ЖУРНАЛ
ПРИКЛАДНОЙ ХИМИИ

Volume 31 No. 10

October 1958

JOURNAL OF
APPLIED CHEMISTRY
OF THE USSR

(ZHURNAL PRIKLADNOI KHIMII)

IN ENGLISH TRANSLATION

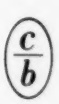

CONSULTANTS BUREAU, INC.

DENDRITIC CRYSTALLIZATION

by **D. D. SARATOVKIN**

2nd Edition,
Revised and Enlarged

Translated from Russian

THIS SIGNIFICANT volume has been extensively revised by the author from the 1953 edition; in particular with *fresh material derived from observations under the stereoscopic microscope.*

The first section deals briefly with some general concepts on crystallization, drawing an important distinction between *genetic* and *structural* types of crystals, including some aspects of the *defect crystal state.* The second section covers at length the illuminating ideas and observations of the 19th-century Russian metallurgist D. K. Chernov, who proposed many of the basic ideas of dendritic crystallization. The third section is an extended survey of current views on dendritic crystallization, in which the ideas of many Soviet and other scientists are briefly summarized and criticized. Section four presents the growth forms of real crystals; all types are reviewed, but only dendritic or closely related forms are selected for subsequent investigation.

Following sections discuss the causes and forms of crystal growth, with *detailed applications* to certain substances that have been extensively studied *(particularly the ammonium halides),* and to eutectics in metal and organic systems; an extensively revised presentation on steel castings which provides a lucid explanation of how the various structures found in real castings can be fitted into the author's theory of dendritic crystallization. Nearly all the concepts developed earlier in the book are utilized in this final section.

The main bulk of the volume contains many *original* and *unpublished* ideas and observations, and is an excellent example of the modern macroscopic approach to the crystalline state by an experienced worker concerned with the infinite variety of real crystals—all of which is enhanced by a *profusion of explanatory line diagrams and sets of stereoscopic photographs.*

CB translations are by bilingual scientists, and include all photographic, diagrammatic and tabular material integral with the text.

CONTENTS

Cloth-bound; 126 pp., illustrated; $6.00

CONSULTANTS BUREAU, INC.
227 WEST 17TH STREET, NEW YORK 11, N. Y.

Volume 31 No. 10

October 1958

JOURNAL OF
APPLIED CHEMISTRY
OF THE USSR

(ZHURNAL PRIKLADNOI KHIMII)

A publication of the Academy of Sciences of the USSR

IN ENGLISH TRANSLATION

Year and issue of first translation:
Vol. 23, No. 1 January 1950

	U. S. and Canada	*Foreign*
Annual subscription	*$60.00*	*$65.00*
Annual subscription for libraries of non-profit academic institutions	*20.00*	*25.00*
Single issue	*7.50*	*7.50*

CONSULTANTS BUREAU INC.
227 W. 17th ST., NEW YORK 11, N. Y.

Printed in the United States of America

JOURNAL OF APPLIED CHEMISTRY OF THE USSR

Volume 31, Number 10 October 1958

CONTENTS

CONTENTS (continued)

PRODUCTION OF A NEW SULFATE FERTILIZER, KALUSZITE, FROM NATIVE KAINITES

G. P. Aleksandrov and V. S. Tikhonova

Mineral Chemistry Laboratory, Institute of the Geology of Useful Minerals, Academy of Sciences Ukrainian USSR

Among the potash fertilizers used in agriculture, the most widely used are of the chloride type: potassium chloride, sylvinite, mixed salts, etc. However, fertilizers of this type should be used for crops of low sensitivity to chloride ions. For a number of other crops (buckwheat, flax, hemp, tobacco, potato, etc.) the best potash fertilizer is potassium sulfate, which not only increases the yield, but improves the quality of the crop [1, 2]. However, owing to the scarcity of potassium sulfate, its use in agriculture is very limited.

We have carried out a search for ways of producing other sulfate fertilizers from the kainite salts which are available in enormous quantities in the Carpathian territories, and which are not being mined at present owing to lack of demand.

It was shown by a number of preliminary experiments that artificial kaluszite (syngenite)* can be made by simple conversion from Carpathian kainites.

The chemical composition of kaluszite corresponds to the double sulfate of potassium and calcium, $K_2SO_4 \cdot CaSO_4 \cdot H_2O$, with a theoretical content of 28.7% K_2O.

Kaluszite consists of colorless acicular crystals, of relatively low solubility in water. When boiled with water, the main bulk of the kaluszite decomposes with formation of calcium sulfate and potassium sulfate.

According to the literature, synthetic kaluszite can be made by the action of potassium chloride solution, containing not less than 8% KCl, on gypsum or anhydrite, or by the action of concentrated potassium sulfate solution on gypsum or calcium chloride. Kaluszite is not formed from solutions saturated with the chlorides of potassium and sodium simultaneously. Neither is it formed from dilute solutions of the above-named salts [4].

K_2O	Na_2O	CaO	MgO	CO_2	SO_3	Cl	Fe_2O_3	H_2O (240°)	Insoluble residue	Total	$Cl_2 = O$	Total
7.84	20.96	1.32	6.02	—	15.00	28.85	—	12.36	13.39	105.74	6.51	99.23
8.28	21.52	1.30	7.06	0.86	15.62	29.91	1.20	9.77	11.36	106.88	6.74	100.14
10.08	18.06	1.92	8.19	—	21.65	25.95	—	5.98	13.17	105.00	5.79	99.21
10.47	20.54	1.43	8.59	—	21.46	29.28	1.27	2.87	8.86	104.77	6.60	98.17
11.30	16.44	1.57	7.91	—	21.66	24.19	1.15	12.36	7.62	104.20	5.46	98.74
12.19	12.79	1.08	10.46	0.49	22.10	23.19	0.75	14.14	7.72	104.91	5.23	99.68
13.86	14.19	0.15	10.79	—	22.22	26.16	—	15·81	2.75	105.93	5.90	100.03

* Native kaluszite was first found in the potash deposits of Kalusz (Ukrainian SSR) from which its name is derived [3].

TABLE 1

Effect of the Amount of Potassium Chloride Added on Kaluszite Yield

Amounts taken					K_2O content		Kaluszite yield	
potassium chloride		kainite (g)	gypsum (g)	water (ml)	in kainite (%)	in kaluszite (%)	g	as K_2O (%)
g	% on weight of kainite							
11	3.1	350	175	500	12.19	10.00	305	61.5
22	6.2	350	175	500	12.19	11.07	332	65.0
33	9.3	350	175	500	12.19	13.17	322	66.8
44	12.4	350	175	500	12.19	13.59	365	70.4
52	14.8	350	260	500	11.30	13.19	484	78.0
65	18.6	350	260	500	11.30	13.12	470	77.1

TABLE 2

Effect of the Amount of Gypsum on Kaluszite Yield

K_2O content of kainite (%)	Amounts taken				Amt. of gypsum (% of theoretical)	K_2O content of kaluszite (%)	Kaluszite yield	
	kainite (g)	gypsum (g)	potassium chloride (g)	water (ml)			g	as K_2O (%)
8.28	300	79	29.4	428	100	13.30	220	66.9
8.28	300	158	29.4	428	200	12.67	289	72.7
10.47	300	108	44.2	428	100	16.82	275	78.0
10.47	300	216	44.2	428	200	13.62	382	87.7
11.30	350	325	52.0	500	250	11.40	549	87.2

EXPERIMENTAL

Kaluszite is formed when powdered gypsum is added to concentrated kainite solution. It is deposited in the form of a coarsely crystalline, easily filterable precipitate.

In all the following experiments kaluszite was prepared by the following procedure: kainite was dissolved at the boil in a definite amount of water, and powdered gypsum was added to the solution with stirring. The precipitated kaluszite was filtered off, pressed out thoroughly on a vacuum filter, and dried. It should be noted that despite the high content of sludge, which usually hinders filtration, in the kainite, the filtration of kaluszite is fairly rapid and a clear filtrate is obtained; therefore the sludge was not removed previously from the kainite solution.

Chemical analysis of the mother liquor showed that the reaction of kainite with gypsum leads to formation of magnesium chloride and sulfate, which are always present in the mother liquors after precipitation of kaluszite. This is because ion exchange takes place when kaluszite is dissolved in water, leading to the equilibrium reaction

$$2\,[KCl \cdot MgSO_4 \cdot 3H_2O] \rightleftarrows K_2SO_4 + MgSO_4 + MgCl_2 + 6H_2O. \quad (1)$$

When gypsum is added, the equilibrium shifts in the direction of the sparingly soluble kaluszite, and the other reaction products remain in solution. Therefore the formation of kaluszite from kainite and gypsum can be represented by the equation

$$2\,[KCl \cdot MgSO_4 \cdot 3H_2O] + CaSO_4 \cdot 2H_2O = K_2SO_4 \cdot CaSO_4 \cdot H_2O + MgSO_4 + MgCl_2 + 7H_2O, \quad (2)$$

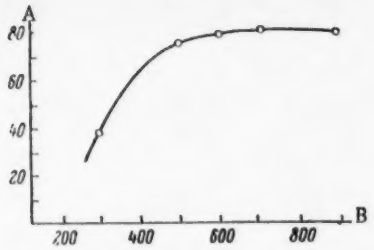

Fig. 1. Effect of the concentration of kainite solution on the kaluszite yield.
A) Yield as K_2O(%), B) kainite content (g per liter H_2O).

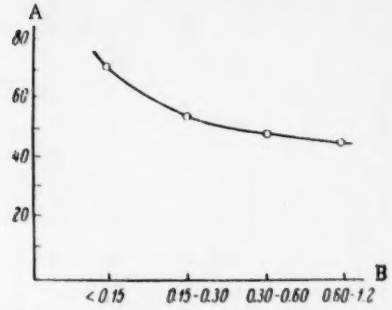

Fig. 2. Effect of gypsum grain size on kaluszite yield.
A) Yield as K_2O (%), B) grain size (mm).

TABLE 3

Effect of Precipitation Temperature on Kaluszite Yield

Precipitation temperature °C	Yield of kaluszite as K_2O (%)	K_2O content of kaluszite (%)
10	82.05	17.62
20	84.83	17.89
30	84.63	17.48
40	81.93	17.08
50	76.17	16.02
60	81.22	15.85
70	65.75	13.80
80	71.88	13.15
90	63.13	13.37

where kainite is the source of the sulfate ions required for the formation of kaluszite. Equation (2) shows that only one half of the sulfate ions in the kainite is expended in kaluszite formation, while the rest remains unused. It is clear that if the deficient quantity of potassium chloride was introduced from outside, the yield of kaluszite would be increased and its K_2O content raised. In fact, when the deficient amount of potassium chloride was added, the product was richer in potassium.

The reaction between kainite, potassium chloride, and gypsum may be represented by the following equation:

$$KCl \cdot MgSO_4 \cdot 3H_2O + CaSO_4 \cdot 2H_2O + KCl = \\ = K_2SO_4 \cdot CaSO_4 \cdot H_2O + MgCl_2 + 4H_2O. \quad (3)$$

This indicated a more rational method for the utilization of kainite, which was studied in detail.

For determination of the optimum conditions of kaluszite formation, experiments were carried out in which the effects of the concentration of the original kainite solution, the amounts of potassium chloride and gypsum added, the temperature of kaluszite precipitation, crystallization time, and other factors influencing the kaluszite yield were studied. Kainite of different grades was used in these experiments, with K_2O contents from 8 to 14%; the chemical compositions are shown in unnumbered table on p.1431 .

Effect of concentration of the original kainite solution. The concentration of the original kainite solution is one important factor which has a strong influence on the kaluszite yield. As was stated earlier, kaluszite is not precipitated from dilute solutions, while the use of highly concentrated kainite solutions may led to in-

TABLE 4

Comparative Field Trials of Kaluszite

Crop, and location of trial	Kainite			Potassium chloride			Potassium sulfate			Kaluszite		
	Yield (centners/ hectare)	yield increase		Yield (centners/ hectare)	yield increase		Yield (centners/ hectare)	yield increase		Yield (centners/ hectare)	yield increase	
		centners/ hectare	%		centners/ hectare	%		centners/ hectare	%		centners/ hectare	%
Potatoes												
Agrobiology Institute, Acad. Sci. Ukrainian SSR, 1952	107.1	42.7	66.3	80.4	16.0	24.8	—	—	—	116.7	52.3	81.2
Poles'e Field Crop Research Station, 1954	183.5	33.5	22.3	180.0	30.0	20.0	184.2	34.2	22.8	194.1	44.1	29.4
L'vov Agricultural Institute, Collective Farm, 1954	110.0	25.0	29.4	—	—	—	—	—	—	122.0	37.0	43.5
The same	135.0	33.0	32.4	—	—	—	—	—	—	163.0	61.0	59.8
Sugar beet												
L'vov Field Crop Research Station, 1953	296.8	37.2	14.3	280.6	21.0	8.1	261.8	2.2	0.82	291.8	32.2	12.4
Buckwheat												
L'vov Agricultural Institute, 1952	13.2	—0.6	—4.4	14.0	0.20	1.4	—	—	—	16.0	2.2	15.9
Poles'e Field Crop Research Station, 1952	4.7	—0.6	—11.9	5.7	0.3	5.6	6.8	1.4	26.6	6.5	1.1	21.0
The same, 1954	5.3	—0.3	—5.4	6.4	0.8	14.3	7.2	1.6	28.6	6.7	1.1	19.7
Flax												
L'vov Agricultural Institute, Collective Farm, 1954												
Seeds	2.7	1.9	237.5	—	—	—	—	—	—	3.1	2.3	287.5
Fibers	3.0	1.5	100	—	—	—	—	—	—	3.3	1.8	120.0
Cabbage												
Agrobiology Institute, Acad. Sci. Ukrainian SSR, Collective Farm, 1952	465.0	77.0	19.9	467.0	79.0	20.4	—	—	—	504.0	116.0	29.9
Tobacco												
Institute of Tobacco, 1954 (dry mass)	—	—	—	—	—	—	22.3	0.4	1.8	24.6	2.7	12.3
The same, 1955 (raw mass)	—	—	—	—	—	—	141.8	9.5	7.2	161.9	29.6	22.4
The same, 1956 (raw mass)	—	—	—	—	—	—	102.6	9.8	10.6	115.8	23.0	24.8

creased contamination of the kaluszite, which would primarily influence its K_2O content. For determination of the optimum concentration of the original kainite solution, we used solutions containing from 300 to 900 g of kainite per liter of water. Kaluszite was precipitated from these solutions by addition of powdered gypsum (75% on the weight of kainite), the precipitation being carried out at 15-20 deg. The amount of potassium chloride added was the amount required theoretically (calculated on the magnesium sulfate), the potassium chloride present in the kainite being taken into account. The effect of the concentration of kainite solution on the kaluszite yield is shown in Fig. 1; it is seen that the yield of kaluszite, calculated as K_2O, increases with increasing concentration of the original kainite solution, the best yields being obtained with solutions containing 650-700 g of kainite per liter of water.

Effect of the amount of potassium chloride added. For determination of the effects of the amount of potassium chloride added to the kainite, a series of experiments was carried out with a kainite solution containing 700 g of the salt per liter of water. The amounts of potassium chloride added ranged from 3 to 19% on the weight of kainite, which corresponded to 16.2 to 103.3% of the amount theoretically required. The potassium chloride was usually dissolved in the kainite solution before addition of gypsum. The amount of powdered gypsum taken was 50-75% on the weight of kainite. The results of the experiments are given in Table 1.

These results show that the kaluszite yield increases with the amount of potassium chloride added, reaching a maximum when the addition is 15% on the weight of kainite, or 83% of the theoretical amount necessary. Further increase of the amount of potassium chloride does not increase either the degree of utilization of K_2O or the K_2O content of the product.

Effect of the amount of gypsum on the kaluszite yield. The original kainite solution used in these experiments contained 700 g per liter of water. Kainite and potassium chloride were dissolved with warming, and the solution was then cooled to 15-20 deg. The amount of potassium chloride taken was 85% of the theoretical. Powdered gypsum was used for precipitation of kaluszite. Sieve analysis showed that the gypsum used was heterogeneous, containing 46.7% of particles < 0.15 mm, and 53.3% of particles between 0.15 mm and 1.2 mm.

In this series of experiments the theoretical amount and also double the theoretical amount of gypsum was used. The slurry was left to settle for 12 hours, after which the kaluszite was filtered off and squeezed out thoroughly on a suction filter. The results of these experiments are given in Table 2.

It follows from these results that, if the theoretical amount of gypsum is used, the kaluszite formed is richer in potassium, but its yield is lower. Therefore in the subsequent experiments double the theoretical amount of gypsum, or about 70% on the weight of kainite, was taken.

Since the reaction of kainite solution with gypsum is a heterogeneous reaction, the degree of subdivision of the gypsum should have a strong influence on the kaluszite yield and on its K_2O content. This is because the reaction between concentrated kainite solution and powdered gypsum occurs at the surface of the latter, and owing to the low solubility of kaluszite under these conditions the gypsum grains become covered with a crystalline coating which prevents further penetration of the kainite solution into the particles. Therefore increase of the specific surface makes a greater mass of gypsum available for the reaction, and this leads not only to an increase of the yield of kaluszite but to an increase of its K_2O content. The effect of gypsum grain size on the yield of kaluszite as K_2O is plotted in Fig. 2.

It was found experimentally that with the use of gypsum of grain size <0.15 mm the yield of kaluszite is 16% higher than with the use of gypsum of grain size 0.15–0.30 mm. The K_2O content of the kaluszite is also higher. Therefore previously-sifted gypsum, with grains < 0.15 mm, was used in the subsequent experiments.

Effect of precipitation temperature on kaluszite yield. The experiments on the influence of precipitation temperature on the kaluszite yield were carried out by the same procedure as in the previous experiments, except that the precipitation by gypsum was performed at definite temperatures, at which the slurry was kept for 4 hours. Vigorous stirring was used during addition of the gypsum and during the subsequent storage of the slurry at constant temperature. The experiments were performed over the temperature range from 10 to 90 deg, with kainite containing 12.19% K_2O. The results are given in Table 3.

It is seen that the best results are obtained if kaluszite is precipitated at 20-30 deg. The kaluszite so formed contains about 18% K_2O, the yields being up to 85%. Experiments on the influence of settling time of the slurry on the kaluszite yield showed that the time is not of great importance, but if the slurry is kept for 2-3 hours after the precipitation the kaluszite yield rises to 88%, and the K_2O content increases by 1-2%.

Treatment of mother liquors. In the production of potassium salts in the existing potash plants, utilization of the mother liquors is of special importance. In the conversion of kainite into kaluszite by the proposed process, about 1.5 cubic meters of a mother liquor containing from 300 to 340 g of salts per kg of solution is obtained per ton of raw material converted. This mother liquor consists mainly of sodium chloride (160-175 g/kg), magnesium sulfate (30-40 g/kg), potassium chloride (44 g/kg), and magnesium chloride (42-52 g/kg). The contents of potassium and magnesium salts merit consideration from the point of view of possible further utilization for kaluszite production. However, the valuable components of the mother liquor can be used only after removal of most of the sodium chloride, which has an adverse effect, if present in large concentrations, on the kaluszite yield. In the conditions existing in the Carpathian deposits, where natural gas, a most efficient and cheap fuel, is available, this problem may be solved by evaporation of the mother liquors. Experiments showed that when the mother liquor is evaporated to 50% of its original volume most of the sodium chloride is precipitated, and can be easily separated from the remaining solution. Further evaporation of the remaining mother liquor (to about 0.1 of the initial volume) precipitates potassium and magnesium salts, mainly kainite, which may be recycled. The final mother liquor is magnesium chloride solution, containing about 280 g of $MgCl_2$ per kg.

After the optimum conditions for the production of kaluszite from Carpathian kainite had been established, the following technological procedure was adopted. To a solution containing 650-700 g of kainite in a liter of water, a weighed quantity of potassium chloride is added, followed by gypsum (65-75% on the weight of kainite), with vigorous stirring. The grain size of the gypsum should not exceed 0.15 mm, while the amount of potassium chloride added depends on the K_2O content of the kainite. The precipitation temperature must not exceed 20-30 deg. The kaluszite slurry is held at this temperature for 2-3 hours, and the kaluszite is then filtered off, dried, and crushed. The conversion of kainite into kaluszite is represented by the following diagram:

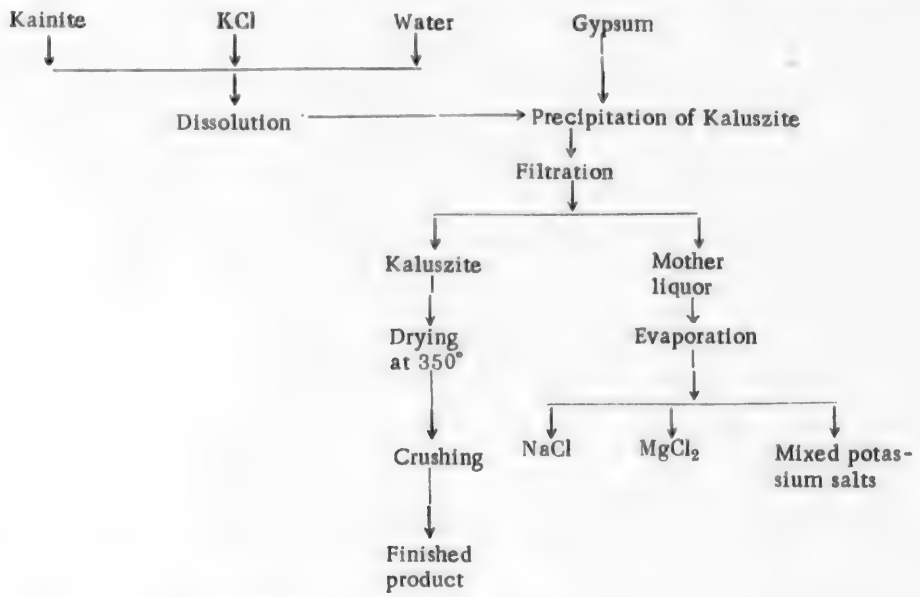

The kaluszite made by this process is a 60-65% concentrate, the principal impurities in which are excess gypsum and the sludge present in the original kainite. The sodium chloride content of the kaluszite does not exceed 1-1.5%. In addition to the main elements in kaluszite, it also contains a number of trace elements (B, Mn, Cu, Sr, Ba, and others), which makes it preferable to other potash fertilizers made artificially. The mother liquors obtained after removal of the kaluszite by filtration can also be utilized in the proposed process. The liquors are evaporated, and after separation of the sodium chloride and further evaporation the precipitated crystals of mixed potassium salts are filtered off and recycled, magnesium chloride being left in the final mother liquor.

Agricultural trials of kaluszite. Kaluszite is a new type of potash fertilizer. Its use for increasing the yields of agricultural crops was first proposed by us in 1953 [5]. Pilot-plant trials of the process yielded 15 tons of kaluszite, which was used for extensive field trials, spread over several years, in various agricultural regions of the Ukraine, for comparison of its effects with those of other types of potash fertilizers on potatoes, sugar beet, buckwheat, flax, cabbage, and cigarette tobacco.

The trials showed that kaluszite is not inferior but is even superior to potassium sulfate as a fertilizer, and produces considerably larger crop increases than sylvinite, 40% potash salts, potassium chloride, and kainite; this places kaluszite in one of the leading positions among the potash fertilizers. Despite this, like other potash fertilizers, kaluszite is not a universal fertilizer and should be used for crops which are adversely affected by chloride fertilizers.

As the result of several years of field trials it was found that kaluszite increases the yield of potatoes by 30 to 81% (with a simultaneous increase of the yield of large tubers), of sugar beet by 12% (with a simultaneous increase of 0.5-1.6% in the sugar content), of buckwheat by 16-21%, of flax seed by 290%, of flax fibers by 120%, of cabbage by 30%, and of tobacco by 22-25% (Table 4).

It follows that the new form of sulfate fertilizer which we recommend, kaluszite, is a highly effective sulfate fertilizer which merits the widest possible agricultural utilization.

SUMMARY

1. The following are the optimum conditions for the production of kaluszite from crude kainite: a) precipitation from solutions containing 700 g of kainite per liter of water; b) the precipitation by gypsum should be carried out at 15-20 deg; c) the proportions of kainite, water, and gypsum should be 1:1.5:0.7, and the gypsum grain size should not exceed 0.15 mm; d) to increase the yield of kaluszite and its K_2O content, 15-17% of potassium chloride, on the weight of kainite, should be added; the kaluszite yield then reaches 82-83%, the K_2O content being 18-19%.

2. The high concentrations of sodium and magnesium chlorides present in the mother liquors lower the kaluszite yield, and therefore they should not be recycled.

3. Potassium salts and magnesium sulfate can be recovered from the mother liquor by evaporation; they may be recycled only after separation of most of the sodium chloride.

4. Agricultural trials of kaluszite with a number of crops showed that it is as effective as potassium sulfate and much more effective than sylvinite, mixed salts, potassium chloride, and kainite; this puts kaluszite in a leading position among the fertilizers.

LITERATURE CITED

[1] I. P. Serdobol'skii, Potassium [In Russian] (Moscow, Izd. AN SSSR, 1944).

[2] I. N. Elagin and G. M. Solov'ev, Cultivation of Buckwheat [In Russian] (Moscow, Agricultural Literature Press, 1954).

[3] E. S. Dana, Descriptive Mineralogy (Leningrad–Moscow, ONTI, 1937) [Russian translation].

[4] I. N. Kepeshkov, Potash Salts of the Volga, Emba, and Carpathian Regions [In Russian] (Moscow–Leningrad, Izd. AN SSSR, 1946).

[5] G. P. Aleksandrov and V. N. Dudnik, Soviet Authors' Certif. Ministry of Agriculture USSR No 96, 316. [In Russian]

Received February 19, 1957

COMPOSITION AND PROPERTIES OF DEFLUORINATED PHOSPHATES

N. N. Postnikov, M. G. Frenkel', B. B. Evzlina, A. I. Smirnov, and V. I. Plotnikova

The production of defluorinated phosphates consists of high-temperature steam treatment (at 1400-1450 deg) of native phosphates [1-15], apatites or phosphorites, mixed with silica or limestone; the process may be schematically represented by the equation

$$2Ca_5(PO_4)F + H_2O + 0.5SiO_2 = 3Ca_3(PO_4)_2 + 0.5Ca_2SiO_4 + 2HF.$$

In our opinion, defluorination without fusion should be represented as involving calcium orthosilicate and not metasilicate [1, 2]. It is known that when a mixture of calcium oxide and silica (in 1:1 ratio) is heated at 1400 deg for one hour, orthosilicate and tricalcium disilicate are formed [3].

This paper contains an account of the composition and properties of defluorinated phosphates made in a pilot unit* from apatite concentrate and from Chulak-Tau phosphorites.

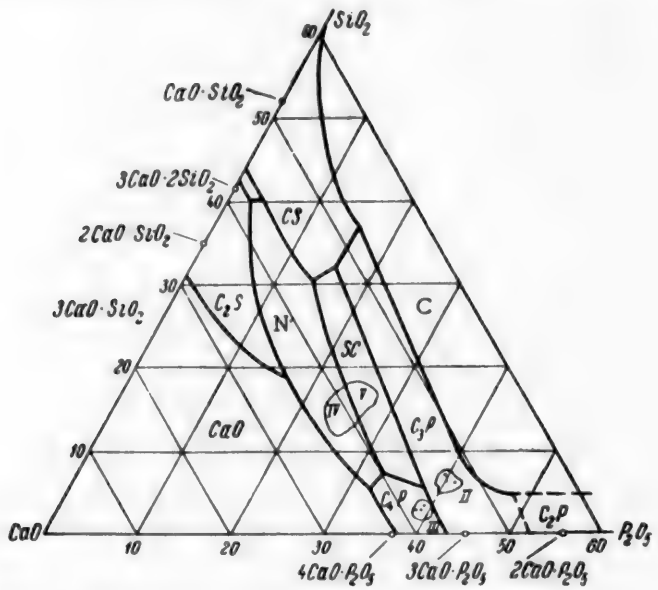

Fig. 1. Distribution of defluorinated phosphates, made from Mixtures I-V, on the phase-stability diagram for the ternary system $CaO-SiO_2-P_2O_5$.
C) Cristobalite, N) nagelschmidtite.

* The pilot trials were carried out at the Experimental Plant of the Scientific Research Institute of Fertilizers and Insectofungicides under the guidance of S. I. Vol'fkovich, N. N. Postnikov, A. A. Ionass, and R. E. Remen [15].

TABLE 1

Average Composition of Defluorinated Phosphates Made from Apatite Concentrate and Chulak-Tau Phosphorites

Mixture	Sample No.	Composition of defluorinated phosphate (%)						Molar comp. of defluorinated phosphate (calculated for the 3 components)		
		P_2O_5	SiO_2	CaO	MgO	Fe_2O_3	F	P_2O_5	SiO_2	CaO
III	5—7	38.35	2.71	51.52	0.52	0.91	0.28	1.0	0.19	3.46
II	3—4	37.84	5.9	49.86	0.54	0.72	0.43	1.0	0.42	3.4
I	1—2	19.55	46.38	26.3	0.68	1.24	0.01	1.0	5.62	3.42
IV	1—3	23.46	13.32	58.7	3.04	1.09	0.65	1.0	1.34	6.33
IV	4—5	22.51	12.57	59.0	3.01	1.18	0.1	1.0	1.32	6.5
V	—	23.18	14.62	55.32	3.1	0.92	0.05	1.0	1.40	5.71

TABLE 2

Composition of Citric-Acid Extracts of Defluorinated Phosphates from Apatite Concentrate and Chulak-Tau Phosphorites

Mixture	Contents in citric-acid extract (%)				Composition of citric-acid extract (molar)		
	P_2O_5	SiO_2	CaO	Fe_2O_3	P_2O_5	SiO_2	CaO
I	16.46	0.23	23.74	0.19	1.0	0.003	3.66
	14.46	0.23	17.85	0.21	1.0	0.003	3.12
II	30.34	2.13	38.6	0.31	1.0	0.17	3.29
	25.25	1.71	33.23	0.25	1.0	0.16	3.34
III	35.29	2.66	46.88	0.35	1.0	0.18	3.37
	23.82	2.48	30.87	0.31	1.0	0.25	3.30
	21.41	0.9	28.00	0.9	1.0	0.1	3.32
IV	22.22	19.63	54.67	1.97	1.0	1.34	6.22
	19.26	13.10	51.33	1.70	1.0	1.61	6.75
	15.38	11.96	49.74	0.80	1.0	1.84	8.22
	10.44	9.24	44.78	0.50	1.0	2.09	10.87
	9.68	9.30	43.70	0.47	1.0	2.28	11.52
V	23.26	13.93	52.32	2.16	1.0	1.41	5.69
	22.44	14.00	50.95	1.61	1.0	1.37	5.75
	21.45	12.80	51.37	1.65	1.0	1.47	6.07
	14.60	11.88	40.18	0.80	1.0	1.92	6.28
	14.12	11.90	40.22	0.80	1.0	1.99	7.22

EXPERIMENTAL

The samples of defluorinated phosphates used in the tests were obtained under different furnace conditions from the following mixtures: I) 100 wt. parts of apatite concentrate and 100 wt. parts of sand, II) 100 wt. parts of apatite concentrate and 5 wt. parts of sand, III) 100 wt. parts of apatite concentrate and 2 wt. parts of sand, IV) 100 wt. parts of Chulak-Tau phosphorite and 60 wt. parts of limestone, V) 100 wt. parts of Chulak-Tau phosphorite and 40 wt. parts of limestone.

The defluorinated phosphates were studied by determinations of their solubility in citric acid and ammonium citrate solution, by optical crystallographic and x-ray structure analysis, and by phase differentiation effected by centrifugation in heavy liquids.

The results of total chemical analyses (average data) are given in Table 1. The primary analytical data, calculated on the sum of the three components $CaO + SiO_2 + P_2O_5$, were used for distribution of defluorinated

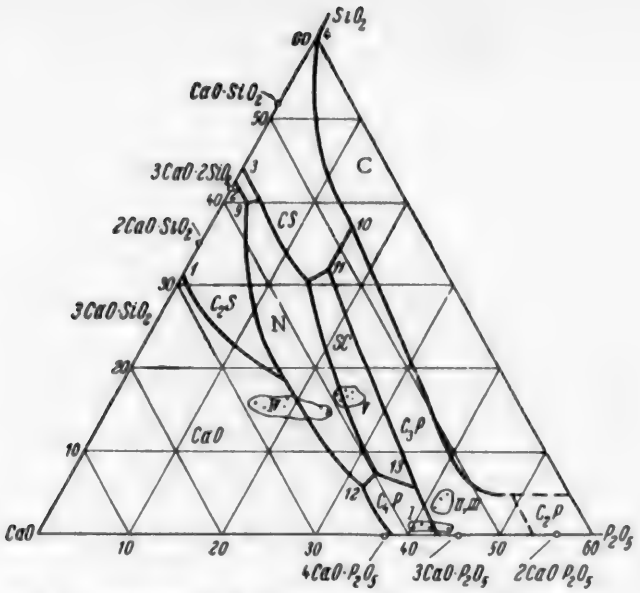

Fig. 2. Distribution of citric-acid extracts from defluorinated phosphates, made from Mixtures I-V, on the phase-stability diagram for the ternary system $CaO-SiO_2-P_2O_5$.

TABLE 3

Composition of Citrate Extracts from Defluorinated Phosphates Made from Apatite Concentrate and Chulak-Tau Phosphorites

Mixture	Composition of citrate extract (%)			Composition of citrate extract (molar)		
	P_2O_5	SiO_2	CaO	P_2O_5	SiO_2	CaO
I	10.70	1.14	17.17	1	0.252	4.08
	3.96	1.18	8.17	1	0.627	5.22
II	16.10	1.49	23.17	1	0.218	3.62
	14.08	1.08	20.38	1	0.218	3.62
III	21.65	2.20	29.30	1	0.239	3.41
	17.87	2.23	21.80	1	0.297	3.13
	12.45	1.80	17.53	1	0.34	3.57
IV	20.34	4.22	55.17	1	0.49	6.89
	17.65	4.73	52.40	1	0.63	7.53
	13.58	2.62	51.30	1	0.46	9.62
	9.40	1.00	48.07	1	0.25	12.98
	8.88	3.00	47.20	1	0.74	13.45
V	21.65	4.72	53.2	1	0.51	6.25
	20.10	5.18	52.70	1	0.60	6.65
	19.90	4.65	52.79	1	0.59	6.71
	13.73	4.44	40.85	1	0.77	7.57
	13.20	4.60	41.10	1	0.82	7.93

phosphates by the phase-stability regions of the ternary system $CaO-SiO_2-P_2O_5$ [6, 10]. The defluorinated phosphates made from Mixture I lie in the stability region of cristobalite, while those made from Mixture II are in the stability region of tricalcium phosphate (Fig. 1). The fact that the phase composition of defluorinated phosphate should correspond to tricalcium phosphate is not a necessary and sufficient criterion of a high degree of assimilability, which is estimated from the solubility of phosphates in 2% citric acid.

TABLE 4

Phase Composition of Defluorinated Phosphates Made From Apatite Concentrate with Sand

Mixture	Sample No	Total P_2O_5 (%)	P_2O_5 soluble in citric acid %	P_2O_5 soluble in citrate %	Mineral composition					
					α-tricalcium phosphate (N_g = 1.594, N_p = 1.588)	β-tricalcium phosphate (N_g = 1.627, N_p = 1.622)	fluorapatite (N_g = 1.632, N_p = 1.630)	quartz (N = 1.55)	ferrosilicates (N = 1.82)
I	1	19.33	16.46	10.70	Principal phase	Absent	Individual grains	Present in considerable amounts	Present
I	2	19.18	14.46	3.96	The same	"	The same	The same	"
II	3	38.11	30.34	16.10	" "	Present	Present	Present	Individual grains
II	4	37.56	25.25	14.08	" "	"	"	Present 1%	"
III*	5	38.25	35.29	21.65	" "	Present (N_g = =1.623, N_p =1.620)	"	Absent	Present in considerable amounts
III	6	38.43	23.82	17.87	" "	Absent	"	"	Absent
III	7	38.41	21.41	12.45	" "	Present	"	Individual grains	Individual grains

*"Principal phase" means that the content of α-tricalcium phosphate is over 50%.

Tricalcium phosphate [7] is dimorphous, and exists in two modifications: the high-temperature α-form is completely soluble in the standard quantity of 2% citric acid, while the solubility of the low-temperature β-form is 1/3 to 1/4 of this.

The α-modification can be stabilized either by means of various stabilizing additives, which lower the temperature of its transition into the β-form, but do not make this transition impossible, or by rapid cooling (quenching). The effects observed here are analogous to those in orthosilicate transitions.

The defluorinated phosphates made from Chulak-Tau phosphorites with additions of limestone lie in the stability region of silicocarnotite and nagelschmidtite (Fig. 1). Defluorinated phosphates containing less silica than the amount required for formation of calcium orthosilicate may be expected to contain free lime as a separate phase, provided that basic solid solutions — silicophosphates of the composition 5.3 $CaO \cdot P_2O_5 \cdot SiO_2$ and 7.3 $CaO \cdot P_2O_5 \cdot SiO_2$ [4] have not been formed. In contrast to apatite, Chulak-Tau phosphorites contain considerable amounts of magnesium in the form of dolomite. The action of heat may cause the formation of magnesium orthosilicates if enough SiO_2 is present. If there is a deficiency of SiO_2, magnesium silicates cannot be formed, and free magnesium oxide must remain [5, 9]. Chulak-Tau phosphorites contain considerable amounts of the oxides of iron and aluminum, which give rise to the formation of a spinel of the $MgO \cdot Al_2O_3$ type [5]; this was confirmed by optical crystallographic analysis of the defluorinated phosphates.

Analytical data for extracts of defluorinated phosphates in 2% citric acid are given in Table 2, which shows that: a) citric acid

TABLE 5

Phase Composition of Defluorinated Phosphates Made from Chulak-Tau Phosphorites (100 wt. parts) Mixed with Limestone (40 wt. parts) (Mixture No.5)

Sample No.	Total P_2O_5 (%)	P_2O_5 soluble in citric acid (%)	P_2O_5 soluble in citrate (%)	Mineral composition (%)										
				silicophosphates of nagelschmidtite type of N_{av} (fraction dens. 3.05-3.15)					silicocarnotite (N_g = 1.644, N_p = 1.630)	silicophosphate phase of silicocarnotite type, N_{av}			apatite (N 1.630)	spinellides and periclase
				1.680–1.669	1.662–1.66	1.658	1.651	1.647		1.644	1.639	1.628		
7	25.13	23.00	20.52	—	—	—	0.41	5.69	14.81	15.0	56.05	0.82	6.79	2.26
9	24.94	14.60	13.73	2.21	6.93	7.65	31.28	6.62	1.70	6.01	10.25	0.12	23.45	3.42
10	25.00	14.12	13.20	0.88	4.19	25.37	27.03	7.62	0.3	3.88	2.04	0.03	24.39	3.78
11	24.54	21.70	20.10	—	0.58	1.84	21.91	39.58	6.56	9.89	12.60	0.02	5.47	1.55
12	24.90	22.50	20.10	—	—	—	—	0.54	13.16	11.62	64.13	1.31	6.66	2.39

extracts P_2O_5, SiO_2, and CaO from defluorinated apatite phosphates in more or less constant proportions, which correspond to 1 mole of $Ca_3(PO_4)_2$ and 0.2 mole of Ca_2SiO_4 for Mixtures II and III, and in a lower ratio (with respect to Ca_2SiO_4) for Mixture I; b) the three-component compositions of the citric-acid extracts lie in the stability regions of tricalcium phosphate (Fig. 2) for Mixtures II and III, and of tetracalcium phosphate (Mixture I); c) citric acid extracts P_2O_5, SiO_2, and CaO from defluorinated phosphorite phosphates in variable proportions, which alter with decrease of P_2O_5 solubility; d) the three-component compositions of the citric-acid extracts lie in the stability regions of silicocarnotite and nagelschmidtite, the silicocarnotite defluorinated phosphates having the highest solubility; e) the proportion of MgO brought into solution increases with decreasing CaO: SiO_2 ratio in the solution.

Analytical data for extracts of defluorinated phosphates in ammonium citrate (citrate extracts) are given in Table 3.

These results show that: a) the solubility of P_2O_5 present in defluorinated apatite phosphates in ammonium citrate solution is only 70-20% of the solubility in citric acid, while the solubility of P_2O_5 present in defluorinated phosphates made from Chulak-Tau phosphorites in ammonium citrate is only 1-3% less than the solubility in citric acid; b) ammonium citrate extracts somewhat more CaO (1-3% more) than does citric acid, while the amount of SiO_2 extracted by citric acid is greater (2-3 times).

In general, the higher the solubility of defluorinated phosphates in citric acid, the higher it is in ammonium citrate. Moreover, defluorinated phosphates which correspond to silicocarnotite in their phase composition are always more soluble in ammonium citrate than defluorinated phosphates corresponding to tricalcium phosphate and nagelschmidtite in phase composition.

Studies of the phase composition of the defluorinated phosphates were carried out with the same samples as those used for detailed chemical analysis. Defluorinated phosphates made from apatite concentrate mixed with sand were studied by the immersion method only. The results, given in Table 4, show that in samples Nos. 3, 4, and 5 the principal phase as indicated by the mineral ratio is tricalcium phosphate. Samples Nos. 1 and 2 contain quartz in addition to α- tricalcium phosphate as a principal phase. Samples Nos. 3, 4, 5, and 7 contain β-tricalcium phosphate; its exact content could not be determined, as N_g for β-tricalcium phosphate is close to N_g for fluorapatite. In addition to undecomposed fluorapatite, quartz is present in large amounts in samples Nos. 1 and 2, and in small amounts in Nos. 3, 4, 6, and 7. Ferrosilicates form isotropic inclusions of a brownish color, characteristic of iron oxides, and a high refractive index (N_g > 1.82).

Investigations under the microscope confirmed that the quality of defluorinated phosphates made from apatite concentrate depends on the α-tricalcium phosphate content. The solubility in citric acid increases with the content of the α-form. The solubility of defluorinated phosphates in 2% citric acid is lowered by the presence of β-tricalcium phosphate (same sample No. 3).

The phase composition of defluorinated phosphates made from Chulak-Tau phosphorites was studied by means of centrifuge analysis and microscopy in immersion liquids (each phase separately). All the samples were previously ground down to −150 mesh and centrifuged in heavy liquids for separation of the individual minerals. The following fractions were isolated: −3.00; +3.00; −3.05; +3.05; −3.10; +3.10; −3.15; +3.15. Each fraction was analyzed under the microscope. The result of chemical determinations of P_2O_5, centrifuge analysis (densities), and microscopical analysis (optical constants) are given in Table 5.

The principal minerals in defluorinated phosphates are calcium silicophosphate phases of variable composition, with low birefringence (0.002-0.003), with an average refractive index of 1.639-1.658. In samples Nos.7 and 12, which have the highest solubility in ammonium citrate, the silicophosphate phases correspond to silicocarnotite of N_g = 1.644 and N_p = 1.630, and a silicocarnotite type of N_g = 1.644 and 1.639. Among the silicophosphates, silicocarnotite is characteristic by its birefringence (0.014). An immersion specimen of this sample, of grain size −150 mesh, had somewhat higher interference colors than those of quartz under the same conditions. The mineral is colorless, with a bluish tinge in some of the granules. The refractive indices of silicocarnotite are N_p = 1.630 and N_g = 1.644.

In samples Nos.9 and 10 the predominant part of the calcium silicophosphates had refractive indices above 1.647, which is characteristic of silicophosphates of the nagelschmidtite type. The decreased content of soluble phosphates is evidently associated with predominance of phases of the nagelschmidtite type. The density of these phosphate phases varies between 3.00 and 3.15. These samples also have high apatite contents (23-24%). The decrease of solubility in citric acid is 35-40%, or much more than would be found in presence of apatite.

Sample No.11 has a high content of phosphoric acid in soluble form. The silicophosphate phase consists of mineral with refractive indices between 1.639 and 1.651, but for most of the minerals the refractive indices do not exceed 1.647, i.e., are close to the values for the silicocarnotite phase. These samples contain appreciable amounts of quartz and portlandite $Ca(OH)_2$ in the form of aggregates of fine transparent crystals (N = 1.562). Spinellides and periclase are found in the high-density mineral fraction (about 3.6). These minerals have high refractive indices: spinellides from 1.718 to 2.39, and periclase, 1.724. Periclase appears in defluorinated phosphates from Chulak-Tau phosphorites only in presence of free lime.

If the name given to the new type of phosphate fertilizers, "defluorinated phosphates," is considered in relation to their composition it is seen that the present name reflects the process by which the fertilizer is made, but not its composition or properties. Indeed, the phase composition of the fertilizer made from apatite concentrate with added sand corresponds to α-tricalcium phosphate (Table 4), irrespective of the amount of sand added. In the same way, the fertilizers made from Chulak-Tau phosphorites with added limestone consist predominantly of calcium silicophosphates, which are solid solutions of calcium orthophosphate and calcium orthosilicate in proportions which depend on the composition of the original phosphate mixture.

We therefore consider that the name of the new fertilizer should be changed from "defluorinated phosphates" to "tricalcium phosphate" for the products obtained from apatite with added sand, and to "calcium silicophosphate" for the products which are silicophosphate phases of variable composition, and which may be obtained from native phosphate and limestone, sand being added if there is not enough silica in the native phosphate.

SUMMARY

1. A chemical and crystallographic study has been made of defluorinated phosphates made from apatite concentrate mixed with sand, and from Chulak-Tau phosphorites mixed with limestone; it was found that the phosphate component of defluorinated phosphates made from apatite concentrate consists of α-tricalcium phosphate, and the phosphate component of those made from Chulak-Tau phosphorites, consists of calcium silicophosphate (a silicocarnotite phase of variable composition).

2. The phase composition of the phosphate components of defluorinated phosphates determines their solubility in citric acid and ammonium citrate. Fertilizers the phase composition of which corresponds to α-tricalcium phosphate and silicocarnotite have the highest solubility in citric acid, and phosphates the phase composition of which corresponds to silicocarnotite have the highest solubility in ammonium citrate.

3. In presence of excess lime in defluorinated phosphates from Chulak-Tau phosphorites, magnesium oxide remains in the form of periclase (MgO).

4. The nomenclature of defluorinated phosphates should be changed by the introduction of the following names: tricalcium phosphate and calcium silicophosphate.

LITERATURE CITED

[1] S. I. Vol'fkovich, V. V. Illarionov, and R. E. Remen, J. Chem. Ind. 4, 11 (1954).

[2] D. S. Reynolds, Ind. Eng. Ch. 26, 4, 406 (1934).

[3] P. S. Mamykin and S. G. Zlatkin, J. Phys. Chem. 9, 3, 392 (1937).

[4] N. A. Toropov and N. A. Borisenko, Cement 6, 10 (1954).

[5] G. V. Kukolev, Chemistry of Silicon [In Russian] (1951).

[6] R. L. Barrett and M. C. Caughey, Amer. Mineral. 27, 10, 680 (1942).

[7] E. V. Britske and B. K. Veselovskii, Bull. Acad. Sci. USSR, Div. Chem. Sci. 4, 479 (1937).

[8] I. Tromel, Stal u. Eisen, 2 (1943).

[9] K. S. Evstrop'ev and N. A. Toropov, Chemistry of Silicon [In Russian] (1950).

[10] D. S. Beliankin et al., Physicochemical Principles of Silicate Technology [In Russian] (1954).

[11] V. I. Plotnikova and A. I. Smirnov (Records of the State Institute of Chemical Raw Materials Obtained by Mining) [In Russian]

[12] W. Jander, E. Hoffmann, Z. Anorg. Chem. 13-46, 4, 576-580 (1933).

[13] K. A. Vasil'ev and B. A. Faktorovich, Light Metals 2, 1 (1936).

[14] Methods of Accelerated Chemical Analysis of Raw Cement Mixes and Clinker [In Russian] (Industrial Construction Press, (1952)).

[15] S. I. Vol'fkovich, N. N. Postnikov, A. A. Ionass, and R. E. Remen, Records of the Sci. Res. Inst. Fertilizers and Insectofungicides Nos.8579 and 8736 (1953-1954): "Pilot trials of the production of defluorinated phosphates from apatite concentrate and sand." Records of the Sci. Res. Inst. Fertilizers and Insectofungicides No 9062 (1954): "Pilot trials of the production of defluorinated phosphates from Chulak-Tau phosphorites."

Received October 24, 1956

CONTRACTION IN THE HARDENING OF PORTLAND CEMENT WITH ADDED CHLORIDES AT POSITIVE AND NEGATIVE TEMPERATURES

V. V. Nekrasov and G. A. Shisho

Chair of Chemistry of the I. V. Michurin Fruit and Vegetable Institute, and the Scientific Research Section of the S. Ia. Zhuk Hydroelectric Project

Calcium chloride (usually 1-2% on the weight of cement) has long been used as an additive for acceleration of the hardening of concretes based on Portland cement. During recent years it has become usual in construction practice to add relatively large amounts of calcium and sodium chlorides in the production of the so-called "cold" concrete, i.e., in the placement of concrete mixed during the cold seasons of the year, at subzero temperatures of the materials and surroundings. In particular, much work was done in this direction from 1951, in connection with the construction of the Volga—Don canal, where the industrial trials were carried out. However, the physiocochemical processes which take place in the hardening of cement in presence of such additives are far from being sufficiently well understood.

For further elucidation of this question, we used the contraction method of studying the hardening of cements, which was described by one of us earlier [1], in which contraction curves, i.e., curves representing the decrease of the sum of the absolute volumes of the solid and liquid phases in the course of hardening, are used to given an indication of the chemistry and kinetics of the process. This method has already yielded useful results in a number of cases [2-5]. Data obtained by us during 1954-1957 are presented in this paper.

EXPERIMENTAL

The experiments were performed with Portland cements from the "Bol'shevik" and "Komsomlets" works, pozzolanic Portland cement from the "Komsomolets" works, individual clinker minerals, and lime. Analytical and test data for the cements and analytical data for the minerals are presented in Tables 1 and 2. Chlorides ($CaCl_2$ and NaCl) were used both in the chemically pure forms and in technical grades; the impurities in the technical products had no appreciable influence on the contraction. In preparation of the cement pastes the chlorides were added in solutions containing from 2.7 to 22% salt (on the weight of water); with the water—cement ratio (W/C) of 0.5 generally used in our experiments, this gave salt contents in the range of 1.3-11% on the cement weight at the moment of mixing.

The method described earlier was used for measurements of contraction. The contractometers were glass vessels coated on the inside with layers of bitumen or paraffin wax to prevent destruction of the vessel. Pastes of cement with water or salt solution were mixed, and introduced into the contractometer in definite weights; the remaining space and measuring tube were filled with water, and in some instances with the same chloride solution. To prevent evaporation of the liquid in the measuring tube, it was covered with a layer of mineral oil or kerosene. In a number of experiments at subzero temperatures the whole space over the paste was also filled with kerosene; special check experiments showed that replacement of water over the paste by solution or kerosene has almost no effect on the contraction curve under these conditions, i.e., the water added to the paste during mixing is sufficient to ensure a normal course of hydration over a long period even in presence of salts. The experiments were performed at different hardening temperatures: +20, 0, −5, −10°. Special thermostatic boxes for the contractometers, placed in cold rooms, made it possible to maintain almost constant temperatures (0, −5, −10°) over long periods. In each series of experiments the comparison standard was a similar

TABLE 1

Cement Characteristics

Portland cement	Activity (kg/cm²)	Mineral composition of clinker (%, works data)			
		C_3S	C_2S	C_3A	C_4AF
Works:					
"Bol'shevik"	454	52	25	3	18
"Komsomolets"	396	45	35	3	14
Pozzolanic, from "Komsomolets" works	356	50	31	3	14

TABLE 2

Analytical Data for Clinker Mineral Samples (%)

Clinker mineral	SiO_2	Al_2O_3	Fe_2O_3	CaO	MgO	SO_3	Calcination loss	Free CaO
C_3S	26.3	—	—	73.7	—	—	—	0.2
C_2S	34.9	—	—	65.1	—	—	—	—
C_3A	0.2	38.2	—	60.0	0.2	0.2	0.7	—
C_4AF	—	20.9	32.9	46.1	—	—	—	0.04

contractometer, containing an equal weight of sand (previously soaked in water) and kept under the same conditions, instead of cement; corrections for thermal contraction were thereby eliminated. For convenient comparison with earlier data, the contraction (in ml) is calculated per 300 g of cement.

The following concordant and reproducible results were obtained in several series of contraction experiments with the above-named cements. At positive temperatures the addition of chlorides to Portland cement during mixing increases the contraction somewhat only in presence of small amounts of salts, and mainly at the initial stages [1]. The contraction curves lie lower, i.e., cement hydration is retarded, with increase of the amounts of salts; this is clearly seen in all cases (although to different extents) with sodium chloride and especially with calcium chloride (Figs. 1 and 2).

Decrease of the hardening temperature to 0 deg (in another series of experiments) naturally reduced the contraction in comparison to the contraction at +20 deg, at all stages in the hardening of cement both with and without added chlorides. However, in presence of considerable amounts of calcium chloride the decrease of contraction due to the temperature change is very small, while with 5 to 10% $CaCl_2$ on the cement weight the contraction curves generally lie even somewhat higher than the curves for the same mixtures at the positive temperature and the curve for cement without added chlorides at 0°C. This unexpected increase of contraction in presence of large amounts of calcium chloride becomes even more prominent on further decrease of temperature. At −10°C the curve for cement with 10% $CaCl_2$ cuts the curve for cement without additive at +20°C. This effect is not observed with sodium chloride, even when large amounts are added (Figs. 3 and 4).

The contraction curves in Figs. 1-4 were obtained in experiments with Portland cement from the "Bol'shevik" works. Very similar results were obtained in experiments with Portland cement from the "Komsomolets" works and pozzolanic Portland cement; the contraction was appreciably greater in presence of considerable amounts of $CaCl_2$ at low temperatures.

In order to find which components of Portland cement clinker cause this contraction effect, experiments were performed with individual clinker minerals, prepared in different institutes. It was found that addition of

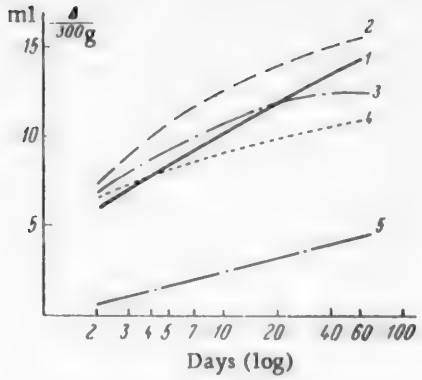

Fig. 1. Effect of additions of $CaCl_2$ on the contraction of Portland cement (W/C 0.5, +20°C). Amounts of $CaCl_2$ (% on cement weight): 1) 0 (pure water), 2) 1.3, 3) 2.8, 4) 5.5, 5) 11.

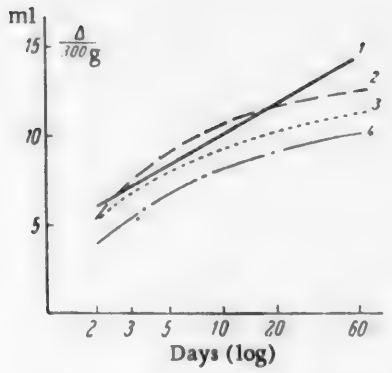

Fig. 2. Effect of additions of NaCl on the contraction of Portland Cement (W/C 0.5, +20°C). Amounts of NaCl (% on cement weight): 1) 0 (pure water), 2) 1.3, 2.8; 3) 5.5; 4) 11.

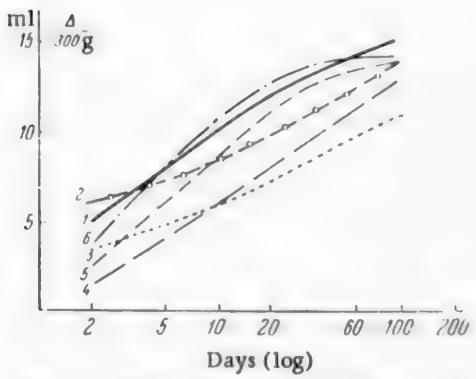

Fig. 3. Effect of additions of $CaCl_2$ on the contraction of Portland cement at various temperatures, with W/C = 0.5. Amounts of $CaCl_2$ (% on cement weight) and temperatures respectively: 1) 0 (pure water), +20°; 2) 5, +20°; 3) 10, +20°; 4) 0 (pure water), 0°; 5) 5, −5°; 6) 10, −10°.

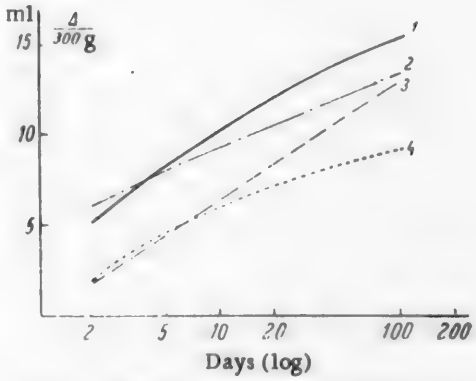

Fig. 4. Effect of additions of NaCl on the contraction of Portland cement at various temperatures, with W/C = 0.5. Amounts of NaCl (% on cement weight) and temperatures respectively; 1) 0 (pure water), +20°; 2) 10, +20°; 3) 0 (pure water), 0°, 4) 10, −10°.

$CaCl_2$ (10% on the weight of mineral) at −10°C sharply increased contraction in the case of tricalcium silicate and decreases it appreciably in the case of the other three minerals, as compared with the contraction of the same mineral with water without additives at +20°C. These data are plotted in Fig. 5 (calculated per 100 g of mineral). The absolute values of the contraction of dicalcium silicate are very low, and the results for this mineral are not given in Fig. 5 (the particle size of the minerals were different, and therefore their absolute contractions are not comparable in this series of experiments).

When these results were obtained, it became necessary to find whether calcium chloride interacts at subzero temperatures with tricalcium silicate as such, or with the free lime formed by its hydrolysis. The former corresponds to formation of complex calcium chlorosilicates, and the latter, of calcium oxychlorides. Experiments were therefore carried out on the contraction of free lime. Lime paste was mixed either with water or with chloride solutions, and held in contractometers at various temperatures. The ratios of added salts to lime

TABLE 3

Alkalinity of Solutions in Contractometers in Contact With Hardening Cement Paste. Portland cement from "Bol'shevik" works, water–cement ratio 0.5, hardening temperature +20 to 0°C (average data)

	Water	Concentrations of salt solutions (% on weight of water)			
		$CaCl_2$		NaCl	
		10	20	10	20
OH' (meq/liter	74	40	36	111	131

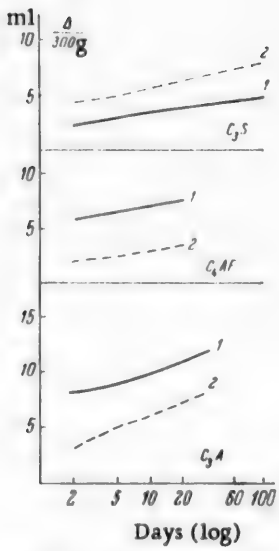

Fig. 5. Combined effect of added $CaCl_2$ and subzero temperature on the contraction of Portland cement clinker minerals.
1) Without addition, +20°C
2) with 10% $CaCl_2$ on the mineral weight, −10°C.

were, of course, higher than the ratios of added salts to cement, because the lime formed in the hydration of cement represents only a small proportion of the latter. The contraction of these mixtures was slight, but after 30 days (per 100 g of lime at W/L* ratio 2.4) it reached, with 20-40% NaCl (on the weight of lime), 2-3 ml at +20°C, and 3.5-4 ml at −10°C; with 20-40% $CaCl_2$ it was 3-4 ml at +20°C and 4-5 ml at −10°C. Comparison of these results with data for the clinker minerals shows that the increase of contraction at lower temperatues, characteristic of tricalcium silicate and alite cements, is also found in the case of lime (with NaCl as well as with $CaCl_2$), but it is mainly the silicate which reacts with calcium chloride under these experimental conditions, as the amount of lime split off during hydrolysis is not enough to give rise to the observed contraction effect.

Analytical data for samples of the lower liquid layer (in contact with the hardening cement) from the contractometer after several months of hardening (Table 3) show both a decrease of the solubility of lime in presence of calcium chloride (decrease of alkalinity), and interaction of lime with sodium chloride (increase of alkalinity) [6, 7]. In some contractometers, at high $CaCl_2$ concentration in the cement paste and with the contractometers filled with the same solution, loose formations appeared on the surface of the hardened cement and gradually occupied a large volume. Samples of this substance after drying contained 20-40% $CaCl_2$ (in some cases, up to 50% calculated from the combined chlorine), 4-8% sesquioxides, and 10-14% SiO_2 on the dry substance, with a calcination loss of 10-15%. It is possible that such substances are formed in the hardening cement paste itself. The sharp increase in the volume of the solid phase then corresponds to the acceleration of the strength increase of cement and concrete which is observed (although not always) at high contents of calcium chloride (in comparison with the strength without added $CaCl_2$), and with the strength decreases, very sharp in some instances, found in these materials at later stages. It must be emphasized here that the strength (compressive or tensile) of a cement-based hardening material does not depend only on the degree of hydration or on the course of other chemical processes reflected by the contraction curves, and these curves in no way correspond directly to the course of the mechanical strength increase.

* W/L is the water – lime ratio.

DISCUSSION OF RESULTS

The retardation of hydration of Portland cement clinker in presence of considerable amounts of chlorides may be attributed both to reactions of the salts with the clinker minerals and their hydration products (as the result of which the newly formed materials become less permeable to water), and to a decrease of the content of free water in the liquid phase of the hardening paste, because part of the water is bound in the hydration layers of the salt ions. This last concept is in harmony with the observed effect of salt concentration on contraction, and explains why calcium chloride produces a greater retardation effect than sodium chloride. The cause of the increased contraction in presence of small amounts of chlorides and at early stages is not yet quite clear.

The effects produced by chlorides added to concrete mixes at subzero temperatures are often attributed merely to a decrease of the freezing point of the aqueous solution surrounding the hydrating cement grains. In that case a decrease of temperature to 0°C and below should progressively retard the hydration of cement, both without additives and in presence of salts. However, the contraction curves show convincingly that the simultaneous influence of high concentrations of calcium chloride and low temperatures leads to the formation of entirely different hydration products of Portland cement; possibly oxychlorides, but predominantly complex salts containing silica. We did not isolate these individual substances, but the contraction experiments indicate that they are chlorohydrosilicates of the general formula $aSiO_2 \cdot bCaO \cdot cCaCl_2 \cdot dH_2O$, the very large contractions indicate that the number of molecules of water of crystallization (d) in them is also very large.

It follows from the considerable increase of alkalinity that sodium chloride may lead to appearance of calcium chloride in the system, but the concentration of the latter is evidently insufficient in this case.

The fact of greatest interest and practical importance is that new hydration products are formed in considerable amounts to judge by the contraction curves, only at temperatures about 0°C and lower. This leads to the conclusion that these new products, like many other crystalline hydrates, are less stable at positive temperatures.

Thus, the specific behavior of Portland cements at low temperatures in presence of considerable amounts of calcium chloride in the hardening pastes is primarily determined by the alite component of the clinker – tricalcium silicate. Here our findings are not in agreement with the recently-published data of Serb-Serbina and Savvina [8-10], obtained by another method; according to their results, not tricalcium silicate but tricalcium aluminate reacts most vigorously with $CaCl_2$ at subzero temperatures. According to these authors, the aluminates (C_3A and C_4AF) are the most important components of Portland cement clinker (with regard to the favorable effects of chlorides, especially on the strength and density) [10, 11]. Unfortunately, the experiments described in these papers were often performed under conditions very far from those actually obtaining in hardening concrete; the observed effects took place at water–cement (W/C) ratios between 5 and 100, i.e., with very high excesses of water and chloride relative to the cement, at ratios 10 to 200-fold greater than those actually found in concrete. The results so obtained are hardly applicable under practical conditions without substantial corrections. The graphs [10, 11] plotted by these authors show that at W/C ratios below 15 the difference between the behavior of C_3A with respect to $CaCl_2$ at positive and negative temperatures respectively disappeared, and the amount of bound $CaCl_2$ fell sharply. It seems that with further increase of the W/C ratio the role of C_3A in the action of $CaCl_2$ on clinker diminishes still further and, as our experiments showed, tricalcium silicate begins to play the more important role.

SUMMARY

1. In the hardening of cements made from Portland cement clinker in presence of considerable amounts of $CaCl_2$ (up to 10-11% on the cement weight), at water – cement ratios of about 0.5, the normal course and the chemistry of cement hydration change sharply at subzero temperatures; with decrease of temperature below 0°C the processes are intensified rather than being suppressed as is normally the case.

2. This change is the consequence of predominant interaction of tricalcium silicate with $CaCl_2$ under these conditions, with formation of highly-hydrated complex calcium chlorosilicates. These substances are less stable at positive temperatures, and therefore the strength and density of such concrete may change in an undesirable direction when the temperature is raised above zero.

3. Similar substances are not formed at subzero temperatures when considerable amounts of sodium chloride are added to the hardening cement.

4. Interaction of calcium aluminates with $CaCl_2$ under these conditions has less influence on the course of hydration of Portland cement.

LITERATURE CITED

[1] V. V. Nekrasov, Bull. Acad. Sci. USSR, Div. Chem. Sci. 6, 592 (1945).

[2] V. V. Nekrasov, J. Appl. Chem. 21, 3, 204 (1948).

[3] V. V. Nekrasov, J. Appl. Chem. 21, 3, 212 (1948).

[4] A. M. Kuznetsov and G. A. Starkov, Bull. Natural Sci. Inst. Molotov Univ. 13, 487 (1952).

[5] Iu. M. Butt and E. M. Kolobov, J. Appl. Chem. 29, 3, 468 (1956).*

[6] V. V. Nekrasov and A. V. Evko, J. Appl. Chem. 22, 2, 179 (1947).

[7] V. V. Nekrasov and A. V. Evko, Hydrotech. Constr. 9, 14 (1948).

[8] Iu. A. Savvina and N. N. Serb-Serbina, Bldg. Industry 9, 6 (1954).

[9] N. N. Serb-Serbina and Iu. A. Savvina, Cement 2, 3 (1955).

[10] Iu. A. Savvina and N. N. Serb-Serbina, Bldg. Industry 9, 31 (1956).

[11] N. N. Serb-Serbina, Iu. A. Savvina, and V. S. Zhurkina, Proc. Acad. Sci. USSR 111, 659 (1956).*

Received June 13, 1957

*Original Russian pagination. See C. B. Translation.

EXTRACTION OF VALUABLE COMPONENTS FROM FLOTATION PYRITE BY SULFATING ROASTING

V. V. Pechkovskii, S. A. Amirova, and V. V. Parkacheva

The A. M. Gor'kii State University, Perm'

Flotation pyrite has the following average composition (%): sulfur, 40-46; iron, 39-42; copper, cobalt, nickel, zinc, and manganese 1.5-2.5; gangue 10-12. The first stage in the conversion of such pyrite is usually oxidative roasting with formation of sulfur dioxide for sulfuric acid production [1]. The subsequent utilization of the pyrite cinders as a source of iron is possible only after extraction of nonferrous metals, especially copper and zinc. Thus, an important stage in the multiple conversion of flotation pyrite is extraction of valuable components, namely copper, cobalt, nickel, zinc, manganese, and certain other metals, from pyrite cinders. The method most widely used for the extraction of nonferrous metals from pyrite cinders is chlorinating roasting, which has been studied fairly extensively [2].

Sulfating roasting is no less promising as a method of multiple treatment of pyrite cinders. Among the great advantages of sulfating roasting is its high selectivity. Smirnov and Iablonskii [3] reported that sulfating roasting and leaching of flotation pyrite containing iron, copper, and cobalt in the proportions of 100:1:1 yielded a solution in which these metals were present in roughly equal amounts. In short, a relatively simple operation results in approximately a 30-fold increase of the relative concentrations of copper and cobalt in the solution as compared with the ore. Therefore sulfating roasting gives much better results than reverberatory smelting in this respect. The high selectivity of sulfating roasting is the consequence of differences in the thermal stability of the sulfates formed in the process.

It is believed [3-5] that sulfate formation in oxidative and sulfating roasting of sulfide ores may occur both by direct oxidation of sulfides and by sulfation of metal oxides by sulfur dioxide.

It must be pointed out, however, that many aspects of the nature of sulfate formation have been studied relatively little.

The purpose of the present investigation was to study the optimum conditions for the extraction of valuable components from flotation pyrite by means of sulfating roasting. The material chosen for the study was flotation pyrite of the following composition: Fe 37.1%, S 40.0%, Cu 0.7%, Co 0.8%, Ni 0.2%, Zn 0.7%, CaO 2.1%, MgO 2.0%, Al_2O_3 5.3%, SiO_2 8.8%.

The influence of various factors on the conditions for the formation of the sulfates of copper, cobalt nickel, and iron was studied. The flotation pyrite of the above composition was subjected to oxidative roasting at various temperatures. The cinders were then sulfated by mixtures of sulfur dioxide and air, and the degree of sulfation of the different components was studied in relation to the temperature, duration of the experiment, concentration of sulfur dioxide in the gas, and the conditions used in the formation of the pyrite cinders. The experimental procedure was as follows.

The oxidative roasting of the flotation pyrite of the above composition was carried out by a procedure approximating to hearth conditions. A weighed sample of about 50 g of the pyrite was spread in an even layer over a ceramic plate and roasted in a muffle furnace at a fixed temperature in a stream of air. The temperature was measured by means of a thermocouple, the hot joint of which, contained in a quartz socket, was immersed directly in the pyrite. The roasting was continued to a total sulfur content not exceeding 2.0%. In ad-

TABLE 1

Variation of the Degree of Sulfation of Cobalt with Roasting Conditions and Temperature in Addition Sulfation SO_2 concentration 10%, sulfation time 15 minutes

Cinders No.	Pyrite roasting temperature (°C)	Degree of conversion of Co into the water-soluble form (%)	Sulfur content of cinders (%)	Degree of sulfation of cobalt (%) after additional sulfation of the cinders at (°C)							
				450	500	550	600	650	700	800	850
1	550	77.0	2.2	77.0	–	77.0	77.5	77.8	79.2	81.4	43.3
2	600	89.5	2.1	89.5	89.5	–	89.5	–	85.7	87.5	61.5
3	700	82.0	1.5	82.0	82.1	82.8	84.0	84.1	84.3	85.6	54.4
4	700	51.0	8.2	61.3	64.5	67.5	84.0	73.8	78.7	81.6	33.0
5	800	35.3	1.2	39.9	48.2	57.7	66.8	79.2	84.0	86.5	66.2
6	900	6.0	0.2	25.6	33.2	41.1	47.7	63.3	80.0	81.0	23.2
7	900	1.1	4.1	33.0	38.0	–	49.0	–	63.4	88.3	12.8
8	Plant (made in hearth furnace)	63.5	1.3	64.2	64.4	65.3	67.7	69.2	71.6	82.2	54.4

dition, cinders with higher sulfur contents were specially prepared. Sieve analysis of the cinders showed that they consisted mainly of particles smaller than 0.15-0.08 mm. The cinders formed by oxidative roasting were then subjected to additional sulfation. For this, a weighed sample of 2 g of the pyrite cinders was placed in a laboratory tubular furnace and heated at a definite temperature in a stream of gas consisting of air and sulfur dioxide. Previously calibrated flow meters were used to produce gas mixtures containing 2.5, 5.0, 7.5, and 10.0% of sulfur dioxide respectively. Water-soluble sulfates were determined in the cinders made by oxidative roasting of pyrite, and in the cinders subjected to additional sulfation. The cinders were leached with hot water, and iron, copper, cobalt, and nickel were determined in the filtrate. Cobalt in the aqueous extract was determined gravimetrically; by weighing as potassium cobaltinitrite, formed by double reprecipitation [6, 7]. The amount of water-soluble cobalt, as a percentage of the total cobalt in the sample taken for analysis, was termed the degree of conversion of cobalt into the water-soluble form, or its degree of sulfation.

The effect of temperature on the degree of conversion of cobalt into the water-soluble form in the oxidative roasting of flotation pyrite is illustrated by the data below.

Roasting temperature (°C)	400	500	550	600	650	700	800	900
Degree of conversion of cobalt into the water-soluble form (%)	24.4	59.8	77.0	89.5	88.2	82.0	35.3	6.0

The final content of total sulfur in the cinders was 1.2-2.2%.

It follows from the above data that the maximum conversion of cobalt into the water-soluble form, as a function of temperature, occurs at about 600°. The explanation of this maximum is that cobalt sulfate decomposes rapidly at temperatures above 600° in presence of sulfide sulfur [7]. This accounts for the necessity of keeping the temperature at a strictly definite level in purely sulfating roasting [3, 8]. Thus, when pyrite is roasted in constant presence of sulfide sulfur in the charge, fairly complete extraction of cobalt into solution can be effected only if the temperature does not exceed 600°.

Data on additional sulfation of cinders obtained by oxidative roasting of flotation pyrite under different conditions are presented in Table 1-3. These results show that the content of water-soluble cobalt in the cinders may be increased by treatment of the cinders with mixtures of sulfur dioxide and air under definite conditions. For example, when cinders made by roasting in a mechanical hearth furnace were subjected to additional sulfation with a gas containing 5% sulfur dioxide at 700° under laboratory conditions, the amount of cobalt converted into the water-soluble form was increased from 63.5 to 89.4%.

TABLE 2

Variation of the Degree of Sulfation of Cobalt with Temperature and Sulfur Dioxide Concentration of the Gas. Duration of experiment 15 minutes

SO_2 concentration (%)	Degree of sulfation of cobalt (%) after additional sulfation of cinders Nos. 5 and 8 at (°C)							
	500		600		700		800	
	5	8	5	8	5	8	5	8
10.0	48.2	64.4	57.7	67.7	84.0	71.6	86.5	82.2
7.5	45.6	71.5	62.0	72.4	86.6	85.8	92.5	89.4
5.0	40.4	67.1	71.0	81.5	80.0	89.4	82.0	88.0
2.5	38.2	63.5	52.0	71.0	77.6	72.4	27.3	38.0

It was found that the rate and extent of the additional sulfation of cobalt depend on various factors, including the temperature, sulfur content of the original cinders, sulfation time, concentration of sulfur dioxide in the gas, and conditions used for the oxidative roasting.

Preliminary analyses showed that virtually no additional sulfation of cobalt takes place in the cinders studied, at temperatures below 400°. It must also be pointed out that cinders in which the initial degree of sulfation of cobalt is high (about 87-89%) do not undergo any appreciable further sulfation.

It follows from Table 1 that sulfation of cobalt in cinders containing not more than 4.0% total sulfur is detected at temperatures above 400°, proceeds at an appreciable rate at 600-650°, and reaches a maximum at 700-750°. When the temperature is raised above 800°, the degree of sulfation of the cobalt decreases, because under these conditions, even in absence of sulfide sulfur, cobalt sulfate decomposes at an appreciable rate.

If the original cinders contain more than 4-5% sulfide sulfur, the situation is somewhat different. Table 1 shows that in this case the degree of sulfation has two maxima, one at 600° and the other at 800°.

In the sulfation of cinders No.7, with a lower sulfur content (6.1%), the degree of sulfation of cobalt as a function of temperature has only one maximum, at 800°. These results suggest that if the sulfide sulfur has not been burned out of the cinders, the degree of sulfation of cobalt decreases at temperatures above 600°.

Further examination of the results in Tables 1-3 shows that by means of additional sulfation it is possible to attain high degrees of sulfation of cobalt in cinders made by oxidative roasting both at low and at high temperatures. Therefore, a high temperature in the oxidative roasting of pyrite does not prevent subsequent very complete sulfation of cobalt in the cinders. It is true that cinders made by oxidative roasting at different temperatures show distinctive differences in sulfation. It should be noted that the sulfation of cobalt in cinders made by oxidative roasting of pyrite in the 600-800° range proceeds fairly easily. The sulfation of cobalt in cinders made by the roasting of pyrite at 550 and 900° is somewhat more difficult. It is known [3, 7] that cobalt is a constituent of pyrite, mainly in the form of an isomorphous mixture with iron, of the $(Co,Fe)S_2$ type. It is probable that this compound is broken down rapidly at temperatures above 550°, and therefore cobalt in cinders made by roasting at 550° and lower is sulfated with somewhat more difficulty. With regard to cinders made by roasting at temperatures of 900° and over, the sulfation of cobalt in such cinders is more difficult because of their partial sintering during the oxidative roasting.

Cinders No.5 (oxidative roasting temperature 800°) and No.8 (works cinders made by sulfating roasting) were used for studies of the effect of sulfur dioxide concentration on the degree of sulfation of cobalt. The results are given in Table 2. It is seen that cobalt in the cinders is effectively sulfated by gas mixtures containing 5-10% SO_2. If the sulfur dioxide concentration of the gas is below 5%, the degree of sulfation of cobalt is somewhat lower. Moreover, if a gas containing 2.5% SO_2 or less is used, the maximum of sulfate formation is shifted toward lower temperatures. This is because the decomposition rate of cobalt sulfate increases with decrease of the sulfur dioxide concentration in the gas phase. Increase of the sulfur dioxide concentration above 7.5% also causes some decrease in the degree of sulfation of cobalt. This is because increase of the

TABLE 3

Effect of the Time of Additional Sulfation of Cinders on the Degree of Sulfation of Cobalt. SO_2 concentration 10%

Cinders No.	Temperature (°C)	Degree of sulfation of cobalt (%) after time (minutes)				
		5	15	30	45	60
5	600	45.7	66.8	75.0	75.2	75.6
	800	62.2	86.5	85.0	84.6	84.0
6	600	30.0	47.7	49.7	51.1	52.0
	800	56.2	81.0	79.5	80.0	81.4
8	600	—	67.7	71.6	72.3	73.6
	800	—	82.2	86.6	89.9	92.2

sulfur dioxide concentration in the gas phase is accompanied by a corresponding decrease of the oxygen concentration. Thus, under laboratory conditions the optimum concentration of SO_2 in the gas phase for additional sulfation of cobalt in cinders made by oxidative roasting of pyrite is about 7.5%.

The effect of time on the degree of sulfation of cobalt in cinders is shown by the data in Table 3. It follows from these results that under certain conditions the sulfation of cobalt proceeds at a fairly high rate. Intensive sulfation occurs during the first 5-15 minutes, after which the process is very slow or virtually stops. This is caused by the formation of a dense coating of cobalt sulfate on the cobalt oxide grains. In some instances (at high degrees of sulfation and high temperatures) there is even some decrease in the degree of sulfation of cobalt with time. Analyses showed that in the oxidative roasting of pyrite and in additional sulfation of the cinders, copper, manganese, nickel, iron, and certain other metals which form water-soluble sulfates, pass into solution together with cobalt. It was found that copper is sulfated to approximately the same extent as cobalt. The maximum conversion of nickel into a water-soluble form was 50-60%. The degree of sulfation of iron also depended strongly on the temperature. The maximum conversion of iron into a water-soluble form during additional sulfation occurred at 600°, and was 2-3%. At temperatures above 700° the amount of iron passing into a water-soluble form fell sharply, and at 750° the cinders contained virtually no soluble iron.

This investigation shows that under certain conditions sulfating roasting can be used for conversion of flotation pyrites with very complete utilization of the sulfur, iron, and nonferrous metals.

It is seen that either ordinary sulfating roasting, or oxidative—sulfating roasting may be carried out, according to the equipment used for the process.

Ordinary sulfating roasting is carried out in such a way that the stages of sulfide oxidation and sulfate formation take place simultaneously or almost simultaneously. This demands strict control of the temperature at which this type of roasting is carried out. It has been shown that in the sulfation of copper and cobalt the temperature of ordinary sulfating roasting must not exceed 600°. However, the relatively low roasting temperature results in a decrease of the process rate. Accordingly, furnaces used for sulfating roasting usually operate at rates 2.0-2.5 times lower than corresponding furnaces for oxidative roasting [3, 8]. This serious disadvantage of ordinary sulfating roasting can be avoided by the use of oxidative—sulfating roasting. For this, the equipment must be designed so that the pyrite is first subjected to ordinary intensive oxidative roasting, and the hot cinders (at 700-750°) are then subjected to the action of furnace gases containing 5-8% of sulfur dioxide.

LITERATURE CITED

[1] K. M. Malin, Sulfuric Acid Technology [In Russian] (Goskhimizdat, 1950).

[2] M. E. Pozin, Technology of Mineral Salts [In Russian] (Goskhimizdat, 1949).

[3] V. I. Smirnov and Iu. A. Iablonskii, Bull. Central Inst. Information 1, 6 (Metallurgy Press, 1954).

[4] V. I. Smirnov, Hydrometallurgy of Copper [In Russian] (Metallurgy Press, 1954).

[5] M. E. Pozin, A. M. Ginstling, and V. V. Pechkovskii, J. Appl. Chem. 27, 12, 1237 (1954). •

[6] P. V. Faleev, Factory Labs. 8, 381 (1939).

[7] R. M. Perel'man, A. Ia. Zvorykin, and N. V. Gudima, Cobalt [In Russian] (Izd. AN SSSR, 1949).

[8] G. Ia. Leizerovich, Roasting in a Fluidized Bed [In Russian] (Metallurgy Press, 1956).

Received February 11, 1957

• Original Russian pagination. See C. B. Translation.

INVESTIGATION OF THE RATE OF ABSORPTION OF HYDROGEN SULFIDE BY ARSENICAL SODA LIQUORS

V. V. Ipat'ev, V. I. Tekhomirov, and N. F. Soboleva

Leningrad Scientific Research Institute of Petroleum Processing and Synthetic Liquid Fuel Production

Despite the fact that the arsenical soda process for removal of hydrogen sulfide from gases is now widely used in industry both in the USSR and abroad, there have been very few studies of the kinetics of absorption of hydrogen sulfide by arsenical soda liquors, or of a number of other important problems in the technology of the arsenical soda process.

Calculations relating to the design of industrial absorption units are based on very scanty and inadequately verified kinetic data. It is assumed in the calculation formulas, without adequate justification, that the driving force in the absorption of hydrogen sulfide by arsenical soda liquors is the concentration difference of hydrogen sulfide at the boundary of the diffusion gas film.

The theoretical and experimental investigations of Pozin [1] have shown that in many cases of chemisorption the concentration difference of the absorbed component in the gas phase cannot be regarded as the driving force of absorption; Pozin showed that the rates of a number of chemisorption processes are independent of the composition of the gaseous medium. In many cases the concentration of the absorbent in solution must be taken into account, as well as the concentration of the absorbed component in the gas phase. This suggests that the driving force of absorption of hydrogen sulfide by arsenical soda liquor (this is abbreviated to a.s. liquor in this paper) is likewise not represented merely by the concentration gradient of hydrogen sulfide in the diffusion gas film.

It is most necessary to understand the absorption process and to have reliable experimental data, both for intelligent design of new plants, and for rational utilization of existing units. Accordingly, a study was made of the rate of absorption of hydrogen sulfide in a.s. liquors under laboratory conditions in a wetted-wall absorber which is shown schematically in Fig. 1.

The liquor passed through the tube 1 into the space between tubes 2 and 3, and then through the slit 4, to wet the inner walls of the vertical absorption tube 5. The tube 6 was open to the air, and served to equalize the pressure in the space between tubes 2 and 3. From the absorption tube the liquor entered the space between tubes 5 and 7, and left the apparatus through the outlet 8. Tube 9, like tube 6, served to equalize the pressure to the atmospheric pressure. Thus the lower end of the absorption tube also acted as a liquid seal which separated the space of the absorption tube from the atmosphere. The gas entered the absorption tube from below through the inlet 10, passed upward through the tube 5, the inner walls of which were wetted with the liquor, and passed out through the dry tube 3. All the above-named parts of the apparatus were enclosed in a glass jacket 11, filled with water, which acted as a thermostat. The water was warmed by an electric heater (not shown in the diagram). Air was fed into the jacket through the tube 12, to agitate the water and maintain the temperature constant along the jacket. The gas mixtures were made from hydrogen sulfide made in a Kipp's apparatus, and technical hydrogen.

The internal diameter of the absorption tube was 0.7 cm, and the wetted portion was 60 cm long. The wetted area was therefore 132 cm^2. The wetted perimeter was 2.2 cm.

The effects of hydrogen sulfide concentration in the gas, temperature, and composition of the liquor on the absorption rate were studied.

TABLE 1

Effect of Hydrogen Sulfide Concentration in the Gas on the Absorption Rate

H_2S content of gas (%)		Feed rate (liters/hour)		Absorption rate ($g \cdot m^{-2} \cdot hour^{-1}$)	
at entry	at exit	gas	liquid		
2.57	2.33	60	0.89	15.6	
2.00	1.72	60	0.82	18.0	
1.31	1.05	62	0.97	17.3	Mean 16.7
1.07	0.83	60	0.91	15.6	
0.91	0.63	60	0.84	18.1	
0.39	0.17	66	0.96	15.7	
2.52	1.97	60	1.45	35.7	
2.41	1.90	60	1.45	33.2	Mean 34.2
1.76	1.32	60	1.56	28.6	
1.12	0.47	60	1.20	42.2	
0.89	0.41	60	1.20	31.2	
0.59	0.32	60	1.50	17.5	
0.27	0	60	1.62	17.5	

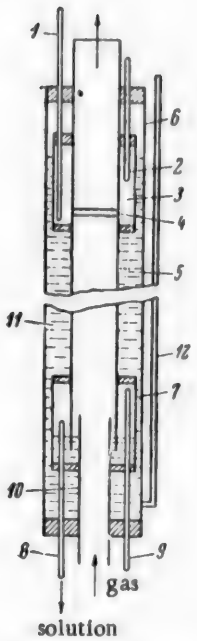

Fig. 1. Wetted-wall absorber.

The results of experiments on the effect of hydrogen sulfide concentration in the gas on the absorption rate are given in Table 1.

The gas feed rate was about 60 liters/hour, which corresponds to a linear gas velocity of 0.46 m/second. The liquid feed rate in the first series of experiments was maintained at about 0.8-0.9 liter/hour, and in the second, at about 1.4-1.5 liters/hour; the temperature was maintained at 40° in all cases. The composition of the a.s. liquor was the same in all the experiments: 10.1 g of As_2O_3 and 12.3 g of Na_2CO_3 per liter. The liquor was regenerated before each experiment to pH = 8.1.

It follows from the data in Table 1 that the rate of absorption of hydrogen sulfide by a.s. liquor remains almost constant over the range of hydrogen sulfide concentrations in the gas studied. Comparison of the two series of experiments shows that the absorption rate increases from 16.9 to 31.3 $g \cdot m^{-2} \cdot hour^{-1}$ (i.e., is doubled) with increase of the liquor rate from 0.9 to 1.4 liters/hour (1.56-fold).

The effect of temperature on the rate of absorption of hydrogen sulfide by a.s. liquor was studied in a series of experiments the results of which are given in Table 2. In this series of experiments the gas rate was constant at about 60 liters/hour. The composition of the solution was as before.

The results in Table 2 show that temperature has no noticeable influence between 17 and 53°. The fact that temperature has no appreciable influence on the absorption rate shows that the temperature coefficient of the process which determines the rate of the whole process is not large.

Table 3 contains the results of experiments carried out at constant solution pH, but with different arsenic contents in the a.s. liquor. The gas composition, gas and liquor rates, and temperature (40°) were kept constant. Solutions with different arsenic contents were made by the mixing, in various proportions, of a.s. liquor of pH 8.2, with 8% sodium bicarbonate solution of pH 8.3; the pH of the mixture was always between 8.2 and 8.3.

The results show that the rate of absorption of hydrogen sulfide by a.s. liquor at constant pH is virtually independent of the arsenic concentration. A series of experiments was then carried out with solutions of different degrees of saturation with hydrogen sulfide, and therefore of different pH. These solutions were prepared by the mixing, in different proportions, of a liquor saturated with the gas, containing 1.03% H_2S, with a completely regenerated liquor. The results of these experiments are given in Table 4 and Fig. 2. These results

TABLE 2

Effect of Temperature on the Absorption Rate of Hydrogen Sulfide

Temperature (°C)	Liquor rate (liters/hour)	H_2S content of gas (%)		Absorption rate ($g \cdot m^{-2} \cdot hour^{-1}$)
		at entry	at exit	
17	1.30	0.64	0.23	22.0
		0.68	0.35	
		0.58	0.33	
		0.64	0.31	
17	1.55	0.54	0.18	25.2
		0.67	0.22	
		0.42	0.12	
		0.34	0.08	
40	1.20—1.59	1.12	0.47	25.2
		0.86	0.54	
		0.89	0.54	
		0.55	0.22	
		0.59	0.32	
		0.34	0.02	
53	1.40	0.60	0.18	24.7
		0.59	0.25	
		0.65	0.25	
		0.63	0.27	

TABLE 3

Effect of the Arsenic Content of A.S. Liquor on the Absorption Rate of Hydrogen Sulfide at Constant pH of the Liquor

Content of a.s. liquor (ml per 100 ml of mixture)	As_2O_3 content (g/liter)	Feed rate (liters/hour)		H_2S content of gas (%)		Absorption rate ($g \cdot m^{-2} \cdot hour^{-1}$)
		gas	liquor	at entry	at exit	
0	0	64	0.88	0.91	0.71	13.6
0	0	63	0.84	0.92	0.66	17.5
33	3.4	62	0.87	0.68	0.47	13.9
33	3.4	62	0.92	0.92	0.68	15.8
100	10.2	63	0.86	1.00	0.81	12.8

show that the rate of absorption of hydrogen sulfide by a.s. liquor decreases as the liquor becomes spent (with increasing saturation with hydrogen sulfide), and the solution pH decreases with it.

Experiments were then carried out on the rate of absorption of hydrogen sulfide by a.s. liquor containing added buffer solutions, and by alkali solutions. In this way both the arsenic content and the pH of the solutions could be varied widely.

The results of this series of experiments are given in Table 5; they show that the rate of absorption of hydrogen sulfide is mainly determined by the solution pH.

Comparison of the first three experiments shows that replacement of a.s. liquor by a buffer mixture of the same pH has almost no effect on the rate of absorption of hydrogen sulfide. However, an artificial increase of the solution pH by addition of small amounts of NaOH results in a sharp increase of the absorption rate, as is seen

TABLE 4

Effect of Rate of Absorption of H_2S on the Degree of Saturation of the Solution with H_2S

Contents of regenerated liquor (ml per 100 ml of mixture)	pH	Feed rate (liters/hour)		Temperature (°C)	H_2S content of gas (%)		Absorption rate ($g \cdot m^{-2} \cdot hour^{-1}$)	
		gas	liquor		at entry	at exit		
100	8.3	60	1.52	37	1.17	0.85	20.8	mean 27.1
					1.11	0.70	26.6	
					1.12	0.64	31.2	
					1.15	0.69	29.8	
67	7.8	60	1.40	45	1.26	0.90	23.4	mean 17.8
					1.27	1.13	9.1	
					1.11	0.90	13.6	
					1.12	0.91	13.6	
					1.13	0.83	19.5	
33	7.5	60	1.30	45	1.06	0.89	11.0	mean 10.4
					1.06	0.87	12.3	
					1.01	0.89	7.8	
0	7.1	60	1.30	20	0.03	1.03	0	

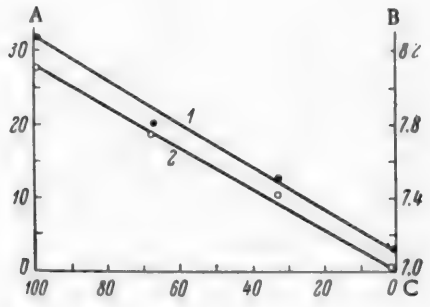

Fig. 2. Effect of the degree of regeneration on the rate of absorption of hydrogen sulfide.
A) Absorption rate ($g \cdot m^{-2} \cdot hour^{-1}$), B) pH, C) degree of regeneration (%). Curves: 1) variation of solution pH, 2) variation of absorption rate.

from a comparison of Experiments 4 and 5. A still greater increase is seen in Experiment 6 and 7, in which the absorption solutions contained no arsenic at all, but had high pH values. Comparison of Experiments 8 and 9 with Experiments 10 and 11 illustrates the influence of solution pH on the rate of hydrogen sulfide absorption at constant arsenic content.

The absorption of hydrogen sulfide by a.s. liquor comprises the following consecutive processes.

1. Diffusion of hydrogen sulfide to the liquor surface through the gas diffusion layer.

2. Dissolution of hydrogen sulfide in the liquor.

3. Reaction of the dissolved hydrogen sulfide with OH' ions according to the equation

$$H_2S + OH' = H_2O + HS' \quad (1)$$

and in part according to the equation

$$H_2S + 2OH' = 2H_2O + S''. \quad (2)$$

4. Diffusion of OH' ions through the liquid diffusion layer to the gas–liquid boundary, and diffusion of the reaction products (HS' and S'') in the opposite direction.

5. Reaction of HS' and S'' ions with oxythioarsenate ions:

$$HS' + AsS_3O''' = AsS_4''' + OH', \quad (3)$$

$$S'' + AsS_3O''' + H_2O = AsS_4''' + 2OH'. \quad (4)$$

The last two reactions may take place either in the liquid diffusion layer or in the bulk of the liquid stream.

Reactions (1) and (2) lower the solution pH. Reactions (3) and (4) raise the pH again. However, Reactions (3) and (4) cannot restore the pH to its original value; this is seen if Equations (1) and (3) and Equations (2) and (4), respectively, are added together. It is known that the pH of a.s. liquor falls as the result of absorption of hydrogen sulfide. The explanation is that the degree of dissociation of thioarsenic acid is higher than the degree of dissociation of oxythioarsenic acid.

The role of pH in determining the absorption rate of hydrogen sulfide by a.s. liquor may be explained on the assumption that the slowest step, which determines the absorption rate as a whole, is Process 4, diffusion of OH', HS', and S'' ions through the liquid diffusion layer. The first three processes are rapid, and this explains why the absorption rate of hydrogen sulfide is independent of the hydrogen sulfide concentration in the gas (Table 1). Reactions (3) and (4) are much slower than Reactions (1)and (2), and occur mainly in the bulk of the liquor. Reactions (3) and (4) do not occur, to any practical extent, in the liquid diffusion layer, as the HS' and S'' ions are able to diffuse into the bulk of the stream. As a result, the OH' ion concentration at the gas boundary drops sharply, and a virtually constant gradient of OH' ion concentration is established across the liquid diffusion layer. The thickness of this layer, in its turn, depends on the velocity and turbulence of the liquid stream.

TABLE 5

Variation of the Rate of Absorption of Hydrogen Sulfide with the Solution pH for A.S. Liquor and Certain Other Alkaline Solutions

Expt. No.	Solution	As_2O_3 (g/liter)	pH at entry	H_2S content at entry (%)	Absorption ($g/m^2 \cdot hour$)
1	A. s. without buffer mixtures	7.0	7.8	1.83	13.2
2	Buffer ($KH_2PO_4 + NaOH$)	0	7.8	1.61	12.0
3	The same	0	7.8	1.95	10.0
4	A. s. without buffer mixtures	10.3	8.0	1.83	12.9
5	500 ml of a. s. + 0.5 ml of 1 N NaOH	10.3	9.8	2.12	48.5
6	1 N NaOH	0	(14)*	1.68	6 .0
7	1 N Na_2CO_3	0	13.5	1.93	62.5
8	800 ml a.s. + 200 ml of buffer solution of pH = 6.6	8	7.3	2.9	11.0
9	The same	8	7.3	2.2	10.1
10	800 ml of a.s. + 200 ml of buffer solution of pH = 11 (borax + NaOH)	8	8.15	2.6	12.7
11	The same	8	8.15	2.3	13.0

* Calculated value in parentheses.

Because of this, the rates of hydrogen sulfide absorption do not differ significantly in Experiments 1-4 (Table 5). The sharp increase of OH' ion concentration in solution produced by addition of bases, whether arsenic compounds are present in the solution (Experiment 5) or not (Experiments 6 and 7), raises the absorption rate sharply.

The presence of oxythioarsenates in the liquor determines its capacity. In absence of these compounds, the solution would be exhausted much more rapidly, as absorption of small amounts of hydrogen sulfide would lower the solution pH and the absorption rate. The presence of oxythioarsenates acts as a kind of buffer by retarding the decrease of solution pH

SUMMARY

1. It was shown experimentally that the rate of absorption of hydrogen sulfide by a.s. liquor varies with the degree of regeneration of the liquor. The liquor pH changes symbatically with it. The rate of absorption of

hydrogen sulfide by a.s. liquors, NaOH, Na_2CO_3, and buffer solutions depends mainly on the solution pH.

2. The rate of absorption of hydrogen sulfide by a.s. liquors is almost independent of the hydrogen sulfide concentration in the gas and the concentration of sodium oxythioarsenate in solution if the solution pH remains constant. Increase of temperature from 17 to 53° has little practical effect on the rate of absorption of hydrogen sulfide by a.s. liquors.

3. The view is put forward that the rate of absorption of hydrogen sulfide by a.s. liquors is determined mainly by the rate of diffusion of the ions involved in neutralization of hydrogen sulfide through the liquid diffusion film. Thioarsenic acid is formed relatively slowly and mainly in the bulk of the liquid stream; it determines the capacity of the solution and thereby exerts only an indirect influence on the rate of absorption of hydrogen sulfide.

LITERATURE CITED

[1] M. E. Pozin, J. Appl. Chem. 19, 10-11, 1201 (1946); 19, 12, 1319 (1946); 20, 4, 345 (1947).

Received November 25, 1956

INVESTIGATION OF THE RATE OF ABSORPTION OF HYDROGEN SULFIDE BY ARSENICAL SODA LIQUORS*

M. I. Gerber, V. P. Teodorovich and A. D. Shusharina

(Leningrad Scientific Research Institute of Petroleum Processing and Synthetic Liquid Fuel Production)

The results of a study of the absorption rate of hydrogen sulfide by arsenical soda liquors in a wetted-wall absorber are presented in the preceding paper [1]. However, in that investigation, the rate characteristics could be determined only at the initial stage of the absorption process, i. e., at the stage in which the free alkali of the solution is neutralized. Further interaction of HS' ions with sodium oxythioarsenate was not investigated.

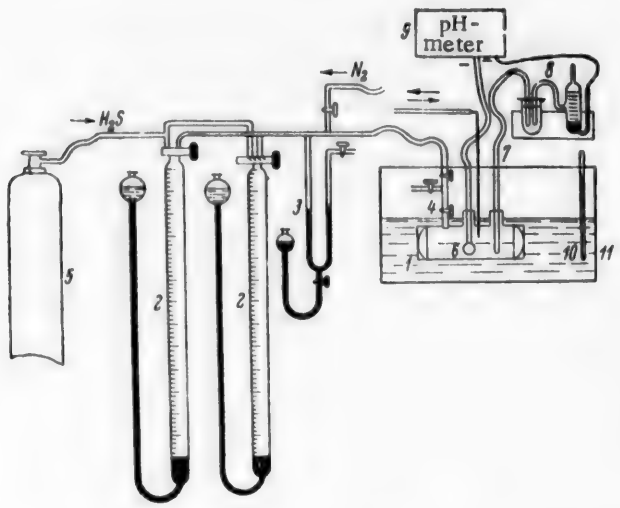

Fig. 1. Apparatus for investigation of the rate of absorption of hydrogen sulfide by sodium arsenate solution.
1) Reaction vessel, 2) gas buret, 3) manometer, 4) stopcock of reaction vessel, 5) cylinder with hydrogen sulfide, 6) glass electrode, 7) electrolytic bridge, 8) saturated calomel electrode, 9) pH meter, 10) thermometer, 11) thermostat.

For a fuller investigation of the absorption process, a method was used in which gas, with a constant partial pressure of hydrogen sulfide, was brought into contact with the absorbent and the absorption process could go to completion.

A diagram of the apparatus used is shown in Fig. 1.

* This work was carried out under the guidance of V. V. Ipat'ev.

The vessel 1, through which oxygen-free nitrogen had been blown, contained 100 ml of the liquor, previously heated to the required temperature. The bulb of one of the burets 2 was then lowered in order to reduce the pressure, measured by means of the manometer 3, in the reaction vessel. The stopcock 4 was then shut, hydrogen sulfide from the cylinder 5 was blown through the connecting tubes between the stopcock and the burets, and the burets were then filled with it. The stopcock 4 was then opened and the pressure in the reaction vessel was brought to atmospheric. The motor which rocked the reaction vessel was then switched on, and the time of start of the experiment was recorded. The rocking rate was 80 per minute. During the experiment, the pressure in the vessel, measured by means of the manometer 3, was kept equal to atmospheric by means of the leveling bulb of the buret 2. Thus, the partial pressure of hydrogen sulfide in the gas phase over the solution remained constant during absorption. The amount of absorbed hydrogen sulfide was found from the change of the gas volume in the buret.

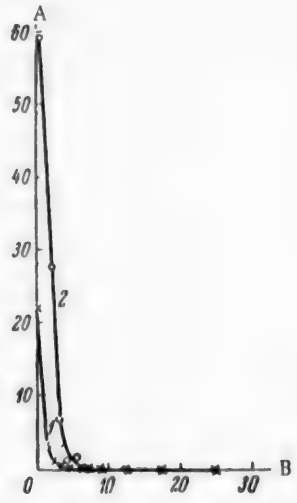

Fig. 2. Variation of the rate of absorption of hydrogen sulfide in water and alkali with time, at 40°.
A) Absorption rate (ml H_2S/min), B) time (minutes).
Curves: 1) H_2O, 2) 0.05 M NaOH.

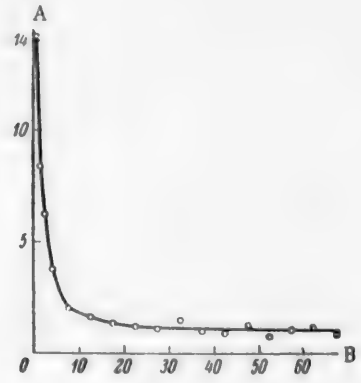

Fig. 3. Variation of the rate of absorption of hydrogen sulfide in 0.5 M $Na_2HAsS_2O_2$ with time, at 40°.
A) Absorption rate (ml H_2S/min),
B) time (minutes).

The solution pH was measured during the experiment. For this, the reaction vessel contained, immersed in the solution, a glass electrode 6 and an electrolytic bridge 7, consisting of a flexible rubber tube filled with agar and connected to the saturated calomel electrode 8. The readings of the pH meter 9 were corrected in accordance with the calibration data for the electrode.

The absorbents used were solutions of individual oxyarsenates and oxythioarsenates, the synthesis of which was described previously [2]. The hydrogen sulfide used for absorption was made in a Kipp's apparatus and liquefied in a test tube immersed in solid carbon dioxide. After the condensation, the tube with the liquid hydrogen sulfide was placed in a high-pressure bomb. The first portions of the hydrogen sulfide which evaporated in the bomb were released into the air. Analysis showed that the subsequent portions were 100% hydrogen sulfide.

This method could not be used for determination of the rate of absorption of hydrogen sulfide per unit interfacial area, but it was suitable for qualitative studies of the absorption of hydrogen sulfide by different absorbents.

In order to obtain comparative data, experiments were carried out on the rates of absorption of hydrogen sulfide by water and by solutions of cadmium chloride, caustic soda, sodium phosphate, sodium arsenate and sodium oxythioarsenate.

Curves showing the variations of the absorption rate in water and alkali with time are plotted in Fig. 2.

In all the absorbents studied, with the exception of arsenic compounds, the absorption process was largely

TABLE 1

Effect of Solution pH and Percentage of Hydrogen Sulfide in the Gas on the Rate of Absorption of Hydrogen Sulfide by Na_2HAsO_4 Solution Containing 0.045 g-atom As Per Liter at 40°

Composition solution	H_2S concentration in gas (%)	pH		H_2S absorbed in 3 minutes (ml)	Time (minutes) in which the S/As ratio in solution increased by 0.5
		original solution	after 3 minutes		
Na_2HAsO_4+NaOH	17.2	10.5	6.90	88.7	55
Na_2HAsO_4	17.0	8.5	6.70	55.5	37
$Na_2HAsO_4+H_2SO_4$	16.8	6.9	6.35	40.7	24
Na_2HAsO_4+NaOH	4.25	10.8	7.90	53.5	120
$Na_2HAsO_4+H_2SO_4$	4.25	6.9	6.55	11.3	92
$Na_2HAsO_4+H_2SO_4$	16.8	6.9	6.35	40.7	24
	8.5	6.9	6.45	17.9	74
	4.25	6.9	6.56	11.3	92

TABLE 2

Absorption of Hydrogen Sulfide by $Na_3AsS_2O_2$ Solution Containing 0.05 g-atom As Per Liter at 40°

Composition of solution	H_2S concentration in gas (%)	pH		H_2S absorbed in 3 minutes (ml)	Time (min.) in which the S/As ratio in solution increased by 0.5
		original solution	after 3 minutes		
$Na_3AsS_{1.88}O_{0.19}$	4.1	>11	7.65	133	60
	4.5	>11	7.75	128	45
	5.4	>11	7.80	140	41
$Na_3AsS_{1.88}O_{0.19}+H_2SO_4$	4.65	9.45	7.00	41	34
	5.0	9.70	7.00	52.5	31
	9.7	9.50	7.20	58	30
$Na_3AsS_{1.88}O_{1.88}$	5.7	>11	7.60	113	33
$Na_3AsS_{1.88}O_{1.88}+H_2SO_4$	6.1	7.85 Solution slightly turbid	6.40	58	19

complete within three minutes from the start of the experiment. During this time, the solutions absorbed 80-90% of the total amount of hydrogen sulfide which they could absorb. The experimental results on the absorption of hydrogen sulfide by water and alkali are in good agreement with literature data.

The absorption of hydrogen sulfide by sodium oxythioarsenate takes an entirely different course. Fig. 3 shows the variation of the rate of absorption of hydrogen sulfide in Na_2HAsS_2O with time, at 40°, with 4.35% hydrogen sulfide in the gas phase, the pH of the original solution being 8.2. Comparison of the curves in Figs. 2 and 3 shows that the absorption of hydrogen sulfide by sodium oxythioarsenate differs greatly from the absorption of hydrogen sulfide by the other absorbents studied. In the case of sodium oxythioarsenate, the process is very complex and probably occurs in three stages. The first stage, a diffusion process, consists of physical dissolution of hydrogen sulfide; the second stage is a rapid chemical reaction between hydrogen sulfide and free alkali in the solution with formation of sodium hydrosulfide; the third stage is a slow chemical reaction between sodium hydrosulfide and sodium oxythioarsenate. The first two stages are rapid and are completed in a few minutes, as in the absorption of hydrogen sulfide by water or pure alkali; the third stage is slow and takes hours. The complexity of the process lies in the fact that all these stages proceed simultaneously to some extent, but the

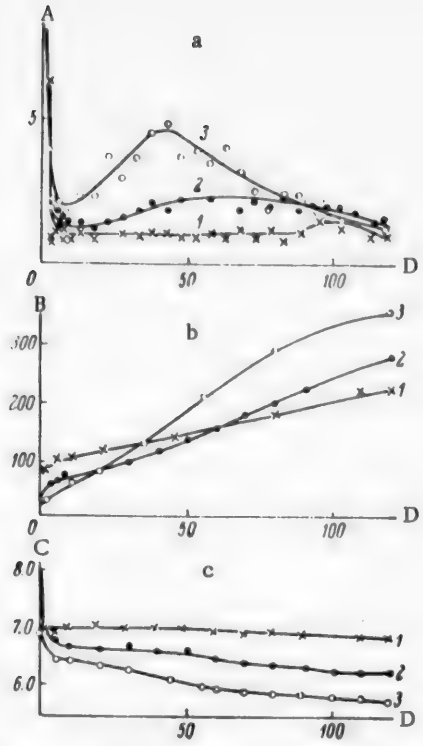

Fig. 4. Absorption of hydrogen sulfide by Na_2HAsO_4 solution at 40°. H_2S concentration, 17%.
a) Variation of the absorption rate of hydrogen sulfide with time, b) integral curves for hydrogen sulfide absorption in the same solutions, c) variation of solution pH with time. A) Absorption rate (ml H_2S/min), B) H_2S content (ml), C) pH, D) time (minutes). pH before experiment: 1)10.5, 2)8.5, 3)6.5.

determining stage is the reaction of sodium hydrosulfide with sodium oxythioarsenate.

For a fuller investigation of the course of absorption of hydrogen sulfide by arsenic compounds, experiments were carried out with Na_2HAsO_4 and $Na_3AsS_2O_2$.

Absorption of H_2S by Na_2HAsO_4 solution. Two series of experiments were carried out with 0.45 M Na_2HAsO_4 solution: in one, the effect of solution pH was studied, and in the other, the effect of the partial pressure of hydrogen sulfide on the rate of replacement of oxygen by sulfur.

The results (Table 1, Fig. 4) show that during the first few minutes after the start of the experiments, most hydrogen sulfide was absorbed by the solution to which alkali had been added. However, subsequently the process was much slower in the solutions to which alkali had been added than in the solutions to which water or acid had been added. The pH of all the solutions fell sharply during the first few minutes, but the subsequent fall was gradual.

Fig. 4 shows curves for the time variations of the absorption rate of hydrogen sulfide, solution pH and total amounts of hydrogen sulfide absorbed. The curves for the absorption rate as a function of time (Fig. 4, a) have maxima, which are most pronounced at low solution pH.

If the sodium arsenate solution is acidified, the addition of 0.5 g-atom of sulfur per 1 g-atom of arsenic requires 24 minutes, instead of the 55 minutes required when alkali had been added to the solution. The same effect was observed at lower partial pressures of hydrogen sulfide (Table 1).

As was to be expected, higher rates of absorption of hydrogen sulfide by sodium arsenate solution corresponded to higher partial pressures of hydrogen sulfide in the gas.

The views advanced above on the course of absorption of hydrogen sulfide as a three-stage process may be developed further as follows, in the light of the experimental results obtained.

The reaction between sodium arsenate and sodium hydrosulfide formed at the second stage of absorption proceeds as follows:

$$Na_2HAsO_4 + NaSH \rightleftarrows Na_2HAsSO_3 + NaOH;$$

$$Na_2HAsSO_3 + NaSH \rightleftarrows Na_2HAsS_2O_2 + NaOH,$$

Sodium hydrosulfide acts as a carrier of sulfur, and its concentration, like the solution pH, largely determines the rate of absorption of hydrogen sulfide at the third stage. The higher the sodium hydrosulfide concentration and the lower the solution pH, the more rapidly is oxygen replaced by sulfur in the sodium oxythioarsenate molecule. The maxima on the kinetic curves for the rate of absorption of hydrogen sulfide as a function of time are caused by the fact that the solution pH falls continuously during absorption.

Absorption of H_2S by $Na_2AsS_2O_2$ solution. It may be assumed that in solutions of high pH (> 11) $Na_3AsS_2O_2$ is hydrolyzed.

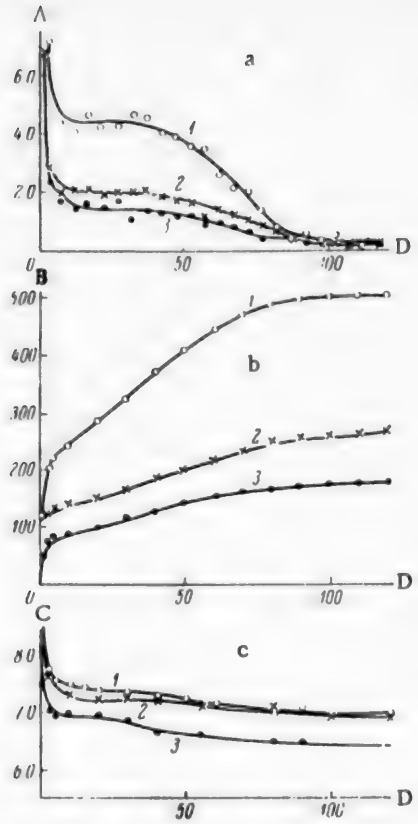

Fig. 5. Absorption of hydrogen sulfide by $Na_3AsS_2O_2$ solution at 40°.
a) Variation of absorption rate with time, b) variation of total amount of hydrogen sulfide absorbed with time, c) variation of pH with time. A) Absorption rate (ml H_2S/min), B) H_2S content (ml), C) pH, D) time (min). Concentration (mole/liter: 1) 0.1, 2) 0.05, 3) 0.025.

$$Na_3AsS_2O_2 + H_2O \rightleftarrows Na_2HAsS_2O_2 + NaOH.$$

Absorbed hydrogen sulfide reacts with NaOH, and the equilibrium shifts to the right. The experimental results (Table 2) show that more than 100 ml of hydrogen sulfide is absorbed during the first 3 minutes. Of this, a few ml is physically dissolved, while the remaining, much larger portion reacts with the free alkali in solution to form NaSH. Replacement of oxygen by sulfur in the $Na_2HAsS_2O_2$ molecule proceeds slowly according to the equation.

$$Na_2HAsS_2O_2 + NaSH \rightleftarrows Na_2HAsS_3O + NaOH.$$

This process is largely complete after 70-80 minutes. There is sometimes a small maximum on the rate–time curve at the start of absorption.

Conversely, if the solution is acidified with sulfuric acid (Table 2), the amount of hydrogen sulfide absorbed during the first three minutes decreases sharply, so that the concentration of SH^- ions falls. However, decrease of the solution pH accelerates the slow reaction of sodium oxythioarsenate formation. Whereas without acidification, 40-60 minutes was needed for replacement of 0.5 g-atom of oxygen, per 1 g-atom of arsenic, by sulfur, if the solution is acidified, 31-34 minutes is sufficient. The above is also confirmed by the last experiment in Table 2, where only 19 minutes was needed for such replacement at pH = 7.85.

It was of interest to study the effect of sodium arsenate concentration in solution on the rate of absorption of hydrogen sulfide. The results, given in Table 3 and Fig. 5, show that the sulfur capacity of the solution increases with the concentration of sodium oxythioarsenate. With a 4-fold increase of the solution concentration, the total amount of hydrogen sulfide absorbed during 2 hours is increased almost 3-fold.

TABLE 3

Absorption of Hydrogen Sulfide by $Na_3AsS_{2.05}O_{1.95}$ Solutions of Different Concentrations at 40°

Solution concentration (mole/liter)	H_2S concentration in gas (%)	pH		H_2S absorbed in 3 minutes (ml)	Time (min) in which the S/As ratio in solution increased by 0.5
		original solution	after 3 minutes		
0.100	6.6	>11	7.7	193	30
0.050	5.7	>11	7.6	113	33
0.025	4.4	>11	7.0	67	22

SUMMARY

1. A new method has been devised for studying absorption rates; the gas can be present at different partial pressures over the absorbent, and the composition of the gas can be kept constant during absorption.

2. In a study of the rate of absorption of hydrogen sulfide by Na_2HAsO_4 and $Na_3AsS_2O_2$ solutions, it was shown that the absorption process takes place in three stages: a) physical solution of hydrogen sulfide; b) rapid chemical reaction between hydrogen sulfide and the alkali present in solution as the result of hydrolysis of sodium arsenate salts; c) the slow chemical reaction in which oxygen is replaced by sulfur in sodium oxythioarsenate.

LITERATURE CITED

[1] V. I. Tikhomirov and N. F. Soboleva, J. Appl. Chem. 31, 10, 1472 (1958). •

[2] N. I. Brodskaia, M. I. Gerber, V. P. Teodorovich and A. D. Shusharina, J. Appl. Chem. 30, 11, 1588 (1957). •

Received November 25, 1958

• Original Russian pagination. See C. B. Translation.

INFLUENCE OF THE SPECIFIC SURFACE OF THE FILLER ON THE OXIDATION OF CHROMITE CHARGES

M. V. Kireeva

The Urals Chemical Scientific Research Institute

The common method for treatment of chromium ores is oxidative roasting of a mixture of chromium ore, soda and dolomite. The soda reacts directly with chromium oxide to form soluble sodium chromate. A dual role is attributed to dolomite. On the one hand, the calcium oxide in dolomite acts as a chemically-active base and combines with the acidic oxides of the ore [1], thereby lowering the consumption of soda for this purpose; on the other hand, the dolomite acts as filler, serves as a "skeleton" in the calcined mass, prevents fusion of the mass, and keeps it permeable to gases.

Although it is now possible to calculate the amount of calcium oxide necessary for the chemical reaction from the mineral composition of the roasted mass [2], the amount of dolomite as filler cannot be calculated; it is found empirically, under the actual production conditions, in each individual case. The reason is that the physical nature of the filler is not yet understood.

Sodium monochromate is formed in a heterogeneous medium, as the process involves three phases: solid (ore), liquid (melt containing sodium carbonate, sodium chromate and calcium carbonate [3]), and gas (oxygen of the gaseous medium). Therefore, the extent of reaction should depend on the interphase area and on the ratio between the amount of liquid phase and the surface area of the filler.

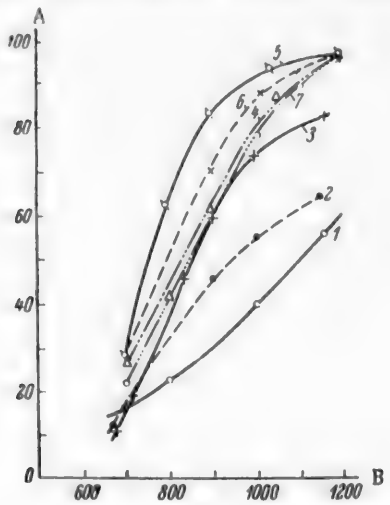

Fig. 1. Effect of the roasting temperature on the degree of oxidation of chromium for different contents of chromium oxide in the charge.
(A) Degree of oxidation of chromium (%), B) temperature (°C).
The numbers on the curves correspond to the charge numbers in Table 1.

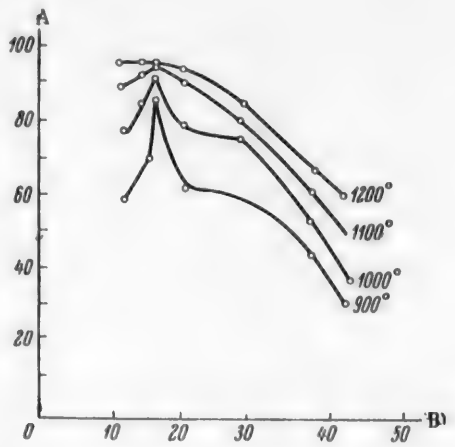

Fig. 2. Effect of chromium oxide content of the original charge on the degree of oxidation of chromium.
A) Degree of oxidation of chromium (%),
B) Cr_2O_3 content of charge (%).

TABLE 1

Effect of the Filler Content of the Charge on the Degree of Oxidation of Chromium

Charge No.	Composition of charge (%)			Roasting temperature (°C)	CrO_3 content of sinter (%)		Degree of oxidation of chromium (%)
	Cr_2O_3	Na_2CO_3	MgO		water-soluble	total	
1	41.80	58.20	—	670	7.90	56.51	13.98
				800	12.62	56.92	22.17
				900	18.01	59.40	30.33
				1000	24.93	63.40	39.32
				1150	37.91	67.25	56.37
2	37.20	51.70	11.1	670	6.21	50.31	12.35
				720	10.26	51.62	19.87
				900	24.08	53.40	45.01
				1000	29.47	53.75	54.83
				1150	35.21	54.08	65.11
3	28.60	40.0	31.4	670	3.97	38.65	10.27
				720	7.60	39.10	19.45
				840	18.00	40.05	45.00
				1000	30.15	40.61	74.25
				1150	34.54	41.25	83.74
4	19.55	27.53	53.0	700	9.05	25.91	28.60
				800	10.67	25.79	41.40
				900	16.48	26.21	62.87
				1050	23.54	27.20	86.55
				1200	26.51	27.22	97.33
5	16.20	22.63	61.2	700	6.61	20.67	31.97
				800	17.21	20.95	64.02
				900	18.29	21.76	84.07
				1050	20.67	22.00	93.93
				1200	21.65	22.33	96.97
6	15.00	20.90	64.1	700	5.83	19.75	29.55
				900	13.85	19.80	70.00
				1000	17.36	19.85	87.46
				1100	18.33	19.98	91.73
				1200	19.91	20.77	95.85
7	12.00	16.75	71.2	700	2.65	12.40	21.02
				900	7.83	12.45	58.92
				1000	9.80	12.51	78.43
				1100	11.30	12.60	90.12
				1200	12.19	12.70	96.01

The purpose of this investigation was to determine the influence of the filler surface on the oxidation process.

EXPERIMENTAL

The influence of the filler surface on the degree of oxidation of chromium was studied by variation of the amount of filler at a constant specific surface and also by variation of the specific surface of the filler while its amount was constant.

In order to exclude the influence of the chemical nature of the filler in the oxidative roasting of chromite charges, chromium oxide and not ore was used as the starting material in the first part of the investigation. The ore contains SiO_2, Al_2O_3, Fe_2O_3 as impurities; it would be necessary to introduce a chemically-active base (lime) to combine with them. The filler used was magnesium oxide; it is known [4] that in the production of sodium chromate, it does not react either with chromium oxide or with the sodium carbonate, which is the third component of the charge.

The chromium oxide content of the charges was varied from 12.0 to 41.8% (by variation of the amount of filler), while the amount of sodium carbonate was the amount theoretically necessary for sodium chromate formation.

TABLE 2

Effect of the Specific Surface of the Filler (Magnesite) on the Degree of Oxidation of Chromium*

Composition of charge (%)					CrO_3 content of charge (%)	CrO_3 content of sinter (%)		Degree of oxidation of chromium (%)
ore	soda	lime	magnesite No. 1	magnesite No. 2		water-soluble	total	
27.6	23.20	6.70	42.50	—	16.5	19.37	22.42	86.49
27.6	23.20	6.70	—	42.50	16.5	17.79	22.21	80.11
32.20	28.31	8.33	31.06	—	20.0	22.73	26.71	85.13
32.20	28.31	8.33	—	31.06	20.0	19.92	25.98	76.66

* Average results from 5-6 experiments are given.

TABLE 3

Effect of the Roasting Temperature on the Degree of Oxidation of Chromium in Charges with Different Fillers (Magnesites)

Roasting temperature	CrO_3 content of sinter (%)		Degree of oxidation of chromium (%)	Roasting temperature	CrO_3 content of sinter (%)		Degree of oxidation of chromium (%)
	water-soluble	total			water-soluble	total	
Charge with magnesite No. 1				Charge with magnesite No. 2			
700	1.79	25.58	7.0	700	2.66	26.30	10.11
800	9.23	25.29	36.50	800	6.68	25.00	26.72
900	18.33	26.31	69.70	900	13.86	25.51	54.31
1000	22.52	26.49	85.10	1000	19.88	25.98	76.52
1150	26.45	27.06	97.74	1150	25.33	26.80	94.50

The charges (4-5 g samples) were heated at the required temperatures (from 670-1200°) in a vertical furnace with an open platinum heater which raised the furnace temperature uniformly. The rate of heating was such as to approximate as much as possible to the heating regime used in industrial conditions and was 8° per minute.

In the second part of the investigation, when the influence of the specific surface of the filler on the degree of oxidation of the chromium was being studied, the charges were based on an ore containing Cr_2O_3 62.00%, SiO_2 2.47%, Al_2O_3 8.47%, Fe_2O_3 12.72%, MgO 14.26%. The main fillers (with regard to the amount added) were two different samples of magnesite, similar in chemical composition but differing in specific surface: 18.2 m^2/g (magnesite No. 1), and 9.65 m^2/g (magnesite No. 2). In addition, a certain amount of lime (CaO content 97.95%) which acted as a chemically-active filler, was introduced. This amount was calculated by means of the formula of the Urals Chemical Scientific Research Institute [2]:

$$CaO = 1.88SiO_2 + 0.82Fe_2O_3 + 0.92Al_2O_3,$$

where CaO represents the amount of calcium oxide (in g) which must be added to 100 g of ore; SiO_2, Fe_2O_3 and Al_2O_3 represent the % contents of these oxides in the original ore.

Because of the presence of lime in the charge, the amount of sodium carbonate added could be limited to the amount necessary for formation of sodium chromate. The chromium oxide contents of the charges were 16.5 and 20%. The charges were roasted under the same conditions as in the first part of the investigation.

The sinters were analyzed for total, water-soluble and acid-soluble chromic anhydride by the methods used in the chromate industry.

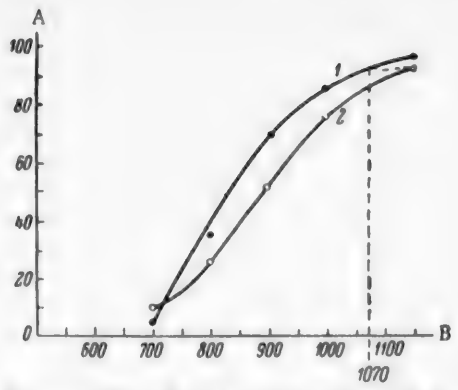

Fig. 3. Effect of the specific surface of the filler on the degree of oxidation of chromium. A) Degree of oxidation of chromium (%), B) roasting temperature (°C). Filler: 1) lime + + magnesite No. 1, 2) lime + magnesite No. 2.

It must be noted that no acid-soluble chromic anhydride was found in any of the sinters. The analytican data were used to calculate the degree of oxidation of the chromium, calculated as the ratio of water-soluble to total chromic anhydride in the sinters, multiplied by 100.

The results of the first series of experiments are given in Table 1 and Fig. 1. The data of Table 1 and Fig. 1 may be presented as shown in Fig. 2, which represents the variation of the degree of oxidation with the chromium oxide content of the original charge for a constant final roasting temperature. The nature of this relationship varies with the roasting temperature. The curves corresponding to final roasting temperatures of 900, 1000 and 1100° (Fig. 2) each have an oxidation maximum at 16.2% of chromic oxide in the charge. The magnitude of the maximum diminishes with increase of the roasting temperature, and at 1200°, the degree of oxidation of the chromium is almost the same for charges containing from 12.0 to 19.5% of chromic oxide. On further increase of the amount of chromic oxide in the charge, the degree of oxidation decreases, and in the charge without filler (41.8% Cr_2O_3), the maximum oxidation at the same roasting temperature is only 60%. This last fact may be attributed to the presence of a large amount of liquid phase, which prevents the penetration of oxygen from the furnace gas to the chromic oxide particles. The probable explanation of the maxima on the curves in Fig. 2 is that with about 16% of chromic oxide in the charge, the best ratio between the amounts of liquid phase and filler, ensuring good gas permeability, is attained. The amount of liquid phase in the roasted mass increases with increasing chromic oxide content, with a consequent increase of the thickness of the liquid film on the surface. More intensive heating is required to increase the degree of oxidation of chromium under these conditions.

Analogous results were obtained (Table 2) on variation of the specific surface of the filler (by the use of different magnesites as fillers). These results show that different degrees of oxidation were reached in the roasting of charges containing magnesite No. 1 and No. 2, respectively, at the same temperatures. This difference is illustrated especially clearly by the data in Table 3 and by Fig. 3, where the variation of the degree of oxidation of chromium with the final roasting temperature of charges with these magnesites is shown. These results also indicate that in order to attain a required degree of oxidation, any decrease in the surface of the filler must be compensated by an increase of the roasting temperature.

SUMMARY

1. Experiments with variations of the amount of filler and of its specific surface showed that the specific surface of the filler influences the degree of oxidation of chromium in the roasting of chromite charges.

2. For a required degree of oxidation, if the surface area of the filler is decreased, the charge should be roasted at a higher temperature.

LITERATURE CITED

[1] L. I. Popova, J. Chem. Ind. 2, 6 (12), 465 (1926).

[2] T. D. Averbukh, M. A. Serebrennikova and N. D. Maslova, J. Appl. Chem. 29, 498 (1956).*

[3] Ia. E. Vil'nianskii and O. I. Pudovkina, J. Appl. Chem. 21, 12 (1948).

[4] I. G. Ryss and R. G. Uritskaia, Bull. Acad. Sci. USSR 4 (1934).

Received March 23, 1957

*Original Russian pagination. See C. B. Translation.

DETERMINATION OF THE PRECIPITATION pH, AND CALCULATION OF THE SOLUBILITY PRODUCT OF ANTIMONY HYDROXIDE BY A POLAROGRAPHIC METHOD

P. N. Kovalenko

The Rostov State University

The polarographic method is used for the solution of many problems in production control, problems relating to the technology or impurity removal from solutions in the production of concentrates consisting of precipitated hydroxides with high contents of given components, etc.

In chemical analysis and in industrial purification of electrolytes for separation of elements as their hydroxides, it is important to know the pH range in which precipitation occurs. The dropping mercury electrode is successfully used for this purpose. By variation of the solution pH, conditions may be set up favoring salt hydrolysis and shift of the hydrolysis equilibrium until hydroxides are precipitated in presence of other components.

For fractional precipitation of hydroxides from solutions of their salts, the range of hydrogen-ion concentrations in which precipitation occurs must be found for each hydroxide. For example, if the precipitation pH of antimony hydroxide is known and if its ionic concentration is determined, its solubility product can be calculated [1]. However, determination of the precipitation pH of antimony hydroxide by the known methods [2, 3] involves great difficulties, and the results are not reproducible. Data on the solubility product (K_s) of antimony hydroxide, published in the literature [4], give no indication of the temperature at which it was determined.

The purpose of the present investigation was to determine the pH at which precipitation of antimony hydroxide begins by the most accurate polarographic method and to calculate K_s from the results. K_s for antimony hydroxide was calculated from experimental polarographic data obtained by determination of antimony concentration in presence of strong electrolytes. Since the ionic strength is considerable in such cases, there are considerable deviations from the true values of K_s.

Denoting the molar concentrations of the ions by $[Sb^{3+}]$ and $[OH^-]$, we have the true solubility product, with the ionic strength of the solution taken into account:

$$K_{a\,Sb(OH)_3} = [Sb^{3+}]\,[OH^-]^3 \cdot \gamma^4,$$

where $K_{aSb(OH)_3}$ is the activity product of $Sb(OH)_3$.

Then

$$K_{a_{Sb(OH)_3}} = K_{s\,Sb(OH)_3} \cdot \gamma^4 \text{ and } \gamma = \sqrt[4]{\frac{K_a}{K_s}},$$

where K_a and K_s are found from experimental data.

It follows from the above expression that despite the classical theory, the product of the molar concentrations of ions in a saturated electrolyte solution is not constant but varies inversely with the power of the activity coefficient, which is a function of the ionic strength of the solution and is directly proportional to $\sqrt[4]{K_a/K_s}$.

In practice, instead of a constant value for K_s, a series of values is obtained corresponding to different values of the ionic strength, which depends on the electrolyte concentration. The true solubility product, as a constant quantity, is determined graphically by extrapolation of the curves for the log $K_s - [Me^{n+}]$.

EXPERIMENTAL

The original solution was antimony chloride solution, prepared from a weighed quantity of $SbCl_3$ dissolved in 2.4 N hydrochloric acid. The titer of the $SbCl_3$ solution was determined by the bromate method; T_{SbCl_3} = = 0.00201 g. $SbCl_3$ solutions of the required concentrations – $1 \cdot 10^{-3}$, $5 \cdot 10^{-4}$ and $2 \cdot 10^{-4}$ mole/liter – were prepared by dilution of the original solution; the supporting electrolyte in the polarographic determinations was hydrochloric acid. For suppression of the current maximum, 3 drops of 0.1% methylene blue was added per 25 ml of solution. The hydrogen-ion concentration was determined potentiometrically by means of the quinhydrone electrode.

The M-7-2000 manual polarograph, made in 1946 at the Scientific Research Institute of Chemistry of Gor'kii University, was used for the determinations. The current strength was measured by a mirror galvanometer of absolute sensitivity $1.2 \cdot 10^{-9}$ amp/mm/m, R_{ext} = 615 ohm, R_{cr} = 1685 ohm. The distance from the center of the mirror to the galvanometer scale was 0.25 m. The capillary constant $m^{2/3} \cdot t^{1/6} = 1.426$ mg$^{2/3} \cdot$sec$^{1/2}$, where m = 1.417 mg/sec and t = 1.007 sec.

The $SbCl_3$ concentration of the solutions was determined polarographically with the aid of a calibration graph (Fig. 1).

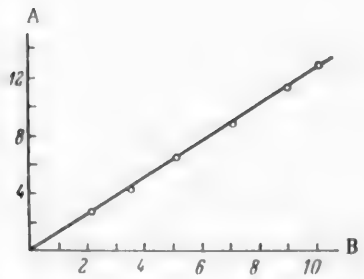

Fig. 1. Calibration graph for diffusion current against antimony concentration.
A) Diffusion current id (μa), B) antimony concentration $C_{Sb^{3+}} \cdot 10^4$ (moles/liter).

For determination of the precipitation pH of antimony hydroxide, a series of solutions was prepared of equal initial concentrations of the antimony salt but of different pH, and after equilibrium had been reached in the solutions, their polarographic curves were determined. The diffusion wave of antimony chloride as a function of solution pH is plotted in Fig. 2.

In polarography of solutions with pH values at which solid antimony hydroxide is not formed, there should be a constant value of the diffusion current. In reality, the current strength decreases slightly; this is probably due to the influence of the ionic strength of the solution, which has a retarding effect on ionic mobility with increase of solution pH from 0.36 to 0.45 (Fig. 2).

At a definite hydrogen-ion concentration, formation of a solid phase (precipitation of $Sb(OH)_3$) begins, and the diffusion current decreases sharply, owing to the rapid fall of

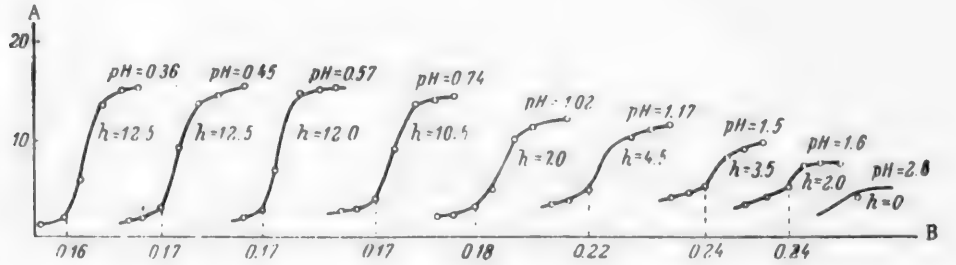

Fig. 2. Effect of solution pH on the diffusion-wave height. Initial concentration of antimony solution $5 \cdot 10^{-4}$ mole/liter, absolute sensitivity of galvanometer $1.2 \cdot 10^{-9}$ amp/mm/m, $m^{2/3} \cdot t^{1/6} = 1.417$ mg$^{2/3} \cdot$sec$^{1/2}$. A) Diffusion-wave height (mm), B) emf (v).

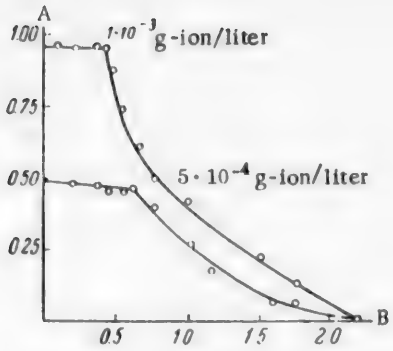

Fig. 3. Course of hydrolysis of antimony chloride (Sb^{3+}) as a function of its concentration, with changes of solution pH at 12°. Galvanometer sensitivity S in polarographic determinations = 1/100. A) Concentration of Sb^{3+} – $C_{Sb^{3+}} \cdot 10^3$ (g-ion/liter), B) solution pH.

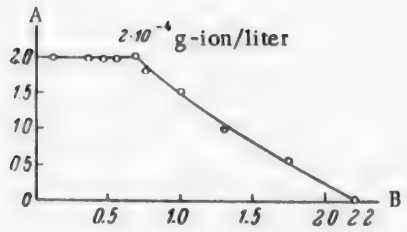

Fig. 4. Course of hydrolysis of antimony chloride (Sb^{3+}) as a function of its concentration, with changes of solution pH at 12°. Galvanometer sensitivity S in polarographic determinations - 1/50. A) Concentration of Sb^{3+} – $C_{Sb^{3+}} \cdot 10^4$ (g-ion/liter), B) solution pH.

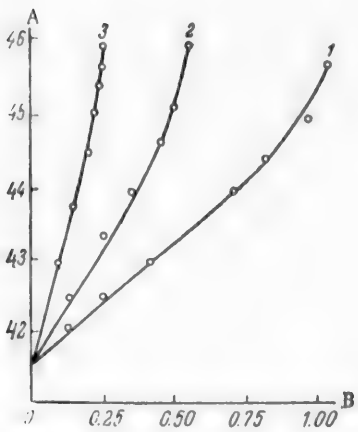

Fig. 5. Variation of – log K_s with the Sb^{3+} concentration, which varies with solution pH. A) Negative log K_s, B) concentration of Sb^{3+} – $C_{Sb^{3+}} \cdot 10^3$ (g-ion/liter). 1) $C'_{Sb^{3+}} = 1 \cdot 10^{-3}$, 2) $5 \cdot 10^{-4}$, 3) $2 \cdot 10^{-4}$ g-ion/liter; – log K_a = 41.5, $K_a = 3.16 \cdot 10^{-42}$.

antimony concentration in the solution. The sharp decrease of the diffusion current is a sign of the start of precipitation of antimony hydroxide.

The results of measurements of the diffusion current and $Sb^{...}$ concentration at different solution pH are plotted in Figs. 3 and 4. The $Sb^{...}$ concentration in solution was found from the calibration graph. These results are quite reproducible.

The diffusion current (id) in μa was calculated from the height h of the polarographic wave in mm by means of the formula [1]:

$$id = \frac{a \cdot b \cdot 10^6 \cdot h}{l},$$

where l = 0.25 m and b is the galvanometer shunt ratio.

It follows from Figs. 3 and 4 that at first, as the solution pH changes from 0.1 to 0.74 (Figs. 3 and 4), the diffusion-current strength in the electrolytic reduction of antimony at the dropping mercury electrode decreases only slightly, and only when the solution pH reaches a certain value does id decrease sharply owing to a decrease of the antimony concentration in solution. The precipitation pH is a definite function of the initial antimony concentration; its value increases with decrease of the antimony concentration. The effect of antimony concentration on the pH value at which precipitation of $Sb(OH)_3$ begins can be derived from the equation for the solubility product [5] of $Sb(OH)_3$:

$$K_s = C_{Sb^{3+}} \cdot \frac{K_w^3}{C_{H^+}^3}, \quad pH = \frac{1}{3} \lg \frac{K_s}{K_w^3 \cdot C_{Sb^{3+}}}$$

and

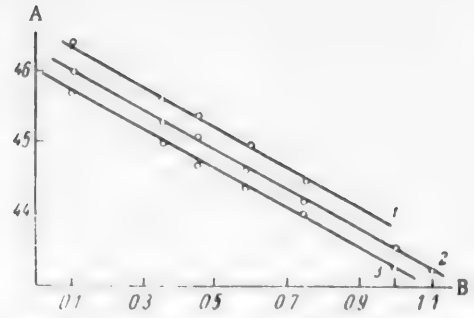

Fig. 6. Variation of $-\log K_s$ with pH of $SbCl_3$ solutions of different concentrations. A) Negative log K_s, B) pH of $SbCl_3$ solution. $SbCl_3$ concentration (mole/liter): 1) $2 \cdot 10^{-4}$, 2) $5 \cdot 10^{-4}$, 3) $1 \cdot 10^{-3}$.

$$C_{Sb^{3+}} = \frac{K_s}{K_w^3} \cdot 10^{-3pH}.$$

Therefore, in practice, there should be an inverse logarithmic relationship between $C_{Sb^{3+}}$ and the solution pH at which $Sb(OH)_3$ is precipitated. This is confirmed by the data in Figs. 3 and 4.

It is interesting to note that, irrespective of the concentrations of the original Sb^{3+} solutions, the precipitation of $Sb(OH)_3$ terminates at the same pH value of 2.2

The diagrams show that in solutions containing $1 \cdot 10^{-3}$ g-ion Sb^{3+} per liter, precipitation of the hydroxide begins at pH = 0.45; with $5 \cdot 10^{-4}$ g-ion/liter, at pH = 0.62, and with $2 \cdot 10^{-4}$ g-ion/liter, at pH = 0.74. The sharpest fall of antimony concentration in solution, from which the pH of the start of precipitation can be determined exactly, is seen in the curve for an initial concentration of $1 \cdot 10^{-3}$ mole $SbCl_3$ per liter. The higher the antimony concentration in solution, the more distinct is this fall; at high concentrations of $SbCl_3$ in solution, a slight increase of pH favors rapid formation of the solid $Sb(OH)_3$ phase. However, as soon as the $SbCl_3$ concentration in solution decreased, hydroxide formation slowed down (Figs. 3 and 4). The experiments were performed at 12°; at this temperature, the ionic product for water (K_W) is $0.44 \cdot 10^{-14}$.

It follows from the results (Fig. 5) that the value of the solubility product calculated from the formula given above does not remain constant. The solubility of $Sb(OH)_3$ in solutions of different pH, up to a certain limit, varies, probably because of differences of ionic strength. However, if the activity product (K_a), instead of the product of the actual concentrations, is taken, the value of K_a remains satisfactorily constant. This product can be determined from the functional relationship between $-\log K_s$ and the concentration of Sb^{3+} ions.

The relationship between $-\log K_s$ and Sb^{3+} concentration in the course of hydrolysis is plotted in Fig. 5. This graph shows that $-\log K_s$ and the Sb^{3+} concentration, which diminishes with increase of pH, owing to intensified hydrolysis over a definite range of $C_{Sb^{3+}}$, are connected by a linear relationship, represented by the equation

$$-\lg K_s = a + b \cdot C_{Sb^{3+}},$$

where a is a constant, equal to the negative logarithm of the product $[Sb^{+3}][OH^-]^3$, with ion activities corresponding to complete dissociation of the antimony salt; b is the slope factor [1].

Extrapolation of the curves to their intersection of the ordinate axis gives the activity product K_a at infinitely low Sb^{3+} concentration, i. e., when the activity coefficient is 1,

$$a = -\lg K_a \quad b = -\frac{\lg K_s - a}{C_{Sb^{3+}}},$$

where $C_{Sb^{3+}}$ is the antimony concentration, varying because of increase of the solution pH. Irrespectively of the initial Sb^{3+} concentration, all the curves meet at the ordinate at one point, corresponding to $-\log K_a$, the average value of which is −41.5, and $K_a = 3.16 \cdot 10^{-42}$.

The lower the concentration of the original $SbCl_3$ solution, the greater is the slope factor b. It is interesting to note that the product of the slope factor and the concentration of the original solution, C_{init}, is constant:

$$b \cdot C_{init} = K = \text{const and } -\log K_s = -\log K_a + \frac{K}{C_{init}} \cdot C_{Sb^{3+}}.$$

The activity product of antimony hydroxide, determined polarographically, is given below:

Initial concentration (mM/liter)	Slope factor (b)	Constant ($K = b \cdot C_{init}$)	Average value of of activity product (K_a)
1.0	3.40	3.40	$3.16 \cdot 10^{-42}$
0.5	6.60	3.30	
0.2	16.0	3.20	
	Mean	3.30	

Variations of $-\log K_s$, with pH of $SbCl_3$ solutions of different concentrations, are plotted in Fig. 6. These graphs represent the course of variation of K_s during hydrolysis of the antimony salt and precipitation of $Sb(OH)_3$ at different solution pH.

SUMMARY

1. The pH of the start of precipitation of antimony (Sb^{3+}) hydroxide for different initial antimony concentrations has been determined by a polarographic method. The precipitation terminates at the same pH value of 2.2, irrespective of the initial concentration.

2. The effects of antimony chloride concentration and solution pH on the diffusion current were studied.

3. The activity product of antimony hydroxide was calculated from polarographic data.

LITERATURE CITED

[1] P. N. Kovalenko, Ukrain. Chem. J. 5, 549 (1954); J. Inorg. Chem. 8, 1717 (1956).

[2] H. T. S. Britton, Hydrogen Ions (ONTI, 1936) [Russian translation].

[3] N. A. Tananaev, Progr. Chem. 10, 621 (1941).

[4] V. Bayerle, Rec. trav. chim. 44, 519 (1925).

[5] P. N. Kovalenko and V. N. Nestorovich, Ukrain. Chem. J. 6, 635 (1952).

Received January 18, 1957

"SHAVINGLESS" DISSOLUTION OF MAGNESIUM, ZINC, TIN, AND IRON IN HYDROCHLORIC ACID*

A. G. Loshkarev

(The V. V. Vakhrushev Mining Institute, Sverdlovsk)

For shavingless sampling and investigation of the corrosion of magnesium, zinc, tin, iron, and their alloys, and also of many other metals (cadmium, aluminum) and alloys, it is important to study the rate of shavingless dissolution accompanied by hydrogen evolution. Shavingless samples of these metals and alloys are usually taken by means of hydrochloric acid solutions of various concentrations.

Magnesium and zinc were the metals chosen for our investigation of the rates of shavingless dissolution of metals in hydrochloric acid solutions. In addition, data are presented on the behavior of iron and tin in hydrochloric acid. These results can be used for comparison of the rates of shavingless dissolution of iron and tin in hydrochloric and nitric acids [1].

The metals in question differ from each other in chemical nature. A common property of all these metals is their electronegativity. They therefore dissolve at various rates in nonoxidizing acids with evolution of hydrogen, according to the equation

$$M^{II} + 2H^{+} \rightarrow M^{2+} + H_2.$$

The rates of ordinary spontaneous solution of magnesium, zinc, and iron in nonoxidizing acids with evolution of hydrogen have been studied in adequate detail.

In the case of very electronegative metals, if the discharge rate of the hydrogen ions is sufficiently high, the rate of spontaneous solution is determined by the diffusion of hydrogen ions to the metal surface. This applies to technically pure, e. g., electrolytic, magnesium and zinc.

In fact, Brunner [2], Zentnerszwer [3], and King and Bravermann [4] showed that the dissolution of magnesium in hydrochloric acid is diffusional in character. Durdin and Markevich [5] reached the same conclusion.

Very pure zinc, made by repeated distillation, dissolves very slowly in hydrochloric acid [6]. This is due to the high hydrogen overvoltage on zinc. Impurities present in technical zinc influence its rate of dissolution in acid in accordance with their respective hydrogen overvoltages. Therefore admixtures of lead, mercury, and cadmium [7] decrease, while admixtures of iron, copper, antimony, and arsenic [8] increase the dissolution rate of zinc in nonoxidizing acids.

The dissolution of iron in nonoxidizing acids is of a different character. Here the processes associated with ionization and discharge of the metal take place slowly, and the process kinetics are determined by a combination of the anode and cathode processes. The dissolution potential of iron is a function of the logarithm of the hydrogen-ion concentration, and the dissolution rate of iron is proportional to a certain fractional power of the hydrogen-ion concentration [9]. These relationships are satisfactorily confirmed by the experimental data of Shultin [10], Kolotyrkin [11], Bodforss [12], and Novikov [13].

*A. V. Aleksandrova took part in the experimental work.

No experimental data are available on the spontaneous dissolution of tin in nonoxidizing acids. According to the views put forward by Durdin [14], the spontaneous dissolution of tin should be of a similar nature to that of iron.

In the present investigation the kinetics of shavingless dissolution of metals in hydrochloric acid was studied experimentally with the following electrolytic metals: magnesium MG1, zinc TzO, tin 01, and "Armco" Al iron. The experimental procedure is described in an earlier paper [1]. All the experiments were carried out at room temperature (17°). The solvent was usually 5.54 N HCl. The acid solution was introduced into a pit in the metal by means of a capillary dropper. The volume of 5.54 N HCl at 17° was 0.141 ml.

As in the preceding studies [1, 15], the amount of metal entering the sample in shavingless dissolution was found from the metal content of the solution. Magnesium in the solution was determined by the volumetric complexometric method developed by Savinovskii, Stiunkel', and Iakimets [16]. A microburet was used for greater accuracy. Zinc was determined gravimetrically as ZnO. Iron was determined by the thiocyanate method with the aid of a photoelectric colorimeter [17]. Tin was determined by Tananaev's nephelometric method [18].

The experimental results are plotted in Fig. 1.

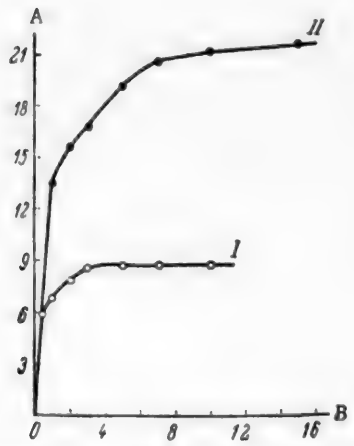

Fig. 1. Shavingless dissolution of magnesium (I) and zinc (II). A) Metal content q (mg), B) time t (minutes).

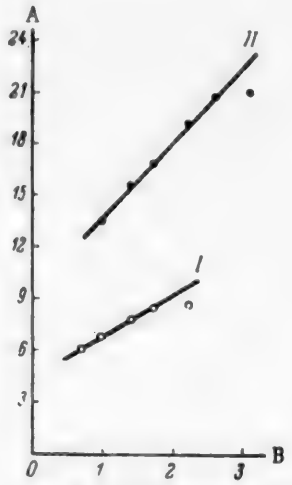

Fig. 2. Nonequilibrium period of shavingless dissolution of magnesium (I) and zinc (II). A) Metal content (mg), B) $\sqrt{t}$.

The most striking fact in the experimental data is the considerable rate at which magnesium and zinc dissolve in hydrochloric acid. 8.70 mg of Mg and 21.0 mg of Zn dissolve in 10 minutes in 0.141 ml of 5.54 N HCl at 17°. The amounts of iron and tin which dissolve in hydrochloric acid under the same conditions are very much less – 0.25 mg of Fe, and 0.95 mg of Sn.

The nature of the shavingless dissolution of these two pairs of metals is also different.

During the first two minutes more than 75% of the amount of zinc which dissolves in 10 minutes passes into solution. Roughly the same is true for magnesium. Because of experimental difficulties, we were unable to determine the dissolution rate during the first few seconds of the process. It seems, however, that here, as in the dissolution of copper, iron, and lead in nitric acid [1], the rate is constant during this period, i. e., it is determined by the rate of steady diffusion of hydrogen ions to the metal surface. The dissolution rate of magnesium and zinc decreases with time, and its change with time is generally analogous to the changes of the dissolution rates of copper, iron, and lead in nitric acid.

In accordance with the nonsteady diffusion equation [1, 15]

$$q = \frac{2nF\sqrt{D}}{\sqrt{\pi}}\sqrt{t}$$

TABLE 1

Shavingless-Dissolution Potentials of Magnesium and Zinc (φZn) in 5.54 N HCl at 17°

Time (min)	$\varphi^{\bullet}$Mg	$\varphi^{\bullet}$Zn	Time (min)	$\varphi^{\bullet}$Mg	$\varphi^{\bullet}$Zn
1/4	−1.682	−0.392	5	−1.603	−0.345
1/2	−1.686	−0.375	6	−1.556	−0.342
3/4	−1.686	−0.371	7	−1.552	−0.340
1	−1.682	−0.366	8	−1.560	−0.340
1 1/2	−1.682	−0.360	9	−1.564	−0.340
2	−1.678	−0.358	10	−1.569	−0.340
3	−1.656	−0.351	12	−1.569	−0.340
4	−1.634	−0.349	15	−1.569	−0.340

• φ in v on the hydrogen scale.

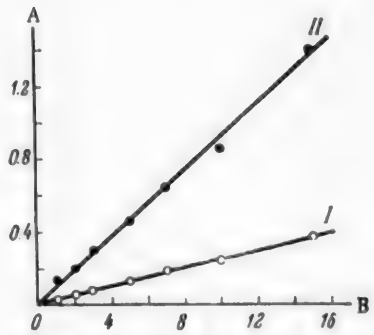

Fig. 3. Shavingless dissolution of iron (I) and tin (II).
A) Metal content q (mg), B) time t (minutes).

Fig. 2 is a plot of the amounts of magnesium and zinc dissolved (q) against the square root of the dissolution time ($\sqrt{t}$). It is seen that this relationship is linear during the middle part of the process. This leads to the conclusion that soon after the start of the dissolution, the dissolution rate of magnesium and zinc is determined by the rate of nonsteady diffusion of hydrogen ions to the surface of the dissolving metal.

A similar effect is to be expected in the dissolution of such electronegative metals as manganese, vanadium, aluminum, titanium, and the alkaline-earth and alkali metals.

Experimental data on variations of potential during the shavingless dissolution of magnesium and zinc in 5.54 N HCl at 17° are summarized in Table 1.

TABLE 2

Shavingless-Dissolution Potentials of Tin (φ_{Sn}) and Iron (φ_{Fe}) in 5.54 N HCl at 17°

Time (min)	$\varphi^{\bullet}_{Sn}$	$\varphi^{\bullet}_{Fe}$	Time (min)	$\varphi^{\bullet}_{Sn}$	$\varphi^{\bullet}_{Fe}$
1/4	−0.384	—	5	−0.382	−0.223
1/2	−0.384	−0.236	6	−0.382	−0.224
1	−0.384	−0.225	7	−0.382	−0.225
2	−0.384	−0.221	8	−0.382	−0.225
3	−0.384	−0.220	9	−0.382	−0.227
4	−0.382	−0.221	10	−0.382	−0.227

• φ in v on the hydrogen scale.

When hydrochloric acid is placed on magnesium, the film of magnesium oxide which is always present on the metal surface dissolves, and the potential of magnesium falls rapidly from − 1.430 to − 1.686 v. During dissolution, the potential increases from − 1.686 to 1.552 v in 6 minutes, and then decreases again to − 1.569 by the 15th minute.

The rates of shavingless dissolution of iron and tin in hydrochloric acid remain constant for 10 minutes

(Fig. 3), and are very much lower than the rates for magnesium and zinc, namely: 0.020 mg/min·cm^2 for iron, and 0.078 mg/min·cm^2 for tin. The solution rate remains constant, evidently because the solution potential of the metal is constant. This hypothesis is confirmed by experimental observations. The solution potentials of iron and tin in 5.54 N HCl are given in Table 2. These potentials remain constant during dissolution (within the limits of experimental error).

The high negative values of the solution potentials of iron ($\varphi_{Fe} = -0.22$ v) and tin ($\varphi_{Sn} = -0.38$ v) account for the relatively low rates of solution of these metals in hydrochloric acid. In turn, the slight change of the concentrations of hydrogen and metal ions in solution leads to stabilization of the solution potential during the time of measurement (10-15 minutes).

The results of our experiments on the shavingless dissolution of iron and tin are in agreement with literature data [12, 13] which show that when nonoxidizing acids are used to dissolve metals for which the ionization and discharge processes are slow, their rates being comparable with the discharge rate of hydrogen ions, the solution potential and rate remain constant with time at a given hydrogen-ion concentration. Thus, here we have a typical case of mixed anodic – cathodic control.

It is seen that the shavingless dissolution of iron in hydrochloric acid differs from dissolution in nitric acid [1] not only by its lower rate, but also by the mechanism of the process itself. The cause of this significant difference is the considerably higher difference of potential between the oxidizing and reducing agent when iron is dissolved in nitric acid, as compared with the difference of potential when iron is dissolved in hydrochloric acid. Increase of this potential difference up to a certain limit makes the process diffusion-controlled instead of being under mixed anodic – cathodic control.

This conclusion is illustrated by the shavingless dissolution of magnesium and zinc in hydrochloric acid.

SUMMARY

1. The shavingless dissolution of magnesium, zinc, tin, and iron in 5.54 N HCl at 17° was studied, and it was shown that the solution rates of magnesium and zinc in hydrochloric acid are determined by the rate of diffusion of the solvent to the metal surface.

2. The rate of shavingless dissolution of tin and iron in hydrochloric acid is determined by the rate of the anodic – cathodic process.

LITERATURE CITED

[1] A. G. Loshkarev, J. Appl. Chem. 30, 10, 1558 (1957). •

[2] E. Brunner, Z. Phys. Ch. 47, 56 (1904).

[3] M. Zentnerszwer, Rec. Trav. Chim. 42, 579, 1065

[4] C. V. King and M. M. Bravermann, J. Am. Chem. Soc. 64, 64 (1932).

[5] Ia. V. Durdin and A. Markevich, J. Gen. Chem. 19, 2131 (1949). •

[6] A. Thiel and J. Eckell, Korr and Metallsch. 6, 122 (1928); 7, 145 (1928).

[7] A. Burkhardt and G. Sachs, Metallwirtsch. 23, 325 (1933)

[8] F. Getman, Z. Phys. Ch. 36, 2655 (1932).

[9] A. N. Frumkin, V. S. Bagotskii, Z. A. Iofa, and B. N. Kabanov, Kinetics of Electrode Processes (Izd. MGU, 1952), 292. [In Russian]

[10] A. I. Shultin, J. Phys. Chem. 15, 370, 399 (1941); 18, 61, 69 (1944).

[11] Ia. M. Kolotyrkin, J. Phys. Chem. 25, 1249 (1951).

[12] S. Bodforss, Z. Phys. Ch. (A), 160, 141 (1932).

[13] S. K. Novikov, Sci. Mem. Moscow Pedagogic Inst. 64, 42 (1947).

• Original Russian pagination. See C. B. Translation.

[14] Ia. V. Durdin, Sci. Mem. Leningrad State Univ. 40, 3 (1939).

[15] A. G. Loshkarev, J. Appl. Chem. 30, 12, 1861 (1957). *

[16] D. A. Savinovskii, T. B. Stiunkel', and E. M. Iakimets, Instructions for Determination of the Hardness of Water (Min. Chem. Ind. 1953). [In Russian]

[17] A. K. Babko and A. T. Pilipenko, Colorimetric Analysis (Goskhimizdat, 1951). [In Russian]

[18] N. A. Tananaev, The Shavingless Method (Metallurgy Press, 1948). [In Russian]

Received November 14, 1956.

* Original Russian pagination. See C. B. Translation.

USE OF THE RESULTS OF ELECTROCAPILLARY DETERMINATIONS IN STUDIES OF ACID-CORROSION INHIBITORS FOR METALS*

L. I. Antropov, V. P. Grigor'ev, and A. T. Petrenko

(The S. Ordzhonikidze Polytechnic Institute, Novocherkassk)

The practical selection and evaluation of inhibitors [1, 3] is carried out almost exclusively by empirical means – by direct determinations of the decrease of corrosion loss resulting from addition of inhibitors to the corrosive medium. Although it has been repeatedly noted [4-13] that such particle properties as molecular weight, size, dipole moment, etc., should play an important role in the mechanism of inhibitor action, these properties have not been used, either individually or jointly, as a basis for the selection of inhibitors. Attempts to evaluate inhibitor effectiveness from shifts of the equilibrium potentials of the corroding metals in their presence [14], from changes of electrical resistance at the metal – solution boundary [5, 14], from the rate of increase of the hydrogen overvoltage with time [15-19], and from their ability to suppress polarographic maxima [20] cannot be regarded as adequately substantiated.

In this paper we discuss the possible use of results of electrocapillary determinations as a method for selection of physical inhibitors and for evaluation of their effectiveness.

METHOD

Bonding between physical inhibitors and metals, leading to protection of the latter, is effected largely by electrostatic and van der Waals forces.** Special importance therefore attaches to the charge of the protected metal surface and the electrical properties of the inhibitor particles (charge, dipole moment, polarizability). It was pointed out earlier by one of us [21] the charge on a metal relative to the solution is determined by the relationship between the equilibrium potential of the metal under corrosion conditions (E_{eq}) and its zero point ($E_{q=0}$), rather than by the cathodic or anodic function of the metal in the given corrosion system. The difference $E_{eq} - E_{q=0} = \varphi_{eq}$ is the equilibrium potential on the zero-point scale. The sign of φ_{eq} coincides with the sign of the charge on the metal surface, while the magnitude of φ_{eq} is a measure of this charge. It was shown in earlier papers [21, 22] that the range of substances among which inhibitors should be sought can be narrowed if φ_{eq} is known. If the condition $\varphi_{eq_{Me_1}} = \varphi_{eq_{Me_2}}$, holds for two metals Me_1 and Me_2, then, in accordance with the foregoing considerations, the conditions of electrostatic adsorption of the same particles on these metals are similar. This makes it possible to use adsorption data for one of the metals (say, Me_1) to estimate adsorption of the same substances on the other metal (say, Me_2). The most accurate and complete characteristics of adsorption effects on metal – solution interfaces are provided by electrocapillary determinations carried out with the aid of a mercury electrode. Data obtained by electrocapillary determinations on mercury may be used in evaluation of the adsorbability of various substances on other metals under corrosion conditions provided that their zero points and equilibrium potentials are known, i.e., provided that φ_{eq} can be determined for them. Substances which, at potential φ_{eq}, produce the greatest decrease of interfacial tension at the mercury – solution boundary would be adsorbed to the greatest extent at the corroding metal – medium boundary, and they should therefore have the

---

*The essential contents of this paper were presented at the Leningrad Interregional Conference on Corrosion in 1956.

**The action of "chemical" inhibitors also usually commenced with physical adsorption. The present discussion can therefore be of some significance in relation to chemical inhibition.

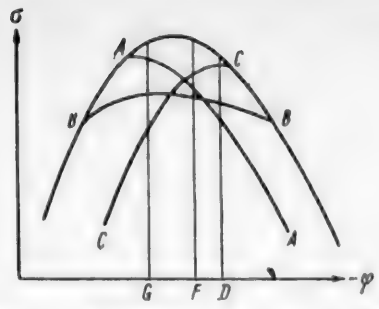

Fig. 1. Electrocapillary curves. Explanation in text.

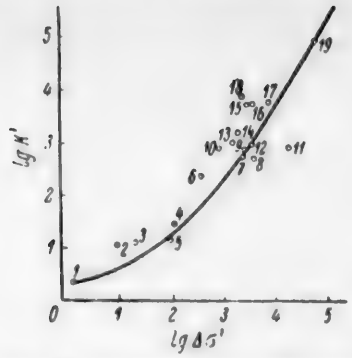

Fig. 2. Variation of specific inhibition coefficients of iron corrosion with specific surface activity of inhibitors (the numbers of the points correspond to the numbers of the substances as given in the text).

greatest inhibiting effect.* Suppose that electrocapillary curves determined in an acid solution (of the same concentration as in corrosion) in absence and presence of 3 additives A, B, and C are of the form shown in Fig. 1. Here the ordinates show the surface tension σ, while the abscissa represents the potential of the mercury electrode φ_{Hg}, which is the difference between the potential of mercury on the hydrogen scale ($E_{H_{Hg}}$) and its zero point ($E_{q=\theta_{Hg}}$). Let D (Fig. 1) represent the equilibrium potential of the metal Me_1, which has the value $\varphi_{eq_{Me_1}}$, under corrosion conditions; it is then evident that the adsorbability of the additives, determined by the lowering of the surface tension $\Delta\sigma$ (Fig. 1), is represented by the sequence: C < B < A. For physical inhibitors, this sequence should correspond to the sequence of increasing inhibiting effects on corrosion of the metal Me_1 at equilibrium potential $\varphi_{eq_{Me_1}}$. For another metal Me_2, corroded in the same medium as Me_1, the value of $\varphi_{eq_{Me_2}}$ would be different; for example, the value of $\varphi_{eq_{Me_2}}$ represented by the point F in Fig. 1. In this case the same additives form a different sequence in order of their inhibiting effects: C < A < B. Thus, in this method, in contrast to the method of Gatos [20], it is possible to take into account the nature of the metal by the use of the zero point, which is a very characteristic constant for each metal.

The proposed method for selection and evaluation of physical inhibitors also takes account of the nature of the corrosive medium, which should have an appreciable influence on inhibitor action. Thus, if the composition of the corrosive medium is changed, as by the introduction of some oxidizing agent**, the equilibrium potential of the metal Me_1 changes also, being shifted in the positive direction in this case. Suppose that the new value of the equilibrium potential is $\varphi'_{eq_{Me_1}}$, and is represented by the point G in Fig. 1. Then, as can be readily seen from the values of $\Delta\sigma$ corresponding to $\varphi_{eq_{Me_1}}$, the additives form a different sequence in order of inhibiting action: A < B < C. Additive A, which was the most effective inhibitor in absence of oxidizing agents, should have hardly any inhibiting action in this case. Conversely, the additive C, ineffective under the original conditions, may acquire appreciable inhibiting properties*** [23, 24].

* This simple connection between adsorbability and inhibiting effect does not hold in every case.

** Introduction of an oxidizing agent may, under certain conditions, change the value of $E_{q=\theta_{Me_1}}$, and therefore the shift of φ_{eq} must in general be regarded as the results of changes both of $E_{q=\theta_{Me_1}}$ and $E_{eq_{Me_1}}$.

*** This fact is ignored in a number of investigations. For example, Fischer and Elze [23, 24] showed that iodoethylquinoline, which inhibits the dissolution of iron in acids, ceases to exert an inhibiting effect if an oxidizing agent (ferric salt, chromic acid, etc.) is introduced into the acid solution. Since under these conditions the reaction of hydrogen liberation is replaced by reduction of the oxidizing agent, while the metal ions continue to pass into solution, they assume that the inhibitor can only inhibit the cathodic process of hydrogen evolution, and has no influence on anodic dissolution of the metal. However, this assumption is clearly unjustified, as on the addition of an oxidizing agent the equilibrium potential of iron is shifted in the positive direction, and adsorption of iodoethylquinoline, an additive of the cationic type, corresponding in behavior to additive A (Fig. 1), may become very slight or even impossible, and its inhibiting action is naturally diminished or lost completely as a result.

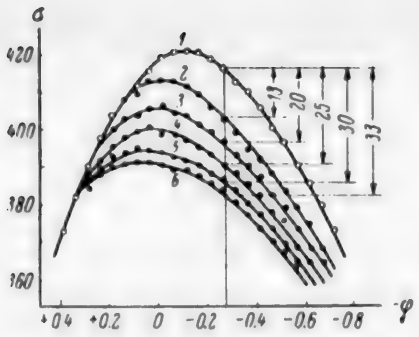

Fig. 3. Decrease of the surface tension of mercury in 1 N HCl solution at $\varphi_{eq_{Fe}} = -0.26$ v in presence of caffeine. Caffeine concentration (millimoles/liter): 1) original solution, 2) 2.15, 3) 4.30, 4) 8.60, 5) 17.20, 6) 34.40.

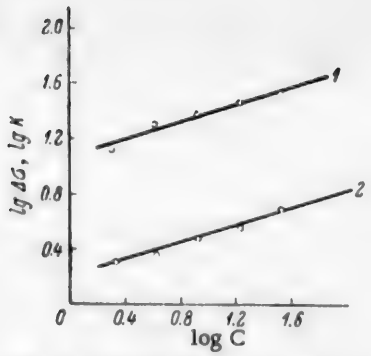

Fig. 4. Plots of log $\Delta\sigma$ − log C (1) and log K − log C (2) for caffeine in 1N HCl at $\varphi_{eq_{Fe}} = -0.26$ v. Values of $\Delta\sigma$ in dynes/cm, C in millimoles/liter.

Determination of a General Relationship Between Surface Activity and Inhibiting Action

By the method described it is possible to estimate the adsorbability of organic compounds on metal surfaces under corrosion conditions, by means of electrocapillary measurements. Although the inhibiting action of organic compounds must be closely related to their adsorbability, this relationship may differ with the nature of the stage of the corrosion process which is influenced by the particular additive [25]. If retardation of corrosion on addition of an inhibitor is caused by its action on the discharge of hydrogen ions or on ionization of the metal atoms, i. e., on reactions in which positively-charged particles are involved, the inhibiting effect, for a given degree of adsorbability, must depend on the electrical nature of the additive, and should be greatest for cations and least for anions. If the action of the additive reduces to mere shielding of the surface or creation of an additional barrier to diffusion, the electrical properties of the particles should play a less important role. Retardation of the recombination of hydrogen atoms into molecules and of their removal from the metal surface should also depend little on the particle charge. In this case, regardless of the nature of the inhibitor particles, the inhibiting effect should increase regularly with increase of the surface activity of the additive.

To test this hypothesis, the relationship between surface activity and inhibiting action was studied for 19 substances (additives), consisting of representatives of different classes of organic compounds: 1) formic acid*, 2) oxalic acid*, 3) acetone*, 4) methyl ethyl ketone* [26, 27], 5) thiourea, 6) sulgin, 7) trimethylbenzylammonium chloride, 8) caffeine, 9) pyramidon, 10) anthranilic acid, 11) tetrabutylammonium sulfate, 12) o-hydroxyquinoline, 13) sulfidine, 14) norsulfazole, 15) (trimethylsilylmethyl) diethylmethylammonium iodide**, 16) (trimethylsilylmethyl) diethylallylammonium iodide**, 17) bis (trimethylsilylmethyl) ethylmethylammonium iodide**, 18) (trimethylsilylmethyl) ethylmethylcyanoethylammonium iodide [28], 19) p-tolylthiourea. The inhibiting action of these substances on the corrosion of iron was tested in 1 N H_2SO_4 at 20°. The electrocapillary curves were plotted and values of $\Delta\sigma$ determined at the equilibrium potential of iron $\varphi_{eq_{Fe}}$, which is − 0.3 v under these conditions [29, 30]***; the specific decreases of surface tension $\Delta\sigma' = \Delta\sigma/C$ were found. The inhibition coefficients $K = j/j_1$, where j is the corrosion rate in acid without inhibitor, and j_1 is the

*Data for calculation of $\Delta\sigma$ were taken from Smirnova's dissertation [26], and for calculation of K', from the paper by Beskov and Balezin [27].

**The authors gratefully acknowledge that the organosilicon compounds were kindly supplied by the laboratory of Corresponding Member (AN SSSR) A. D. Petrov.

***The zero-charge potential of iron was taken as ± 0.00 v in accordance with data on the electronic exit work function for iron [29]. Vasenin's equation [30], with some changes in the values of the constants, was used for the calculations.

corrosion rate in the acid containing inhibitor, and the specific inhibition coefficients $K' = K/C$ were determined; the concentrations (C) of the added organic substances were expressed in moles/liter. The experimental data are plotted in $\log\Delta\sigma' - \log K'$ coordinates in Fig. 2. It follows from Fig. 2 that the specific surface activities and specific inhibition coefficients vary over very wide ranges. Despite this, all the experimental data for iron and a great variety of inhibitors, when plotted in $\log\Delta\sigma' - \log K'$ coordinates, lie around one common curve, which indicates a regular increase of inhibiting action with increasing surface activity. This evidently suggests that the action of physical inhibitors of iron corrosion is primarily determined by their adsorbability, and it can also be regarded as confirmation of the earlier hypothesis concerning the action of physical inhibitors. Deviations from the course of the $\log \sigma' - \log K'$ curve, which differ in character for different types of additives, indicate that, apart from surface activity, inhibiting action is associated with molecular properties which do not have a direct influence on adsorbability. For example, tetrasubstituted ammonium derivatives with organosilicon radicals are more powerful inhibitors than aromatic amines and tetrasubstituted ammonium bases, although their surface activities are the same. The greatest inhibiting effect is produced by Additive 18, which contains a cyano group as well as an organosilicon radical.

Thus, the proposed method can be used for seeking new inhibitors and evaluating their effectiveness. Moreover, correlation of electrocapillary data with corrosion data may prove useful for determination of the inhibiting effects of individual functional groups and clarification of the mechanism of inhibition.

Estimation of Changes of Inhibitor Effectiveness with Concentration from the Results of Electrocapillary Measurements

Literature data relating to different inhibitor concentrations were used in plotting the $\log\Delta\sigma' - \log K'$ relationship. Since, at a given φ_{eq}, the specific surface activity and specific inhibition coefficient depend not only on the nature of the substance but also on its concentration, this may be an additional cause of the deviations of the experimental points from the curve, apart from the causes discussed earlier. Therefore the relationship between $\log\Delta\sigma'$ and $\log K'$, which provides a correct qualitative picture of the variation of inhibiting action with surface activity, cannot be used for exact quantitative characterization of inhibitors. It must be supplemented by data on variations of $\Delta\sigma$ and K with the volume concentration of the inhibibitors. Such data were determined for 9 different substances: caffeine, sulgin, norsulfazole, sulfidine, o-hydroxyquinoline, anthranilic acid, pyramidon, bis(trimethylsilylmethyl)ethylmethylammonium iodide, and (trimethylsilylmethyl) diethylallylammonium iodide.

Electrocapillary curves for 1 N HCl solutions containing various amounts of these inhibitors were determined The curves were then used to find values of $\Delta\sigma$ at φ_{eq}* corresponding to different inhibitor concentrations.

As an example, Fig. 3 shows electrocapillary curves for caffeine; values of $\Delta\sigma$ are also given. A plot of these values of $\Delta\sigma$ against the inhibitor concentration, in logarithmic coordinates (Fig. 4) gives a straight line; its slope γ depends on the nature of the inhibitor.

The corrosion rates of iron in 1 N HCl in presence of the same additives were measured, and the inhibition coefficients determined. A linear relationship, represented by the equation

$$K = \beta \cdot \Delta\sigma, \qquad (1)$$

was found to exist between the inhibition coefficient and the decrease of surface tension; here β is the inhibition coefficient at $\Delta\sigma = 1$ dyne/cm, and it may be regarded as a quantitative measure of inhibitor effectiveness. Within the concentration range studied, log K is a linear function of $\log C_i$. The slopes of the $\log K - \log C$ and of the $\log \Delta\sigma - \log C$ plots coincide for all the additives (for caffeine, see Fig. 4). Therefore the relationship between the inhibition coefficient and concentration can be represented by the equation

$$\log K = \log K_1 + \gamma \log C, \qquad (2)$$

where K_1 is the inhibition coefficient when the inhbitor concentration is unity. Since γ can be found from the results of electrocapillary measurements, to determine the inhbiting action of any substance over a wide concentration range it is sufficient to determine the inhibition coefficient at any one inhibitor concentration.

Thus, considerations of the zero-charge potentials of corroding metals and the use of the φ-potential scale

*Here φ_{eq} was assumed to be equal to the equilibrium potential of iron in 1 N HCl without additives; the small changes of φ_{eq} caused by the presence of inhibitors were disregarded.

give rise to a new method for quantitative study of the inhibiting properties of various substances, based on determination of electrocapillary curves. Equation (1) should be used for selection of new effective inhibitors and quantitative determinations of the inhibiting effect contributed by each functional group in a given compound.

Equation (2) can be used to determine variations of the inhibiting action of a given compound with its concentration with hardly any need for direct corrosion experiments.

SUMMARY

1. The effectiveness of physical inhibitors of acid corrosion of metals is directly related to lowering of the surface tension at the mercury – solution boundary at a potential corresponding to the equilibrium potential of the corroding metal expressed on the zero-point scale.

2. The regular increase of inhibiting action with increasing surface activity can be applied in evaluation of the inhibiting properties of various substances and in searches for new inhibitors.

3. Deviations from this regularity may provide the basis for qualitative studies of the inhibiting effect of individual functional groups in organic compounds, and for elucidation of the mechanism of inhibition of acid corrosion of metals.

4. Quantitative characterization of an inhibitor and of the individual functional groups in its molecules is possible on the basis of the relationship between the inhibition coefficient and the decrease of surface tension at different volume concentrations of the inhibitor.

5. Changes of inhibiting effect caused by changes in the inhibitor concentration can be calculated from electrocapillary curves and the inhibition coefficient determined at one particular inhibitor concentration.

LITERATURE CITED

[1] H. Fischer, Z. Metallkunde, 46, 350 (1955); Werkstoffe and Korr. 6, 26, (1955).

[2] G. Schikorr, Schiff and Hafen, 7, 90 (1955).

[3] I. N. Putilova and L. G. Gindin, J. Appl. Chem. 28, 1298 (1955). •

[4] A. Sieverts and P. Lueg, Z. anorg. Ch. 126, 193 (1923).

[5] F. Rhodes and W. Kuhn, Ind. Eng. Ch. 21, 421 (1927).

[6] C. Mann, B. Zaner, and C. Hultin, Ind. Eng. Ch. 28, 159, 1048 (1953).

[7] I. N. Putilova, S. A. Balezin, and V. P. Barannik, Protection of Metals Against Acid Corrosion (Goskhimizdat, 1945). [In Russian]

[8] S. A. Balezin and S. K. Novikov, Sci. Mem. V. I. Lenin Moscow State Pedagogic Inst. 44, 25 (1947).

[9] J. Ch'Jao and C. Mann, Ind. Eng. Ch. 39, 910 (1947).

[10] N. Hackermann and H. Schmidt, Corrosion 5, 237 (1949).

[11] U. Fischer, Z. Elektroch. 55, 92 (1951).

[12] C. Roht and H. Zeidheizer, J. Electroch. Soc. 100, 553 (1953).

[13] R. George and N. Hackerman, Corrosion 11, 6, 19 (1955).

[14] W. Machu, Korr. and Metallsch. 13, 1, 20 (1937). Z. ang. Ch. 51, 583 (1938).

[15] J. O. M. Bockris and B. Conwey, J. Phys. Chem. 53, 527 (1949).

[16] V. A. Kuznetsov and Z. A. Iofa, J. Phys. Chem. 21, 201 (1947).

[17] J. Jewell, J. Electroch. Soc. 102, 198 (1955).

[18] W. Müller, Trans. Electroch. Soc. 76, 167 (1933).

[19] V. Cupr, Z. Electroch. 45, 297 (1939).

• Original Russian pagination. See C. B. Translation.

[20] H. Gatos, J. Electroch. Soc. 101, 433 (1954).

[21] L. I. Antropov, J. Phys. Chem. 25, 1494 (1951); Proc. Conf. on Electrochemistry (Izd. AN SSSR, 1953), 380. [In Russian]

[22] L. I. Antropov, Trans. Novocherkassk Polytech. Inst. 25, 5 (1954).

[23] J. Elze and H. Fischer, J. Electroch. Soc. 99, 259 (1952).

[24] J. Elze, Metalloberfläche 8, A, 177 (1954).

[25] L. I. Antropov, Problems of Corrosion and Metal Protection (Izd. AN SSSR, 1956), 79. [In Russian]

[26] M. G. Smirnova, Candidate's dissertation (Novocherkassk, 1955). [In Russian]

[27] S. D. Beskov and S. A. Balezin, Sci. Mem. V. I. Lenin Moscow State Pedagogic Inst. 44, 3 (1947).

[28] V. F. Mironov, A. D. Petrov, and N. A. Pogonkina, Bull. Acad. Sci. USSR, Div. Chem. Sci. 64, 762 (1953). *

[29] W. Sachtler, Z. Elektroch. 59, 119 (1955).

[30] R. M. Vasenin, J. Phys. Chem. 27, 878 (1953).

Received December 28, 1956.

* Original Russian pagination. See C. B. Translation.

ANODIC POLARIZATION OF ZINC IN SULFURIC ACID

G. P. Maitak

(Institute of General and Inorganic Chemistry, Academy of Sciences Ukrainian SSR)

This paper contains the results of a study of anodic polarization of zinc in sulfuric acid solutions, carried out by determination of voltage – current curves. This comprises the first part of an experimental investigation carried out in order to establish the possibility and conditions of anodic electrochemical polishing of zinc in sulfuric acid. The shapes and parameters of voltage – current curves, which characterize anodic polarization of a metal in a solution used or tested for electrochemical polishing, are among the most important characteristics of the electrochemical polishing of a metal in particular solutions. Therefore the study commenced with determinations of voltage – current curves.

Research into the electrochemical polishing of zinc and other, softer metals has been stimulated by the fact that the advantages of electrochemical over mechanical polishing of metals, which have frequently been noted, are even more pronounced with these metals because of the difficulties involved in their mechanical polishing. Difficulties in the production of a mirror surface on zinc by mechanical polishing have long existed, and have not been overcome as yet.

In earlier work [1, 2] on the measurement of the optical properties of metals, the results of which have been accepted in reference works [3], satisfactory specular surfaces could not be obtained on zinc. In later studies of the optical constants of metals [4], zinc with a specular surface was obtained, but it was noted that this required great experience and much time. However, it is stated that the presence of layers difficult to remove, which is inevitable in mechanical polishing of metals "distorts the optical constants so much that there is still considerable uncertainty about the numerical values of n and k" [5].

Difficulties in the mechanical polishing of zinc are also met in metallographic studies [6], because of the ease with which the structure can be changed in pure, and especially in coarse-grained zinc.

Attempts to improve the mechanical polishing process are still being made [7] while in work on the electrochemical polishing of metals much attention is devoted to studies of the electrochemical polishing of zinc. The electrochemical polishing of metals was discovered [8] in studies of the anodic dissolution of zinc and silver. It is thought [9] that the electrochemical polishing of zinc and zinc alloys has a promising industrial future.

Numerous electrolytes have already been recommended for the electrochemical polishing of zinc [10-29].

Electrochemical polishing takes place ". . . in a solution containing an electrolyte (usually one which forms complex ions with the particular metal) in presence of which anodic polarization results in unstable passivation of the metal, primarily manifested by the fact that the current strength does not increase with the voltage, i. e., by an anomalous current – voltage curve" [8]. Therefore, although new solutions for electrochemical polishing of metals are still being found by empirical methods, it may be assumed that, as has already been noted [30-32] solutions used for electrochemical polishing of metals are characterized by the presence of passivators, oxidizing agents, and activators which dissolve the film formed on the metal during anodic polarization.

It is known that the oxidizing properties of sulfuric acid, its ability to dissolve metals, and the solubility of sulfates, all change with increasing concentration of the acid. The composition of the products formed on an insoluble anode in electrolysis also changes, and, although the process taking place at the anode in electrolysis of concentrated sulfuric acid solutions are not yet fully understood, the important fact is that strong oxidizing agents

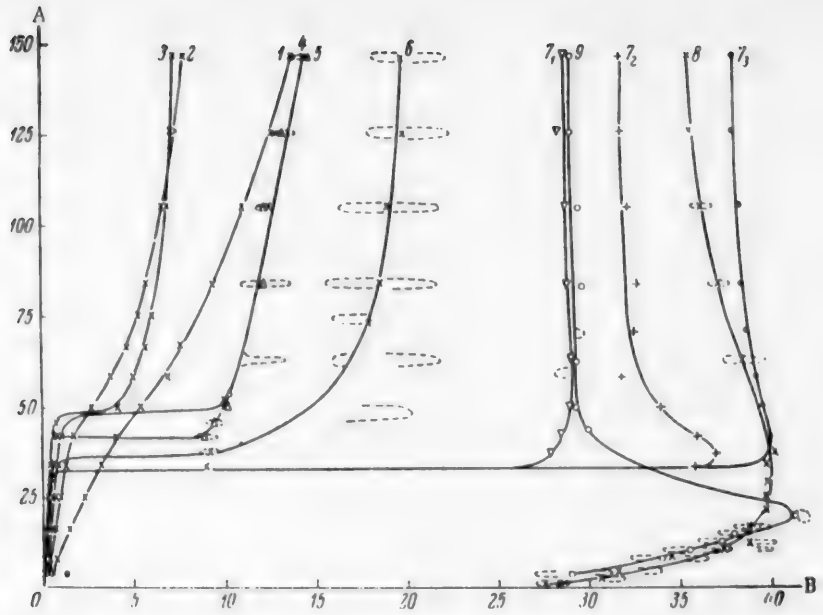

Fig. 1. Voltage – current curves showing variations of the anodic polarization of zinc with current density in unstirred solutions of sulfuric acid, in measurements at increasing current strength.
A) Anodic current density (amps/dm^2), B) voltage between electrodes (v). Sulfuric acid concentration (wt. %): 1) 2; 2) 5; 3) 10; 4) 20; 5) 30; 6) 40; 7_1, 7_2, 7_3) 50; 8) 70; 9) 85.

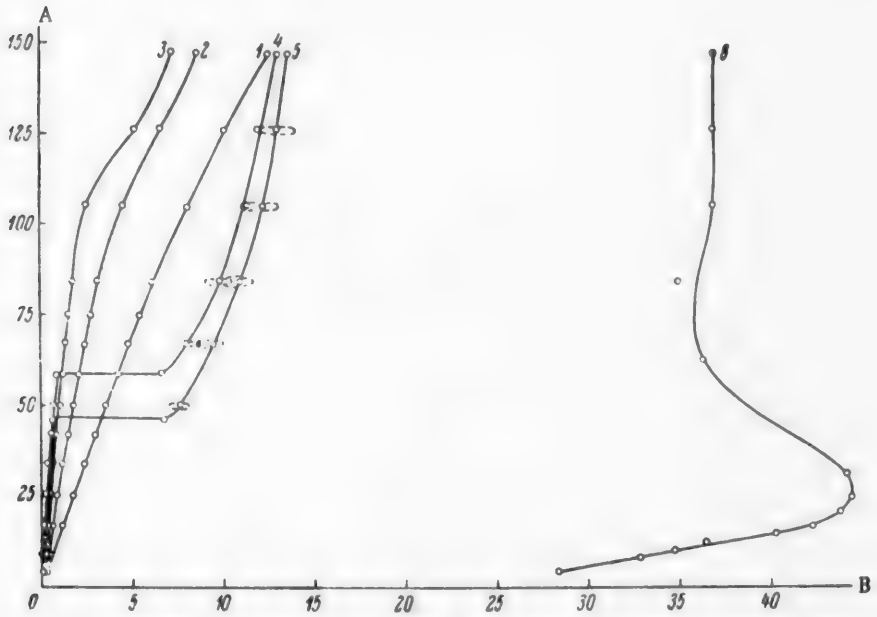

Fig. 2. Voltage – current curves showing variations of the anodic polarization of zinc with current density in stirred solutions of sulfuric acid, in measurements at increasing current strength.
A) Anodic current density (amps/dm^2), B) voltage between electrodes (v). Sulfuric acid concentration (wt. %): 1) 2, 2) 5, 3) 10, 4) 20, 5) 30, 6) 85.

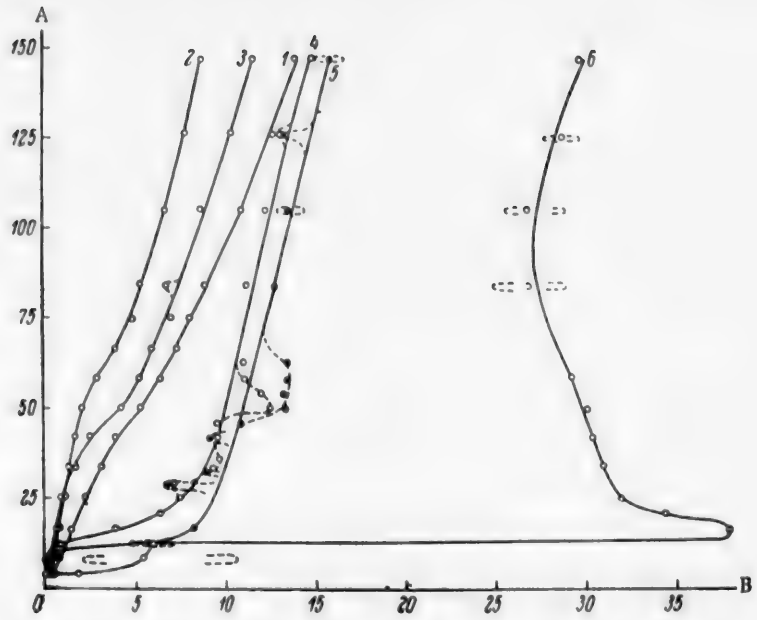

Fig. 3. Voltage – current curves showing variations of the anodic polarization of zinc with current density in unstirred solutions of sulfuric acid, in measurements at decreasing current strength.
A) Anodic current density (amps/dm^2), B) voltage between electrodes (v). Sulfuric acid concentration (wt. %): 1) 2, 2) 5, 3) 10, 4) 20, 5) 30, 6) 40.

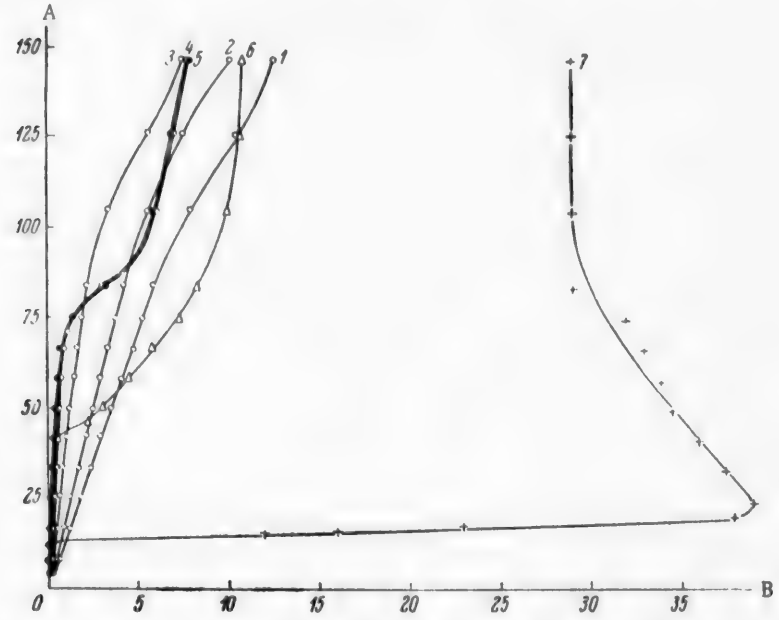

Fig. 4. Voltage – current curves showing variations of the cathodic polarization of zinc with current density in stirred solutions of sulfuric acid, in measurements at decreasing current strength.
A) Anodic current density (amps/dm^2), B) voltage between electrodes (v). Sulfuric acid concentration (wt. %): 1) 2, 2) 5, 3) 10, 4) 20, 5) 30, 6) 40, 7) 50.

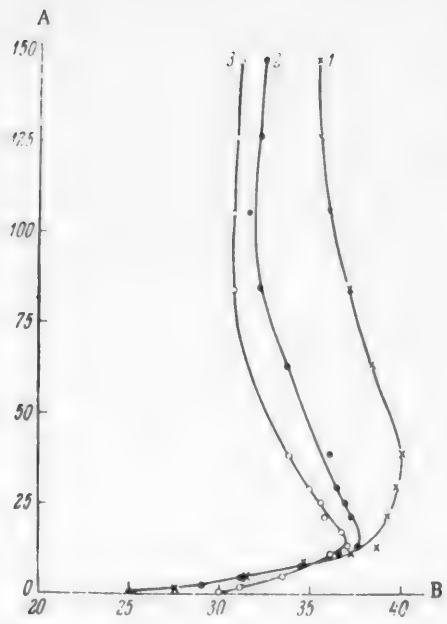

Fig. 5. Effect of temperature on the voltage – current curves showing variations of cathodic polarization of zinc with current density in 70% sulfuric acid, in measurements at increasing current strength (solution not stirred).
A) Anodic current density (amps/dm^2), B) voltage between electrodes (v). Solution temperature (°C): 1) 20, 2) 50, 3) 80.

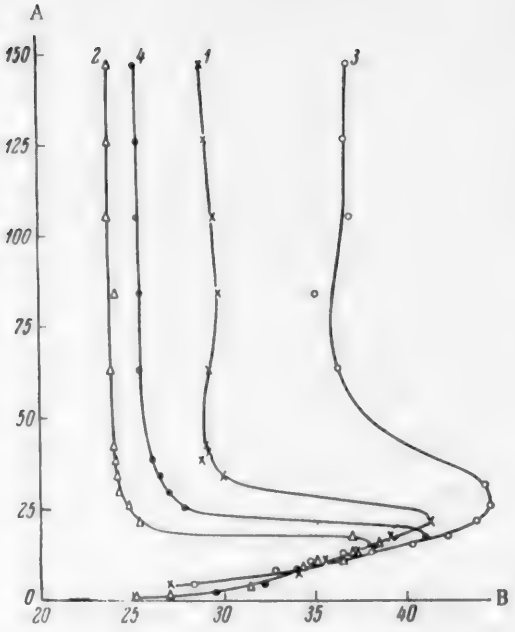

Fig. 6. Effects of temperature and stirring on the voltage – current curves showing variations of cathodic polarization of zinc with current density in 85% sulfuric acid, in measurements at increasing current strength.
A) Anodic current density (amps/dm^2), B) voltage between electrodes (v). 1, 2) Solution not stirred; 3, 4) solution stirred. Temperature (°C): 1, 3) 20; 2, 4) 80.

are formed at high current densities. It is therefore natural to assume that by variation of the sulfuric acid concentration, current density and other electrolysis conditions it is possible to vary the relative oxidizing, passivating, and solvent effects at the anode in such a way as to make possible the electrolytic polishing, in sulfuric acid, of metals which formerly could not be treated by this process. Effects have already been observed in the anodic dissolution of zinc in sulfuric acid [33, 34], which confirm this assumption with regard to zinc.

In determinations of the voltage – current curves the voltage at the cell terminals was measured at each given current density. Curves of a different shape are obtained if the current strength is measured at each given voltage, but the effects revealed by the one method are also revealed by the other, since the variations of current density and voltage are interconnected by Ohm's law.

All the experiments were performed with electrodes cut from sheet zinc, 1.0 and 1.5 mm thick, containing the following impurities (%): Fe 0.0030, Cu 0.012, Cd 0.0017 and Sn 0.0005. The working areas of the electrodes were: anodes, 0.024 dm^2 (width 6 mm and immersion depth 20 mm), and cathodes, 0.71 dm^2 (width 74 mm and immersion depth 48 mm). The cathode and anode were placed vertically. The distance between them was about 2 cm in all the experiments. This distance was adjusted and checked by means of a gage, but variations of 1.0-1.5 mm were possible. In every experiment a new zinc anode was used, the surface being always prepared by the same method – coarse polishing on a corundum disk. To prevent spontaneous dissolution of the zinc cathode during the intervals between determinations, the electrolysis was not discontinued, but the current was switched over to an auxiliary platinum anode. This increased the service life of the zinc cathodes.

The current source was a storage battery in parallel with a selenium rectifier. The electrolytic cell in all the experiments was a glass beaker, 1 liter in capacity, containing 400 ml of solution.

Sulfuric acid solutions of the following concentrations (in wt. %) were used: 2, 5, 10, 20, 30, 40, 50, 70 and 85; both static (unstirred) and stirred electrolytes were used. The solutions were stirred by means of a glass stirrer rotating at 300 revolutions/minute. The solution temperature was 18-20°. Some experiments with concentrated solutions, in which zinc anodes were strongly passivated, were carried out at 50 and 80°.

The measurements required for the plotting of the voltage – current curves were carried out at increasing current densities, and in most cases also at decreasing current densities. Each type of determination was performed in triplicate, each time in a different experiment with new specimens. The voltage – current curves (Figs. 1-6) were plotted from the average voltages for each current density in these triplicate experiments. The results of the individual experiments in most cases agreed to within a few hundredths of a volt, but in some solutions the polarization of zinc is unstable, and at a given current strength the voltage in a given experiment fluctuates, while the variations between duplicate experiments may be a few volts. In such cases the average values from three triplicate experiments were also used, but the limits of the observed fluctuations are indicated by dash lines. The second ascending branches of the voltage – current curves for 50% sulfuric acid are greatly displaced for some experiments, and are therefore plotted separately (Fig. 1, Curves 7_1, 7_2, and 7_3).

It follows from Figs. 1-6 that the shapes of the voltage – current curves and the voltage ranges in which they lie vary considerably with the sulfuric acid concentration.

The curves for 2, 5, 10, 20, 30, and 40% sulfuric acid solutions (Figs. 1-4) each have a clear inflection between the first and second ascending branches. Under the conditions corresponding to the first ascending branch of the voltage – current curve, zinc undergoes spontaneous and anodic dissolution, with formation of a pitted and corroded surface. After the limiting current has been reached, under conditions corresponding to the second ascending branch of the voltage – current curve, which is not subject to a limiting current, spontaneous dissolution of zinc ceases, and it is subject to anodic dissolution only, with formation of a mirror surface, accompanied by decomposition of water [35] with liberation of oxygen at the anode. Electrochemical polishing occurs only after spontaneous dissolution of the zinc anodes in sulfuric acid has ceased, after the limiting current has been reached.

The following effects were observed visually at the zinc anode in all the sulfuric acid solutions for which the voltage – current curves are of the form described. When the zinc anodes are immersed in the acid, without current flowing, with current below the limiting value, or even above the limiting value (but in the latter case only until the kick of the galvanometer needle corresponding to the inflection on the voltage – current curve is recorded), zinc dissolves spontaneously at a rate which depends on the acid concentration. In the more concentrated solutions (20, 30, and 40%) the process is very vigorous, with violent evolution of gas near the zinc anode. In solutions between 2 and 40% concentration, decrease or increase of current strength to the limiting value or even above it (but in the latter case only for a brief time, so that no kick is yet recorded on the voltmeter) has no influence on the effects visually observed. However, after the kick on the voltmeter corresponding to the limiting current has been observed, there is an immediate qualitative change of the picture observed at the anode. Spontaneous solution of zinc in sulfuric acid of all these concentrations ceases, the surface of the metal becomes bright and lustrous, and streams of heavy liquid flow down it. If the current is only a little above the limiting value, gas evolution at the anode is almost imperceptible. With further increase of the current strength during the voltage – current determinations, no qualitative changes were observed either visually at the anode, or in the voltage – current curves. Gas evolution at the anode became more vigorous, but the bubbles were smaller than in spontaneous dissolution. These effects were observed in the reverse sequence in determinations at decreasing current strengths.

If the solutions are stirred, the voltage – current curves are smoothed out, the hysteresis loop between the direct and reverse voltage – current curves decreases, the limiting current is shifted toward higher values, while the second ascending branches are shifted toward lower interelectrode voltages.

The anodic passivation of zinc increases with increasing acid concentration in these and in more concentrated solutions. The voltage – current curves for unstirred 20, 30, and 40% sulfuric acid solutions (Fig. 1), and especially curves for 40% solutions, lie in a region of much higher voltages than the curves for anodic polarization of zinc in more dilute solutions. In the voltage – current curves determined at increasing current strengths in unstirred 20, 30, and 40% sulfuric acid solutions, the second ascent begins at similar voltages, while higher current densities (150 amps/dm^2) correspond to much higher voltages in 40% than in 30 or 20% acid. This last effect cannot be attributed to ohmic drop of potential in the solution, as these three solutions differ little in specific conductance, which is higher for 40% than for 20% solution. Other data also suggest that the cause of these changes

in the voltage – current curves with change of acid concentration lies in greater anodic passivation in 40% sulfuric acid, and in more highly concentrated solutions in general, than in 20 and 30% acids. For example, this view is supported by the indications of changes in oxidation processes at the anode in the electrolysis of sulfuric acid with variations of concentration and current density, which follow from data on the yields of persulfuric acid at platinum anodes [36]. At a current density of 5 amps/dm^2 formation of persulfuric acid can be detected in sulfuric acid solutions of about 40% strength and higher. At 50 amps/dm^2 the yield of persulfuric acid in 40% sulfuric acid solution is considerable, while at 100 amps/dm^2 it is 70%.

However, the passivation of zinc in these solutions is unstable, and the reverse voltage – current curve, determined with decreasing current strength, is similar in form to the curve determined with increasing current strength; it reproduces the course of the latter, although with some hysteresis, and after a reverse jump of potential it approaches the abscissa axis along the first ascending branch.

In 50% sulfuric acid the anodic passivation of zinc is considerably greater, and the second ascending branch of the voltage – current curve is displaced sharply toward higher voltages.

Anodic passivation of zinc is even more pronounced in 70 and 85% sulfuric acid solutions (in solutions of higher concentrations than these, the current soon ceases to flow because of the formation of a nonconducting film). The voltage – current curves for 70 and 85% sulfuric acid solutions lie in the region of higher voltages, and are quite different in form from the curves for more dilute solutions. In these solutions, immediately after the current is switched on, and with only a slight increase of current, the voltage rapidly rises to a maximum value, beyond which it decreases rapidly with further increase of current strength, so that the points on this branch of the curve cannot be recorded. After this, with further increase of current strength to the maximum values, which reached about 150 amps/dm^2, the voltage changes slightly and the curve ascends. The surface of the zinc anodes in these solutions becomes coated with a grayish-white film which offers resistance and limits the process. even at the start of the determinations, when the voltage is rising rapidly to a maximum. At the critical point, when the voltage begins to fall after having reached a maximum, the specimen becomes vigorously attacked at some single region. At the end of the determination, a small region of the specimen is found to be strongly attacked while the rest is merely coated.

The voltage – current curves are shifted in the direction of lower voltages with increase of temperature (Figs. 5 and 6). This is probably due to increasing corrosiveness of the solutions.

The voltage – current curves corresponding to 70 and 85% sulfuric acid solutions, and the effects observed at the zinc anodes in these solutions, are similar to the known voltage – current characteristics of solid dielectrics and to processes observed in the breakdown of solid dielectrics [37]. In electrolysis at high current densities processes may apparently take place at the electrodes which are similar to the processes which occur in the breakdown both of liquid [35] and of solid dielectrics.

The voltage – current curves described above indicate the great variations of passivation and solubility of zinc anodes with acid concentration and current density. The specimens obtained in these determinations could be used to estimate the concentrations of sulfuric acid solutions in which electrochemical polishing of zinc is possible.

The specimens used for determinations of the voltage – current curves for 85, 70, and 50% sulfuric acid solutions were coated with a dull white film, and were corroded; in each of the first two cases, only at one region, but right through the plate, while the specimens from 50% solution were corroded all over the surface, sometimes to a greater extent near one edge, which became sharpened.

The specimens used in determinations of the voltage – current curves at increasing current strength in stirred 2, 5, 10, 20, 30, and 40% solutions of sulfuric acid were mirror-bright and polished on the surface. Stirring always resulted in better leveling and polishing of the surface. In determinations in unstirred solutions, zinc was polished only in 5 and 10% sulfuric acid solutions; 30 and 40% solutions gave no polishing effect at all, while in 2 and 20% solutions the zinc was polished, but the effect was much worse than in stirred solutions of the same concentrations. The specimens used in determinations of voltage – current curves in sulfuric acid solutions from 2 to 40% concentration at decreasing current strength were coated with a black deposit, which was easily removed.

SUMMARY

1. Anodic polarization of zinc in sulfuric acid is accompanied by anodic passivation and electrochemical polishing. The anodic passivation is unstable under the experimental conditions used, and increases with increasing acid concentration.

2. The voltage – current curves for the anodic polarization of zinc in sulfuric acid solutions from 2 to 40% concentration, determined both at increasing and at decreasing current strengths, are similar in form, although with some hysteresis, and consist of two ascending branches connected by a plateau which is caused by passivation. The voltage – current curves for anodic polarization of zinc in 70 and 85% sulfuric acid solutions lie in the region of considerably higher voltages, and resemble the known voltage – current characteristics of solid dielectrics.

3. Electrochemical polishing of zinc occurs in stirred sulfuric acid solutions, from 2 to 40% concentration, under conditions corresponding to the second ascending branch of the voltage – current curve. In anodic polarization in more highly concentrated (50, 70, and 85%) sulfuric acid solutions, zinc becomes coated with a high-resistance film.

LITERATURE CITED

[1] P. Drude, Ann. Phys. Chem. (Neue Folge), 39, 481 (1890).

[2] W. Meier, Ann. Phys. (Vierte Folge), 31, 1017 (1910).

[3] Landolt – Börnstein, Phys. Chem. Tabelle. Fünfte Auflage. Berlin II, 905 (1923); ibid. I, Ergbd. 476 (1927).

[4] G. Pfestorf, Ann. Phys. (Vierte Folge), 81, 906 (1926).

[5] C. Schaefer, Theoretical Physics, III, part 2, optics (Moscow-Leningrad, GONTI, 1938), 73 [Russian translation].

[6] E. E. Levin, Microscope Studies of Metals (Practical Handbook) (Moscow-Leningrad, Mashgiz, 1951) 76. [In Russian].

[7] B. Kleinschmidt, Metall, 6, 522 (1952).

[8] E. Shpital'skii, "Method for conferring a bright polished appearance on metal surfaces and galvanic metal deposits." Patent presented in Moscow, April 19, 1911 (certif. No. 46,537) and issued April 30, 1913 (No. 23,897, class 48). •

[9] S. Wernick, Electrolytic Polishing and Bright Plating of Metals. London, 68 (1951).

[10] H. Strecker, German Patent 302,902.

[11] W. H. J. Vernon and E. G. Stroud, Nature, London 142, 477, 1161 (1938).

[12] C. Schaefer, Met. Ind. 38, 22 (1940).

[13] E. Raub and B. Wullhorst, Ztb. I, 1553 (1942).

[14] R. W. Parcel, Met. Progr. 42, 209 (1942); Met. Ind. 62, 69 (1943); A. De Sy and H. Haemers, Met. Progr. 53, 368 (1948).

[15] A. De Sy and H. Haemers, St. and E. 61, 185 (1941).

[16] J. L. Rodda, Mining and Met. 24, 323 (1943); O. Smeskal, Met. Progr. 47, 729 (1945); G. Tolley, Metallurgia, 37, 71 (1947).

[17] F. C. Mathers and R. E. Ricks, Proc. Ind. Acad. Sci. 53, 130 (1943).

[18] R. W. Manuel, U. S. Patent 2,330,170 (1943). •

[19] A. I. Levin, Machine Tools and Instruments 3, 9 (1944).

[20] P. A. Jacquet, Metaux corrosion – usure, 19, 71 (1944).

• Original Russian pagination. See C. B. Translation.

[21] C. L. Faust, U. S. Patent 2,373,466 (1945).

[22] Danish Patents 75,527 and 75,489 (1945).

[23] I. Glayman and I. Skogh, French Patent 1,001,514 (1946).

[24] J. Itsumi and I. A. Akamutsu, Japanese Patents 1507, 1510, and 1511 (1950).

[25] T. Furukawa, J. Electroch. Soc. Japan, 19, 372 (1950); C. A, 46, 4929 (1952).

[26] K. Nagai and K. Mano, C.. A. 46, 3426 (1952); M. Krieg and E. Lange, Naturwiss. 39, 209 (1952).

[27] J. Miyoshi and J. Kitano, Japanese Patent 2204 (1951).

[28] S. Tajuma et T. Mori, C. r. 234, 1976 (1952).

[29] E. Knuth-Winterfeldt, Kemisk, 34, 1, 1 (1953).

[30] B. P. Artamonov, N. P. Fedot'ev, and N. I. Razmetov, Jubilee Volume on the Twentieth Anniversary of the State Institute of Applied Chemistry (Leningrad, State Chem. Tech. Press, 1939), 22. [In Russian].

[31] L. Ia. Popilov, Electropolishing of Metals (Moscow-Leningrad, Mashgiz, 1947), 13. [In Russian].

[32] V. I. Lainer, Electrolytic Polishing of Metallic Articles (Moscow, State Local Industries Press, 1948), 5. [In Russian].

[33] E. S. Hedges, J. Chem. Soc. 2580 (1926).

[34] W. J. Muller and L. Holleck, Monatsh. 52, 425 (1929).

[35] G. P. Maitak, Ukrain. Chem. J. 17, 317 (1951).

[36] J. W. Mellor, A Comprehensive Treatise on Inorganic andTheoretical Chemistry, 10, 454 (1935).

[37] A. Gemant, Electrophysics of Insulating Materials (published by the Commission for Improving the Living Conditions of Students, Leningrad, 1932) 112 and 197 [Russian translation].

Received May 30, 1958.

ELECTROLYTIC DEPOSITION OF SILVER WITH PERIODIC REVERSAL OF DIRECT CURRENT

N. A. Marchenko, I. N. Leknovitskii, and A. N. Buianova

(The V. I. Lenin Polytechnic Institute, Khar'kov)

Silvering is a process very widely used in electroplating. The chief merits of silver are its high chemical resistance and bright luster. The good electrical properties (conductivity) of silver are frequently used. However, silver plating is an unproductive process, as the current densities used in industrial practice do not exceed 0.3-0.5 amp/dm^2. Dense deposits are obtained only if their thickness does not exceed 10μ; thicker deposits are loose and require scratch finishing. Another disadvantage of silver coatings is their low hardness. In consequence the question of improving the technology of silver plating has often been raised. One of the most progressive methods used at the present time is metal deposition with reversal of current.

Perodic current reversal creates conditions for the formation of smooth, dense deposits at higher current densities; the reason is that while the article acts as the anode, surface irregularities are removed from it. Reversal of current in electrolysis processes has been used for a long time, but detailed studies of this procedure have been started only recently.

Numerous investigations [1-20] have shown that the use of current reversal in the deposition of nickel, zinc, copper, and other metals gives favorable results, with higher productivity and improved deposit quality.

Until recently the literature contained no data on the use of current reversal in silver plating. Some work has now been done on the subject [21-25], but the process has not been studied in sufficient detail, and there are no recommendations relating to its industrial use.

EXPERIMENTAL

The electrolyte used had the following composition (in g/liter): $AgNO_3$ 35, KCN_{total} 54, KCN_{free} 27. The electrolysis was carried out at 20° in a rectangular cell, 500 ml in capacity, without stirring. The anodes were silver plates, and the cathodes were of copper or silver. The anodes and cathodes were equal in area ($S_c : S_a = 1$).

For investigation of the potential – time relationship, the potential difference between the test electrode and a calomel electrode was fed through a direct-current tube amplifier to an electromagnetic 8-loop oscillograph type MPO-2. Variations of current strength with time were also studied by means of the oscillograph. The results were mechanically recorded on a highly sensitive photographic film moving at 4 mm/second. The current efficiency was determined by means of a copper coulometer in the direct-current circuit. The circuit diagram of the electrolysis apparatus is given in Fig. 1, and of the reverser, in Fig. 2.

The effects of the current-reversal conditions on the productivity of the process, and on such quality characteristics of the deposits as dispersity, texture, uniformity of metal distribution, and microhardness were studied. The dispersity of the deposits was determined by the metallographic method. Grain area was calculated from the formula:

$$F = \frac{f \cdot 10^6}{N \cdot v^2},$$

where F is the grain area (in μ^2), f is the measured area (mm^2), N is the number of grains in area f, and v is the magnification.

The number of grains in the measured area was calculated statistically, and results from 15 determinations were taken. The texture was studied with the aid of x-ray patterns taken in a Debye camera by the polished section method.

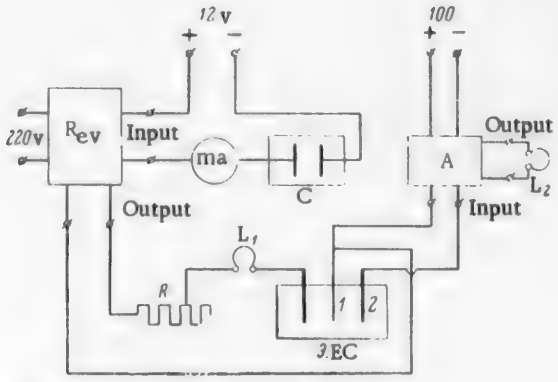

Fig. 1. Electrolytic circuit diagram.
Rev) reverser; ma) milliammeter; C) coulometer; R) rheostat; L_1) loop for measurement of current strength; EC) electrolytic cell; 1) test electrode; 2) calomel electrode; A) amplifier; L_2) loop for measurement of potential difference.

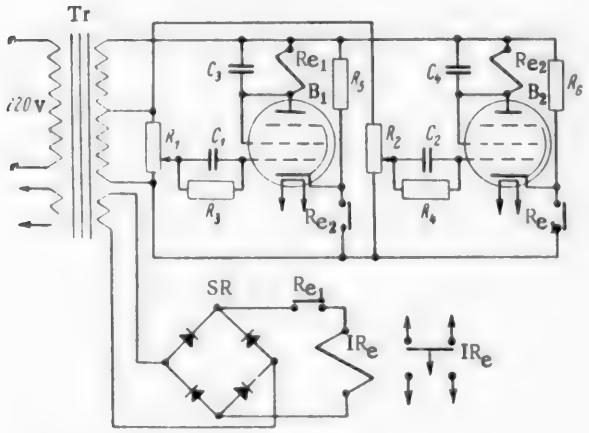

Fig. 2. Reverser circuit.
Tr) Transformer; R_1 and R_2) potentiometers; R_3, R_4, R_5, and R_6) resistances; Re_1 and Re_2) relays; C_1 and C_2) grid capacitors; C_3 and C_4) blocking capacitors; B_1 and B_2) beam tetrode; IRe) intermediate relays; SR) selenium rectifier.

Microhardness was determined by means of the PMT-3 instrument by indentation of the pyramid at an angle of 136° and a load of 25g.

The uniformity of metal distribution was tested in a cell with cathodes connected in parallel. The cell consisted of a rectangular vessel 140 x 80 x 80 mm. The distance between the cathode centers and between the nearest cathode and anode was 40 mm. The anode was of silver, and the cathodes of copper, 20 x 20 mm in size.

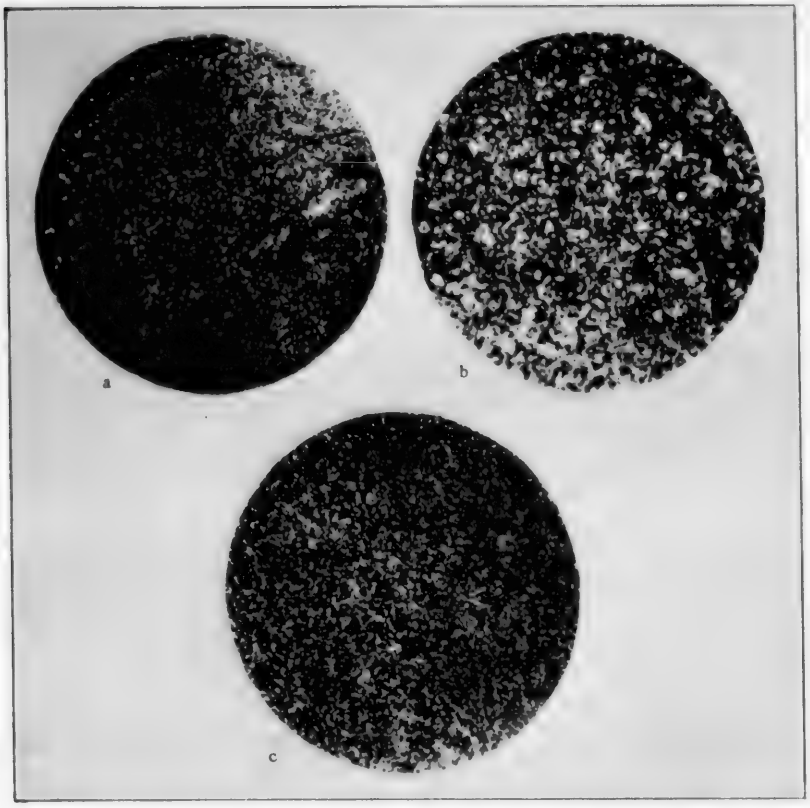

Fig. 3. Surface structure of electrolytic deposits formed at d = 0.5 amp/dm^2. a, b) With direct current, electrolysis time 30 and 120 minutes respectively; c) T = 11 seconds, t_c/t_a = 10, electrolysis time 120 minutes.

TABLE 1

Characteristics of Deposits

Current density (amps/dm^2)	Deposition time (minutes)	Electrolyte temperature (°C)	Deposits formed with			
			reversed current		steady current	
			external appearance	grain size (μ^2)	external appearance	grain size (μ^2)
0.5	30	20	Fine-grained, dull	—	Fine-grained, dull	4.5
0.5	60	20	the same	4.15	the same	6.25
0.5	120	20	" "	4.46	Coarse-grained, dull	62.5
1	30	20	" "	4.35	the same	104
1	60	20	" "	4.62	—	—
1	120	20	" "	5.9	—	—
1	180	20	Coarse-grained, dull	213	—	—

In each determination the electrolysis was continued for 30 minutes, and the weight increase of each cathode (as a percentage of the total increase) was found.

2 series of experiments were carried out.

In the first series of experiments the total period T was 11 seconds, and the ratio of the cathode and anode periods, t_c/t_a, was 10.

TABLE 2

Uniformity of Metal Distribution

Current	Current density (amps/dm²)	Uniformity of distribution on cathodes (%)		
		I	II	III
Reversed	1	41.45	31.15	27.4
The same	0.5	44.45	27.9	27.65
Steady	0.5	46.5	29	24.5

TABLE 3

Effects of the Electrical Deposition Conditions on the External Appearance of the Deposits and the Deposition rate

T (seconds)	t_c/t_a	Reversal frequency (per minute)	Maximum operating current density (amps/dm²)	Deposit	Current efficiency (%)	Deposition rate (μ/minute)
11	10	5.5	1.5	Dull	82	0.82
5	9	12	1.75	Semibright.	80	0.88
12	5	5	1.5	The same	66.6	0.62
3	5	20	2	Almost bright.	66.6	0.83
21	2	2.9	1.5	Semibright.	33.3	0.31
2.5	2.3	24	2.5	Bright.	40	0.63

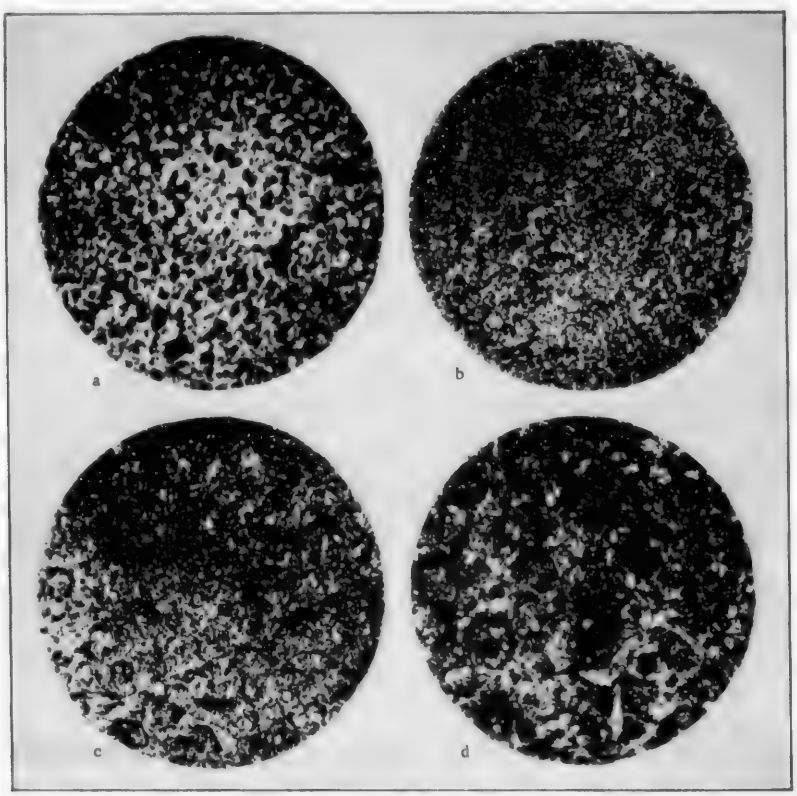

Fig. 4. Surface structure of deposits formed at d = • amps/dm².
a) With direct current, electrolysis time 30 minutes; b, c, d) T = 11 seconds, t_c/t_a = 10, electrolysis time 30, 120, and 180 minutes respectively.

• Omission in Russian - Publishers note.

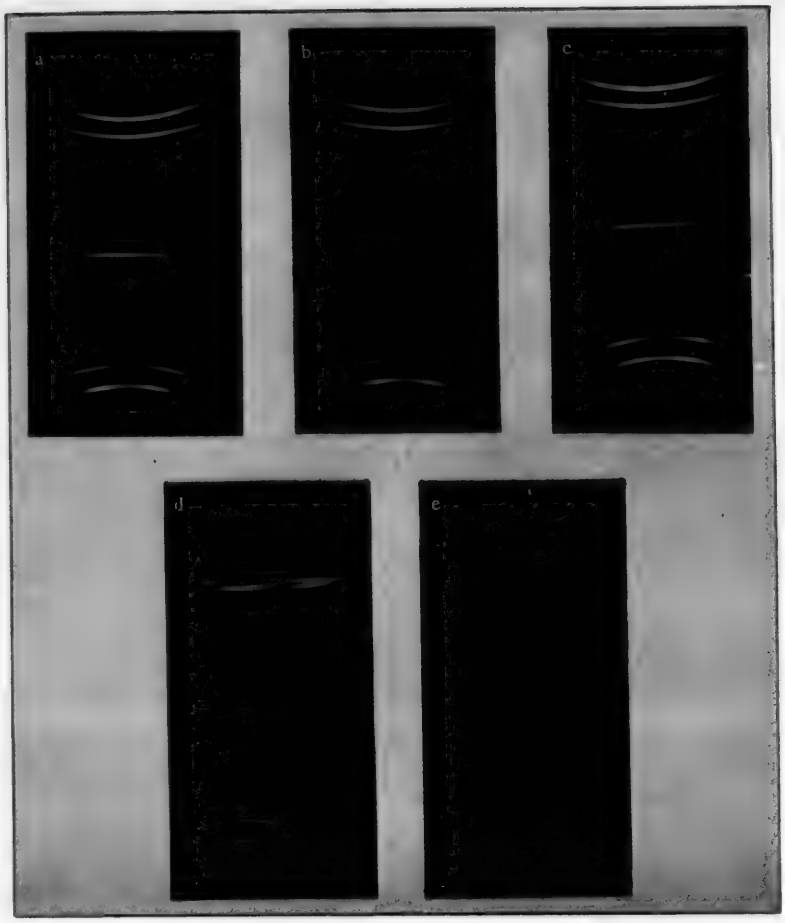

Fig. 5. x-Ray patterns of the deposits.
a) Direct current, d_c = 0.5 amp/dm^2, single crystal size (s. c.) ~ 5μ; b) t_c/t_a = 10/1, d = 1.5 amps/dm^2, s. c. ~ 2μ; c) t_c/t_a = 10/2, d = 1.5 amps/dm^2, s. c. ~ 1μ; d) t_c/t_a = 14/7, d = 1.5 amps/dm^2, s. c. ~ 1μ; e) t_c/t_a = 1.75/0.75, d = 3 amps/dm^2, s. c. < 1μ.

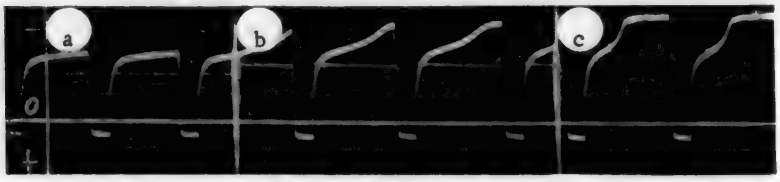

Fig. 6. Variations of polarization and current strength with time at t_c/t_a = = 2.5/0.5. Current density (amps/dm^2): a) 2, b) 2.5, c) 3.

It follows from the data in Table 1 and Figs. 3 and 4 that deposits formed with reversal of current have a finer crystal structure than deposits formed with the use of direct current. This effect is especially prominent with increase of the electrolysis time. For example, in deposition lasting two hours (d = 0.5 amp/dm^2) the grains formed with the use of direct current are about 14 times the size of the grains formed with the use of current reversal.

At a current density of 1 amp/dm^2 the deposits formed with the use of direct current are coarse-grained

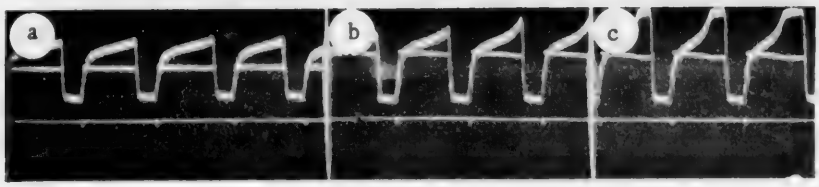

Fig. 7. Variations of polarization and current strength with time at t_c/t_a = = 1.75/0.75. Current density (amps/dm^2): a) 2.5, b) 3, c) 3.5.

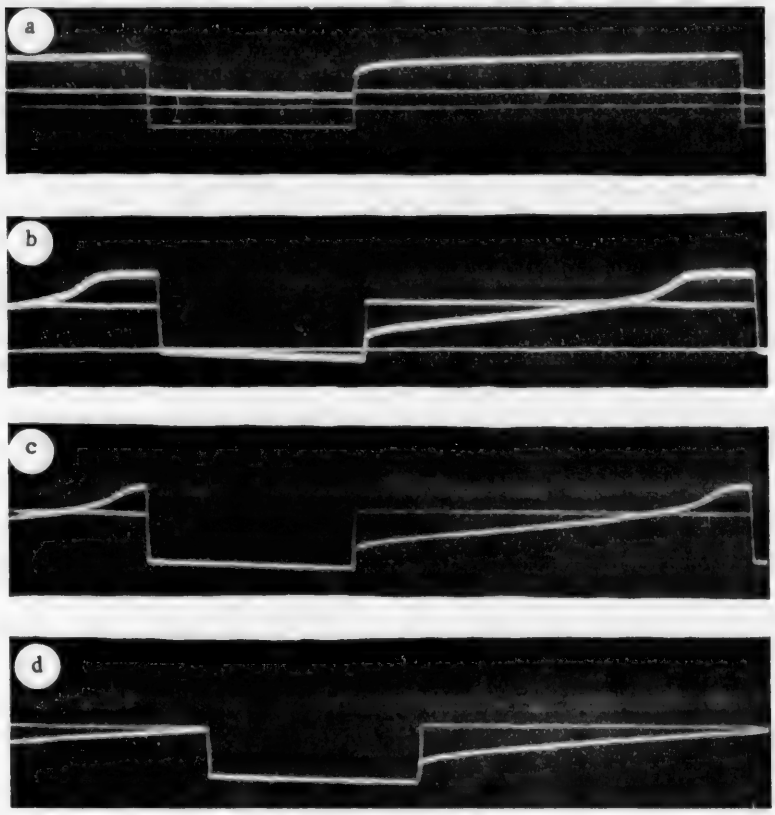

Fig. 8. Variations of polarization and current strength with time. Current density (amps/dm^2) and time (minutes) respectively: a) 1 and 15, b) 2 and 15, c) 2 and 30, d) 2 and 60.

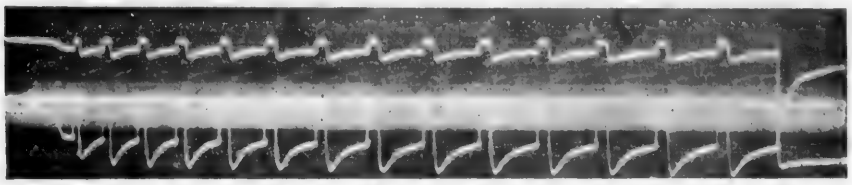

Fig. 9. Variations of polarization and current strength with time at d = 4 amps/dm^2.

and loose even after brief electrolysis. The deposits formed at this current density with current reversal are fine-grained, dense, and do not need scratch polishing even after two hours of electrolysis. By this procedure it

is possible to obtain compact deposits up to 60μ thick, with little variation of grain size. It follows from the data in Table 2 that the uniformity of metal distribution is better with the use of current reversal, and with increase of current density. The deposits formed by the reversal procedure are harder than those obtained with steady current (the hardness on the H_v scale is 105-100 in the former case, and 76-78 in the latter).

In the second series of experiments different current-reversal regimes were studied in order to find deposition conditions in which bright coatings are formed, with maximum increase of productivity.

The deposition conditions were chosen so as to reveal the effects of the t_c/t_a ratio, duration of the anode period (t_a), and number of reversals per minute (n) on deposit quality.

Since the structure and external appearance of deposits depend on the current density and deposition time, the deposits taken for comparison were obtained at the maximum operating current density for each regime, the deposit thickness being 15μ.

It follows from Table 3 that the greatest influence on the external appearance of the deposits is exerted by the reversal frequency and duration of the anode period, and not by t_c/t_a, as stated in some papers [17].

Bright, microcrystalline deposits are obtained at n = 20-24. For determination of the effect of current reversal on orientation, x-ray photographs were taken; some of these are shown in Fig. 5.

The deposits formed with and without current reversal give similar x-ray patterns with regard to perfection of structure and crystal axes. However, the single crystals in deposits formed under reversal conditions are considerably smaller than in deposits formed under steady current; the smallest single crystals are formed at t_c/t_a = 1.75/0.75, that is, at the highest reversal frequency. This explains why the densest, bright deposits, probably of minimum porosity, are formed under precisely these conditions.

The reversal frequency also influences the productivity of the process, as the higher the reversal frequency, the greater is the limiting current density.

The current efficiency is determined by the ratio of the cathode and anode periods (t_c/t_a), as the cathodic and anodic current efficiencies are 100% in the current-density range used; this is fully confirmed by experimental data.

Under all the deposition conditions with current deversal (except for t_c/t_a = 2), the deposition rate is 2-2.5 times the rate under steady conditions.

Examination of the oscillograms (Figs. 6-8) leads to the conclusion that the anode and cathode processes take place without the so-called "overvoltage," i. e., current reversal does not result in increased polarization during the first instant of electrolysis; this is in agreement with the results of Vagramian and Solov'eva [26].

In all cases the anode potential changes in the electropositive direction immediately after reversal, sharply at first and then slightly. However, at current densities considerably in excess of the operating values, and with prolonged anode periods, there are spontaneous periodic variations of potential (Fig. 9), evidently associated with periodic formation and breakdown of an oxide film.

The variation of potential is accompanied by periodic variation of current strength; a change of potential in the electropositive direction corresponds to a decrease of current strength, and vice versa. The periodic variations begin some time after reversal of current. The shape of the cathodic-polarization curve depends on the current density and duration of electrolysis.

It is interesting to note that, with every regime, above a certain limiting current density a bend appears on the cathodic branch of the oscillogram, after which the potential remains almost constant. The explanation of this effect is that at this current density the catholyte layer becomes impoverished fairly rapidly, with formation of a spongy deposit and evolution of hydrogen.

As electrolysis proceeds, the position of the bend shifts, and finally the bend disappears with a simultaneous decrease of polarization (Fig. 8); this is evidently caused by a decrease of the true current density owing to increase of the growing surface.

Thus, the oscillographic method of studying the potential – time relationship, as used in the present work, may serve as an objective method for finding the maximum operating current densities.

SUMMARY

1. With the use of reversing current in the deposition of silver, the productivity of the process is increased 2 to 2.5-fold owing to the use of higher current densities, fine-grained deposits (bright in some cases) are obtained, the uniformity of metal distribution is improved, hardness increases nearly 1.5-fold, and thick deposits may be obtained without the need for periodic scratch treatment.

2. The following electrolyte composition (g/liter) and deposition regime may be recommended for industrial use: $AgNO_3$ 35, KCN_{total} 54, KCN_{free} 27, temperature 18-20°, no stirring, d = 2-2.5 amps/dm^2, T = 2.5 seconds, t_c/t_a = 1.75/0.75.

LITERATURE CITED

[1] H. Leblan and K. Schick, Z. Phys. Ch. 46, 213 (1903).

[2] H. C. Cocks, Trans. Far. Soc. 24, 348 (1928).

[3] G. W. Jernstedt, U. S. Patent 2,451,341; 12, 10 (1948).

[4] G. W. Jernstedt, Plating, VII, 35, 7, 708 (1948).

[5] G. T. Bakhvalov, Proc. 2nd All-Union Conference on Theoretical and Applied Electrochemistry (Kiev, Acad. Sci. Ukrainian SSR Press, 1949). [In Russian]

[6] G. T. Bakhvalov, Jubilee Volume of Scientific Papers from the M. I. Kalinin Institute of Nonferrous Metals and Gold, Moscow (Metallurgy Press, 1950). [In Russian]

[7] A. D. Rupasova, Soviet Author's Certif. No 99,518 (1952). [In Russian]

[8] A. E. Chester, U. S. Patent 2,651,610 (1953).

[9] Rosi Dino, Galvanotechnica, 4, 12, 293 (1953).

[10] E. Costa, Galvanotechnica, 4, 6, 145 (1953).

[11] M. S. Borozdina and L. S. Lukasheva, Tech. Inf. Bull. Ministry of the Electrical Industry 63 (1954).

[12] P. P. Beliaev, M. K. Korolenko, and V. V. Filimonova, Metallic Coatings in Chemical Equipment Construction, Coll. 15 (Moscow, Mashgiz, 1954). [In Russian]

[13] S. Herzer, Swiss Patent 294,350 (1954).

[14] E. Gerber, Metalloberfläche, 8, 11, 161 (1954).

[15] A. I. Stasova, Tech. Transport Machine Construction 2, 60 (1955).

[16] P. P. Feigel'shtein, Exchange of Technical Experience, All-Union Technological Planning Inst. 3, 18 (1955).

[17] Iu. Ia. Vene and S. A. Nikolaeva, J. Phys. Chem. 5, 29, 811 (1955).

[18] H. M. Heiting, Metall, 9, 17-18, 764 (1955).

[19] A. Whittaker, Machinery, 86, 2206, 416 (1955).

[20] N. I. Zhinovich, M. M. Menkina, and K. F. Rubenchik, Coll. Sci. Trans. Belorussian Polytech. Inst. (Minsk, Acad. Sci. Belorussian SSR Press, 1956) 55, 103. [In Russian]

[21] L. Bosdorf and A. Beyer, Metalloberfläche, 138, 8 (1954).

[22] G. W. Jerstedt and J. D. Patrick, U. S. Patent 2,678,909 (1954), 18 V 1954.

[23] A. P. Popkov and A. T. Vagramian, Bull. Acad. Sci. USSR 6, 966 (1954).

[24] A. L. Ferguson and D. K. Turner, J. Electroch. Soc. 101, 7, 382 (1954).

[25] G. T. Bakhvalov, Author's Summary of Doctorate Dissertation, M. I. Kalinin Inst. of Nonferrous Metals and Gold (Moscow, 1955). [In Russian]

[26] A. T. Vagramian and Z. A. Solov'eva, J. Phys. Chem. 24, 10, 1253 (1950).

Received February 11, 1957.

DEPOSITION OF COPPER FROM ACID ELECTROLYTES BY MEANS OF PERIODICALLY REVERSED CURRENT

V. V. Ostroumov and I. F. Plotnikova

Since the first work in this field [1, 2] electrolysis with the use of periodically reversed current has attracted considerable attention [3-8]. Alkaline and acid electrolytes have been tested for various metals, but most of the work has been done with cyanide electrolytes.

It was found that with periodic reversal of current during electrolysis the deposition rate could be increased severalfold above the usual rates of metal deposition with the use of direct current. In some cases bright metal deposits were obtained.

Copper can also be deposited from acid electrolytes at a high rate, and with a simultaneous improvement of the deposit quality. However, the literature contains no references to the possible formation of bright copper deposits from such electrolytes without the use of special brighteners. Bibikov [5] studied the deposition of copper and zinc from acid solutions, but the deposits obtained by him were far from mirror-bright.

In this paper is given a description of the conditions for the production of mirror-bright copper deposits from acid electrolytes with the use of periodically reversed current. No organic brighteners are added to the electrolytes. Bright copper deposits of virtually any thickness can be obtained.

EXPERIMENTAL

The electrolyte used in most of the experiments contained 200 g of copper sulfate and 100 g of sulfuric acid per liter.

A mechanical or an electronic reverser was used for periodic reversal of the current. The former consisted of a cylinder made from insulating material, carrying two pairs of brass rings of different heights, under potentials of opposite sign. As the cylinder rotated, two spring contact plates fell periodically from the upper to the lower rings, thereby changing the sign of the potential at the cell terminals. The reverser was rotated by a motor of the Warren type.

The principle of the electronic reverser was based on constancy of the time necessary for the discharge of a capacitor through a high impedance to a certain definite potential. At that instant an emission current which switched over a relay began to flow in the tube circuit. Simultaneously, a second capacitor was brought into a state of discharge, and at a certain instant a second relay was switched over in the same manner. The switching of the two relays was automatically repeated at a fixed rate. The durations of the cathode and anode periods in the flow of the current were regulated independently by turns of the levers of two high-resistance potentiometers. If the duration of the cathode period is, say, 4.8 seconds, and that of the anode period 1.2 seconds, the duration of a complete cycle is 6 seconds.

Copper was deposited on flat, carefully polished brass disks 4 mm thick and 25 mm in diameter. The inactive electrode surfaces were coated with nitrocellulose varnish. The anode consisted of pure copper, enclosed in a cylindrical ceramic diaphragm.

The specular properties of the deposits were measured in terms of their reflective power, determined in a beam of white light by means of a selenium photocell.

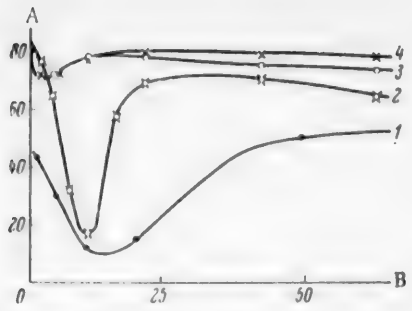

Fig. 1. Effect of the thickness and formation conditions of the nickel underlayer on the reflectance of copper deposits. Current density in copper deposition 80 ma/cm², current ratio 4.8 : 1.2 seconds, stirred electrolyte.
A) Reflectance of copper deposits (%), B) thickness of copper deposits (μ). Thickness of nickel underlayers (μ) and current density in their deposition (ma/cm²) respectively: 1) without underlayer (on brass), 2) 1 and 5, 3) 2 and 10, 4) 5 and 15.

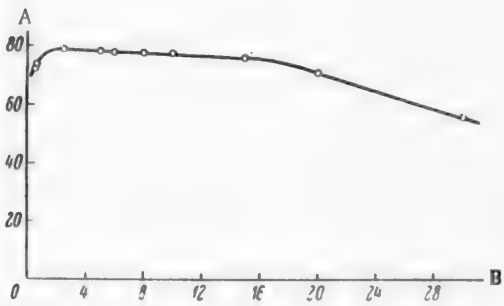

Fig. 2. Effect of the length of the cycle on the reflectance of copper deposits. Thickness of copper layer 25μ, current density 80 ma/cm².
A) Reflectance (%), B) length of cycle (seconds).

The thickness of the copper deposits was found by weighing, or by calculation from the duration of electrolysis and current density. The changes in the weight of copper corresponded to 100% current efficiency at the cathode and anode over a wide range of current densities. Hence the "efficiency" of electrolysis with periodically reversed current could be calculated from data on the current characteristics. For example, for current of the periodicity given above, the efficiency is:

$$\frac{4.8 - 1.2}{4.8 + 1.2} \cdot 100 = 60\%.$$

This means that the amount of copper deposited is 60% of the amount which would be deposited in electrolysis with direct current in the same time and at the same current density.

Preliminary experiments showed that the reflectance of copper deposits depends considerably on the nature of the electrode surface. Mirrorlike copper deposits with maximum reflectance cannot be obtained on polished brass, bright copper layers deposited from baths containing gelatin, amalgamated brass, bright palladium or rhodium deposits, and polished deposits of nickel from ordinary baths. Copper deposits with 80-82% reflectance can be obtained with certainty only on underlayers of bright nickel. If such copper deposits are used as intermediate layers, they do not require polishing before being coated with nickel, chromium, etc.

However, the underlayers of bright nickel on which specular deposits of copper are formed must be obtained under certain definite conditions.

The final result is not influenced by the potassium fluoride content of the nickel electrolyte, stirring conditions, or electrolyte temperature. Increase of the pH of the nickel electrolyte, increase of current density during deposition of nickel, increased thickness of the nickel underlayers, increase of the content of sulfonated naphthalene, and "conditioning" of the nickel electrolyte all have a favorable effect. We used a nickel electrolyte, of pH 6.0-6.6, of the following composition (g/liter): nickel sulfate 170, boric acid 30, potassium chloride 5, potassium fluoride 4, sulfonated naphthalene 8. The bright nickel underlayers must be deposited at a current density not less than 10-15 ma/cm², to a thickness of 2μ (Fig. 1).

Only the results obtained with the use of a bright nickel underlayers deposited under these conditions are given below.

The reflectance of the copper deposits formed depends little on the length of the total cycle. For example, for a constant ratio of 4 : 1 between the cathode and anode periods, the reflectance of copper deposits remains almost constant with cycles from 2 to 15 seconds (Fig. 2).

Variations of the anode period from 0.5 to 2.0 seconds also have little effect if the cathode period remains constant (4.8 seconds), under otherwise equal electrolysis conditions (Fig. 3).

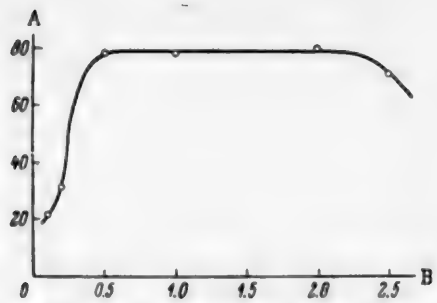

Fig. 3. Effect of the length of the anode period on the reflectance of copper deposits. Thickness of copper layer 25μ, current density 80 ma/cm².
A) Reflectance (%), B) length of anode period (seconds).

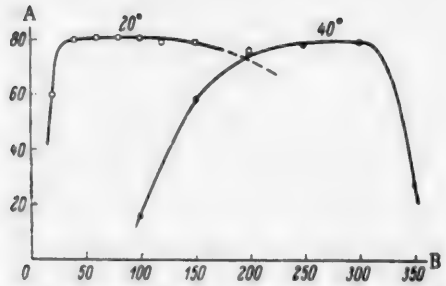

Fig. 4. Effect of electrolyte temperature on the reflectance of copper deposits. Current ratio 4.8 : 1.2 seconds, stirred electrolyte containing 50 g of sulfuric acid per liter.
A) Reflectance (%), B) current density (ma/cm²).

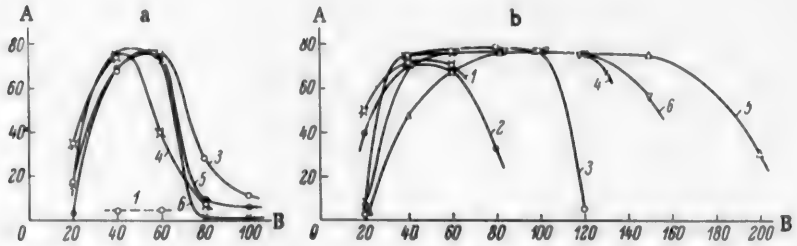

Fig. 5. Effect of the sulfuric acid content of the electrolyte on the reflectance of copper deposits. Thickness of copper layer 25μ, current ratio 4.8 : 1.2 seconds.
A) Not stirred, b) stirred electrolyte. Sulfuric acid content (g/liter): 1) 25, 2) 50, 3) 75, 4) 100, 5) 150, 6) 200.

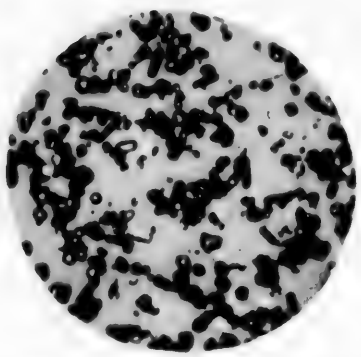

Fig. 6. Copper crystals deposited from an electrolyte supersaturated with cuprous copper. Magnification × 200.

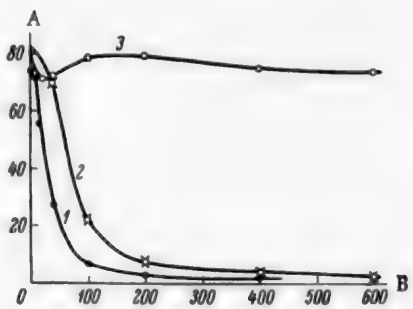

Fig. 7. Effect of the number of current pulses on the reflectance of copper deposits.
A) Reflectance (%), B) number of current pulses (or cycles). Curves: 1) anodic current pulses, 1.2 seconds long with pauses of 4.8 seconds, 2) cathodic current pulses 4.8 seconds long, with pauses of 1.2 seconds, 3) combination of anodic and cathodic pulses of the above durations.

Experiments with electrolysis at different anodic current densities and constant cathodic current density showed that the best results are obtained when the two current densities are equal.

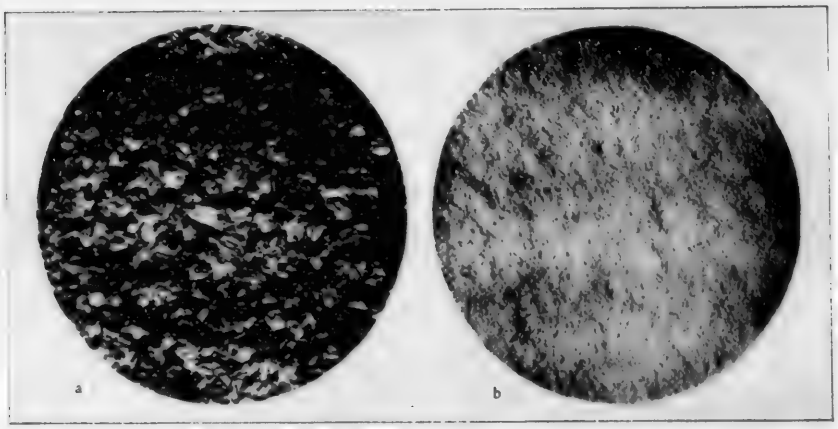

Fig. 8. Etched surface of copper deposits: a) deposit formed by the action of direct current, b) deposit formed under the action of periodically reversed current (4.8 : 1.2). Magnification × 375.

As a rule, brighter copper deposits are obtained if the electrolyte is stirred during electrolysis.

The electrolyte temperature had a very appreciable influence (Fig. 4). With increase of temperature from 20 to 40°, the region in which bright deposits are obtained shifts in the direction of higher current densities. This fact may be useful for raising the rate of metal deposition.

The sulfuric acid content of the electrolyte must be maintained at a high level, not only because high current densities are used in the process, but also because sulfuric acid probably has a certain specific influence. In a static electrolyte, variations of the sulfuric acid concentration from 50 to 200 g/liter have almost no influence on the nature of the copper deposits. Relatively bright deposits can be obtained only in a narrow current-density range, from 40 to 50 ma/cm^2 (Fig. 5, a). However, if the electrolyte is stirred, increase of the sulfuric acid content widens considerably the range in which bright deposits are formed, which extends from 40 to 150 ma/cm^2 (Fig. 5, b). A concentration of sulfuric acid above 100 g/liter is unlikely to be useful, as the solution then approaches saturation with copper sulfate.

The presence of certain impurities in the electrolyte prevents the formation of bright copper deposits. Accumulation of particles of anode sludge in the electrolyte has an adverse effect on the deposit surface owing to the appearance of various irregularities, growths, etc. The original properties of the electrolyte are restored by filtration. If electrolytes are used for a long time with anodes without diaphragms, continuous filtration is probably necessary.

Admixtures of gelatin, dextrin, tannin, silver salts, and sulfites were found to be harmful. Alcohol, sulfonated naphthalene, and cellulose treated with sulfuric acid were found to be inert admixtures. Strong oxidizing agents, such as hydrogen peroxide, nitric acid and its salts, and potassium persulfate, usually raise the reflectance of the deposits. Strong reducing agents such as hydrazine sulfate have the same effect as oxidizing agents. Deposits with the maximum possible reflectance (82%) were generally obtained by electrolysis in a hydrogen atmosphere in a closed vessel after prolonged saturation of the electrolyte with the gas.

Chloride ions occupy a special position. A chloride content close to 10 mg per liter in the electrolyte makes the formation of bright deposits impossible.

When the electrolyte volume is several liters, harmful impurities which are often present in "pure" reagents and in water may be removed by one of the two following methods.

In the first purification method the prepared electrolyte is heated almost to boiling with metallic copper (coiled wire), kept in that condition for about 1-2 hours, and then cooled rapidly. Numerous fine crystals of metallic copper appear in the liquid immediately or after some time, and they take with them most of the impurities. The cooled solution is filtered through a glass filter*.

*After purification by this method the copper and sulfuric acid contents of the electrolyte must be adjusted.

Crystallization of copper takes place as the result of the following processes. When heated, copper dissolves in the cuprous form

$$Cu + Cu^{++} \rightleftharpoons 2Cu^{+},$$

but the equilibrium concentration of cuprous ions falls with decrease of temperature. This fall can only be effected by a shift of equilibrium with formation of metallic copper [9-14]. The copper is precipitated in the form of crystals of the cubic system, as cubes, octahedrons, tetrahedrons, and combinations of these forms (Fig. 6).

The second purification method, which is also suitable for small volumes of solution, consists of saturation of the prepared electrolyte with copper sulfate on heating, followed by rapid cooling. The precipitated fine crystals of sulfate take most of the impurities with them. The solution is filtered and adjusted by addition of water and sulfuric acid.

If the contents of impurities are fairly high, both purification procedures must be repeated.

DISCUSSION OF RESULTS

Most authors consider that smooth (or bright) electrode deposits are formed under the action of periodically reversed current because of preferential dissolution of all kinds of surface projections during the anode current pulses. It has been found, however, that this kind of dissolution cannot cause the formation of smooth surfaces on copper deposited from acid baths. The action of anodic current pulses only, with intermediate pauses, should convert an original rough copper surface into a smooth one, while an initially polished surface should remain unchanged, if the projections are really removed in this way.

Fig. 7 (Curve 1) shows variations of the reflectance of a polished surface of an electrolytic copper deposit under the action of an increasing number of anodic pulses lasting 1.2 seconds, with pauses of 4.8 seconds between them. The reflectance of the polished copper decreases appreciably after only 5-10 current pulses.

The decrease of reflectance is caused by the formation of a film, transparent at first and then of a brown color on the copper surface. When the film is thick enough it can be easily detached from the electrode. It was found that films of this kind can be formed very simply in the anodic polarization of copper by direct current in a hydrogen atmosphere. Under these conditions a film is formed at the anode at 80 ma/cm^2, even in very acid electrolytes; it stops the flow of current almost entirely 1 minute after the start of electrolysis. It consists of a conglomerate of yellow, rather closely packed grains, with visible inclusions of transparent red crystals of cuprous oxide. The film possibly consists of a mixture of grains of cuprous hydroxide, cuprous oxide, and metallic copper [15]*.

The reflectance of copper layers formed during the action of cathodic pulses on a bright nickel underlayer was studied similarly. The duration of each cathodic pulse was 4.8 seconds, with pauses of 1.2 seconds (Fig. 7, Curve 2). The copper deposits formed after the first few pulses had an ideal mirror surface and high reflectance (80%). On further growth, as Fig. 7 shows, the reflectance of the deposits fell to very low values (2-3%). This decrease is undoubtedly caused by growth of individual copper grains and formation of a rough surface.

Each of the individual processes, the anodic and the cathodic, results in a sharp decrease in the reflectance of the electrode surface. However, if the two processes are combined in electrolysis with periodic reversal of current, with the same durations of the anodic and cathodic pulses (1.2 and 4.8 seconds), an unexpected result is obtained – the deposit retains its luster almost without change right from the start of electrolysis, to almost any desired thickness (Fig. 7, Curve 3).

In the light of the foregoing, we consider the following to be the probable interpretation of the cause of formation of bright copper deposits from acid electrolytes by means of periodically reversed current.

The first layer of copper deposited on the surface of bright nickel by the first cathodic pulse consists of small crystallites of copper, oriented in a definite manner by the underlayer (a grain-oriented deposit). The anodic current pulse creates a thin transparent film of cuprous oxide (or hydroxide) on the surface of this layer. During the next cathodic pulse the second layer of copper grows on the oxide film, which has the same (or almost

* Vene and Nikolaeva [15] correctly draw attention to the importance of anodic passivation of copper in this process.

the same) orientation effect on the copper crystallites as the underlayer of bright nickel had on the first copper layer. Therefore the reflectance of the second copper layer also remains high. During the subsequent deposition cycles the crystallite orientation is renewed each time owing to the presence of an oxide film. The deposit as a whole retains its initial orientation, irrespectively of its thickness.

Fig. 8 shows two photographs of copper surfaces deposited by means of direct and periodically reversed current respectively. Each deposit was 100μ thick. The etching was effected by the action of concentrated nitric acid for 1-2 seconds. Both deposits were formed on bright nickel underlayers. The electrolyte was stirred. The current density was 80 ma/cm^2. It is easily seen that the bright copper deposit has an extremely fine structure, difficult to distinguish under the microscope. Structure studies of polished cross sections of copper deposits confirmed the above hypothesis on the mechanism of formation of bright deposits during electrolysis by means of periodically reversed current.

SUMMARY

1. It is shown that bright copper deposits can be obtained from acid electrolytes by electrolysis with periodically reversed current, without the use of organic brighteners.

2. Copper deposits of maximum reflectance (80-82%) can be obtained on bright nickel underlayers.

3. A hypothesis is put forward to explain the mechanism whereby bright copper deposits are formed in electrolysis from acid electrolytes by means of periodically reversed current.

LITERATURE CITED

[1] G. T. Bakhvalov, Proc. 2nd All-Union Conf. on Theoretical and Applied Electrochemistry (Acad. Sci. Ukrainian SSR, 1949). [In Russian]

[2] G. W. Jernstedt, Metal Finish. 45, 2, 68 (1948); Plating 35, 7, 708 (1948).

[3] G. T. Bakhvalov, Jubilee Volume of Scientific Papers, Moscow Inst. of Nonferrous Metals and Gold (1950), 222, [In Russian]; Bull. Eng. and Technol. 4, 161 (1953).

[4] G. W. Jernstedt, Proc. Am. Electropl. Soc. 36, 63 (1949); 37, 151 (1950); Westinghouse Eng. 10, 2, 133 (1950).

[5] N. N. Bibikov, Inform. Pamphlet, Leningrad Inst. of Sci. Tech. Information, 14 (1953-1954).

[6] Collected papers: Corrosion and Metal Coatings 43, Urals Polytech. Inst. (Moscow – Sverdlovsk, State Sci. Tech. Press, 1953). [In Russian]

[7] Collected papers: Improvement and Automation of Electroplating Processes 3, Ministry of Transport Machine Building USSR, (Moscow, VPTI,*1955). [In Russian]

[8] N. W. Hovey, J. L. Griffin, and A. Krohn, J. Electroch. Soc. 102, 8, 470 (1955).

[9] F. Foerster and O. Seidel, Z. anorg. Ch. 14, 106 (1897); F. Foerster, Z. Electroch. 5, 508 (1898-1899).

[10] R. Luther, Z. Phys. Chem. 36, 385 (1901).

[11] E. Heinerth, Z. Electroch. 37, 2, 61 (1931).

[12] O. A. Esin, Z. Phys. Chem. 156, 41 (1931).

[13] A. I. Gaev and O. A. Esin, Electrolytic Refining of Copper (Sverdlovsk – Moscow – Leningrad, ONTI, 1934). [In Russian]

[14] M. Thompson, Chem. Met. Eng. 33, 298 (1926).

[15] Iu. Ia. Vene and S. A. Nikolaeva. J. Phys. Chem. 29, 5, 811 (1955).

Received January 31, 1957.

*All-Union Design and Planning Technological Institute.

THE CHEMICAL NATURE OF SULFONATED-NOVOLAC ION-EXCHANGE RESINS

A. A. Vasil'ev and A. A. Vansheidt

(Institute of High-Molecular Compounds, Academy of Sciences USSR)

In earlier papers [1, 2, 3] we described methods of preparation of ion-exchange sorbents with the use of phenol – formaldehyde novolac resins as starting materials.

By one of these methods [1], insoluble products were made by the action of formaldehyde on soluble products formed by sulfonation of novolacs (SNF resins). By the other methods, insoluble products were obtained when the novolac was dissolved in sulfuric acid [2] or in chlorosulfonic acid [3], and the sulfonated mass was heated at temperatures above 150° until a gel was formed (SN and SN-2 resins). Further heating of the gels for several hours to 100° in the first method, and to 160-180° in the other two methods, led to a decrease of the swelling capacity and sulfo group contents of the resins, and increase of their mechanical strength. Sulfonated novolac cation exchangers are similar in properties to sulfonated phenolic resins, such as MSF, KU-1 and others made by different methods; but SN and especially SN-2 resins are appreciably superior to them in exchange capacity, while SNF resins have a high degree of swelling and satisfactory mechanical strength.

With regard to the mechanism by which insoluble sulfonated-novolac products are formed, in the case of SNF resins it evidently consists mainly of cross linkage of the sulfonated-novolac molecules by the methylene groups of the added formaldehyde; therefore the swelling capacity of the resins can be varied by variations of the amount of formaldehyde.

When sulfonated novolacs are hardened by simple heat treatment, the mechanism of the processes taking place is less clear, although some views on this question can be put forward on the basis of existing experimental data.

The structure of novolacs can be represented by the formula [4]

$$H[C_6H_3(OH)CH_2]_n - C_6H_4OH$$

if it is assumed that sulfonation results in substitution of all the H atoms in the o- and p-positions to the phenolic hydroxyls in the benzene nuclei, the structure of soluble, fully sulfonated novolacs can be represented by the formula

$$HO_3S[\underset{\displaystyle SO_3H}{\underset{|}{C_6H_2(OH)}}CH_2]_n - \underset{\displaystyle SO_3H}{\underset{|}{C_6H_2(OH)}}SO_3H.$$

This corresponds to the presence, in the sulfonated-novolac molecules, of (n + 3) SO_3H groups or sulfur atoms, or of (x + 2) S atoms per molecule containing x aromatic nuclei.

Thus, in the case of our 5-nucleate novolac of molecular weight close to 500 (n = 4), its content of sulfo-group sulfur should not exceed 20.7%, and should by 17.4% if one sulfo group is present in each nucleus, i. e., if the structure is

$$H[\underset{\displaystyle SO_3H}{\underset{|}{C_6H_2(OH)}}CH_2]_4 - \underset{\displaystyle SO_3H}{\underset{|}{C_6H_3OH}}.$$

As was described earlier [1], insoluble sulfonation products of novolacs (SNF resins) are formed by the action

TABLE 1

Consumption of Sulfuric Acid in the Preparation of Cation Exchangers from Novolac Resins

Sample No.	Sulfonating agent and concentration used	Weight ratio of sulfonating agent to resin	Gel heat treatment conditions		Sulfuric acid found (% of original amount)			Swelling coefficient	Sulfur content of cation exchangers (%)		
			temperature (°C)	time (hours)	expended in formation SO_2	in wash waters	in sulfonated resin		total (S)	active (S_a)	inactive ($S - S_a$)
1	Oleum (14.9% SO_3)	4:1	No heat treatment		6.00	—	—	—	15.50	12.16	3.34
2	The same	4:1	160	4	9.70	64.8	15.1	—	12.90	10.85	2.05
3	" "	4:1	180	4	15.5	61.8	14.2	—	13.23	11.70	1.53
4	Sulfuric acid (96.2%)	2:1	No heat treatment		6.19	65.9	10.3	5.2	12.13	8.85	3.28
5	The same	2:1	160	4	13.5	58.7	16.2	2.3	11.12	8.49	2.63
6	" "	2:1	160	8	17.9	52.9	16.7	1.7	10.15	7.34	2.81
7	Sulfuric acid (91%)	4:1	160	4	10.2	71.2	13.3	3.0	11.63	9.63	2.00
8	The same	4:1	160	4	16.2	—	—	—	10.71	8.51	2.20

TABLE 2

Variations of Sulfur Content of SNF Cation Exchangers after Treatment with Solutions of Sodium Sulfite and Formaldehyde, and with Alkali Solutions

Sample No.*	Amount of Na_2SO_3 or NaOH per g of resin** (in g)	Treatment conditions		Swelling coefficient	Sulfur content (%)			Increase of sulfur content in comparison with the original (untreated) product (%)	
		temperature (°C)	time (hours)		total (S)	active (S_a)	inactive ($S - S_a$)	ΔS	ΔS_a
1	—	—	—	1.8	9.65	7.74	1.95	—	—
1a	3.2 Na_2SO_3	20	48	2.2	9.80	8.77	1.03	0.15	1.03
1b	1.6 Na_2SO_3	20 and additionally 98	48 and additionally 5	2.5	10.77	9.60	1.17	1.12	1.86
2	—	—	—	3.2	11.07	9.25	1.82	—	—
2a	0.43 NaOH	20	312	3.3	—	9.95	0.88	—	0.70
2b	0.43 NaOH	98	24	—	10.95	10.38	0.57	—	1.13
3	—	—	—	1.6	8.35	6.85	1.50	—	—
3a	2.5 Na_2SO_3	98	10	1.6	8.66	8.48	0.18	0.31	1.63
3b	1.6 NaOH	98	10	1.8	—	7.55	—	—	0.70

*Samples Nos. 3, 3a, and 3b refer to comparative experiments on the treatment of KU-1 sulfonated phenolic resin with the reagents.

**10% solutions of sodium sulfite and 36-38% formaldehyde solution (amount of CH_2O equivalent to the Na_2SO_3) and 12% (Experiments 2a, 2b) and 6.4% (Experiment 3b) NaOH solutions were used.

TABLE 3

Variations of Sulfur Content of SN Cation Exchangers after Treatment with Solutions of Sodium Sulfite and Formaldehyde, and with Alkali Solutions

Sample No.	Amount of Na_2SO_3 per g of resin*	Treatment conditions		Swelling coefficient	Sulfur content (%)			Increase of sulfur content in comparison with the original (untreated) product (%)	
		temperature (°C)	time (hours)		total (S)	active (S_a)	inactive ($S - S_a$)	ΔS	ΔS_a
1	—	—	—	5.2	12.13	8.85	3.28	—	—
1a	5.0	20	120	6.3	12.87	11.00	1.87	0.74	2.15
1b	2.5	98	10	6.8	13.73	12.45	1.28	1.60	3.60
2	—	—	—	2.3	11.12	8.49	2.63	—	—
2a	5.0	20	120	2.3	11.36	9.15	2.21	0.24	0.66
2b	2.5	98	10	2.6	11.87	10.95	1.28	0.75	2.10
3	—	—	—	1.7	10.15	7.34	2.81	—	—
3a	5.0	20	120	1.7	10.09	7.78	2.31	0	0.44
3b	2.5	98	10	2.4	10.35	9.49	0.86	0.20	2.15
4	—	—	—	1.9	11.46	9.86	1.60	—	—
4a	0.43 NaOH	20	48	2.1	11.95	10.75	1.20	—	0.89
4b	0.43 NaOH	20 and additionally 98	48 and additionally 8	—	11.88	11.15	0.73	—	1.29

*10% solutions of sodium sulfite and 36-38% formaldehyde solution (amount of CH_2O equivalent to the Na_2SO_3) and 12% (Experiments 2a, 2b) and 6.4% (Experiment 3b) NaOH solutions were used.

of formaldehyde on soluble novolac sulfonic acids. Evidently some of the phenolic nuclei of the sulfonated novolac undergo desulfonation and become cross linked by methylene groups. The extent of the desulfonation increases with the amount of formaldehyde added. On the assumption that the molecules are cross linked by $-CH_2$ groups only, the hypothetical composition of SNF resins may be represented by the formula

$$H[C_6H_2(OH)-CH_2]_{n-2m}-[C_6H_2(OH)-CH_2]_m-[C_6H_2(OH)CH_2]_m-C_6H_3OH.$$

(SO_3H on the first unit; CH_2 on the bridging unit; SO_3H on the last unit)

For a 5-nucleate sulfonated novolac (with n = 4, and m = 1), the sulfur content should be 12.5%.

The maximum sulfur contents determined by titration ("active" sulfur) of resins of this type are close to this value if about 1 mole of formaldehyde is taken per mole of the original novolac after sulfonation.

The insoluble sulfonation products formed when the sulfonated mass is heated (SN [2] and SN-2 [3] resins) always contain "inactive" sulfur (not determined by titration) in addition to the sulfur which is contained in the sulfur group and determined by titration. Small amounts of inactive sulfur are also present in SNF resins.

With regard to the nature and origin of this sulfur, it seemed possible that it is present in the $>SO_2$ sulfone groups, which effect the cross linkage of the sulfonated-novolac molecules in SN and SN-2 resins, as it is known [5] that sulfones are frequently formed during sulfonation processes at temperatures above 150° and high concentrations of sulfonic acids. It should be noted, however, that although further heating (thermal treatment) of insoluble sulfonated novolacs results in a considerable decrease of their swelling coefficient, their contents of inactive sulfur (which is about 2% in SN and SN-2 resins) change little during heat treatment ([2], table). Therefore the cross linkage of the molecules during heat treatment of the insoluble sulfonated resins cannot be attribu-

ted to formation of new $-SO_2$ bridges. Evidently the great decrease of swelling and increased cross linking of the sulfonated-novolac molecules as the result of heat treatment are due to other reactions, including oxidation – reduction processes. This follows from the fact that when the sulfonated products in gel form are heated at 160° and at higher temperatures considerable amounts of sulfur dioxide are evolved, i. e., SO_3 is reduced by oxidation of the sulfonated resins. Thus, it follows from Table 1 that in the sulfonation of novolac about 6% of the sulfuric acid is reduced to SO_2 even before heat treatment of the gel. During the subsequent heating of the gel for 8 hours at 160° this amount is trebled, with a simultaneous threefold decrease of the swelling coefficient of the resin, whereas the inactive-sulfur content of the latter does not rise but falls.

Thus, the cross linking of the molecules of the sulfonated resins when they are heated above 160° is most likely associated with oxidation and dehydrogenation processes in the resins. These processes, which favor the formation of conjugated quinoid structures, which are powerful chromophores are probably also the cause of the deep black color characteristic of sulfonated phenolic and novolac cation exchangers prepared at high temperatures [6].

In further experiments, in which the action of sodium sulfite and formaldehyde or alkali on SN and SNF sulfonated novolac resins was studied, it was found that the nature of the inactive sulfur presents a more complicated problem. The combined action of sodium sulfite and formaldehyde on the resins resulted (as expected) in a small increase of the total sulfur content, probably owing to a sulfomethylation reaction:

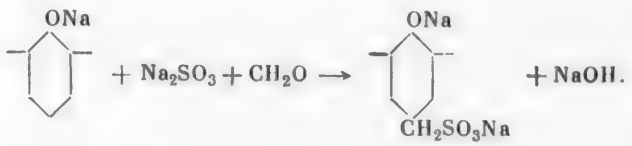

It was found, however, that the increase of the exchange capacity of the resins is largely due to partial (in some cases total) conversion of the inactive sulfur into an active form, i. e., to formation of $-SO_3H$ groups, rather than to formation of sulfomethyl ($-CH_2SO_3H$) groups. The simultaneous increase of the swelling coefficients was probably the consequence of partial breakdown of the bonds between the molecules of the space polymer. It was also found that the exchange capacity of the sulfonated novolac cation exchangers is not increased if sodium bisulfite is used instead of sulfite. This led to the hypothesis that the increase of exchange capacity and swelling coefficients of the cation exchangers produced by treatment with sodium sulfite in presence of formaldehyde is the result of a secondary reaction, caused by the action of the alkali, formed in the reaction between sulfite and aldehyde, on the cation exchangers. It was found in special experiments that when sulfonated novolac cation exchangers were treated with alkali the same effects were observed as in the treatment of the cation exchangers with sodium sulfite. It should be noted that changes in the exchange capacity of the sulfonated novolac resins were observed only as the result of treatment with fairly concentrated alkali solutions (3 N) for a long time (several days) at room temperature, or for several hours at 95-98°. The exchange capacities were not affected by brief treatment (20 minutes) of SN resins with 1 N NaOH at 98° [2], or prolonged treatment (3 days) of SNF resins with 0.1 NaOH at room temperature [1].

Tables 2 and 3 show the effect of the action of sodium sulfite and formaldehyde, and of alkali, on the sulfur contents of SNF and SN resins.

Increase of temperature in the treatment of the cation exchangers with Na_2SO_3 and CH_2O, and with alkali, resulted in a considerable increase of their exchange capacities. When sodium sulfite and formaldehyde were used, the active-sulfur content increased appreciably, not only by partial conversion of inactive sulfur, but also (especially at higher reaction temperatures) as the result of additional formation of methylenesulfonic groups ($-CH_2SO_3H$). If the reaction with Na_2SO_3 and CH_2O was carried out at room temperature, the increase of the total sulfur content took place mainly at the initial reaction stages, and was slower later; the increase of exchange capacity in these cases took place mainly by conversion of groups containing inactive sulfur.

Samples Nos.1, 2, and 3 in Table 3 correspond to Samples Nos.4, 5, and 6 in Table 1, where their synthesis conditions are given. Comparison of data for Samples Nos.1a, 2a, and 3a, and Nos.1b, 2b, and 3b (Table 3) shows that the more cross linked the original resins, the greater is the difficulty with which the sulfur content is increased by treatment with Na_2SO_3 and CH_2O.

In comparative experiments on the treatment of KU-1 sulfonated phenolic resin with sodium sulfite and alkali solutions its behavior was found to be the same as that of SN and SNF sulfonated novolac resins. The nature of the inactive sulfur is therefore probably the same in sulfonated phenol – formaldehyde resins of different origin.

The possibility of sulfo group formation from inactive sulfur suggests that the latter may be present not only in sulfone groups, but also in other groups, such as sulfonate ester groups. It is difficult to believe that sulfones were hydrolyzed with formation of sulfo groups under the conditions used for the action of alkali on the resins (3 N NaOH solution at 20 and 98° for 48 and 8 hours respectively).

For example, heating for 2 hours at 250° with excess of aqueous alkali has no effect on p-cresyl sulfone [7]

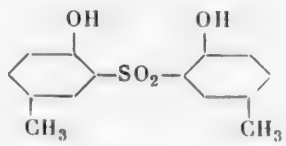

the structure of which can be regarded as analogous to the structure of the sulfones formed when sulfonated novolacs are heated

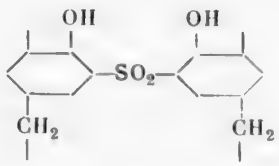

The thermal stability of the sodium salt of 4, 4'-dihydrozydiphenyl sulfone

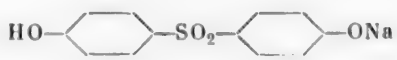

which does not decompose when heated considerably above 100° [8], may also be mentioned in this context.

It is known that when certain substituted phenols (p- and o-cresol, p- and o-chlorophenol, etc.)are subjected to vigorous sulfonation (by means of sulfuric acid and oleum, or chlorosulfonic acid), cyclic compounds with two ester bonds (known as sulfonylides) [9] are formed, for example:

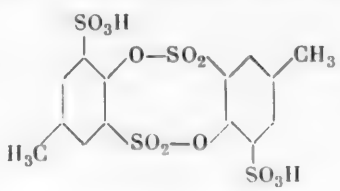

Some compounds of this type are hydrolyzed by caustic alkalies even at room temperatures, with formation of the corresponding sulfonate salts [10].

Thus, the possibility is not excluded that sulfonated novolac cation exchangers may contain, in addition to sulfone bonds, ring ester bond structures of the type:

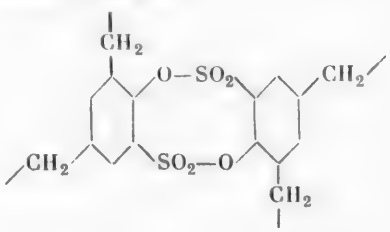

which are stable during determinations of the exchange capacity of sulfonated resins, but are split by the more vigorous action of alkali. Therefore the sulfur of these groups may be inactive, but may pass under certain conditions into active sulfur of the sulfo groups. Saponification of the intermolecular ester bonds should increase the swelling coefficients of the resins.

From the data presented in this paper, only preliminary conclusions may be drawn concerning the processes taking place in the formation of sulfonated ion exchangers from phenol – formaldehyde novolacs, and the possible structures of these resins.

EXPERIMENTAL*

Experiments on the determination of by-products and unreacted substances in the synthesis of sulfonated cation exchangers made from novolacs (SN resins). The sulfonation of the novolacs, and the subsequent gel formation and heat treatment, was carried out in a Wurtz flask, 1 liter in capacity, connected consecutively with four absorption flasks containing 10% caustic potash solution. Novolacs of different molecular weight (usually 400-500) and different sulfonating agents (oleum, sulfuric acid) were used, and the ratio of novolac to sulfonating agent was varied (from 1:2 to 1:4). The reaction mixtures were heated on an oil bath, and the heating was stopped at different stages of the process (after gel formation, after 4 and 8 hours of heat treatment of the gel, etc.).

For determination of combined CO_2 and SO_2, the alkaline solution from the absorption vessels was analyzed by the acidimetric method, by titration with hydrochloric acid first in presence of phenolphthalein and then in presence of Methyl orange. In addition, combined SO_2 in the solution in the absorption vessels was determined by the iodometric method (after neutralization). Comparison of the results of $CO_2 + SO_2$ determinations by the acidimetric and iodometric methods showed that the amount of CO_2 formed during preparation of the sulfonated ion exchangers is negligible; in most cases the same values were obtained in CO_2 determinations in the alkaline solution before and after it was used for absorption.

The amount of SO_3 liberated and absorbed was calculated from the difference between the initial amount of caustic potash and the sum of the amounts of the latter which did not react and which was used for binding SO_2 and CO_2.

The sulfonated product was extracted from the flask and washed thoroughly with water to removed unreacted sulfuric acid. The wash waters were analyzed for sulfuric acid, acidimetrically and by precipitation of $BaSO_4$. Absence of SO_2 in the wash waters was proved (qualitatively by the iodometric method, and also by agreement between the results of titration of the wash waters in presence of phenolphthalein and Methyl orange respectively). The sulfur (total and active) contents and the swelling coefficients of the sulfonated resins were determined.

Some of the experimental results are given in Table 1.

Experiments on the sulfomethylation and alkali treatment of cation exchangers. A weighed sample of sulfonated novolac cation exchanger was covered with 10% sodium sulfite solution and 36-38% formaldehyde solution (in other experiments, with 6.4-17% caustic soda solution) and kept at room temperature or on a water bath with intermittent stirring. The resin was then separated from excess alkali, regenerated with 2 N hydrochloric acid, washed with water to a neutral reaction to Methyl orange, and dried at room temperature.

Both the original resins and samples treated with sodium sulfite and formaldehyde and alkali were analyzed for total sulfur (by fusion with alkali and saltpeter) and for active sulfur (by titration of the resin in presence of excess of neutral salt, with Methyl orange indicator), and the swelling coefficients of air-dry samples were determined.

The methods used for determination of the principal characteristics of sulfonated resins are described in our earlier papers [1, 2].

SUMMARY

1. All sulfonated cation exchangers (SNF, SN, SN-2) formed by sulfonation of phenol – formaldehyde novolacs in presence or absence of formaldehyde, and also sulfonated phenolic cation-exchange resin KU-1,

*V. S. Matrosova, V. A. Orestova, and G. A. Petrova took part in the experimental work.

contain, in addition to the active sulfur of their sulfo groups, small amounts of "inactive" sulfur which is not determined by titration of the sulfo groups of the resins.

2. When sulfonated novolac cation exchangers are treated with alkali or sodium sulfite in presence of formaldehyde, their exchange capacity increases (owing to conversion of some of the inactive sulfur into the active form) and the swelling coefficient is also increased; this indicates that the inactive sulfur is involved in cross linking of the sulfonated novolac molecules.

3. The inactive sulfur is evidently present in the resins mainly in the form of sulfonic ester groups, formed by the interaction of phenolic hydroxyls with sulfo groups; and possibly also in the form of sulfone groups.

4. When the gels are heated above 160° in order to lower their swelling coefficients, the inactive-sulfur content does not increase; this shows that inactive sulfur is not involved in additional cross linking at this reaction stage.

5. In the sulfonation of novolacs at high temperatues, the decrease of the swelling coefficient is accompanied by liberation of sulfur dioxide as the result of partial oxidation and dehydrogenation of the resins by the sulfonating agent; this evidently accounts for the increased cross linking and the deep color of the resins.

LITERATURE CITED

[1] A. A. Vasil'ev and A. A. Vansheidt, J. Appl. Chem. 31, 7, 1075 (1958).*

[2] A. A. Vasil'ev and A. A. Vansheidt, J. Appl. Chem. 31, 8, 1273 (1958).*

[3] A. A. Vasil'ev and A. A. Vansheidt, J. Appl. Chem. 31, 9, 1436 (1958).*

[4] A. A. Vansheidt, Proc. Session of the Acad. Sci. USSR on Organic Chemistry (Moscow – Leningrad, Izd. AN SSSR, 1939), 71. [In Russian]

[5] N. N. Vorozhtsov, Principles of the Synthesis of Intermediates and Dyes (Moscow, Goskhimizdat, 1955), 69. [In Russian]

[6] A. A. Vansheidt and O. N. Simonova, in the book: Plastics 3, 130 (1939). [In Russian]

[7] L. A. Warren and S. Smiles, J. Chem. Soc. 2207 (1931).

[8] L. Glūtz, Ann. 147, 52 (1868).

[9] C. M. Suter, The Organic Chemistry of Sulfur, II (IL, 1951) 7, 8 [Russian translation].

[10] C. S. Schoepfle, F. J. von Natta, and R. G. Clarkson, J. Am. Chem. Soc. 50, 1171 (1928).

Received June 20, 1957.

* Original Russian pagination. See C. B. Translation.

SYNTHESIS OF FLUOROPRENE OVER A SOLID CATALYST

I. M. Dolgopol'skii, I. M. Dobromil'skaia, and B. A. Byzov

(The S. V. Lebedev All-Union Scientific Research Institute of Synthetic Rubber)

In recent years a number of organic fluorine compounds have been synthesized; these have become important for the preparation of a great variety of organic products, including polymers with very valuable properties [1].

The methods of preparation of organic fluoro derivatives are much more complex than the methods for synthesis of other halogen derivatives, but the success achieved in improvement of existing and discovery of new methods for formation of fluorine – carbon bonds has made this class of compounds available not only for research but also for technical uses [2].

One widely-used method for introducting fluorine into organic molecules is by addition of hydrogen fluoride to unsaturated compounds [3]. The reaction of hydrogen fluoride with acetylene hydrocarbons was first studied by Grosse and Linn; it was found to proceed with relative ease in the case of substituted acetylenes. Acetylene itself reacts with HF only at high pressures, mainly with formation of vinyl fluoride. The reaction of acetylene with hydrogen fluoride can be brought about under normal pressure with the use of $HgCl_2$ or $HgCl_2$ + + $BaCl_2$ catalysts on activated wood charcoal [4].

Henne and Pludemann [5] tested a number of methods for the hydrofluorination of acetylene hydrocarbons, and concluded that the choice of the method depends mainly on the nature of the alkyne used. Mochel et al. [6] described the reaction of hydrogen fluoride with vinylacetylene. They found that when a mixture of hydrogen fluoride and vinylacetylene is passed through a catalyst (mercuric nitrate on activated carbon) a mixture of fluoroprene and difluorobutene is formed.

Studies of polyfluoroprene rubber, performed in the All-Union Scientific Research Institute of Synthetic Rubber, showed that it is superior in a number of respects to other known hydrocarbon-resistant and frost-resistant rubbers. The frost resistance of fluoroprene rubber is considerably higher than that of chloroprene and divinyl – nitrile rubbers, while their hydrocarbon resistance is the same [7]. Work was therefore undertaken to develop an industrial process for fluoroprene synthesis. By analogy with the known method for chloroprene synthesis, a study was made of the reaction of vinylacetylene with hydrogen fluoride in aqueous solution in presence and in absence of copper salts. These experiments showed that the reaction does not proceed in aqueous solutions of hydrogen fluoride of various concentrations either in presence or in absence of cuprous salts, and unchanged vinylacetylene is recovered. Negative results were also obtained in attempts to bring about the reaction in the gas phase over active carbon (the temperature rose sharply, and the entire carbon surface became coated with resin, probably as the result of polymerization of vinylacetylene).

Subsequently vinylacetylene was hydrofluorinated in the gas phase over a solid catalyst (mercuric oxide on activated wood charcoal).

As the results of studies of the effects of temperature, component ratio, dilution of the reaction mixture with an inert gas, and contact time, a method was developed for hydrofluorination of vinylacetylene over a solid catalyst, with fluoroprene yields of about 65-70% on the converted and 30-35% on the passed vinylacetylene. In view of the high heat of reaction in the addition of hydrogen fluoride to unsaturated compounds, and the considerable polymerization activity of hydrogen fluoride, attention was devoted mainly to the question of removal of the heat of reaction, with retention of adequate catalyst activity and maximum increase of its service life. The

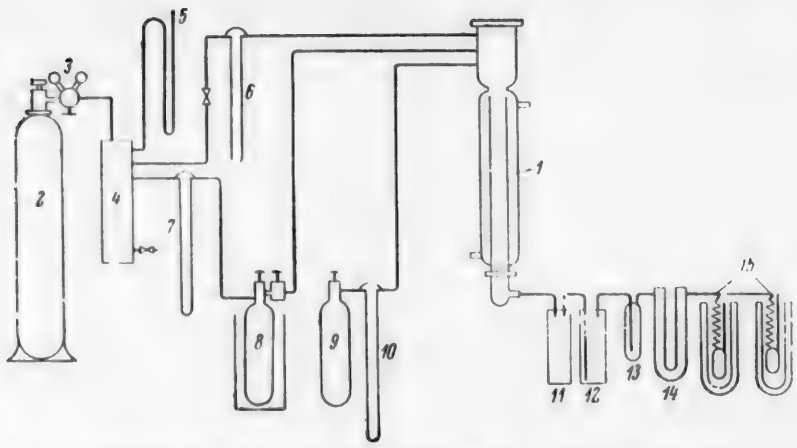

Fig. 1. Synthesis of fluoroprene in the gas phase. Explanation in text.

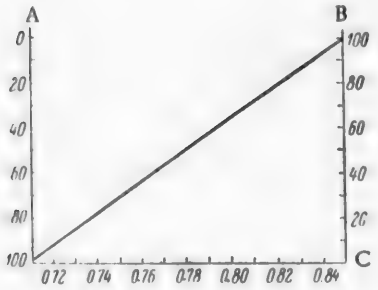

Fig. 2. Variation of the density of the mixture with composition.
A) Vinylacetylene content (%), B) fluoroprene content (%), C) density.

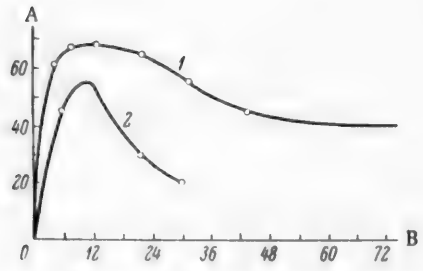

Fig. 3. Variation of catalyst activity with time.
A) Conversion of vinylacetylene (%), B) time (hours). Curves for variation of catalyst activity: 1) in presence of oxygen, 2) in absence of oxygen.

appreciable decrease of catalyst activity which was observed after 10-12 hours of continuous operation resulted in decreased conversion of vinylacetylene, and was accompanied by considerable resinification as the result of polymerization of vinylacetylene and fluoroprene in the catalytic zone. The strong resinification caused complete clogging of the reactor by the cemented mass, the removal of which presented considerable difficulty. The activity fell also as the result of chemical changes in the principal catalyst components – mercury salts. This is confirmed by the fact that metallic mercury was found on the reactor walls and on the support (carbon).

As is known, ferric salts or other oxidizing agents are added to the catalyst to prevent reduction of mercuric salts in the hydration of acetylene or vinylacetylene; this leads to a considerable increase of catalyst activity and service life.

In our experiments up to 6% of oxygen, calculated on the reaction mixture, was introduced into the reaction zone for this purpose. It was found that this produced a considerable increase of the time for which the catalyst could be used continuously. The spent catalyst was easily removed from the tube; this indicates a decrease of resinification due to polymerization of vinylacetylene and fluoroprene on the catalyst.

EXPERIMENTAL

One of the main difficulties in laboratory work involving the continuous supply of hydrogen fluoride is estimation of the amount of hydrogen fluoride supplied in the gas phase.

For exact determination of the amount of hydrogen fluoride supplied, we developed and used a method based on saturation of nitrogen with hydrogen fluoride at a constant predetermined temperature. The degree of saturation of nitrogen with hydrogen fluoride at various temperatures was first determined experimentally; thus, by variation of the amount of nitrogen the amount of hydrogen fluoride fed into the reaction could be regulated.

The apparatus used for hydrofluorination of vinylacetylene over a solid catalyst (mercuric oxide on carbon) in the laboratory is shown schematically in Fig. 1.

The reactor was an iron tube 1, 25 mm in diameter and 300 mm long. One end of the tube was connected to a mixing vessel for gases entering the reactor, and the tube was provided with a thermocouple socket. The reactor was surrounded by a jacket through which water, warmed by means of an external electric heater, was circulated. The temperature was regulated by means of a contact thermometer.

Nitrogen from the cylinder 2, fitted with a reducing valve 3, entered the mixing vessel through the buffer flask 4 to which a manometer 5 was attached, and a flow meter 6. Some of the nitrogen passed through a second tube through a flow meter 7 into a cylinder 8 with liquid hydrogen fluoride, contained in a thermostat, and the nitrogen saturated with hydrogen fluoride then also entered the mixing vessel. Gaseous vinylacetylene was fed from the cylinder 9 through the flow meter 10 into the mixing vessel. The reaction products passed from the reactor 1, through the buffer flask 11, alkaline absorption flask 12, and trap 13 into the drying column 14. The dried gaseous mixture was then condensed at -70 to $-75°$ in the low-temperature condensers 15.

The course of hydrofluorination was checked by an analytical method based on determination of the density of the reaction products (vinylacetylene, fluoroprene, and difluorobutene), and on chemical determination of one of the components (vinylacetylene).

The determination of vinylacetylene was based on its reaction with an alkaline solution of K_2HgI_4, with subsequent titration of excess alkali.

$$K_2HgI_4 + 2C_4H_4 + 2KOH \rightarrow Hg(C_4H_3)_2 + 4KI + 2H_2O$$

The fluoroprene content of difluorobutene was calculated from the formula for a 3-component mixture (from the density of the mixture and its vinylacetylene content).

$$C = 8.323 \cdot \left[\left(\frac{100}{d} - \frac{a}{0.7085}\right) \cdot 0.951\right] + a - 100,$$

where C is the fluoroprene content of the condensate (%), a is the vinylacetylene content (%); d is the density of the mixture; 0.7085 is the density of vinylacetylene; 0.951 is the density of difluorobutene; 8.323 is a coefficient found by calculation.

As the difluorobutene content of the reaction products did not exceed 1-1.5% and varied relatively little, in a number of experiments it was not taken into account, and the fluoroprene content, i. e., the degree of conversion of vinylacetylene, was estimated approximately from a density graph (Fig. 2) for a 2-component mixture (of vinylacetylene and fluoroprene).

Preparation of the catalyst. 82 g of mercuric nitrate was dissolved in 400 ml of water acidified with 12 ml of nitric acid (sp. gr. 1.40). 100 g of chemically pure NaOH was dissolved in 1 liter of water. The alkali solution was gradually added to the mercuric nitrate solution. The precipitate was washed with water by decantation to a neutral reaction, and then suspended in 150 ml of water.

The aqueous suspension of mercuric oxide was poured onto previously sifted and dried carbon (1 liter), with continuous shaking. The carbon with the catalyst was dried under vacuum at 80°.

Influence of certain factors on hydrofluorination of vinylacetylene over a solid catalyst. The effects of temperature (30, 50, 60, and 70°) and contact time (30, 60, and 80 seconds) were studied. The molar ratio of vinylacetylene and nitrogen (dilution of the reaction mixture by inert gas) was varied from 1:2 to 1:3, with molar ratios of vinylacetylene to hydrogen fluoride of 1:1, 1:0.5, and 1:1.5.

The results given below were obtained with a contact time of 30 seconds at temperatures of 50 and 30°, with vinylacetylene, hydrogen fluoride, and nitrogen in the molar proportions of 1:1:2; the experiments were carried out in total absence of oxygen:

Molar ratio of vinylacetylene to hydrogen fluoride	1:1.06	1:0.9	1:0.95	1:1.06
Temperature (°C)	50	50	30	30
Time (hours)	25	25	22	19.5

Composition of reaction products (%):				
vinylacetylene	41.4	33.8	35.0	32.5
fluoroprene	51.2	58.7	58.1	60.3
difluorobutene	7.4	7.5	6.9	7.2
Yield of fluoroprene (%) calculated on vinylacetylene:				
converted	53.1	59.2	45.0	42.4
passed	33.3	40.3	32.2	32.2

Under these conditions the resistance increased sharply owing to serious resinification of the catalyst in the reaction zone, and the time of continuous operation did not exceed 20-25 hours. In experiments carried out at 50° the fluoroprene yield on the converted vinylacetylene varied from 51 to 59%, while in experiments at 30° the yield was 42.4-45%.

The results given below were obtained with a contact time of 30 seconds at temperatures of 50 and 30°, with the same molar proportions, but with 4-6% of oxygen introduced into the reaction zone:

Molar ratio (actual) of vinylacetylene to hydrogen fluoride	1:0.92	1:1.0	1:1.05	1:0.97	1:0.85
Temperature (°C)	50	50	30	30	30
Time (hours)	21	19	17.5	21	18
Composition of reaction products (%):					
vinylacetylene	59.0	42.5	46.5	53.3	52.6
fluoroprene	39.0	57.1	50.0	44.2	45.6
difluorobutene	2.0	0.4	3.4	2.5	1.8
Yield of fluoroprene (%) calculated on vinylacetylene:					
converted	66.8	66.7	58.9	60.5	60.5
passed	37.8	39.4	33.4	30.4	30.8

Under these conditions, the fluoroprene yield on the converted vinylacetylene was 65-67% at 50°, and about 60% at 30°*. It should be noted that in the experiments in which oxygen was supplied into the reaction zone there was less resinification of the catalyst in the reaction zone. The resistance of the system increased only slightly, and therefore the operating time of the catalyst can be increased considerably.

The results given below were obtained with a contact time of 60 seconds at 50°; the component ratio was the same as in the preceding series:

Molar ratio of vinylacetylene to hydrogen fluoride	1:1	1:0.91	1:0.8	1:0.75
Time (hours)	38	36	34	37
Composition of reaction products (%):				
vinylacetylene	44.6	44.8	53.8	48.4
fluoroprene	53.4	52.8	45.6	49.0
difluorobutene	2.0	2.4	0.63	2.6
Yield of fluoroprene (%) calculated on vinylacetylene:				
converted	71.3	73.1	73.3	69.6
passed	39.1	39.3	33.4	35.6

This series of experiments was carried out in complete absence of oxygen. The service time of the catalyst varied in the range of 34-38 hours, after which the experiments were terminated owing to the sharp increase of pressure in the system (resinification of the catalyst). The fluoroprene yield on the converted vinylacetylene was 70-73%.

---

* These results show that decrease of the reaction temperature to 30° decreases the conversion of vinylacetylene appreciably. Further studies of the effects of individual factors were therefore carried out at 50°.

The results of experiments with a contact time of 60 seconds at 50°, at the same molar ratios of the reaction components, are given below:

Molar ratio of vinylacetylene to hydrogen fluoride	1:1.06	1:1.02	1:1.04	1:1.05	1:1.0
Time (hours)	24	24	24	73.5	50
Composition of reaction products (%):					
vinylacetylene	32.7	39.4	38.2	32.5	47.6
fluoroprene	65.5	57.7	59.9	64.7	51.0
difluorobutene	1.8	2.9	1.9	2.8	1.4
Yield of fluoroprene (%) calculated on vinylacetylene:					
converted	67.7	66.3	63.8	70.6	74.8
passed	46.1	40.8	38.0	50.6	36.7

In these experiments from 4 to 6% of oxygen was introduced into the reaction zone during the reaction. Under these conditions the service life of the catalyst increased considerably. There was no resinification after 20 hours of use, and the catalyst retained a considerable part of its activity. Further experiments showed that the catalyst can operate for up to 80-100 hours if oxygen is introduced into the reaction zone.

As the above results show, the fluoroprene yield on the converted vinylacetylene reaches 75%.

Thus, it is evident from all the above data in conjunction with the curve in Fig. 3 that, other conditions being equal, introduction of oxygen into the reaction zone lengthens the service life of the catalyst considerably, with a relatively slight decrease of activity.

Therefore in all the subsequent experiments oxygen was introduced into the reaction zone.

Experiments on the effect of the molar ratio of vinylacetylene to hydrogen fluoride, carried out with ratios of 1:0.5, 1:1, and 1:1.5 at 50° and a contact time of 60 seconds, showed that under these conditions the optimum molar ratio of vinylacetylene to hydrogen fluoride is 1:1. The results of these experiments are given below.

Molar ratio of vinylacetylene to hydrogen fluoride	1:0.39	1:0.41	1:1.0	1:1.0	1:1.49	1:1.46
Time (hours)	12.0	12.0	38.0	56.0	24.0	21.0
Composition of reaction products (%):						
vinylacetylene	87.6	83.3	44.6	49.6	24.8	12.5
fluoroprene	12.4	16.7	53.4	50.0	60.2	73.1
difluorobutene	—	—	2.0	0.4	15.0	14.4
Yield of fluoroprene (%) calculated on vinylacetylene:						
converted	24.7	38.3	71.3	74.8	56.4	52.5
passed	7.2	9.4	39.1	36.7	42.2	46.7

A decrease of the amount of hydrogen fluoride to a ratio of 1:0.5 results in a sharp decrease of vinylacetylene conversion. Increase of the amount of hydrogen fluoride to a ratio of 1:1.5 increases the rate of the secondary reaction (addition of hydrogen fluoride to fluoroprene) of difluorobutene formation.

Studies of the effect of dilution of the gas mixture with nitrogen showed that when the molar ratio of vinylacetylene to nitrogen is increased from 1:2 to 1:3, the catalyst life is increased somewhat (from 70-80 to 100 hours) while the productivity is retained.

The results are given below:

Molar ratio of vinylacetylene to nitrogen	1:2	1:2	1:3	1:3
Molar ratio of vinylacetylene to hydrogen fluoride	1:0.97	1:0.84	1:1	1:0.87
Time (hours)	70.0	88.0	100	100

Yield of fluoroprene (%) calculated on vinylacetylene:				
converted	68.2	65.8	78.5	74.0
passed	35.9	30.8	32.9	28.5
Productivity of 1 liter of catalyst (g of fluoroprene per hour)	18.0	15.5	13.3	13.6
Productivity of 1 kg of mercuric oxide per cycle (in kg of fluoroprene)	26.8	27.3	26.6	27.3

Decrease of the contact time from 60 to 30 seconds reduces the catalyst productivity, calculated on the mercuric oxide, by about one half, as the catalyst becomes unserviceable earlier (the service life of the catalyst is reduced to 45-50 hours).

The influence of contact time is shown below:

Molar ratio of vinylacetylene to nitrogen	1:3	1:3	1:3	1:3
Contact time (seconds)	60	60	30	30
Time (hours)	100	100	45	47
Yield of fluoroprene (%) calculated on vinylacetylene:				
converted	78.5	74.0	47.2	52.2
passed	32.9	28.5	19.0	18.5
Productivity of 1 liter of catalyst (g of fluoroprene per hour)	13.3	13.6	17.0	14.0
Productivity of 1 kg of mercuric oxide per cycle (in kg of fluoroprene)	26.6	27.3	15.3	13.1

As was to be expected, hydrofluorination of vinylacetylene over a solid catalyst in a larger unit involved considerable difficulties because of the need to remove the large quantity of heat evolved in the reaction.

It was found that when the reactor diameter (catalyst layer) is increased above 50 mm the required temperature cannot be maintained by removal of the heat of reaction by means of external cooling. Local overheating results in considerable resinification of the catalyst, which rapidly becomes unserviceable.

The best results obtained in the process carried out on a larger scale at 50°, with a contact time of 60 seconds, and a molar ratio of vinylacetylene to nitrogen of 1:2, are given below:

Molar ratio of vinylacetylene to hydrogen fluoride	1:0.9	1:0.8	1:0.8	1:0.97	1:0.84
Catalyst taken (ml)	1100	1100	1700	3100	3100
Time (hours)	76	64	87	70	88.5
Yield of fluoroprene (%) calculated on vinylacetylene:					
converted	58	78	79	68.2	65.8
passed	33.8	35.5	33.5	35.9	30.8
Productivity of 1 liter of catalyst (kg of fluoroprene per hour)	17.7	19.8	16.9	18.0	15.5
Productivity of 1 kg of mercuric oxide per cycle (in kg of fluoroprene)	26.8	25.5	29.6	25.0	27.4

The above results show that the maximum catalyst productivity reached was 15-20 kg of fluoroprene per liter of catalyst per hour. The productivity of 1 kg of mercury does not exceed 30 kg of fluoroprene per cycle.

90-95% of the mercury can be recovered from the spent catalyst. The recovery method will be described in the next communication.

SUMMARY

1. The conditions for synthesis of fluoroprene from vinylacetylene and hydrogen fluoride in the gas phase over a solid catalyst were studied.

INVESTIGATION OF THE BY-PRODUCT FORMED IN THE NITRATION OF TOLUENE

E. Iu. Orlova and S. S. Romanova

(The D. I. Mendeleev Institute of Chemical Technology, Moscow)

When toluene is nitrated to mononitrotoluene (MNT) under certain conditions, especially with circulation of the acid, the whole mass becomes dark and sometimes a flocculent reddish black precipitate is formed. The degree of darkening and the subsequent course of the process vary in different instances. Sometimes the process is very violent, the reaction mass froths, and is often ejected from the apparatus.

Darkening of the reaction mass lowers the yield, contaminates the main product with a by-product, and increases the hazards of the process.

The formation of a black by-product in the nitration of aromatic hydrocarbons (benzene) was first described by Battegay [1], who observed its formation in the course of nitration by nitrogen oxides in sulfuric acid, and noted the fairly stable black color of the spent acids. The color was lost only on addition of water or nitric acid. Battegay assumed that the spent acid contains a colored complex consisting of benzene, nitrosylsulfuric, and sulfuric acids: $xC_6H_6 \ldots yNSO_5H \ldots zH_2SO_4$. Similar effects were observed in the case of toluene by Kholevo and Eitingon [2] and by Titov and Baryshnikova [3].

In the present investigation the dark by-product was made by the addition (in one step) of toluene to sulfuric acid containing nitrosylsulfuric acid. The toluene dissolved, and the whole mass became almost black (with a reddish tinge). On addition of water to the colored mass nitrogen oxides were evolved, and the mass gradually lost its color and separated into two layers.

Analysis showed that the lower layer is sulfuric acid, and the upper is toluene. This supports Battegay's view that the reaction product of toluene and nitrosylsulfuric acid is a complex.

Tests of the colored mass by the Liebermann reaction [4] showed the presence of a substance containing the nitroso group. The presence of the nitroso group was also found in solutions of nitrosylsulfuric acid in sulfuric acid; nitroso groups were not detected in dry nitrosylsulfuric acid. These facts are in agreement with the results of Hantzsch [5], who showed by means of spectrum analysis that nitrosylsulfuric acid has a saltlike structure – $(NO \cdot SO_4H)$.

Therefore, if the product in question is a complex of toluene, sulfuric acid, and nitrosylsulfuric acid, the latter must be present as the saltlike form – $(NO \cdot SO_4H)$.

It was found that in the formation of the dark product 1 molecule of toluene binds 2 molecules of nitrosylsulfuric acid and 3 molecules of sulfuric acid. Therefore the complex has the following composition: $(C_6H_5CH_3) \cdot (NO \cdot SO_4H)_2 \cdot (H_2SO_4)_3$.

We attempted to isolate the complex from its solution in sulfuric acid by means of extraction in a solvent. However, solvents such as toluene, benzene, carbon tetrachloride, dichloroethane, and mononitrotoluene do not dissolve the complex, which does not enter the organic layer. When acetone, ethyl or methyl alcohol, diethyl ether, or nitric acid were added, they apparently reacted with the whole mass, which usually became decolorized with liberation of nitrogen oxides.

On addition of dilute nitric acid (56.5%) the mass became pale yellow in color and separated into two layers, the upper being mononitrotoluene, and the lower, nitric – sulfuric acid mixture. It was found that 2 moles

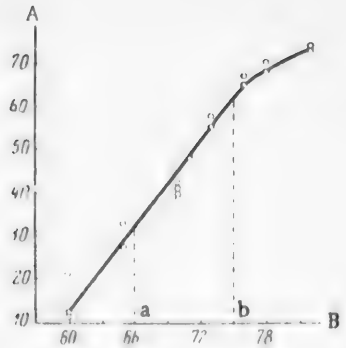

Fig. 1. Effect of sulfuric acid concentration on the stability of the by-product.
A) Time (minutes), B) H_2SO_4 concentration (%). a – b) Limits of H_2SO_4 concentration in the acid mixture in industrial nitration of toluene.

of nitric acid is needed per mole of toluene for complete conversion. Decolorization of the mass on addition of 2 moles of nitric acid per mole of toluene is gradual; we were able to show that the rate of this process, which we define as the "stability" of the by-product, depends on a number of factors in the formation of the dark product. The "stability" of the by-product is apparently determined to a considerable extent by its concentration in solution.

The data in the graphs show that the "stability" of the by-product depends on the following factors.

1. It increases with increase of the sulfuric acid concentration (Fig. 1).

The effect of the sulfuric acid concentration on the stability of the by-product is given below.

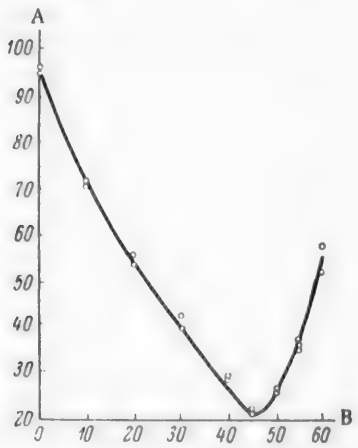

Fig. 2. Effect of temperature on the stability of the by-product.
A) Time (minutes), B) temperature (°C).

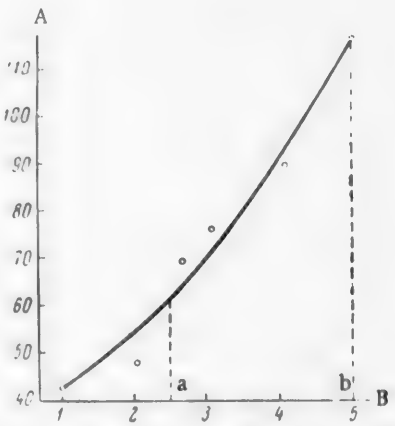

Fig. 3. Effect of N_2O_3 concentration on the stability of the by-product.
A) Time (minutes) B) N_2O_3 concentration (%). a – b) Limits of N_2O_3 concentration in the acid mixture in industrial nitration of toluene.

Reaction Time 10 Minutes at 30°, 5 g of Toluene, 25 g of Sulfuric Acid Containing 1.02% N_2O_3

H_2SO_4 concentration (%) 60 60 65 65 70 70 70 70 73 73 76 76 78 78 82 82
(minutes) 11 12 33 27 40 39 42 41 58 55 67 65 70 68 73 74

1. 1.4-fold change of sulfuric acid concentration (from 60 to 82% H_2SO_4) results in a 6-fold increase of the decolorization time (to 75 minutes from 11).

2. The stability depends on the temperature at which the dark product was formed.

The effect of temperature on the stability of the by-product is given below.

Reaction Time 10 Minutes, 5 g of Toluene, 25 g of Sulfuric Acid Containing 70% H_2SO_4, 1.02% N_2O_3

Temperature (°C) 0 0 10 10 20 20 30 30 40 40 45 45 50 50 55 55 55 60 60
Time for decolorization (minutes) 95 96 71 71 56 54 40 41 28 30 21 22 26 26 37 36 37 58 53

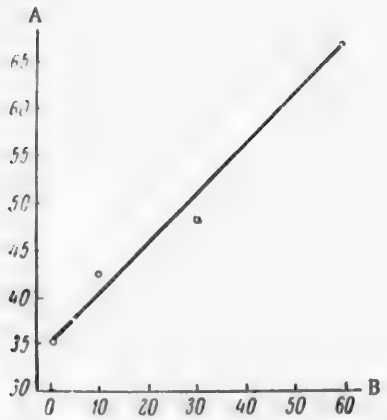

Fig. 4. Effect of the formation time of the by-product on its stability. A) Decomposition time (minutes), B) formation time (minutes).

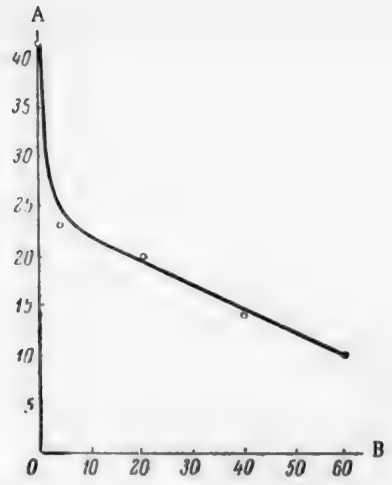

Fig. 5. Effect of mononitrotoluene on the stability of the by-product. A) Time (minutes), B) amount of mononitrotoluene (%).

The decolorization rate at low temperatures (up to 45°) is evidently higher than the rate of formation. At higher temperatures the formation rate exceeds the decolorization rate, as is clearly seen in Fig. 2. Increase of the temperature of the mass above 65° results in frothing, a spontaneous temperature rise to 85-90°, and, on addition of nitric acid, in precipitation of a brown flocculent substance.

3. The stability increases with increasing concentration of nitrogen oxides (Fig. 3).

The effect of N_2O_3 concentration on the stability of the by-product is given below.

Reaction Time 10 Minutes at 30°, 5 g of Toluene, 25 g of Sulfuric Acid Containing 70% H_2SO_4

N_2O_3 in medium (%)	1.02	2.05	2.67	3.09	4.11	5.13
Time for decolorization (minutes)	42	47	69	76	90	116

A 5-fold change in the concentration of nitrogen oxides in the formation of the by-product (from 1.02 to 5.13%) increases the time of decolorization 2.8-fold (from 42 to 116 minutes).

4. The stability increases with the time of formation of the by-product (Fig. 4).

The effect of the time of formation of the by-product on its stability is given below.

5 g of Toluene, 25 g of Sulfuric Acid Containing 70% H_2SO_4 and 1.029% N_2O_3, Reaction Temperature 30°

Reaction time (minutes)	1	5	10	30	60	120
Time for decolorization (minutes)	35	37	42	48	66	Not decolorized in 24 hours.*

5. The stability decreases with increasing concentration of mononitrotoluene in the reaction mass (Fig. 5).

The effect of mononitrotoluene on the stability of the by-product is given below.

* The by-product formed after 120 minutes was stirred for 24 hours with two moles of nitric acid; 2 more moles of nitric acid was added and the liquid was kept for 2 more hours, but it was not decolorized. Water was then added; after 2 hours a brown flocculent precipitate was formed.

Reaction Time 10 Minutes at 30°, 5 g of Toluene, 25 g of Sulfuric Acid Containing 70% H_2SO_4 and 1.02% N_2O_3

Amount of MNT (%)	0	4	20	40	60
Time for decolorization (minutes)	42	23	20	14	10

These results can be used for selection of conditions for nitration of toluene in which the by-product is not formed. In order to avoid the formation of the by-product in nitration of toluene by sulfuric – nitric acid mixture, it is necessary to prevent contact between toluene and the spent acid, free from nitric acid. If such conditions nevertheless arise and the complex is formed, immediate steps must be taken to decompose it. The decomposition of the complex should be carried out preferably at 40-50°. At these temperatures the rate of decomposition of the complex by dilute nitric acid is higher than the rate of its formation. When the nitration mass darkens, so long as the complex is not decomposed, the temperature must not be allowed to rise above 65°, as otherwise frothing occurs and leads to formation of a brown amorphous substance.

The most dangerous stage, with regard to formation of the complex, is the early stage of nitration; subsequently, as toluene is converted into mononitrotoluene, the latter prevents formation of the complex.

EXPERIMENTAL

Starting materials. Toluene, from petroleum, was purified by repeated shaking with concentrated sulfuric acid and then distilled; the fraction in the 109-110.5° range was taken with sp. gr. 0.8580 at 22°. Chemically pure sulfuric acid (93.3% H_2SO_4), technical strong nitric acid (98% HNO_3), and dilute nitric acid (56.6% HNO_3) were used.

Nitrosylsulfuric acid was prepared as follows. Sodium sulfite was put in a Wurtz flask, and concentrated sulfuric acid was added to it (dropwise) from a dropping funnel to give a stream of SO_2. The sulfur dioxide was lead off through a side tube into concentrated nitric acid (98% NHO_3) dissolved in a 20-fold amount of dichloroethane and contained in an Erlenmeyer flask. The temperature in the flask was not allowed to exceed 10° by means of cooling by water and snow. The precipitated crystals of nitrosylsulfuric acid were pressed out in a Schott funnel and kept in the dry state or dissolved in concentrated sulfuric acid. This solution had the following % composition by analysis: H_2SO_4 92.25, HNO_3 0.174, N_2O_3 5.136. The "dry" nitrosylsulfuric acid contained 23.9% N_2O_3; the theoretical N_2O_3 content is 29.8%.

Analytical methods and experimental conditions. The total acidity of the mixture, and the strengths of the sulfuric and nitric acids, were determined by titration with 1 N NaOH solution. The nitric acid content of the mixture was determined by titration with $FeSO_4$ solution. Nitrogen oxides were determined by titration with 0.1 N potassium permanganate solution. A definite quantity of the acid mixture consisting of sulfuric and nitrosylsulfuric acids was introduced into a 3-necked flask provided with a stirrer, thermometer, and dropping funnel. The contents of the flask were cooled to 7-10° in a water bath, so that the toluene could all be added at once, and the temperature was then kept at a fixed level for the required time by means of a water bath. In all cases when toluene came into contact with sulfuric acid containing nitrosylsulfuric acid the reaction mass darkened almost instantaneously, with varying degrees of intensity.

At the end of the experiment 56.5% nitric acid (2 moles per mole of toluene) was added in one step to the reaction mass; the temperature of the solution was kept constant, and the time required for decolorization was recorded. On addition of nitric acid the color changed from black to dark red, then orange, and finally yellow; the transition from orange to yellow was taken as the end of decolorization. The amount of by-product was assumed to be proportional to the decolorization time.

Influence of Various Factors on the Formation Rate of the By-Product

The by-product has limited stability, and the action of nitric acid converts it into a new compound, as shown by the decolorization which occurs.

The effects of temperature, and concentrations of sulfuric acid, nitrogen oxides, and mononitrotoluene on the rate of this reaction were studied.

Investigation of Some of the Properties of the By-Product

The by-product was prepared under the following conditions: 5 g of nitrosylsulfuric acid and 5 g of toluene were added to 20 g of 70% sulfuric acid. The mixture was stirred for 10 minutes at 30°.

No solvent was found which would extract the product from sulfuric acid solution. The substance is either insoluble in the solvents tested (toluene, carbon tetrachloride, dichloroethane, mononitrotoluene), or it reacts with them (acetone, ethyl alcohol, diethyl ether, water, nitric acid).

On addition of water, the product decomposed with liberation of nitrogen oxides. The solution was gradually decolorized. The lower layer was found, by analysis, to consist of sulfuric acid, and the upper layer, of toluene (sp. gr. 0.8590, and characteristic odor).

Decomposition of the product by water led Battegay [1] to assume that it is a complex.

On addition of nitric acid, the product decomposed with liberation of nitrogen oxides, gradual decolorization to a pale yellow color, and separation of the liquid into two layers. The upper layer was found to be mononitrotoluene (sp. gr. 1.15 and characteristic odor), and the lower, a mixture of sulfuric and nitric acids.

It was found that 2 moles of nitric acid is consumed per mole of toluene in decolorization of the product.

The nitroso group was detected by means of the Liebermann reaction in the by-product and in a solution of nitrosylsulfuric acid in sulfuric acid. Dry nitrosylsulfuric acid does not give this reaction. Hantzsch [5], who studied the structure of nitrosylsulfuric acid, showed that it may have a saltlike structure $-(NO)\cdot(SO_4H)$. Presence of the nitrosyl group in the product suggests that if the latter is a complex it contains nitrosylsulfuric acid in the saltlike form.

Determination of the Proportions of Toluene, Nitrosylsulfuric Acid, and Sulfuric Acid in the Product

0.9455 g of nitrosylsulfuric acid was mixed with toluene (by shaking) in a weighing bottle until the characteristic dark color appeared. The open bottle was placed in a desiccator connected to a vacuum pump, in order to remove excess toluene. The bottle was weighed from time to time in order to determine the amount of toluene entering the reaction. At the end of 2 days the weight became constant at 0.9611 g. The product was dissolved in sulfuric acid (16.7470 g) and analyzed for nitrogen oxides. The mixture was found to contain 0.103 g of N_2O_3, which corresponds to 0.430 g of nitrosylsulfuric acid. The amount of nitrogen oxides introduced with the nitrosylsulfuric acid was 0.226 g. Therefore a part of the nitrogen oxides evaporated together with toluene, and nitrosylsulfuric acid was converted into sulfuric acid. Evaporation of the oxides was confirmed by a yellow color formed on filter paper, and by the presence of yellow vapor.

The amount of nitrogen oxides evaporated was 0.226 − 0.103 = 0.123 g. Therefore, 0.9611 − (0.9455 − − 0.123) = 0.138 g of toluene, 0.430 g of nitrosylsulfuric acid, and 0.393 g of sulfuric acid (0.9611 − 0.138 − 0.430 = = 0.393) entered the reaction; the corresponding molecular proportions are: toluene 0.138/92 = 0.0015, nitrosylsulfuric acid 0.430/127 = 0.0033, sulfuric acid 0.393/98 = 0.0040. Similar proportions were found in a duplicate experiment. This shows that the by-product is a complex of the following composition: $-(C_6H_5CH_3)\,(NO\cdot SO_4H)_2\,(H_2SO_4)_3$.

SUMMARY

1. When toluene is mixed with nitrosylsulfuric acid in sulfuric acid, a black complex compound is formed.

2. This compound is composed of a molecule of toluene, two molecules of nitrosylsulfuric acid, and three molecules of sulfuric acid. The nitrosylsulfuric acid in the complex is in the nitroso form. The following formula is proposed for the complex:

$$(C_6H_5CH_3)\,(NO\cdot SO_4H)_2\,(H_2SO_4)_3.$$

3. The complex may be decomposed by dilute nitric acid. Its stability depends on the formation conditions. The stability increases with increasing concentration of sulfuric acid, increasing temperature, increasing concentration of nitrogen oxides, and decreasing concentration of mononitrotoluene.

4. A solution of the complex in sulfuric acid froths at temperatures above 65°. Dilution of the frothing mass with water causes precipitation of a flocculent brown substance.

5. In order to avoid formation of the complex compound in the nitration of toluene by sulfuric – nitric acid mixture, it is necessary to prevent contact between toluene and spent acid, free from nitric acid. If such conditions nevertheless arise and the complex is formed, immediate steps must be taken to decompose it. The complex should be decomposed at 40-50°. At these temperatures the rate of decomposition of the complex by dilute nitric acid is higher than its formation rate.

6. When the nitration mass darkens, so long as the complex has not been destroyed, the temperature must not be allowed to rise above 65°; otherwise frothing takes place, leading to formation of a brown amorphous substance.

7. The initial stage of nitration is particularly dangerous with regard to formation of the complex; subsequently, as the toluene is converted into mononitrotoluene, the latter prevents formation of the complex compound.

LITERATURE CITED

[1] M. Battegay, Bull. Soc. Chim. 43, 109 (1928).

[2] N. A. Kholevo and I. I. Eitingon, J. Appl. Chem. 9, 1465 (1936).

[3] A. I. Titov and A. N. Baryshnikova, J. Gen. Chem. 6, 12, 1801 (1937).

[4] C. Liebermann, Ber. 15 (1882); 2, 457 (1869); K. Bauer, Organic Analysis (Moscow, 1953) 133 [Russian translation].

[5] A. Hantzsch and K. Berger, Z. anorg. Chem. 190, 321 (1930); Zbl. II, 2112, (1930).

Received February 2, 1957.

LUMINESCENCE METHOD FOR DETERMINATION OF GOSSYPOL

S. N. Vil'kova and A. L. Markman

(The Polytechnic Institute of Central Asia)

Purely chemical methods for determination of gossypol in cottonseed and cottonseed products – oil, oil cake, and meal – have well-known disadvantages: precipitation as dianilinogossypol [1] or as dianilinodipyridinogossypol [2-4] requires 7-14 days; Podol'skaia's volumetric method, based on the reduction of Fehling's solution [5], is rapid but often gives high results in presence of other reducing agents in addition to gossypol in the samples.

Several methods have been proposed for spectrophotometric determination of gossypol in the form of various derivatives, such as anilides [6, 7], and compounds with antimony trichloride [8] or p-anisidine [9].

Recently Markman and Kolesov [10] described a polarographic method for determination of gossypol. All these methods can be used for determination of native or slightly-modified gossypol. The colorimetric method developed by Rzhekhin and Chudnovskaia [11] for determination of the total contents of gossypol and its derivatives gives only approximate values, while calculation of the individual content of deeply-modified gossypol from the total content is, according to the authors themselves, arbitrary in character.

As gossypol contains condensed aromatic rings, it was assumed that its molecules should exhibit luminescence when its solutions are irradiated. This hypothesis was tested with the aid of a Zeiss quartz spectrograph. The source of light for exciting luminescene was a PRK-2 mercury – quartz lamp. The luminescence radiation was directed onto a photographic plate; for quantitative analysis the degree of blackening of the plate was determined by means of the MF-2 microphotometer.

The experiments were performed with gossypol extracted by means of ethyl ether from high-quality cottonseed kernels previously extracted with ligroine.

The gossypol was purified by repeated precipitation by means of ligroine from concentrated solutions in ethyl ether. The purified product was in the form of fine crystals.

Found % C 69.26, H 5.99.

$C_{30}H_{30}O_8$. Calculated % C 69.48, H 5.83.

The solvent used was chloroform (medical, for anesthesia). When tested it was found to exhibit blue luminescence in the 491.6 – 314.5 mμ region. This is evidently due to some impurities. Tests on the luminescence of chloroform solutions of gossypol showed that gossypol itself does not exhibit luminescence, but quenches the blue luminescence due to chloroform; this quenching increases with the gossypol concentration, and becomes complete beyond a certain concentration limit.

Similar results were obtained with acetone as solvent. Acetone, even if repeatedly distilled, gives a blue luminescence; gossypol dissolved in acetone weakens this luminescence and ultimately quenches it completely.

This showed that even if gossypol itself does not luminesce, it is a powerful quencher of luminescence. It is highly probable that absence of luminescence in this case is due to freedom of rotation of both naphthalene radicals about the 2 – 2' axis.

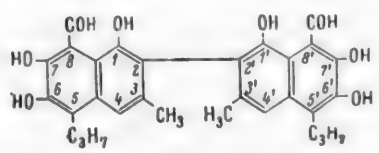

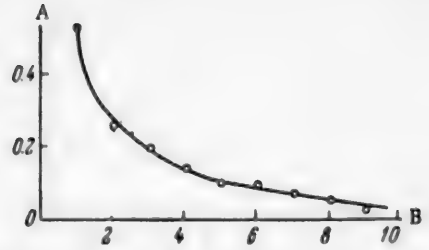

Fig. 1. Effect of gossypol concentration on the quenching luminescence.
A) log I/log I_0, B) gossypol concentration $C \cdot 10^5$ (g/ml).

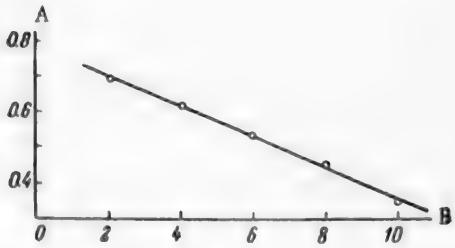

Fig. 2. Effect of the concentration of gossypol extracted from soybean oil on the quenching of luminescence.
A) log I/log I_0, B) gossypol concentration $C \cdot 10^5$ (g/ml).

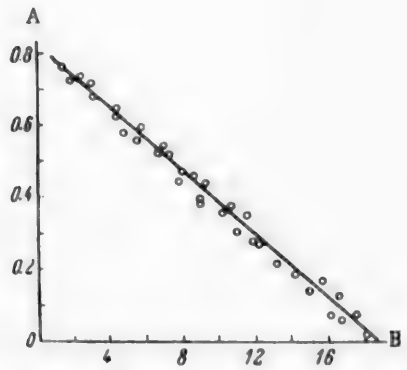

Fig. 3. Effect of the concentration of gossypol extracted from cottonseed oil on the quenching of luminescence.
A) log I/log I_0, B) gossypol concentration $C \cdot 10^5$ (g/ml).

However, this effect, which reduces to a transformation of the absorbed energy, together with the great tendency of gossypol to undergo oxidation, i. e., to lose electrons, should confer qenching properties on it. It was therefore decided to study the quenching of luminescence by gossypol, and to use the quenching effect as an analytical characteristic. The luminescent substance chosen was fluorescein, the molecule of which

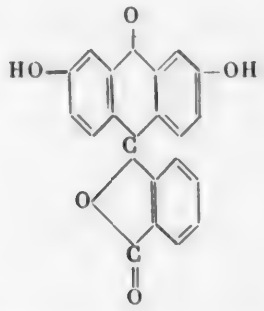

has a number of features in common with the gossypol molecule; this is very important in the light of the views put forward by Vavilov and Galanin [12] on the quenching of dye luminescence by dyes. Such molecular similarity must result in quenching, and the concentration of the quenching agent needed to cause it would be thousands of times less than the concentration of ordinary quenching agents.

Another important fact is that fluorescein is readily soluble in alkali, and gives the highest luminescence yield in alkaline solution; this is important because in work with oil gossypol is extracted from oil by means of shaking with alkali solution.

The experiments were performed with an ISP-51 spectrograph with a glass optical system. Light from a mercury – quartz lamp was passed through a blue filter, which absorbed all the lines of the mercury spectrum with the exception of the 336 mμ line, which excited yellow-green luminescence in fluorescein. Preliminary experiments showed that, if methyl or ethyl alcohol is used as solvent, gossypol quenches the luminescence of fluorescein, and the quenching effect increases with the amount of gossypol in the solution. However, the relationship between the quenching effect and gossypol concentration is not linear, but is of a more complex nature, as is clear from Fig. 1, where this relationship is plotted for the quenching of the luminescence of fluorescein in ethyl alcohol (concentration $1 \cdot 10^{-3}$ g/ml) by native gossypol; the abscissa represents the gossypol concentration ($1 \cdot 10^{-3} - 1 \cdot 10^{-2}$ g/ml), and the ordinate represents the logarithmic ratio of the blackening intensities caused by luminescence partially quenched by gossypol, and the initial luminescence respectively. Special experiments were carried out to find whether any photochemical reactions take place during irradiation of fluorescein solutions containing dissolved gossypol: to an alcoholic solution of fluorescein ($1 \cdot 10^{-3}$ g/ml)

TABLE 1

Comparison of the Polarographic and Luminescence Methods for Determination of Gossypol in Oil

Heating conditions for model solution	Gossypol content of oil in g/ml ($C \cdot 10^4$)	
	polarographic determination	luminescence determination
Not heated	1.16	1.20
Heated at 80°	0.46	0.42
Not heated	2.98	3.00
Heated at 80°	0.91	1.00
Not heated	4.84	4.80
Heated at 100°	0.80	0.85
Not heated	7.28	7.21
Heated at:		
80°	3.21	3.29
100°	1.10	1.50
120°	0.22	0.25
Not heated	8.44	8.40
Heated at:		
80°	4.70	4.80
100°	2.22	2.25
120°	0.60	0.40

TABLE 2

Results of Gossypol Determinations in Black Cottonseed Oils

Type of oil	Heating conditions	Gossypol content of oil in g/ml ($C \cdot 10^4$)	
		polarographic determination	luminescence determination
Screw-pressed oil from the Yangi-Yul' factory	Not heated	9.10	9.40
	Heated at:		
	80°	8.82	8.25
	100°	5.65	5.21
	120°	4.41	4.20
	140°	0.65	0.55
Pre-pressed oil from the Chimkent factory	Not heated	5.65	5.25
	Heated at:		
	80°	5.10	5.00
	100°	2.62	2.25
	120°	1.00	0.90
	140°	0.60	0.45
Extracted oil from the Chimkent factory	Not heated	3.40	3.20
	Heated at:		
	80°	3.25	3.00
	100°	1.65	1.45
	120°	0.65	0.45
	140°	0.19	0.10

gossypol was added in concentrations from $1 \cdot 10^{-3}$ g/ml to $3 \cdot 10^{-3}$ g/ml, each sample was then irradiated for 30 minutes, and the spectra of the solutions were photographed. Photometric examination of the photographs showed that the blackening intensity remains unchanged even after irradiation for 1 hour, the luminescence yield remains constant, and no photochemical reactions take place in the cell.

In the following experiments we used aqueous alkali (0.25 N NaOH) as solvent. It was found that the luminescence yield of fluorescein is considerably higher in alkali than in alcohols, and therefore the alkaline solutions of fluorescein were more dilute ($1 \cdot 10^{-4}$ g/ml), and whereas an exposure time of 5 minutes was used in experiments with alcohols, this was shortened to 5 seconds with the use of alkali. The concentrations of gossypol use previously were also too high. In a series of preliminary experiments it was found that with the use of alkalies the most suitable concentrations of gossypol lie in the range of $1 \cdot 10^{-6}$ to $1 \cdot 10^{-5}$ g/ml. With such low concentrations of gossypol the plot of log I/log I_0 against C should evidently be linear.

In fact, the values of log I/log I_0 for aqueous alkaline gossypol solutions plotted against gossypol concentration fit satisfactorily on a straight line.

The experimental results are given below:

$C \cdot 10^6$ g/ml	2	4	6	8	10
log I/log I_0	0.83	0.64	0.44	0.34	0.23

For tests of the possible use of the luminescence-quenching effect in quantitative determination of gossypol, solutions of gossypol in refined soybean oil were prepared and used as model samples. This oil was chosen as solvent because it does not contain gossypol or any other substances which might influence the quenching of luminescence. The method chosen for quantitative extraction of gossypol from the oil was by shaking with 0.25 N alkali [10].

First, it was necessary to determine whether the alkaline solution of fluorescein loses its power of luminescence after contact with oil. For this purpose 10 ml of oil was mixed with 10 ml of alkaline fluorescein solution

(concentration $1 \cdot 10^{-4}$ g/ml) in a separating funnel. After vigorous agitation for 1 minute a fairly stable emulsion was formed, half an hour being required for its distinct separation: the lower, alkaline layer was slightly turbid, although it did not lose the delicate green color due to fluorescein. The spectrum of the alkaline layer was photographed on the same plate as the spectrum of a control solution of fluorescein which had not been in contact with oil. The average values (from triplicate experiments) for log of the blackening intensity were 0.581 for the control solution, and 0.417 for the solution which had been shaken with oil. This shows that a fluorescein solution which has been in contact with oil does not lose its luminescence, but absorbs light to a somewhat greater extent than a pure solution. This is caused by the presence of minute particles of emulsified oil and possibly also of traces of soap formed by the reaction of free fatty acids in the oil with alkali.

It was decided to accelerate separation of the emulsions and to decrease the oil content of the alkaline layer as much as possible, by salting out. For this, definite amounts of oil and alkaline fluorescein solution were put into a separating funnel, and 1 g of common salt was added; otherwise the procedure was as described above. Separation began within a few seconds after shaking was stopped, the alkaline layer was quite clear, and the difference of blackening intensities from those of fluorescein which had not been in contact with oil were within the limits of experimental error.

The results of experiments in which the oil was shaken with fluorescein solution for 2, 3, and 5 minutes coincided with the results after 1 minute of shaking.

Next, a gossypol solution containing $1 \cdot 10^{-4}$g/ml was prepared in oil, 1, 2, 3, 4, and 5 ml lots of this solution were taken into separating funnels, 5 ml of alkaline fluorescein solution was added to each, and gossypol was extracted from the oil as described above. The luminescence-quenching effects obtained in these solutions are represented by the data below and by the graph in Fig. 2.

$C \cdot 10^5$ g/ml	2	4	6	8	10
log I/log I_0	0.701	0.628	0.546	0.458	0.358

The graph shows that the extinction effect produced by gossypol extracted from soybean oil is proportional to the gossypol concentration.

The experiments with model solutions of gossypol in soybean oil were followed by experiments with cottonseed oil. A series of solutions of gossypol was prepared in refined cottonseed oil; a definite weight of gossypol was taken in each case and dissolved in a definite volume of oil. Gossypol was then extracted from 1 ml of the oil solution by 5 ml of alkaline fluorescein solution, and the luminescence yield of the solution was compared with that of a fluorescein solution without gossypol. The results of these experiments are given below and plotted in Fig. 3.

$C \cdot 10^5$	log I/log I_0	$C \cdot 10^5$	log I/log I_0	$C \cdot 10^5$	log I/log I_0	$C \cdot 10^5$	log I/log I_0
1.2	0.770	6.2	0.530	10.6	0.380	15.0	0.150
1.6	0.730	6.4	0.550	10.8	0.305	15.5	0.170
2.2	0.740	6.8	0.520	11.0	0.330	16.0	0.070
2.8	0.685	7.6	0.450	11.4	0.350	16.5	0.130
2.8	0.720	7.8	0.475	11.8	0.280	16.6	0.060
4.2	0.653	8.6	0.465	12.0	0.270	17.4	0.070
4.2	0.635	8.8	0.386	13.0	0.220	18.0	0.020
4.6	0.585	9.0	0.400	13.8	0.218	18.0	0.025
5.4	0.565	9.2	0.445	14.0	0.190		
5.6	0.600	10.0	0.360	14.8	0.140		

It follows from these results (Figs. 2 and 3) that the quenching of luminescence by gossypol extracted from soybean and cottonseed oil respectively is of the same character.

Finally, the luminescence method for determination of gossypol in oil was compared with the polarographic method of Markman and Kolesov [10]. A series of samples of gossypol was dissolved in refined cottonseed oil; the solutions were heated in a drying oven for half an hour at 80, 100, and 120°, when part of the gossypol was converted into a modified form which could not be determined by analysis. The results of these experiments are summarized in Table 1.

The next series of comparative experiments was carried out with black (crude) cottonseed oils made by different technological processes, unheated and heated in a drying oven for 1 hour at 80-140°. The results of these experiments are given in Table 2.

As the results of this experimental work, the following method is recommended for quantitative determination of gossypol in cottonseed oils. 1 or 2 ml of the oil, 5 ml of alkaline fluorescein solution ($1 \cdot 10^{-4}$ g/ml in 0.25 N caustic soda or potash), and 1 g of common salt are put in a serarating funnel; the funnel is closed and shaken vigorously for 1 minute. The stopper is removed and the solution is allowed to separate; the aqueous alkaline layer containing the gossypol extracted out of the oil is separated off, placed in a cell, and the luminescence spectrum of fluorescein partially quenched by gossypol is photographed. For comparison, the spectrum of a control solution of fluorescein without gossypol is photographed on the same film.

Because of the irregular distribution of the silver bromide grains in the emulsion layer on the photographic film, the photometric results sometimes differ a little from each other. Therefore several (2-4) photographs should be taken on different parts of the film. Isopanchromatic film should be used, as it is the most sensitive in the yellow – green region of the spectrum in which the luminescence of fluorescein occurs. The luminescence spectra are photographed, the film is developed, and the results examined photometrically. The logarithmic ratio of the blackening intensities for the unknown and standard solutions is determined, the average value for several photographs is found, and the gossypol concentration is found from the calibration graph (Fig. 3).

The results obtained by the luminescence method are in satisfactory agreement with polarographic data; if a spectrophotometer is used, one determination takes 5-6 minutes.

This investigation was carried out in the Laboratory of Experimental Physics of the State Institute of Central Asia. We are grateful to the Head of the Department, G. N. Shuppe, for this opportunity.

LITERATURE CITED

[1] A. E. Bailey, Cottonseed and Cottonseed Products, N Y. (1948).

[2] H. D. Royce, Oil and Soap, 10, 183 (1933).

[3] H. D. Royce, J. R. Harrison, and P. D. Deans, Ind. Eng. Ch. 12, 741 (1940).

[4] Technical Control in the Oil and Fat Processing Industries 1 (Moscow, 1952), 532. [In Russian]

[5] M. Z. Podol'skaia, J. Appl. Chem. 27, 657 (1944).

[6] C. M. Lyman, B. R. Holland, and F. Hale, Ind. Eng. Ch. 15, 489 (1943).

[7] F. H. Smith, Ind. Eng. Ch. 18, 41 (1946).

[8] C. H. Boatner, N. Caravella, and L. Kyame, Ind. Eng. Ch. 16, 566 (1944).

[9] W. A. Pons Jr., I. Carrol, Hoffpaner, and R. T. O'Connor, J. Am. Oil Chem. Soc. 28, 8 (1951).

[10] A. L. Markman and S. N. Kolesov, J. Appl. Chem. 29, 242 (1956).*

[11] V. P. Rzhekhin, Gossypol and its Derivatives (Leningrad, 1955), 132. [In Russian]

[12] S. I. Vavilov and M. D. Galanin, Proc. Acad. Sci. USSR 67, 811 (1949).

Received December 24, 1956.

*Original Russian pagination. See C. B. Translation.

SEPARATION OF TANNINS INTO FRACTIONS BY MEANS OF ADSORBENTS

V. M. Glezin

Chair of Pharmaceutical Chemistry and Pharmacognosy, Pharmaceutical

Faculty of the Irkutsk Medical Instutite

Fractionation of tannins, for determination of the nature of the individual components, attracted the attention of eminent Russian and foreign chemists at the end of the last and the beginning of the present century. Many of these studies were devoted to only one problem – investigation of the tannin obtained from Turkish or Chinese galls. Other plant tannins were studied very little; there have been only a few papers by Russian and foreign scientists.

Much work was done by Il'in [1-3] on tannin from Turkish galls. He carefully purified tannin supplied by different German firms, and showed it to be heteregeneous. Tannin was found to be dextrorotatory; no carboxyl groups were found in the tannin studied. Il'in refuted the assertion of E. Fischer, Freudenberg, Herzig, Renner and Schmiedinger [4] that the principal constituent of commercial tannin is pentadigalloylglucose; in his opinion, commercial tannin is a mixture of two substances. Ordinary commercial tannin has maximum rotation in the range $[\alpha]_D$= 70-75°, but if it is purified and fractionated by precipitation with zinc acetate, the optical activity changes, and becomes $[\alpha]_D$ = 115-117°.

Other Russian investigators studied the fractionation of tannins. The dissertation by Kol'o [5] contains methods for separation of tannins from snakeweed and tormentil rhizomes by means of sodium chloride, lead acetate, copper acetate, and stannic chloride.

Eissfeldt [6] used lead acetate to separate tannins from snakeweed and tormentil rhizomes into two groups: one gave a blue and the other a green precipitate with iron salts. It was concluded that the tannins of snakeweed and tormentil rhizomes form a mixed group.

Karrer, Salomon, and Payer [7] fractionated Chinese tannin with the aid of aluminum hydroxide, by the following method: a small portion of aluminum hydroxide was added to an aqueous tannin solution; a precipitate was formed fairly quickly, and this was filtered off. A fresh portion of aluminum hydroxide was added to the filtrate, and a second precipitate was formed; a third precipitate was formed on addition of yet another portion, etc. 80 fractions were obtained from Chinese tannin in this way. The fractions were dissolved in water, pyridine, and alcohol. In aqueous solution the substances had $[\alpha]_D$ from 30° to 157°, in pyridine, between 40.6° and 51.5°, and in alcohol, from 13.8° to 27°.

The method of precipitation by aluminum hydroxide showed, first, that different fractions have different angles of rotation, and second, that fractions of low rotation contain much more ellagic acid and less gallic acid than the fractions of high rotation.

Karrer, Widmer, and Staub [8] isolated tannin from Turkish galls, purified it thoroughly, and then fractionated it by means of aluminum hydroxide. Up to 80 fractions were obtained.

Munz [9] used the method of Karrer and his co-workers to obtain individual fractions of tannin from sumac. He obtained only four fractions, and studied each one in detail.

We studied the tannins of Bergenia and snakeweed rhizomes, dog rose root, burnet root, leaves of the golden rhododendron, oblepikha* leaves, and alder cones. The fractional-adsorption method, devised by the

* Hippophae rhammoides.

Russian scientist Tsvet (Tswett) [10, 11] and later used by Karrer and his co-workers, was used. The precipitants were magnesium oxide, lead oxide, calcium carbonate, and alunite. The oxides of lead and magnesium were used in order to compare the effects of heavy and light metal oxides, and calcium carbonate was used as a neutral salt. According to Tsvet, the most active adsorbents are aluminum hydroxide, precipitated silica, and magnesium oxide. The mineral alunite which we had available contains all these substances. It is found in many parts of our country. After calcination of alunite at 800-900°, potassium sulfate is leached out and a residue containing aluminium, silica, magnesium, and iron remains.

The alunite used had the following composition by analysis (%):

Silicon	Aluminum	Magnesium	Iron
41.52	29.79	0.66	0.73
41.48	29.49	–	0.62
41.73	28.24	0.22	Traces
42.30	30.20	0.20	"

TABLE 1

Amounts of Fractions Obtained by Precipitation with Different Adsorbents

Part of plant	Adsorbents			
	magnesium oxide	lead oxide	calcium carbonate	alunite
Rhizome:				
of Bergenia	9	7	10	25
of snakeweed	2	7	6	9
Root:				
of burnet	8	14	10	22
of dog rose	2	9	6	14
Leaf:				
of golden rhododendron	18	7	8	26
of oblepikha	20	8	10	11
Alder cones	10	2	2	0

The fractional adsorption was carried out as follows: 50 ml of tannin extract was put into a conical flask, followed by a definite amount of adsorbent: 0.15 g of magnesium oxide, lead oxide, or calcium carbonate, or 0.3 g of alunite (exact weights). The required weights of the adsorbents were determined experimentally. The mixture of extract and adsorbent was left overnight. The precipitate was filtered off, similar portions of the adsorbents were again added to the filtrate, and so on; the second, third, and subsequent precipitates were obtained in this way (Table 1).

It follows from the data in Table 1 that the maximum yields of the fractions are obtained with alunite in nearly every case, apart from the tannins of oblepikha leaves and alder cones, where better results are obtained with magnesium oxide. In general, each tannin requires the use of its own adsorbent, one with which it has the greatest affinity.

Lederer [12] states that metal oxides adsorb substances containing phenolic, hydroxyl, and carboxyl groups. Calcium carbonate is recommended as an adsorbent for unsaturated compounds containing several functional groups. In the light of Lederer's views our results show that the tannins of Bergenia rhizome, burnet root, and rhododendron leaf have high phenolic-group contents. This is in agreement with our determinations of polyphenol contents. The method of A. L. Kursanov was used for these determinations. The following results were obtained:

Part of plant	Polyphenol content (%)
Bergenia rhizome	4.80—5.38
Golden rhododendron leaf	2.04—2.32
Burnet root	1.30—1.40

TABLE 2

Amounts of Individual Tannin Fractions Obtained from Bergenia Rhizome (%) with Different Adsorbents

Fraction	Adsorbent		
	magnesium oxide	calcium carbonate	lead oxide
I	7.485	1.446—1.456	2.047—2.035
II	0.587	0.979—0.973	0.734—0.730
III	0.293	0.179—0.161	0.801—0.794
IV	0.411	0.133—0.133	0.556—0.556
V	0.137	0.166—0.166	0.179—0.179
VI	0.195	0.266—0.266	0.801—0.801
VII	0.049	0.055—0.055	2.782—2.782
VIII	0.098	0.066—0.066	— —
IX	0.058	0.055—0.055	— —
X	—	0.055—0.055	— —

Fraction	Alunite adsorbent	Fraction	Alunite adsorbent
I	1.550	XIV	0.235
II	4.350	XV	0.219
III	1.398	XVI	0.235
IV	3.107	XVII	0.160
V	1.881	XVIII	0.053
VI	2.198	XIX	0.035
VII	0.313	XX	0.035
VIII	0.235	XXI	0.160
IX	0.235	XXII	0.177
X	0.117	XXIII	0.177
XI	0.117	XXIV	0.118
XII	0.117	XXV	0.118
XIII	0.117		

TABLE 3

Amounts of Individual Tannin Fractions Obtained from Snakeweed Rhizome (%) with Different Adsorbents

Fraction	Adsorbent			
	alunite	magnesium oxide	lead oxide	calcium carbonate
I	2.71—2.72	9.07	1.19—1.187	0.63—0.636
II	1.76—1.76	3.12	0.58—0.595	0.38—0.384
III	2.21—2.21	—	0.97—0.985	0.36—0.360
IV	8.16—8.61	—	0.54—0.551	0.315—0.318
V	0.718—0.723	—	0.63—0.641	0.162—0.165
VI	2.996—2.722	—	0.09—0.091	0.108—0.110
VII	0.38—0.37	—	0.144—0.146	—
VIII	0.36—0.37	—	—	—
IX	0.10—0.10	—	—	—

TABLE 4

Amounts of Individual Tannin Fractions Obtained from the Root of the Dog Rose (%) with Different Adsorbents

Fraction	Adsorbent			
	alunite	magnesium oxide	lead oxide	calcium carbonate
I	0.73	4.199	2.799	1.06
II	4.21	0.622	0.324	1.02
III	0.89	1.311	0.259	0.38
IV	0.83	0.170	0.170	0.25
V	2.37	0.08	0.220	0.16
VI	1.15	0.05	0.08	0.09
VII	0.86	0.05	0.24	0.06
VIII	0.54	0.03	0.48	0.06
IX	0.44	—	0.38	0.03
X	0.38	—	0.36	0.03
XI	0.53	—	0.18	—
XII	0.57	—	0.79	—
XIII	0.41	—	0.65	—
XIV	0.25	—	0.16	—
XV	0.22	—	—	—
XVI	0.34	—	—	—
XVII	0.22	—	—	—
XVIII	0.19	—	—	—
XIX	0.12	—	—	—
XX	0.09	—	—	—
XXI	0.09	—	—	—
XXII	0.03	—	—	—

TABLE 5

Amounts of Individual Tannin Fractions Obtained from Leaves of the Golden Rhododendron (%) with Different Adsorbents

Fraction	Adsorbent			
	alunite	magnesium oxide	lead oxide	calcium carbonate
I	1.007—1.008	1.008	4.372—4.747	0.666—0.416
II	2.149—2.149	0.672	0.832—1.145	0.624—0.312
III	1.343—1.343	0.672	0.728—0.728	0.666—0.416
IV	1.074—1.074	0.672	0.624—0.624	0.083—0.166
V	1.007—1.007	0.537	0.583—0.665	0.250—0.249
VI	0.805—0.806	0.268	0.416—0.416	0.330—0.332
VII	1.074—1.074	0.268	0.250—0.249	0.250—0.249
VIII	1.874—1.550	0.06	—	0.083—0.166
IX	0.362—0.300	0.06	—	—
X	0.463—0.384	0.161	—	—
XI	0.133—0.133	0.022	—	—
XII	0.178—0.177	0.066	—	—
XIII	0.066—0.066	0.066	—	—
XIV	0.133—0.133	0.066	—	—
XV	0.089—0.088	0.057	—	—
XVI	0.133—0.133	0.088	—	—
XVII	0.199—0.199	0.088	—	—
XVIII	0.089—0.088	0.088	—	—
XIX	0.044—0.044	—	—	—
XX	0.089—0.088	—	—	—
XXI	0.066—0.066	—	—	—
XXII	0.044—0.044	—	—	—
XXIII	0.044—0.044	—	—	—
XXIV	0.044—0.044	—	—	—
XXV	0.089—0.088	—	—	—
XXVI	0.044—0.044	—	—	—

TABLE 6

Amounts of Individual Tannin Fractions Obtained from Burnet Root (%) with Different Adsorbents

Fraction	Adsorbent			
	alunite	magnesium oxide	lead oxide	calcium carbonate
I	0.50	6.89	1.15	0.50
II	0.50	1.60	0.92	1.38
III	0.39	—	0.50	0.39
IV	0.27	—	0.39	0.39

TABLE 7

Amounts of Individual Tannin Fractions Obtained from Oblepikha leaves (%) with Different Adsorbents

Fraction	Adsorbent			
	alunite	magnesium oxide	lead oxide	calcium carbonate
I	1.546	5.409	2.070—2.760	1.260—1.265
II	1.546	2.318	0.992—0.992	1.801—1.820
III	1.236	0.618	0.360—0.360	0.360—0.360
IV	2.782	0.510	0.720—0.720	0.451—0.450
V	1.700	0.309	0.270—0.270	0.360—0.360
VI	0.232	0.309	0.450—0.411	0.451—0.450
VII	1.313	0.309	0.360—0.360	0.451—0.450
VIII	0.463	0.154	0.090—0.087	0.087—0.090
IX	0.185	0.185	—	0.087—0.090
X	0.069	0.069	—	0.180—0.180
XI	0.139	0.069	—	—
XII	—	0.128	—	—
XIII	—	0.025	—	—
XIV	—	0.077	—	—
XV	—	0.077	—	—
XVI	—	0.077	—	—
XVII	—	0.077	—	—
XVIII	—	0.077	—	—
XIX	—	0.077	—	—
XX	—	0.025	—	—

TABLE 8

Amounts of Individual Tannin Fractions Obtained from Alder Cones (%) with Different Adsorbents

Fraction	Adsorbent			
	alunite	magnesium oxide	lead oxide	calcium carbonate
I	0.603—0.51	0.29	0.096	0.165
II	0.188—0.19	0.19	0.055	0.027
III	0.235—0.35	0.046	—	—
IV	0.235—0.23	0.14	—	—
V	0.09—0.09	0.19	—	—
VI	0.14—0.14	0.14	—	—
VII	0.14—0.14	0.14	—	—
VIII	0.19—0.19	0.09	—	—
IX	0.14—0.14	0.09	—	—
X	—	0.09	—	—

The use of calcium carbonate as adsorbent should reveal unsaturated compounds containing several functional groups. Table 1 shows that this applies to the tannins of Bergenia rhizome, burnet root, and oblepikha leaves, as calcium carbonate gave the maximum amounts of fractions with the tannins from these. This fact leads to the hypothesis that the tannins of Bergenia, burnet, and oblepikha consist of unsaturated compounds.

The tannin content of each fraction was determined by titration with 0.1 N potassium permanganate solution in presence of indigo carmine indicator. The precipitate was dissolved in hot water and made up to a definite volume in a measuring flask; 10 or 25 ml of the solution was withdrawn using a pipet, 10 ml of indigo carmine solution and 750 ml of distilled water were added, and the solution was titrated with 0.1 N potassium permanganate to a yellow color. According to Neubauer, 1 ml of 0.1 N potassium permanganate solution oxidizes 0.004157 g of tannin. The tannin contents of all the fractions are given in Tables 2-8.

In addition to quantitative determinations of tannins, the qualitative reactions of individual fractions were investigated. The reagents were lead acetate (neutral salt) in acetic acid, and bromine water. These reagents were used because pyrogallol tannins are precipitated by lead acetate in acetic-acid solution, while pyrocatechol tannins do not form a precipitate. Pyrocatechol tannins are precipitated by bromine water, while pyrogallol tannins are not. This made it possible to classify the individual fractions in the pyrogallol or the pyrocatechol group.

SUMMARY

1. The tannins of Bergenia rhizome, snakeweed rhizome, burnet root, dog rose root, leaves of the golden rhododendron and oblepikha, and alder cones were fractionated and the amounts of different fractions in the tannins were determined.

2. The tannin content of each fraction was determined, and the fractions were identified as belonging to the pyrogallol or the pyrocatechol group, by means of qualitative reactions.

LITERATURE CITED

[1] L. F. Il'in, J. Russ. Phys.-Chem. Soc. 39, 6 (1907).

[2] L. F. Il'in, J. Russ. Phys.-Chem. Soc. 45, 1 (1913).

[3] L. F. Il'in, Tannin and Digallic Acid [In Russian] (Petrograd, (1918)).

[4] K. Freudenberg, Chemie der naturlichen Gerbstoffe. Berlin (1920).

[5] N. Kol'o, Dissertation (Peterburg, (1884)). [In Russian]

[6] H. Eissfeldt, Ann. Ch. Pharmac. 148, 218.

[7] P. Karrer, D. Salomon and I. Payer, Helv chim. Acta 6, 3 (1923).

[8] P. Karrer, R. Widmer and M. Staub, Ann. Chem. 433 (1923).

[9] W. Munz, Uber den Gerbstoff der Edelkastanie und des sicilianischen Sumachs, Collegium 714, X, 499 (1929).

[10] M. S. Tsvet, Trans. Warsaw Soc. Naturalists, Biology Section 14 (1903).

[11] M. S. Tsvet, Chromatographic Adsorption Analysis [In Russian] (Izd. AN SSSR, (1946)).

[12] E. Lederer, Progr. Chem. 9, 10 (1940).

Received January 25, 1957

INVESTIGATION OF THE "RECRYSTALLIZATION" EFFECT IN CELLULOSE

I. I. Korol'kov, V. I. Sharkov, and A. V. Krupnova

Workers studying the heterogeneity of cellulose structure [1-4] have frequently reported that under the influence of acid hydrolysis in an aqueous medium the loose or "amorphous" cellulose fraction becomes more closely packed; this process has been named "recrystallization." It has been shown [5] that this process is sharply retarded or nonexistent during acid hydrolysis in anhydrous ethanol.

Ethanolysis was therefore proposed [5] as a method for determination of the heterogeneity of cellulose. This method was used to show that cellulose samples ground in a vibratory mill, and regenerated cellulose of the viscose-rayon type, contain 50% and more of the amorphous fraction. Experiments on the treatment of ground cellulose with water at various temperatures showed that the recrystallization process can be detected at 0°, and intensifies gradually with increase of temperature.

The previous investigation gave rise to a number of problems which required further study. In particular, it was desired to find out why viscose fibers, which are formed in an aqueous medium, show little recrystallization and, conversely, why the content of the amorphous fraction in ground fibers decreases rapidly during treatment with water at low temperatures.

The effect was studied by means of the ethanolysis method, described previously. In particular, the method was used for determinations of the contents of the fraction readily susceptible to ethanolysis in different samples of regenerated viscose cellulose, of different degrees of stretching. The sample of the lowest degree of stretching was cellulose gel made by precipitation of viscose in an acid bath without tension; one sample was washed with water, and another, with water and ethyl alcohol. The samples of different degrees of stretching were: Cellophane, unstretched viscose yarn, viscose yarn made with 10 and 50 stretch, and superstrong cord of breaking length 54 km.

The results of ethanolysis of these samples are given in Table 1.

These results show that about 14% of cellulose passed into solution during 6 hours of ethanolysis from a cellulose gel washed with water; i.e., this sample is very close-packed. The contents of the loose (amorphous) fraction in the other samples increase with the degree of stretching, reaching a maximum of 50%.

These results are in agreement with density determinations on these samples, carried out by the flotation method in carbon tetrachloride. For example, our results show that the density of viscose yarn of 50% stretch is 1.521, while the density of cellulose gel is 1.537.

It should be noted that these results confirm the conclusion of V. A. Kargin and N. V. Mihailov that orientation of fibers by means of stretching apparently does not involve a phase transition, i.e., crystallization. Stretching of the fiber brings the cellulose into a special state in which, on the one hand, the degree of orientation and fiber strength are increased, and on the other, there is an increase in the amount of loose fraction, which is more reactive in ethanolysis.

This effect requires further investigation.

However, it is quite clear that cellulose fibers formed in an aqueous medium without stretching can become closely packed almost completely at the instant of formation, and that orientation by means of stretching prevents this process. This hindrance to the packing is apparently due to the fact that the loosely arranged macromolecular chains take up fixed positions and lose mobility.

TABLE 1

Results of Experiments on the Ethanolysis of Cellulose Samples

Samples	Amount of cellulose passing into solution (%) of weight taken) during time (minutes)				Content of amorphous fraction (%)
	20	60	180	300	
Gel washed with					
water	1.0	4.0	10.0	14.0	14
water and ethanol	2.0	6.0	16.0	20.5	21.0
Cellophane	8.0	18.0	29.7	34.1	37.5
Yarn					
unstretched	10.0	26.0	36.5	39.5	39.0
10% stretch	12.0	28.6	39.4	44.0	48.0
50% stretch	13.6	30.5	44.5	49.5	51
Superstrong cord	13.0	32.1	46.3	49.0	51.0

TABLE 2

Degree of Polymerization of Cellulose

Samples	Weight loss in aqueous treatment (in %)	Degree of polymerization (DP)	Amount of cellulose passing into solution (%) during ethanolysis in time (minutes)				Content of amorphous fraction (%)
			20	60	180	300	
Original	–	264	13.6	30.5	44.5	49.5	51
Recrystallized at							
100° for 60 minutes	2.5	264	15.0	30.0	38.8	42.5	45
160° for 30 minutes	3.7	192	14.0	25.6	32.4	36.0	38.0
180° for 30 minutes	4.9	56	13.0	20.0	22.5	24.4	25.0

This probably explains why aqueous treatment of oriented viscose fibers at room temperature does not result in any appreciable recrystallization.

However, as the data in Table 2 show, viscose yarn undergoes recrystallization when treated with water at high temperatures.

It must be pointed out that this is accompanied by a small loss of fiber weight, from 2.5 to 5%, and a decrease of the degree of polymerization, determined by Staudinger's method in cuprammonium solution.

The decrease of the degree of polymerization of cellulose during recrystallization was confirmed with samples of ground and bleached spruce sulfite cellulose. Samples of this cellulose were kept in water at various temperatures, for periods of 20 to 300 minutes. The results are given in Table 3.

The results in Table 3 show that the recrystallization of ground wood cellulose, containing about 68% of the amorphous fraction, appears to proceed in two stages.

The first stage takes place at low temperatures without a decrease in the degree of polymerization of cellulose. In this case the content of the amorphous fraction falls rapidly from 68 to 39-44%. The process of fiber packing which takes place here is apparently caused by formation of hydrogen bonds between the separated cellulose chains under the influence of the water present, with utilization of the freedom of movement of the individual macromolecular segments.

The second recrystallization stage occurs on an appreciable scale only at high temperatures, and it is accompanied by a small loss of fiber weight and a decrease of the degree of polymerization. This stage is

TABLE 3

Degree of Polymerization of Ground Spruce Sulfite Cellulose

Aqueous treatment of cellulose		Weight loss in aqueous treatment	Degree of polymerization (DP)	Amount of cellulose passing into solution (%) during ethanolysis in time (minutes)				Content of amorphous fraction
temperature in °C	time (minutes)			20	60	180	300	
Sample 1								
Untreated		—	368	30.3	44.2	62.3	67.1	68
1	30	—	360	20.1	28.5	38.5	42.0	44
20	30	—	368	18.2	24.5	33.8	38.4	39
100	30	—	336	13.4	18.3	27.0	30.8	31
140	30	—	280	10.3	15.4	24.0	28.1	27
180	30	—	88	6.0	10.6	16.4	20.3	20
Sample 2								
Untreated		—	256	28.5	44	61	69	67
100	60	1.9	272	9.5	19.5	29.5	32.5	38
100	300	2.7	270	9.0	20.0	27.5	30.0	30.0
160	20	3.9	160	9.5	18.0	27.0	31.0	31
180	30	7.8	64	7.0	15.5	22.0	24.0	24.0

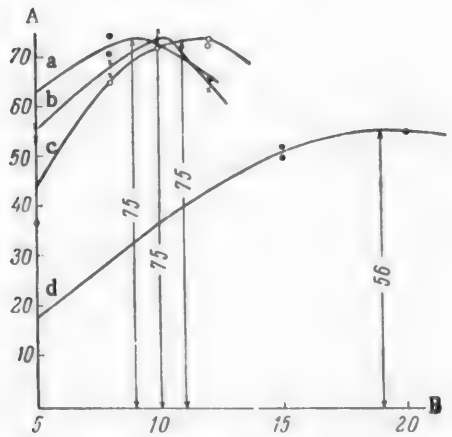

Fig. 1. Yields of reducing substances (RS) in the hydrolysis of recrystallized samples of wood cellulose (t = 200°). A) RS yield (%), B) time (minutes). Explanation in text.

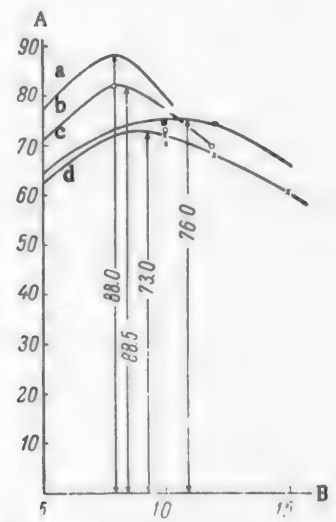

Fig. 2. Yields of reducing substances (RS) in the hydrolysis of regenerated cellulose samples (t = 200°). A) RS yield (%), B) time (minutes). Cellulose samples: a) superstrong cord, b) viscose yarn, 50% stretch, c) Cellophane, d) cellulose gel.

analogous to recrystallization in oriented viscose fibers, and occurs only as the result of rupture of the macromolecular chains, whereby individual chain segments regain freedom of movement.

In order to determine how closely similar the properties of recrystallized samples of ground wood cellulose and the properties of the original wood cellulose are, they were subjected to comparative hydrolysis experiments at 200° in presence of 0.5% sulfuric acid.

TABLE 4

Hydrolysis-Rate Constants of Cellulose

Samples	Hydrolysis time (minutes)	Remaining cellulose (% of original	One-minute constant	
			experimental	average
Ground wood cellulose	5	74.2	–	0.0469
	15	46.8	0.0460	
	30	22.4	0.0478	
Ground cellulose, recrystallized at 160° during 20 minutes	5	83.2	–	0.0505
	15	50.2	0.0505	
Ground cellulose, recrystallized at 180° during 30 minutes	5	85.2	–	0.0466
	15	53.1	0.0472	
	20	42.2	0.0463	
	30	26.6	0.0464	
Cellophane	5	79.8	–	0.0401
	15	53.1	0.0406	
	30	29.2	0.0402	
	40	19.1	0.0390	
	45	15.9	0.0403	
Superstrong cord	5	75.9	–	0.0768
	15	35.1	0.0770	
	25	11.4	0.0765	

In Fig. 1 the yields of reducing substances are plotted against the times of hydrolysis for the following wood cellulose samples: a) ground, b) ground, recrystallized at 160°, c) ground, recrystallized at 180°, and d) original, not ground. The curves show that the maximum yields of sugar formed in hydrolysis are almost the same for ground and recrystallized celluloses, and considerably higher than the yield from the original wood cellulose.

This leads to the conclusion that recrystallized cellulose is much more easy to hydrolyze under harsh conditions than native cellulose. Thus, the properties of native and recrystallized cellulose differ in this respect.

Interesting results were obtained in the hydrolysis of samples of regenerated cellulose by 0.5% sulfuric acid at 200°. Here also the sugar yields were considerably higher than in the hydrolysis of native wood cellulose.

For example, Fig. 2 shows that the maximum sugar yield in the hydrolysis of superstrong cord under these conditions was 88%, and in the hydrolysis of viscose yarn, 82%. A high sugar yield, 73%, was also obtained in the hydrolysis of unoriented cellulose gel.

Consideration of all the foregoing data leads to the conclusion that the high sugar yields obtained in the hydrolysis of regenerated and recrystallized celluloses can be primarily accounted for by the higher hydrolysis rates of these celluloses as compared with native wood cellulose. It is also possible that the results are influenced by the fact that at high temperatures the amorphous fraction may undergo partial hydrolysis before recrystallization.

For studies of the hydrolysis rates of these cellulose samples, the hydrolysis-rate constants at 180° were determined. The constants were calculated from the first-order equation; the calculations were based on data for hydrolysis of 5 minutes and over, as the result of which the undissolved residues of the cellulose samples crystallized completely. The results are presented in Table 4.

It is known that under these conditions the rate constant for hydrolysis of wood cellulose is 0.015. It follows that ground wood cellulose and its recrystallized products are hydrolyzed at 3.2 times the hydrolysis rate of native wood cellulose. Cellophane is hydrolyzed at 2.6 times the rate, and superstrong cord at 5.1 times the rate. Calculations show that this increase of the hydrolysis rate fully accounts for the sugar yields given above.

Thus we may conclude that ground, recrystallized, and regenerated cellulose samples, even after complete recrystallization, are hydrolyzed much more rapidly than the original native cellulose. This result is an indication of the different nature of the packing of cellulose macromolecules in native and fully recrystallized samples respectively, and it shows that their other properties, including the density*, should also differ.

SUMMARY

1. It was found that the content of the loose fraction in viscose fibers increases with increasing stretch during spinning.

2. When viscose fibers are heated in water at high temperatures, the macromolecules are split and the cellulose becomes more densely packed because individual segments of the macromolecules become free to move.

3. When ground native cellulose is treated with water, its recrystallization proceeds in two stages. The first stage in which the packing becomes more dense proceeds at low temperatures without chain rupture. The second stage proceeds at high temperatures and is accompanied by chain rupture.

4. Ground native cellulose differs from viscose fibers by the presence of loosely-packed macromolecules, which are weakly bonded and which are capable of forming dense aggregates under the action of water at ordinary temperatures.

5. Cellulose which has been ground and recrystallized by the action of water, or regenerated from aqueous solutions, is hydrolyzed at 3-5 times the rate of native wood cellulose. This difference is a sign of considerable structural differences between the two types of cellulose.

LITERATURE CITED

[1] K. Hess, E. Steurer, and H. Fromm, Koll. Zt., B. 98, H. 2, 148 (1942).

[2] O. Battista, Ind. Eng. Ch. 42, 3, 502 (1950).

[3] P. Hermans, and A. Weidinger, J. Am. Soc. 68, 12, 2547 (1946).

[4] F. Brenner, V. Frilette, and H. Mark, J. Am. Soc. 70, 2, 877 (1948).

[5] P. I. Korol'kov, V. I. Sharkov, and E. N. Garmanova, J. Appl. Chem. 30, 4, 586 (1957).**

Received April 29, 1957

* The previous paper [5] contains a misprint in the equation for calculation of the amorphous fraction of cellulose from density data. This equation should be:

$$a = 100 - \frac{100\,(d_i - d_a)}{d_f - d_a}.$$

** Original Russian pagination. See C. B. Translation.

STUDY OF THE EXTRACTION OF VEGETABLE OILS FROM OIL CAKES

V. V. Beloborodov

The All-Union Scientific Research Institute of Fats

Extraction of vegetable oils by means of organic solvents is one of the commonest processes for extraction of substances from solids. However, the basic laws governing the extraction of vegetable oils have not been established as yet. The present paper is an attempt to fill this gap.

General considerations of the mechanism of extraction of vegetable oils are contained in publications by Goldovskii [1], Coats and Karnofsky [2], and Osburn and Katz [3]. Boucher et al. [4] showed that the extraction of oil from oil-impregnated clay plates can be represented by equations for nonequilibrium diffusion. Fan, Morris, and Wakeham [5] reached a similar conclusion in relation to microtome sections of Arachis. Il'in [6] showed that the extraction of vegetable oils is a process consisting of two periods (he uses the term "stages"). This view was later confirmed and developed by numerous workers (for examples, Bailey [7]).

King, Katz, and Brier [8] consider that the extraction of oil from soybean flakes is represented by an equation of the form

$$-\frac{dc'}{d\tau} = f(c' - c_1),$$

where c' is the oil content of the flake at time τ, and c_1 is the oil content of the flake at equilibrium.

Smith [9] used data of other workers to derive the following expression for the extraction rate:

$$\frac{dx}{d\tau} = K(x + b)^2,$$

where x is the oil content of the material at time τ, b is a constant, and K is the extraction-rate constant; the values of b and K are calculated from experimental data.

In a recent paper by Othmer and Agarwal [10] the view is put forward that the extraction of oil from soybean flakes is a problem of flow dynamics in capillaries, and it should, in their opinion, conform to the Hagan-Poiseuille law.

The effect of the moisture content of the material was studied by Goldovskii [1], Arnold and Juhl [11], Arnold and Patel [12], and others. Wingard and Phillips [13], Arnold and Pool [14], and Goldovskii [15] demonstrated the favorable effect of temperature on the efficiency of the extraction process. Coats and Wingard [16] showed that the time required to reach a residual oil content of 1%, calculated on the dry material, is proportional to a positive power of the particle size of the material. The effect of particle size has also been discussed by Arnold and Juhl [11] and by Gavrilenko and Beloborodov [17].

It is known [18] that simultaneous consideration of equations for steady diffusion and mass transfer in a moving stream, with the influence of hydrodynamic conditions taken into account, leads to the following expression for the similarity criteria (the action of volume forces, i.e., the Froude criterion, is ignored).

$$Nu' = f(Re,\ Pr'), \tag{1}$$

where Nu' = Kd/D is the Nusselt diffusion criterion, Pr'= ν/D is the Prandtl diffusion criterion, Re = wd/ν is the Reynolds criterion, K is the coefficient of mass transfer, d is a geometrical parameter (particle size in this instance), D is the diffusion coefficient, w is the velocity of the liquid, and ν is the kinematic viscosity.

The extractionof vegetable oils, like the extraction of most substances from solids, is a process of non-equilibrium diffusion. Therefore Equation (1) must be supplemented by terms found by solution of the non-equilibrium diffusion equation in presence of convection, with the aid of the theory of similarity. These terms must be [19]: the concentration ratio E, the Peclet diffusion criterion Pe', and the Fourier diffusion criterion Fo'.

Since Nu' includes the mass-transfer coefficient, E may be omitted. Since Equation (1) contains Pr', it is also permissible to omit Pe'. Therefore, on introduction of the geometrical similarity ratio Γ_1 = h/ d (h is the height of the layer of particles and d is the most characteristic dimension of the system in this instance), we finally have

$$Nu' = f(Fo', Pr', Re, \Gamma_1). \tag{2}$$

The mass-transfer coefficient was calculated from the known equation

$$K = \frac{m}{f_1 \Delta c_m \tau}, \tag{3}$$

where m is the amount of oil obtained per unit weight of the extracted material, f_1 is the surface area per unit weight of the extracted material, Δc_m is the average concentration difference, and τ is the extraction time.

The expression for determination of f_1 is derived on the assumption that the extracted material consists of spherical particles equal in size. If d_e is the effective diameter of the particles, n is the number of particles per unit volume, and γ_b is the bulk density of the material, we have

$$f_1 = \pi d_e^2 n \frac{1}{\gamma_b}. \tag{4}$$

If ψ is the porosity of the layer of particles, then

$$n \frac{\pi d_e^3}{6} = 1 - \psi,$$

and hence (5)

$$n = \frac{6(1-\psi)}{\pi d_e^3}.$$

Since ψ_{av} = 0.3675 [20], it follows that n = 1.208/ d_e^3. Putting n = 1.208/ d_e^3 in Equation (4), we have

$$f_1 = \frac{1.208\pi}{d_e \gamma_b}. \tag{6}$$

The values of d_e were determined from sieve-analysis data. Because of the assumptions made, Equation (6) does not give true values of f_1, but only values proportional to them. Therefore the values of K given by Equation (3) are merely proportional to the true values. However, this does not prevent the determination of the true values of all the other quantities from Equation (3), as the proportionality factors enter the values of f_1 and K, and cancel out when they are multiplied together. Δc_m was calculated as the logarithmic mean difference. In accordance with the dimensions of the quantities in Equation (3), it must be expressed in g/ cc. Conversion formulas for the initial (Δc_i) and final (Δc_f) concentration differences were derived on the assumption that the density of the oil is 0.9 g/ cc, and the density of the solvent petroleum fraction is 0.7 g/ cc (at 50-55°, which is the extraction temperature):

$$\Delta c_i = 0.9 - 0.7 c_{mc} - 0.2 c^2_{mc} \tag{7}$$

$$\Delta c_f = 0.7 c_p + 0.2 c^2_p \tag{8}$$

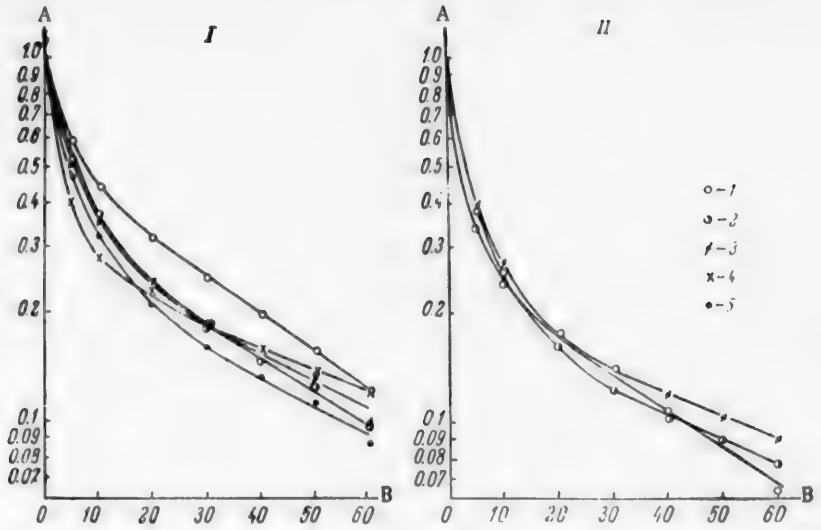

Fig. 1. Extraction curves.
A) Ratio of oil contents of the material at time τ and at $\tau = 0$; B) time τ (minutes). Extracted material: I) expeller-cake particles of $d_e = 4.5$ mm from dehulled cottonseed, II) expeller-cake particles of $d_e = 4.5$ mm from undehulled cottonseed. 1, 2, 3, 4, 5) numbers of experiments.

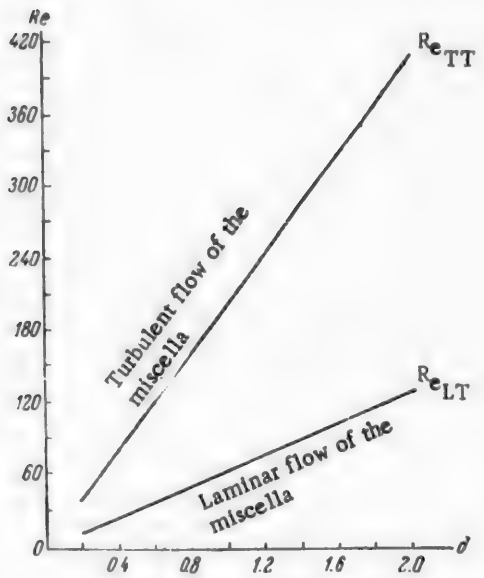

Fig. 2. Critical values of the Reynolds number.
Re_{LT}) transition from laminar to transitional motion, Re_{TT}) transition from transitional to turbulent motion.

where c_{mc} is the solution concentration outside the particles (in weight fractions) and c_p is the solution concentration within the particles (in weight fractions).

It is evident that $c_p = O_p/(O_p + S_p)$, where O_p and S_p are the amounts of oil and solvent within the particles (in % on the dry oil-free substance).

The plant trials were carried out in a vertical screw extractor [21], in which the true time of extraction could not be determined purely by analytical methods, because of the turning of the material together with the screw blades carrying it. A correction factor ϵ must be introduced; this is the slippage coefficient, equal to the ratio of the theoretical time during which the material remains in the extractor, to the actual measured time. The calculation formula then becomes

$$\tau = \frac{100}{\varepsilon s}(6.1t_f + 1.5t_c + 8.33t_e), \qquad (9)$$

where τ is the time (seconds); s is the pitch of the extractor screws (cm); t_f, t_c, and t_e are the times of a single turn of the screw in the feed, conveyor, and extraction columns respectively (in seconds); 6.1, 1.5, and 8.33 (in meters) are respectively: the height of the feed column, the length of the conveyor, and the height of the extraction column, over which the extracted material comes in contact with the solvent.

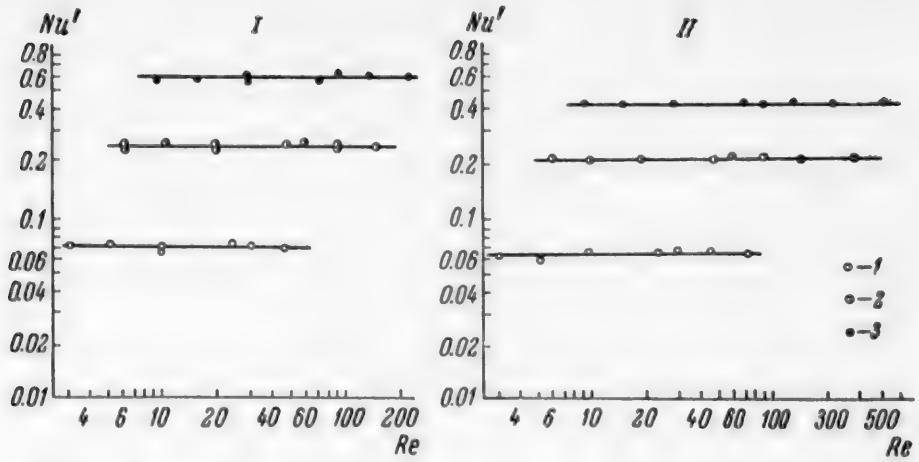

Fig. 3. The Nu' = f (Re) relationship. Extracted material: I) Cottonseed cake formed by single pre-pressing of dehulled cottonseed, II) sunflower-seed cake formed by single pre-pressing. Particle size d_e (from results of laboratory experiments) in mm: 1) 2, 2) 4, 3) 6.

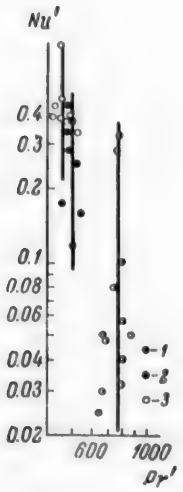

Fig. 4. The Nu' = f (Pr') relationship. Extracted material (from results of plant trials): 1) Soybean cake formed by single pre-pressing, 2) expeller cake from dehulled cottonseed, 3) expeller cake from undehulled cottonseed.

The laboratory experiments were performed in an apparatus described earlier [22].

The extraction curves in Fig. 1 were obtained for a solvent passed at 25-30° through a layer of particles at 30 cc/ minute.*

In experiments on the determination of critical values of Re, based on the conditions that $H/w_0 = \text{const}$ and $H/w_0^2 = \text{const}$, where H is the pressure of the solvent column and w_0 is the velocity calculated for the empty tube [20], different amounts of solvent were passed through a tube 20 mm in diameter, with variations of the height of the layer of material from 100 to 500 mm, and of particle size from $d_e = 2.0$ mm to $d_e = 6.0$ mm.

The critical values of Re calculated from the results of these experiments are presented in Fig. 2**. The value $Re/d_e = 66.3$ corresponds to the transition from laminar to transitional flow, and the value $Re/d_e = 206.0$, to the transition from transitional to turbulent flow.

In experiments on determination of the flow velocity and regime on the extraction effect, various amounts of solvent were passed at 50-55° through tubes of different diameters, with variations of the particle size from 2.0 to 6.0 mm. The amount of solvent and tube diameter were so chosen as to give a definite flow regime. In all these experiments the ratio of solvent to extracted material was very high (from 34.5 to 501.0), so that the solution concentration outside the particles was

* The densities of the oil and solvent used for calculation of Δc_i and Δc_f were correspondingly higher than 0.9 and 0.7 g/ cc.

** The viscosity of the petroleum solvent and the viscosity of oil solutions in the solvent, as used below, are taken from our earlier data [24,25].

Effect of Layer Height of Particles of Cottonseed and Sunflower-Seed Pre-pressed Cake on the Oil Content of the Residue

Data		Average particle size of material d_e (mm)									
		2.0		4.0				6.0			
Solvent velocity w_0 (cm/second)		0.15		0.15		0.70		0.15		0.70	
Cottonseed cake	Height of particle layer (cm)	29.5	9.3	25.0	8.0	25.0	8.3	23.4	7.0	22.0	7.0
	Oil content of residue, % on dry material	0.37	0.48	0.50	0.45	0.38	0.49	0.51	0.56	0.47	0.49
Sunflower-seed-cake	Height of particle layer (cm)	17.0	5.5	21.5	6.5	20.0	6.5	20.0	6.5	20.0	6.5
	Oil content of residue, % on dry material	1.40	1.39	2.51	2.45	2.36	2.22	2.30	2.29	2.02	2.20

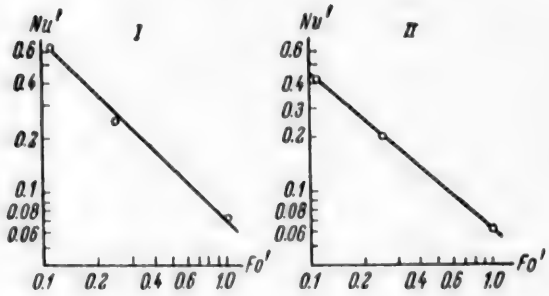

Fig. 5. The Nu' = f (Fo') relationship. Extracted material (from results of laboratory experiments): I) Cottonseed cake formed by single pre-pressing of dehulled cottonseed, II) sunflower-seed cake formed by single pre-pressing.

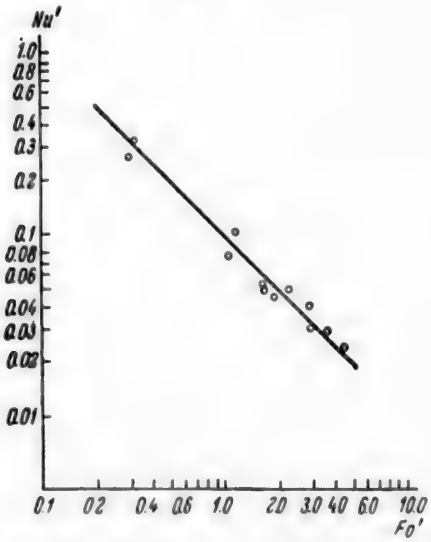

Fig. 6. The Nu' = f(Fo'). relationship. Extracted material-soybean oilcake formed by single pre-pressing (from the results of plant trials).

close to zero, and the influence of the concentration difference was thereby excluded. The same experiments provided data on the effect of the layer height on extraction efficiency.

The Nu' = f (Re) relationship is plotted in Fig. 3*. These results show that the Nusselt diffusion criterion is virtually independent of the Reynolds number over a very wide range of the ratio Re/ d_e (from 10.5 to 490) covering the laminar, transitional, and turbulent flow regions.

The relationship Nu' = f(Pr') is plotted in Fig. 4. This graph shows that there is no interdependence between the Nusselt and Prandtl diffusion criteria; this is probably because the viscosity variations of oil solutions in the extraction solvent in the concentration range from 0 to 60-70 wt.% are small [24]. Therefore Pr' can enter the criterial equation as a proportionality factor.

The table shows the effect of layer height on the extraction efficiency, in terms of the oil content of the residue after extraction. It is seen that the layer height has virtually no influence on the extraction efficiency. This is consistent with the hardness (incompressibility) of the particles obtained from various oilcakes.

Thus, Equation (2) becomes the following simple relationship:

$$Nu' = f(Fo'). \qquad (10)$$

* The diffusion coefficients of vegetable oils at 20° are given in an earlier paper [26]. For other temperatures, these coefficients were found by calculation with the aid of the temperature-viscosity ratio T/η.

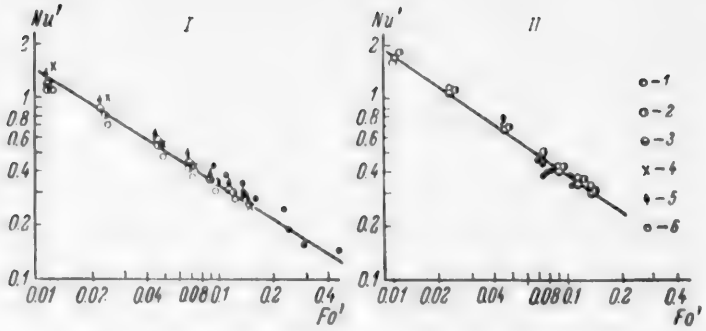

Fig. 7. The Nu' = f(Fo').relationship. Extracted material: I) expeller cake from dehulled cottonseed, II) expeller cake from undehulled cottonseed. 1, 2, 3, 4, 5) Laboratory experiments, 6) plant trials.

The results of extraction of various materials in laboratory and works extractors are presented in Figs. 5-7. These data were used to derive the following explicit form of the relationship between Nu' and Fo' for various materials.

For cottonseed cake made by single pre-pressing from dehulled seeds

$$Nu' = 0.0676 \cdot (Fo')^{-1,0} \qquad \text{at} \quad \tau = 0 \; O_{em} = 10.15\%, \; W_{em} = 6.53\%.$$

For cottonseed expeller cake from dehulled seeds

$$Nu' = 0.0781 \cdot (Fo')^{-0,832} \qquad \text{at} \quad \tau = 0 \; O_{em} = 6.22\%, \; W_{em} = 4.82\%.$$

For cottonseed expeller cake from undehulled seeds

$$Nu' = 0.0780 \cdot (Fo')^{-0,693} \qquad \text{at} \quad \tau = 0 \; O_{em} = 6.68\%, \; W_{em} = 5.48\%.$$

For sunflower-seed cake made by single pre-pressing

$$Nu' = 0.0621 \cdot (Fo')^{-0,858} \qquad \text{at} \quad \tau = 0 \; O_{em} = 14.64\%, \; W_{em} = 4.18\%.$$

For soybean cake made by single pre-pressing

$$Nu' = 0.1 \cdot (Fo')^{-1,0} \qquad \text{at} \quad \tau = 0 \; O_{em} = 16.79\%, \; W_{em} = 4.56\%.$$

The above relationships are valid for Re/d_e = 10.5 to 490.

The above relationships are accompanied by data on the oil contents of the extracted material, O_{em} (at moisture content W_{em}) for which they were determined. As the first portions of oil are extracted very rapidly (Fig. 1), the value of the mass-transfer coefficient for any other oil content can be easily calculated from the formula

$$K' = K \frac{m'}{m}, \qquad (11)$$

where K and m are the mass-transfer coefficient and oil yield at the values of O_{em} given above; K' and m' are the mass transfer and oil yield at any other value of O_{em}.

The results of laboratory experiments and plant trials are compared in Fig. 7.

SUMMARY

1. Results obtained by other workers and the theory of similarity were used to derive the implicit form of the criterial equation for nonequilibrium mass transfer in a layer of particles:

$$Nu' = f(Fo', Pr', Re, \Gamma_1).$$

2. Analysis of our experimental data on the extraction of oil from oil cake showed that the Nusselt diffusion criterion is virtually independent of the Prandtl diffusion criterion, the Reynolds number (within the range of Re/d_e between 10.5 and 490), and the geometrical similarity ratio. The criterial equation for the extraction of oil from oil cake has the following simple form:

$$Nu' = f(Fo').$$

Thus, the extraction of vegetable oils from oil cakes is an instance of nonequilibrium mass transfer in a layer of incompressible particles of high internal resistance.

3. The explicit form of the relationship has been found for different materials.

$$Nu' = f(Fo').$$

4. The results of laboratory and plant experiments are in good agreement, confirming the validity of the relationship established between the similarity criteria, and indicating the similarity of the processes in laboratory and works extractors.

In conclusion, the author thanks Doctor of Technical Sciences, Professor P. G. Romankov, for advice on application of the similarity theory to the experimental data.

LITERATURE CITED

[1] A. M. Goldovskii, Physiocochemical and Biological Principles of the Production of Vegetable Oils [In Russian] (Food Industry Press, (1937)).

[2] H. Coats, and G. Karnofsky, J. Am. Oil Chem. Soc. 27, 251-255 (1950).

[3] J. O. Osburn, and D. L. Katz, Trans. Am. Inst. Chem. Eng. 40, 5, 511-531 (1944).

[4] D. F. Boucher, J. C. Brier, and J. O. Osburn, Trans. Am. Inst. Chem. Eng. 38, 967-993 (1942).

[5] H. P. Fan, J. C. Morris, and H. Wakeham, Ind. Eng. Ch. 40, 2, 195-199 (1948).

[6] S. S. Il'in, Oil and Fat Ind. 3 (1938).

[7] A. Bailey, Industrial Oil and Fat Products (New York, (1951)).

[8] C. O. King, D. L. Katz, and J. C. Brier, Trans. Am. Inst. Chem. Eng. 40, 5, 533-556 (1944).

[9] A. S. Smith, J. Am. Oil Chem. Soc. 29, 10, 421-425 (1952).

[10] D. F. Othmer, and J. C. Agarwal, Ch. Eng. Progr. 51, 8, 372-378 (1955).

[11] L. K. Arnold, and W. G. Juhl, J. Am. Oil Chem. Soc. 31, 12, 613-618 (1954).

[12] L. K. Arnold, and D. J. Patel, J. Am. Oil. Chem. Soc. 30, 5, 216-218 (1953).

[13] M. R. Wingard, and R. C. Phillips, J. Am. Oil Chem. Soc. 28, 4, 149-152 (1951).

[14] L. K. Arnold, and S. P. Pool, J. Am. Oil. Chem. Soc. 30, 12, 611-613 (1953).

[15] A. M. Goldovskii, Trans. All-Union Sci. Res. Inst. Fats 14 (1952).

[16] H. B. Coats, and M. R. Wingard, J. Am. Oil Chem. Soc. 27, 2, 93-96 (1950).

[17] I. V. Gavrilenko and V. V. Beloborodov, Oil and Fat Ind. 7 (1953).

[18] A. G. Kasatkin, Fundamental Principles and Equipment of Chemical Technology [In Russian] (Goskhimizdat, (1955)).

[19] Pao Chih-ch'uan, Candidate's Dissertation, Lensoviet Technol. Inst. (Leningrad, (1955)).

[20] L. S. Leibenzon, Motion of Natural Liquids and Gases in Porous Media [In Russian] (State United Press, (1947)).

[21] R. I. Psinov, M. G. Pitkevich and I. T. Belikov, Report of a Study of the Continuous Extraction of Oil Seeds and Cakes, Leipzig [In Russian] (1946).

[22] V. V. Beloborodov, Oil and Fat Ind. 2 (1957).

[23] F. N. Shakhov and V. A. Zhelekhovskii, Calculations, Design, and Investigations of Chemical Equipment and Machinery, Sci. Res. Inst. Chem. Machinery. Coll. No 5 [In Russian] (Mashgiz, (1950)).

[24] V. V. Beloborodov, Oil and Fat Ind. 3 (1956).

[25] I. V. Gavrilenko and V. V. Beloborodov, Oil and Fat Ind. 11 (1953).

[26] V. V. Beloborodov, J. Appl. Chem. 29, 1437 (1956). •

Received November 14, 1956

• Original Russian pagination. See C. B. Translation.

STUDY OF THE PENTOSE HYDROLYSIS OF CORNCOB CORES*

B. M. Nakhmanovich

The Scientific Research Laboratory of the Dokshakino Acetone Works

In the resolutions of the XXth Congress of the CPSU it is proposed to introduce new sources of raw materials "and to make wider industrial use of synthetic raw materials and substitutes in order to replace completely all the food products used for industrial purposes, during the Sixth Five-Year Plan."

Our searches for possible substitutes for foodstuffs in the acetone and butanol industry indicated that the most promising and most readily available substitute is corncob cores, containing up to 40% pentosans. Our investigations showed that the xylose and arabinose obtained from pentose hydrolyzates from corncob cores are effectively fermented by acetobutylic bacteria.

Among the work of Soviet and foreign scientists on pentose hydrolysis of various kinds of vegetable raw materials, mention should be made of the work of Sharkov [1, 2], Zakoshchikov et al. [3-5], Pliushkin, Chetverikov, and Lazarev [6-8], Gutgerts [9], Sokolov [10, 11], Keller [12], Prianishnikov and Mashevitskaia [13], Brigner [14], Heuser [15], and Hudson et al. [16].

Relatively little work has been done on the hydrolysis of hemicellulose from corncob cores.

EXPERIMENTAL

The corncob cores used were from the 1955 crop grown in the Kabardino–Balkar Autonomous SSR. The cores, containing 19.5% moisture, were shredded to a particle size of 0.5-2.0 mm and dried to constant weight at 105°. The cores contained (% on the bone-dry substance) 33.8% pentosans, equivalent to 38.4% pentoses (by the Tollens method) [17]; 38.6% reducing substances (RS) after 3 hours of hydrolysis with 2% HCl; 0.5% uronic acids (by the Tollens–Lefevre method [18]); no hexosans; ash 1.7%; nitrogenous substances 1.9% (Kjeldahl).

Kinetics of the hydrolysis of corncob-core pentosans by 1% H_2SO_4 at various temperatures. Special copper tubes with airtight screw tops fitted with rubber washers were made for the hydrolysis (the tubes were 20 mm in internal diameter, 150 mm high, with walls 2 mm thick). Into each copper tube there was inserted a closely fitting glass test tube containing 2 g of shredded corncob core and 20 ml of 1% sulfuric acid; the liquor ratio (M) was 10. The tubes were kept for 5 minutes in a water bath at 70° in order to impregnate the corncob material with the acid solution and to remove air; the tops were than screwed down and the tubes were completely immersed in an oil bath, in which they were suspended in a vertical position. The bath was heated a few degrees above the required temperature; after 5 minutes after immersion of the tubes the tube and bath temperature reached the required level and was then kept constant. The hydrolysis was carried out at 100, 110, 120, and 130°. At definite time intervals pairs of tubes (to give two duplicate points) were removed from the bath, cooled rapidly, opened, shaken, and filtered by suction through a funnel with a copper gauze. The following determinations were carried out on the hydrolyzates from these and all subsequent experiments: 1) dry solids (by means of a precision refractometer), 2) reducing substances (RS, by the Bertrand method), 3) acidity (titration with phenolphthalien indicator), 4) RS after additional hydrolysis by 2% HCl (100°; 3 hours) with 5-fold dilution of the hydrolyzates. The solution therefore contained 0.2% H_2SO_4 in addition to the 2% HCl.

The contents of soluble pentosans were found from the difference between the RS contents before and after additional hydrolysis. Calculations based on the experimental results (see Table) show that the hydrolysis

*N. A. Prianishnikova and L. P. Dokhlikova took part in the experimental work.

Hydrolysis of Corncob-Core Pentosans at Various Temperatures (1% H_2SO_4; M = 10)

Hydrolysis time t (minutes)	100°			110°			120°			130°		
	amount of pentosans hydrolyzed		reaction-rate constant $K = \frac{1}{t} \ln \frac{a}{a-x}$	amount of pentosans hydrolyzed		reaction-rate constant $K = \frac{1}{t} \ln \frac{a}{a-x}$	amount of pentosans hydrolyzed		reaction-rate constant $K = \frac{1}{t} \ln \frac{a}{a-x}$	amount of pentosans hydrolyzed		reaction-rate constant $K = \frac{1}{t} \ln \frac{a}{a-x}$
	x (in g/100 ml)	% of total		x (in g/100 ml)	% of total		x (in g/100 ml)	% of total		x (in g/100 ml)	% of total	
15	–	–	–	–	–	–	1.01	29.9	0.0236	–	–	–
30	0.56	16.5	0.0061	1.06	31.4	0.0125	1.58	46.7	0.0210	2.67	79.5	0.0520
45	–	–	–	1.50	44.4	0.0130	2.20	65.1	0.0234	3.05	90.2	0.0517
60	0.86	25.4	(0.0049)	1.85	54.9	0.0132	2.50	74.0	0.0224	3.19	94.4	0.0480
90	1.355	40.1	0.0058	2.38	70.6	0.0135	2.87	85.0	0.0210	3.36	99.7	0.0506
120	1.74	51.5	0.0060	2.56	76.0	(0.0118)	3.14	92.9	0.0220			
150	2.00	59.2	0.0060	2.92	86.7	0.0133	3.15	93.2	(0.0179)			
180	2.24	66.3	0.0060	3.04	90.2	0.0128	3.19	94.4	(0.0160)			
210	2.43	71.9	0.0060	–	–	–	3.19	94.4				
240	2.58	76.2	0.0060	3.21	95.0	0.0125	3.18	94.1	0.0222			
300	2.81	83.0	0.0059	3.21	95.0		–	–				
360	2.81	83.0		3.13	93.0	0.0130	3.34	98.8				
∞	3.38	100.0	0.0060	3.38	100.0		3.38	100.0				

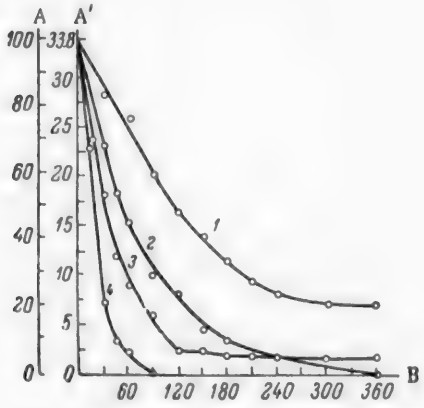

Fig. 1. Rates of hydrolysis of corncob-core pentosans by 1% H_2SO_4 at various temperatures; liquor ratio M = 10. A, A') Pentosans (in % and in g/liter on the weight of bone-dry material respectively), B) time (minutes). Temperature (in °C): 1) 100, 2) 110, 3) 120, 4) 130.

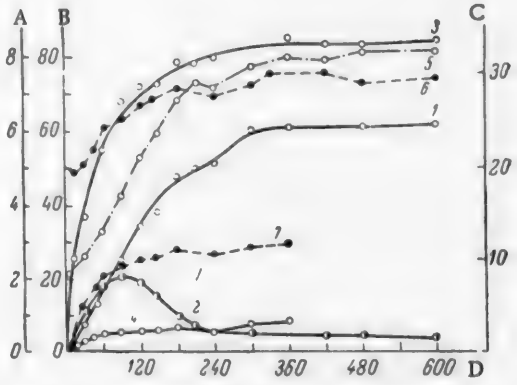

Fig. 2. Hydrolysis of corncob cores by 1% H_2SO_4 at 100°; liquor ratio M = 5. A) Contents in hydrolyzate (in g/100 ml) of: 1) pentoses (RS), 2) pentosans, 3) total solids, 4) organic acids; B) purity of hydrolyzate (%), 5; C) acidity of hydrolyzate (in ml of 0.1 N acid per 10 ml); 6) total, 7) organic; D) time (minutes).

of corncob-core pentosans conforms to the monomolecular-reaction law, with one-minute rate constants of 0.0060 at 100°, 0.0130 at 110°, 0.0222 at 120°, and 0.0506 at 130°. The symbol ∞ represents total hydrolysis of all the original pentosans in the core (a = 3.38 g/100 ml). The curves representing the hydrolysis rates of pentosans are plotted in Fig. 1.

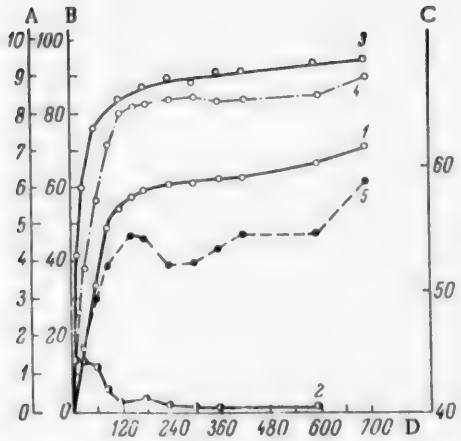

Fig. 3. Hydrolysis of corncob-core pentosans by 2% H_2SO_4 at 100°, with liquor ratio M = 5.
A) Contents in hydrolyzate (in g/100 ml) of: 1) pentoses (RS), 2) pentosans, 3) total solids; B) purity of hydrolyzate (%), 4); C) acidity of hydrolyzate (in ml of 0.1 N acid per 10 ml), 5; D) time (minutes).

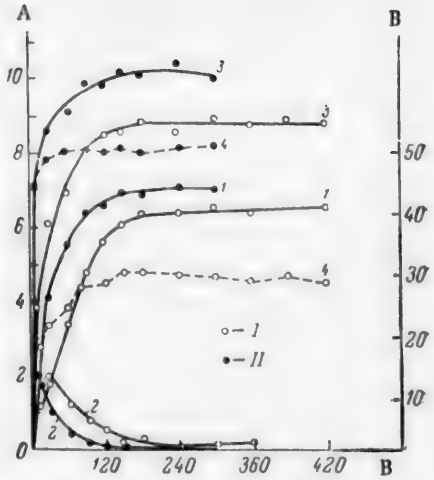

Fig. 4. Hydrolysis of corncob core by hydrochloric acid at 100°, with liquor ratio M = 5.
A) Contents in hydrolyzate (in g/100 ml) of: 1) pentoses (RS), 2) pentosans, 3) total solids; B) acidity of hydrolyzate (in ml of 0.1 N acid per 100 ml), 4; C) time (minutes). HCl concentration (normality): I) 0.2, II) 0.4.

The hydrolyzate acidity was in the range of 27-29 ml of 0.1 N acid per 10 ml.

Hydrolysis of corncob-core pentosans at 100°. Effect of the nature and concentration of the acid. The hydrolysis of corncob cores by sulfuric and hydrochloric acids at 100° (on a boiling water bath) was also studied. 20 g of the corncob material and 100 ml of acid solution was put in a flask fitted with a reflux condenser; at definite intervals the contents of the flask were cooled rapidly, the hydrolyzate was separated from the lignocellulose, and analyzed. The results of the experiments are presented in Figs. 2, 3, and 4.

A decrease of the liquor ratio from 10 to 5 retarded the hydrolysis, and the reaction-rate constant fell from 0.0060 to 0.0048 (in 1% H_2SO_4). With 2% H_2SO_4 (M = 5) the average hydrolysis-rate constant was 0.0101, or double the value of the constant for 1% H_2SO_4.

The rate constants for hydrolysis of the corncob material by 0.2 N and 0.4 N HCl (100°, M = 5) were 0.0102 and 0.0208 respectively. Therefore the rate of hydrolysis of corncob-core pentosans is directly proportional to the acid concentration; this is true for sulfuric and for hydrochloric acids. Equal hydrolysis-rate constants were obtained with 0.2 N HCl and 0.4 N H_2SO_4 (2% H_2SO_4). Therefore in hydrolysis by different acids but of equal normality the rate constant is proportional to the degree of dissociation (the activities of 0.1 N acids are: HCl 1.0, H_2SO_4 0.51). Sharkov [1] found a similar relationship between the hydrolysis of cellulose and the nature and concentration of the acid.

The formation of volatile acids during hydrolysis was determined (by the method of Virtanen and Pulkki, modified by Bekhterova and Ierusalimskii [19]. The volatile acids consist of about 90% acetic and about 10% formic acid. After 3 hours of hydrolysis by 1% H_2SO_4 at 100° the accumulation of volatile acids in solution ceased (Fig. 2), the content being 3.2% on the weight of the bone-dry material or 10.5% on the pentose (RS) weight. Since the RS of pentose hydrolyzates made from corncob cores consist of pentoses only, the amounts of xylose and arabinose may be found from reduction and polarimetric data for the hydrolyzates. Here we make use of the expression for the angle of rotation

$$\alpha = \frac{[\alpha]_D \cdot l \cdot C}{100 \cdot 0.347}, \quad (1)$$

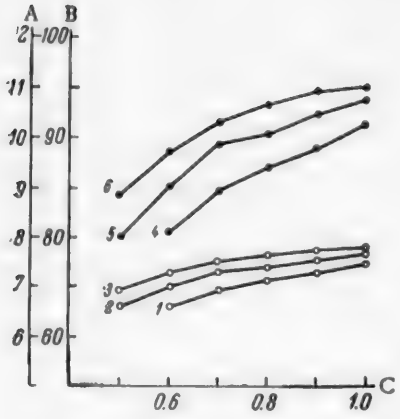

Fig. 5. Variation of pentose (RS) yield with the sulfuric acid concentration at various temperatures of corncob-core hydrolysis, at liquor ratio M = 5.
A) Pentoses in hydrolyzate (g/100 ml), 1, 2, 3; B) pentose yields (% of theoretical), 4, 5, 6; C) H_2SO_4 concentration in solution (%). Pressure during hydrolysis (atmos): 1, 4) 0.8 (117°); 2, 5) 1.0 (121°); 3, 6) 1.2 (124°).

where $[\alpha]_D$ is the specific rotation, which is +108° for L-arabinose and +19° for D-xylose; l = 2 is the length of the polarimeter tube (in dm); C is the concentration of sugar in solution (in g/100 ml).

The rotation of a mixture of arabinose and xylose is the sum of the rotations of the two sugars

$$\alpha = \alpha_a + \alpha_x \qquad (2)$$

Expressing the rotation of the sugars in terms of their concentrations (by means of Equation (1)) we have

$$\alpha = 6.225C_a + 1.095C_x. \qquad (3)$$

In the Bertrand method of sugar determination the reducing power of xylose is the same as that of glucose, and about 5% higher than this in the case of arabinose. Therefore, in determinations of RS by the Bertrand method with the aid of the table for glucose

$$C = 0.95C + C_x \qquad (4)$$

Equations (3) and (4) are used to find C_a and C_x (in g/100 ml) from polarimetric (α) and reduction (C) data:

$$C_a = \frac{\alpha - 1.095C}{5.185}, \quad C_x = C - 0.95C.$$

For the polarimetric determinations, 5 ml of the hydrolyzate was clarified by addition of 5 ml of basic lead acetate (in a 100 ml flask), excess lead was precipitated by the addition of 5 ml of saturated NaH_2PO_4 solution, the liquid was made up to the mark, shaken and filtered. The pentose hydrolyzates contained 16-17% arabinose and about 84% xylose (C = 7.5 g/100 ml, α = +14.6° at M = 5). This method was used to determine the arabinose and xylose in hydrolyzates during hydrolysis of corncob cores by 1% H_2SO_4 at 100°, M = 5. A correction was applied for the rotation of soluble pentosans, the value taken being $[\alpha]_D = -90°$ (mean of different literature data). It was found that corncob-core araban is hydrolyzed much more easily than the xylan. The hydrolysis of araban under these conditions was complete in 1.5 hours, whereas the total content of hydrolyzed pentosans at the time was only 32%.

Corncob-core pentosans can be classified in the following fractions according to their hydrolyzability:

Fraction	Amount (% of total pentosans)	Conditions for complete hydrolysis of the fraction (by 1% H_2SO_4 with M = 10)
Araban	16–17	100°, 1.5 hrs.
Xylan I	62–66	100°, 5 hrs.
Xylan II	12–15	110°, 4 hrs.
Xylan III	5–6	130°, 1.5 hrs.

Fig. 5 represents the effect of the sulfuric acid concentration on the degree of hydrolysis of corncob-core pentosans. In these experiments the hydrolysis was performed in an autoclave for 4 hours. Flasks each containing 100 g of shredded corncob cores and 500 ml of acid solution (of different concentrations) were placed in the autoclave.

The following conditions may be recommended for the production of pentose hydrolyzates, easily fermented by acetobutylic bacteria, from corncob cores: 0.9-1.0% H_2SO_4, 0.6-1.2 atmos (114-124°), hydrolysis

time 3-4 hours, liquor ratio 4-5. The yield of pentoses is about 95% of the theoretical. The hydrolyzates contained about 0.08% furfural.

SUMMARY

1. The kinetics of the hydrolysis of corncob-core pentosans was studied. It was shown that the hydrolysis conforms to the law for monomolecular reactions. The one-minute rate constants for the hydrolysis of corncob-core pentosans at 100, 110, 120 and 130°, at liquor ratio M = 10, by 1% H_2SO_4 were found to be 0.0060, 0.0130, 0.0222 and 0.0506 respectively.

2. Corncob-core pentosans consist of araban (17%) and xylan (83%). The part of the xylan most resistant to hydrolysis comprises 5-6% of the total pentosan content.

3. The rate of hydrolysis of corncob-core pentosans is directly proportional to the acid content of the solution. In hydrolysis by sulfuric and hydrochloric acids of the same normality, the hydrolysis rate was proportional to the degrees of dissociation of these acids.

4. Hydrolysis of the hemicelluloses of corncob-cores is accompanied by formation of volatile acids (90% acetic and 10% formic), the total amount of which was 3.2% on the weight of the bone-dry material.

5. Conditions are specified for the hydrolysis of corncob cores, in which the pentose yield is 95% of the theoretical, with not more than 0.1% furfural in the hydrolyzates.

LITERATURE CITED

[1] V. I. Sharkov, The Hydrolysis Industry, [In Russian] (State Wood Technology Press 1, 1945; 2 (1948)).

[2] V. I. Sharkov and A. P. Petrochenko, Wood Chem. Ind. 3, 11 (1933).

[3] A P. Zakoshchikov, Hydrol. Ind. USSR 5, 1, 5; 6, 11 (1952).

[4] A. P. Zakoshchikov and B. G. Malikov, Hydrol. and Wood Chem. Ind. 3, 4 (1956).

[5] A. P. Zakoshchikov, A. Ia. Kolosova and M. E. Shpuntova, J. Appl. Chem. 29, 7, 1093 (1953). •

[6] E. Z. Pliushkin and N. M. Chetverikov, J. Appl. Chem. 7, 6, 1008 (1934).

[7] N. M. Chetverikov and A. I. Lazarev, Chemical Utilization of Plant Wastes (Leningrad, Food Industry Press, (1935)). [In Russian]

[8] E. Z. Pliushkin, Hydrol. Ind. USSR 1, 4, 8 (1948); 6 (1952).

[9] N. I. Gutgerts, Trans. VNILRO, 1 (Dnepropetrovsk, (1937)).

[10] V. F. Sokolov, Soviet Sugar 2-3 (1935).

[11] V. F. Sokolov, J. Appl.Chem. 9, 1, 113 (1936).

[12] R. E. Keller, J. Appl. Chem. 10, 12, 2041 (1937).

[13] N. D. Prianishnikov and S. G. Moshevitskaia, J. Appl. Chem. 10, 9, 1573 (1937).

[14] L. C. Brigner, C. A., 29, 5687[4] (1935).

[15] E. Heuser, Zbl., I, 505; III, 368 (1923).

[16] G. S. Hudson, and T. S. Harding, J. Am. Chem. Soc., 39, 1038 (1917); 40, 1601 (1918).

[17] A. L. Malchenko, L. I. Iasinskii, S. V. Atamanenko, and A. V. Pelikhova, Technological Chemical Control and Accounting in the Alcohol Industry [In Russian] (Moscow, Food Industry Press, (1946)), p. 183.

[18] N. Ia. Dem'ianov and N. D. Prianishnikov, General Methods of Analysis for Plant Materials [In Russian] (State Chem. Tech. Press, (1934)).

[19] M. N. Bekhtereva and N. D. Ierusalimskii, Factory Labs. 6, 3, 312 (1937).

Received February 26, 1957

• Original Russian pagination. See C. B. Translation.

CONVERSIONS OF β-CHLORO ETHERS IN PRESENCE OF METALS*

V. I. Isaguliants and I. S. Maksimova

The previous communication [1] dealt with the activity of the chlorine atoms in β-chloro ethers, as indicated by studies of their reactions with alkalies under various conditions.

The present communication is concerned with a study of the behavior of β-chloro ethers in presence of metals. The experiments were performed mainly with the methyl ether of α-amylene chlorohydrin and the following metals: sodium, copper, aluminum, and magnesium.

The action of metallic sodium on the methyl ether of α-amylene chlorohydrin might be expected to result in the reaction

$$CH_3-CH_2-CH_2-\underset{\displaystyle OCH_3}{\underset{|}{CH}}-CH_2Cl + Na + Na + ClCH_2-\underset{\displaystyle OCH_3}{\underset{|}{CH}}-CH_2-CH_2-CH_3 \rightarrow$$
$$\rightarrow CH_3CH_2CH_2\underset{\displaystyle OCH_3}{\underset{|}{CH}}-CH_2-CH_2-\underset{\displaystyle OCH_3}{\underset{|}{CH}}-CH_2-CH_2-CH_3 + 2NaCl$$

with formation the dimethyl ether of decanediol as the final reaction product. However, the reaction yielded amylene, sodium methylate, and sodium chloride:

$$CH_3-CH_2-CH_2-\underset{\displaystyle OCH_3}{\underset{|}{CH}}-CH_2Cl + 2Na \rightarrow$$
$$\rightarrow CH_3-CH_2-CH_2-CH=CH_2 + CH_3ONa + NaCl,$$

i.e., the $-\overset{|}{C}-Cl$ and $-\overset{|}{C}-OCH_3$ bonds were broken. According to Shorygin [2], the action of metallic sodium on ethers results in rupture of R−O−R' bonds as follows:

$$\begin{matrix} R \\ R' \end{matrix}\!\!>\!O + 2Na \rightarrow \left[\begin{matrix} R \\ R' \end{matrix}\!\!>\!O\!<\!\begin{matrix} Na \\ Na \end{matrix} \right] \begin{matrix} \nearrow R'Na + RONa \\ \searrow R'ONa + RNa \end{matrix}$$

If this reaction mechanism is applied to the β-chloro ether (with the chlorine atom disregarded), the rupture of the R−O−R bond by the action of metallic sodium may be represented as follows:

$$CH_3-CH_2-CH_2-\underset{\displaystyle CH_2Cl}{\overset{\displaystyle OCH_3}{CH}} + 2Na \rightarrow \left[CH_3-CH_2-CH_2-\underset{\displaystyle CH_2Cl}{CH}-O\!<\!\begin{matrix} Na \\ Na \end{matrix} \right] \rightarrow$$

$$\begin{matrix} \nearrow CH_3ONa + [CH_3-CH_2-CH_2-\underset{\displaystyle Na}{\underset{|}{CH}}-CH_2Cl] & (I) \\ \searrow CH_3Na + [CH_3-CH_2-CH_2-\underset{\displaystyle ONa}{\underset{|}{CH}}-CH_2Cl] & (II) \end{matrix}$$

* Communication II in the series on the synthesis and chemical conversion of β-chloro ethers made from olefins obtained by the cracking of petroleum.

Sodium methylate, i.e., an alcoholate with a radical not containing chlorine, was isolated from the reaction products; therefore the reaction proceeds in the direction (I).

Because of the presence of a chlorine atom in close proximity to a sodium atom in the intermediate organosodium compound, sodium chloride is readily split off with formation of a double bond:

$$[CH_3-CH_2-CH_2-\underset{\displaystyle Na}{\underset{|}{CH}}-\underset{\displaystyle Cl}{\underset{|}{CH_2}}] \rightarrow CH_3-CH_2-CH_2-CH=CH_2 + NaCl.$$

It was found in experiments on the action of metallic sodium on the methyl and butyl ethers of amylene chlorohydrin that metallic sodium does not react with β-chloro ethers in the cold, and decomposition of the ethers by the reaction scheme indicated above commences only when the reaction mixture is heated to 60-70°; the conversion of the ether reaches 55-60%.

The catalytic action of copper on organic compounds containing inactive halogens has long been known (in the case of halogen-substituted aromatic compounds, the Gattermann reaction). It was therefore of interest to investigate its action on β-chloro ethers. When the β-chloro ether had been heated with copper dust at the boil for three hours, it was recovered unchanged.

However, at temperatures of 170-300° and under pressures of 10 to 40 atmos HCl is split off with formation of a substituted vinyl ether and its hydrolysis and polymerization products. The conversion of the original β-chloro ether is 86-96%, according to the experimental conditions. In the course of the experiment the following products were isolated: a gas containing from 16 to 20% unsaturated compounds, a fraction boiling in the 80-120° range, consisting of a mixture of a vinyl ether and methyl propyl ketone, and high-boiling fractions, consisting of condensation products of the substituted vinyl ether. It may be assumed that in presence of copper HCl is first split off from the original β-chloro ether

$$CH_3-CH_2-CH_2-\underset{\displaystyle OCH_3}{\underset{|}{CH}}-CH_2Cl \rightarrow CH_3-CH_2-CH_2-\underset{\displaystyle OCH_3}{\underset{|}{C}}=CH_2 + HCl.$$

The liberated hydrogen chloride reacts with copper to form the chloride. The copper chloride assists further removal of hydrogen chloride.

Many examples are known of the use of copper and its chlorides as catalysts accelerating the reaction in the direction described [3-6].

It is also known that vinyl ethers are easily hydrolyzed in presence of metal chlorides [7]; therefore under the conditions described the substituted vinyl ether which is formed is partially hydrolyzed and converted into a ketone

$$CH_3-CH_2-CH_2-\underset{\displaystyle OCH_3}{\underset{|}{C}}=CH_2 \xrightarrow{CuCl} [CH_3-CH_2-CH_2-\underset{\displaystyle OH}{\underset{|}{C}}=CH_2] \rightarrow CH_3-CH_2-CH_2-\underset{\displaystyle O}{\underset{\|}{C}}-CH_3$$

Methyl propyl ketone was shown to be present in the reaction products.

Copper chloride also causes polymerization of the vinyl ether, but the degree of polymerization is not high. The molecular weight of the polymers formed, determined cryoscopically, was 400-470. The low degree of polymerization may be attributed to the presence of a ketone in the reaction mixture. Polymer chains are terminated in presence even of traces of aldehydes, ketones, or other compounds containing oxygen, because of peroxide formation.

Finely-divided aluminum, like copper, is used as a catalyst for removal of hydrogen halides from halogenated organic compounds [8, 9].

Experiments with aluminum dust were carried out in an autoclave. The temperature was varied from 180 to 280°, and the pressure from 10 to 25 atmos. The conversion of the original chloro ether reached 75.0-91%. The course of the reaction was the same as with copper, but with a higher yield of polymerization products.

The most probable course of the reaction between magnesium and β-chloro ethers is formation of organomagnesium compounds, but in fact the reaction results, as in the case of copper or aluminum, in removal of hydrogen chloride from the β-chloro ether.

The characteristic property of magnesium in this reaction is its ability to catalyze hydrolysis of the vinyl ether. The light-boiling portion of the catalyzate consists of almost pure methyl propyl ketone with a small admixture of the vinyl ether.

Experiments with magnesium were carried out in the temperature range 180-280°, under pressures from 10 to 30 atmos. The conversion of the original ether was 12 to 80%, according to the experimental conditions.

Comparison of the action of copper, aluminum, and magnesium on β-chloro ethers leads to the conclusion that all these metals act by the same reaction mechanism – they all first catalyze the removal of HCl from the ether (as described above), and then the liberated hydrogen chloride reacts with the free metals to give their chlorides.

The chlorides increase the removal of hydrogen chloride and catalyze the secondary reactions of hydrolysis and polymerization of the α-substituted vinyl ether formed.

EXPERIMENTAL

Action of metallic sodium on the β-chloro ether. The methyl ether of amylene chlorohydrin used in the experiment had the following constants: b.p. 140–143°, $n_D^{20} = 1.4295$, $d_4^{20} = 0.9720$. The experiment was carried out in a round-bottomed flask fitted with a fractionating column, dropping funnel, a thermometer inserted in the reaction mixture, a condenser, and a receiver cooled in ice. 9 g of finely-divided metallic sodium and 20 g of the dry methyl ether (about one half of the calculated amount) was introduced into the flask. There was no reaction between the β-chloro ether and sodium in the cold. On slow heating, the surface of the metallic sodium became blue, gas bubbles appeared, and at 65-70° there was a violent reaction with evolution of heat; the temperature rose to 90-95°, the metallic sodium melted, and a substance boiling at 30-35° was distilled off, fresh portions of the ether being added from the dropping funnel. A brown precipitate was formed in the flask after the end of the reaction.

This precipitate was carefully decomposed by water and extracted by ethyl ether. The ether extract was dried over calcium chloride and distilled. Sodium chloride was detected qualitatively in the aqueous solution. The fraction boiling in the 30-35° range had the following constants after it had been washed and redistilled: b.p. 30–32°, $d_4^{20} = 0.6620$, $n_D^{20} = 1.3738$, i.e., it was almost pure α-amylene.

9g of metallic sodium and 43.6 g of the methyl ether was taken for the reaction. 19.5 g of the unchanged ether and 12 g of amylene was obtained. The converted 24 g of the ether should theoretically yield 12.9 g of amylene. The degree of decomposition of the ether was 55%. The unchanged ether had the following constants: b.p. 140-145°, $n_D^{20} = 1.4290$. This ether was again subjected to the action of metallic sodium as described above. 19.5 g of the methyl ether and 4 g of sodium was taken. The reaction started at 65°. 5.8 g of amylene was condensed in the ice-cooled receiver; after redistillation, it had the following constants: b.p. 30–35°, $n_D^{20} = 1.3730$.

From the residue decomposed by water, 8 g of unchanged methyl ether of b.p. 140–144°, $n_D^{20} = 1.4295$ was isolated after extraction in ether and fractionation. The converted 11.5 g of the ether should theoretically yield 6.3 g of amylene. The degree of decomposition of the ether was 59%.

In order to verify whether an alkoxy group is really split off in accordance with Reaction (I), the same reaction was carried out with the butyl instead of the methyl ether of amylene chlorohydrin. The sodium butylate formed by decomposition of the ether should yield butyl alcohol on hydrolysis; because of the relatively slow solubility in water, butyl alcohol can easily be isolated and investigated. 13 g of the butyl ether, with the following constants: b.p. 191–193°, $n_D^{20} = 1.4309$, was taken for the reaction.

The butyl ether did not react with metallic sodium in the cold; when the temperature was raised to 70-75° the reaction proceeded violently, as in the case of the methyl ether, with evolution of heat. As a result of the reaction, 2.9 g of amylene with the following constants: b.p. 37–40°, $n_D^{20} = 1.3780$, was isolated.

The residue was decomposed by water and extracted by ethyl ether. Fractionation yielded 4.3 g of the unchanged butyl ether, 0.8 g of a fraction of b.p. 110–116°, $n_D^{20} = 1.3920$, and 1 g of a fraction of b.p. 116–117°, $n_D^{20} = 1.4000$.

This fraction corresponds to butyl alcohol. Therefore the experimental results confirm the suggested reaction scheme.

Action of copper on the β-chloro ether. When β-chloro ethers were heated with metallic copper to the boiling point, no reactions took place. The subsequent experiments were performed under pressure.

Experiment I. 25 g of the methyl ether and about 1 g of copper dust was put into an autoclave. The autoclave was heated for 4 hours at 280-300° at a pressure of 30-40 atmos.

The outlet tube of the autoclave was connected to a gas holder through a small coil (immersed in freezing mixture). At the end of the reaction, when the autoclave had been cooled to room temperature, two liters of gas containing 19% unsaturated compounds was collected in the holder; this gas was not investigated further.

0.8 g of a liquid, $n_D^{20} = 1.3725$ condensed in a coil.

A drop of this liquid instantly decolorized bromine water. This liquid was probably amylene. The liquid catalyzate was pale brown in color. The bottom and walls of the autoclave were coated with a deposit in which Cl and Cu were detected qualitatively. The reaction mixture was decomposed by a small quantity of water; the upper layer was separated off, dried over calcined potash, and fractionated. The lower aqueous layer was extracted with ethyl ether, and the ether extract was also fractionated.

Balance of Experiment I. 25 g of the chloro ether taken for the reaction, 2 liters of gas collected, 0.8 g of amylene condensed.

Fractionation of upper layer:

Fraction 60–70° — 1.0 g, $n_D^{20} = 1.3840$;

Fraction 70–80° — 1.0 g, $n_D^{20} = 1.3890$;

Fraction 80–107° — 6 g, $n_D^{20} = 1.3895$;

Fraction 110–120° — 0.6 g, $n_D^{20} = 1.4080$;

Fraction 120–135° — 1.0 g, $n_D^{20} = 1.4165$.

Residue in flask, 7.5 g.

Fractionation of ether extract:

Fraction 70–80° — 0.5 g, $n_D^{20} = 1.3900$;

Fraction 80–120° — 0.4 g, $n_D^{20} = 1.4180$.

Total liquid reaction products 18.8 g.

The unchanged ether was assumed to be the 120-135° fraction, 1 g, or 4% of the amount of β-chloro ether taken. The conversion of the original β-chloro ether was 96%.

The first three fractions obtained in distillation under atmospheric pressure were combined and fractionated again; a 98-103° fraction with the following properties was isolated: $n_D^{20} = 1.3900$, bromine number, by the Kaufmann method 25.6-27.9, unsaturated compounds 15.85%; M = 90.99, 94.94.

The ketone content of the mixture was determined by the Idlis* method. The weight of substance taken was 0.3626 g, the yield of 2, 4-dinitrophenylhydrazone was 0.829 g; the theoretical yield is 0.829** g and therefore the mixture contained 67.2% of the ketone.

The melting point of the 2,4-dinitrophenylhydrazone after recrystallization from absolute alcohol was 142.5° (the melting point of the pure compound is 143°).

---

* Transliteration of Russian — Publisher's note.

** As in original — Publisher's note.

Therefore the 98-103° fraction consisted of a mixture of vinyl ether (15.85%) and methyl propyl ketone (67.2%).

The residue was distilled under vacuum, and the following fractions were isolated:

fraction b.p. $_{3-5}$ 120-150°, 3.0 g, $n_D^{20} = 1.4702$, bromine number 61.90 M = 234.2;

fraction b.p. 190-200°, 4.0g, $n_D^{20} = 1.4840$, bromine number 49.0 M = 130.2.

Experiment II. 20 g of the methyl ether and about 1 g of copper dust was put into the autoclave. The experiment was carried out at 200-220° under a pressure of 20-25 atmos; the heating time was 4 hours.

1.2 liters of gas containing 16% unsaturated compounds was collected, and 0.5 g of amylene was condensed.

Fractionation of the catalyzate:

fraction 80–90°–1g, $n_D^{20} = 1.3800$

fraction 95–105°–6.5 g, $n_D^{20} = 1.3905$;

bromine number 29.9–26.1, M = 88.1 and 84.9.

fraction 105–120°–3 g, $n_D^{20} = 1.3990$;

fraction 120–140°–1.6 g. $n_D^{20} = 1.4240$.

The residue in the flask was distilled under vacuum:

Fraction b. p. 5 120—140° — 0.8 g, $n_D^{20} = 1.4690$;

Fraction b. p. 5 160—200° — 2 g, $n_D^{20} = 1.4915$, bromine number54.2, $M = 42.4$.

The total yield of reaction products was 15.4 g.

1.6 g of unchanged ether was isolated. The amount of ether converted was 92%.

Experiment III. 25 g of the ether was put into the autoclave. The temperature was 160-170°, pressure 10-12 atmos; the heating time was 4 hours.

The gas yield was 0.8 liter, containing 20% of unsaturated compounds.

Fractionation of the catalyzate:

Fraction 80—95° — 2.3 g, $n_D^{20} = 1.3895$;

Fraction 95—105° — 5.8 g, $n_D^{20} = 1.3950$,

after a second fractionation the bromine number was 68.03–76.3, M = 85.6 and 83.4:

Fraction 105—120° — 5 g, $n_D^{20} = 1.4020$;

Fraction 120—140° — 3.5 g, $n_D^{20} = 1.4190$.

The residue boiling above 140° was distilled under vacuum; the fraction of b.p.$_8$ 140-180° comprised 1.5 g, and the residue was 2 g; the total yield of reaction products was 20.1 g, 3.5 g of the unchanged ether was isolated; the ether was 86% converted, bromine number 74.5, M = 470.6.

Action of aluminum on the β-chloro ether. The autoclave walls were sprinkled with 2 g of aluminum dust. 20 g of the methyl ether was taken for the reaction. The experiment was performed at 280° and 20-25 atmos; the heating time was 4 hours.

When the autoclave was cooled, 1.8 liters of gas containing 18% of unsaturated compounds was collected. The liquid product was pale brown in color, and the bottom and walls of the autoclave were covered with a precipitate. The precipitate was collected and washed with ethyl ether. Cl' and Al were detected qualitatively in the precipitate.

Balance of the experiment: 20 g of the β-chloro ether was taken; 1.8 liters of gas was obtained and 1 g of amylene condensed.

Fractionation of the reaction product:

Fraction 80—100° — 2 g, $n_D^{20} = 1.3990$;

Fraction 100—120° — 8 g, $n_D^{20} = 1.4008$;

Fraction 120—140° — 1.5 g, $n_D^{20} = 1.4260$.

The residue was fractionated under vacuum, and the following fractions were isolated:

Fraction b. p. $_5$ 140—160° — 2 g, $n_D^{20} = 1.4890$, $M = 253.9$;

Fraction b. p. $_5$ 160—210° — 2.5 g, $n_D^{20} = 1.4920$, $M = 357.2$.

The total yield of reaction products was 17 g. 1.5 g of unchanged ether was isolated; the ether was 92% converted.

After a second fractionation the 98-103° fraction was isolated; it had the following characteristics: $n_D^{20} = 1.3905$, bromine number 74.15, unsaturated compounds 41.65%, M = 89.1 and 90.9.

Experiment II. 25 g of the methyl ether was taken for the reaction. The temperature was 200-220°, pressure 15-10 atmos; the heating time was 4 hours.

0.8 liter of gas was obtained; the content of unsaturated compounds was 15%.

Fractionation of the liquid reaction product:

Fraction 80—100° — 2 g, $n_D^{20} = 1.3990$;

Fraction 100—110° — 6 g, $n_D^{20} = 1.4030$;

Fraction 110—120° — 1.8 g, $n_D^{20} = 1.4090$;

Fraction 120—140° — 4.1 g, $n_D^{20} = 1.4230$.

The residue was fractionated under vacuum, and the following fractions were isolated:

Fraction number b. p. $_5$ 75—120° — 2 r, $n_D^{20} = 1.4370$, bromine number 103.8, $M = 261.3$;

Fraction number b. p. $_5$ 120—160° — 3 r, $n_D^{20} = 1.4860$, bromine number 55.2, $M = 288.2$;

Fraction number b. p. $_5$ 160—200° — 3.5 r, $n_D^{20} = 1.4920$, bromine number 52.0, $M = 452.5$.

The total yield of reaction products was 22.4 g; the ether was 83.6% converted.

A second fractionation yielded a fraction boiling at 98-105°, with the following characteristics: $n_D^{20} = 1.3995$, bromine number 96.4, unsaturated compounds 58.9%, M = 97.8.

Experiment III. 25 g of the ether was taken. The experiment was carried out at 170-180° and 10 atmos.

6.2 g of the unchanged ether was isolated. The conversion was 75%.

Action of metallic magnesium on the β-chloro ether. Experiment I. 25 g of the ether and 6 g of magnesium shavings was put into the autoclave. The experiment was performed at 280° and 25-30 atmos; the heating time was 4 hours.

When the autoclave was opened, its walls and socket were found to be coated with a precipitate in which Cl' and Mg were detected qualitatively.

The gas yield was 2 liters, containing 28% of unsaturated compounds; 1.8 g of amylene was condensed in the coil.

Fractionation of the reaction product:

Fraction 80—120° — 8 g, $n_D^{20} = 1.3990$;
Fraction 120—135° — 3.5 g, $n_D^{20} = 1.4240$.

Fractionation of the ether extract:

Fraction 80—90° — 1 g, $n_D^{20} = 1.3680$;
Fraction 90—115° — 1 g, $n_D^{20} = 1.3995$;
Fraction 115—130° — 1.5 g, $n_D^{20} = 1.4180$.

Vacuum distillation of the residue:

Fraction b. p. $_2$ 75—100° — 1 g, $n_D^{20} = 1.4610$, bromine number 114.9, $M = 182.3$;
Fraction b. p. $_2$ 100—140° — 1 g, $n_D^{20} = 1.4810$, bromine number 69.6, $M = 271.9$;
Fraction b. p. $_2$ 140—180° — 2 g, $n_D^{20} = 1.5020$, bromine number 48.62, $M = 474.5$.

The total yield of reaction products was 20.8 g, the amount of unchanged ether isolated was 3.5 g + 1.5 g = = 5 g; the conversion was 80%.

Experiment II. 25 g of the ether and 6 g of magnesium shavings was taken. The temperature was 180-200°, and the pressure, 18 atmos; the heating time was 4 hours.

1 liter of gas containing 24% of unsaturated compounds was obtained; about 0.8 g of amylene was condensed.

Fractionation of the reaction product:

Fraction 80—95° — 2 g, $n_D^{20} = 1.3906$;
Fraction 95—120° — 4 g, $n_D^{20} = 1.3995$;
Fraction 120—140° — 4 g, $n_D^{20} = 1.4235$.

Ether extract:

95—120° — 1 g, $n_D^{20} = 1.3940$;
120—145° — 2 g, $n_D^{20} = 1.4225$.

Vacuum distillation of the residue:

Fraction b. p. $_2$ 120—140° — 0.8 g, $n_D^{20} = 1.4850$;
Fraction b. p. $_2$ 140—160° — 2 g, $n_D^{20} = 1.4980$.
residue in column 2g

The total yield of the reaction products was 18.6 g; 6 g of unchanged ether was isolated, the conversion being 76%.

Experiment III. 25 g of the ether was taken. The temperature was 180°, pressure 5-7 atmos; heating time 4 hours. 7 g of unchanged ether was isolated; the conversion was 72%.

SUMMARY

1. In a study of the conversion of β-chloro ethers in presence of various metals it was shown that β-chloro ethers, which are stable under normal conditions, readily undergo conversion under harsh conditions (high temperatures and pressures).

2. It has been shown for the first time that when β-chloro ethers are heated with metallic sodium they are decomposed with formation of hydrogen chloride, olefins, and the corresponding alcoholates. A reaction mechanism for the decomposition of β-chloro ethers is postulated.

3. It was shown that when β-chloro ethers are heated in presence of finely-divided copper, aluminum, or magnesium shavings, hydrogen chloride is split off and vinyl ethers are formed. The reaction is most vigorous in presence of copper. The vinyl ethers are converted into ketones under the action of the metal chlorides formed; magnesium chloride is more active in this conversion than chlorides of other metals.

LITERATURE CITED

[1] V. I. Isaguliants and I. S. Maksimova, Proc. Acad. Sci. Armenian SSR 20, 4 (1955); J. Appl. Chem. 30, 5, 775 (1957). •

[2] P. P. Shorygin, Selected Works [In Russian] (Izd. AN SSSR, (1950)), pp. 204-212.

[3] N. I. Matusevich, J. Gen. Chem. 13, 1913 (1937).

[4] German Patent 274, 208 (1913).

[5] U. S. Patent 1,376,665 (1921).

[6] M. F. Shostakovskii, Vinyl Ethers [In Russian] (Izd. AN SSSR, (1952)).

[7] M. F. Shostakovskii, Bull. Acad. Sci. USSR 6, 1056 (1953).

[8] D. A. Pospekhov and N. M. Atamanenko, J. Gen. Chem. 7, 1319 (1948).

[9] V. D. Azatian, Proc. Acad. Sci. USSR 5, 901 (1948).

Received February 15, 1956

• Original Russian pagination. See C. B. Translation.

THE PRINCIPLES OF HEXACHLOROCYCLOPENTADIENE TECHNOLOGY

L. M. Kogan and N. M. Burmakin

Scientific Research Institute of Fertilizers and Insectofungicides

Hexachlorocyclopentadiene (C_5Cl_6) is a cyclic chlorinated hydrocarbon containing two mobile chlorine atoms and a system of conjugated double bonds in the molecule. These characteristics determine the great diversity of the chemical reactions of this compound. C_5Cl_6 is used as a starting material in the production of a number of new insecticides [1], and in the future it is likely to be used in the production of incombustible plastics [2, 3], and for other purposes.

The most important of the methods for preparation of C_5Cl_6 is based on the reactions of polychloropentanes with chlorine. According to the data in the paper by McBee and Baranauckas [4], and also their patent [5], polychloropentanes and chlorine are passed through a hollow tube at 470° and normal pressure*. The yield of C_5Cl_6 is about 50%. A large amount of by-products is formed together with C_5Cl_6. The velocity of the polychloropentanes and chlorine, and other process conditions, are given in the paper [4]. In another patent [6] it is stated that the chlorination products of pentane are passed through a tube partially filled with a substance of large surface area. The temperature in the reaction tube is kept between 350 and 500°. The yield of C_5Cl_6 exceeds 86%.

In the investigation carried out by McBee and Baranauckas the production of C_5Cl_6 is regarded as a single process.

The aim of the present investigation was to choose the main directions of a technological study of the production of C_5Cl_6. The choice was based on thermodynamic analysis of the constituent reactions of the process, followed by experimental vertification of the chosen directions. Kinetic relationships are not considered here.

It was found experimentally [7] that the conversion of polychloropentanes into C_5Cl_6 consists of five consecutive reactions, with intermediate formation of decachloropentanes, nonachloropentanes, octachloropentadiene-1, 3, and octachlorocyclopentene, as follows:

$$C_5H_6Cl_6 + 4Cl_2 \rightarrow C_5H_2Cl_{10} + 4HCl, \quad \text{(a)}$$

$$C_5H_2Cl_{10} \rightarrow C_5HCl_9 + HCl, \quad \text{(b)}$$

$$C_5HCl_9 \rightarrow C_5Cl_8 + HCl, \quad \text{(c)}$$

$$CCl_2{=}CCl{-}CCl{=}CCl{-}CCl_3 \rightarrow$$ 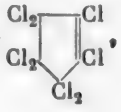 (d)

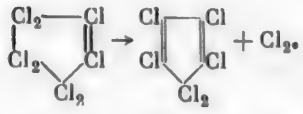 (e)

*Polychloropentanes are prepared by liquid-phase chlorination of pentane – amylene mixtures.

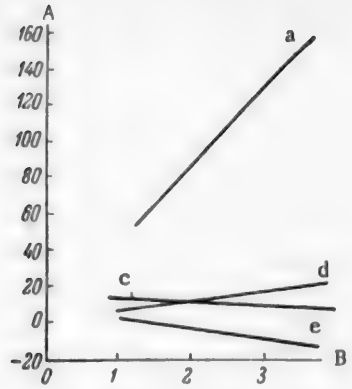

Fig. 1. Effect of reciprocal temperature on the equilibrium constants of reactions taking place in the interaction of polychloropentanes with chlorine (from approximate thermodynamic calculations).
A) In K_c, B)$(1 / T) \cdot 10^3$.

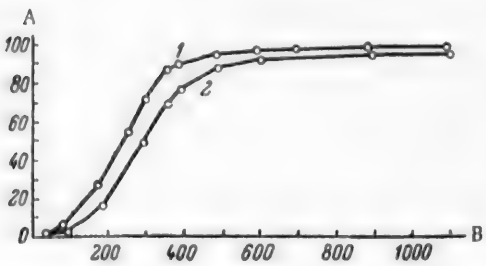

Fig. 2. Effect of temperature on the equilibrium yield of hexachlorocyclopentadiene from octachlorocyclopentene.
A) Yield (%), B) temperature (°C). 1) System diluted with HCl, 2) without dilution.

In addition to the compounds indicated above, decomposition products are obtained: CCl_4, C_2Cl_4 and C_4Cl_6, and also cyclo-C_6Cl_6 formed in the course of secondary processes, and small amounts of other compounds of undetermined composition. The reaction system in question is therefore a complex chemical system, and exact thermodynamic calculations cannot be carried out at present. Our thermodynamic calculations were carried out by the method of Hougen and Watson [8]. The numerical thermodynamic data were taken from the books by Karapet'iants [9], Vvedenskii [10], and Korobov and Frost [11]. The results of the calculations are plotted in Fig. 1. The following conclusions may be drawn from these data.

1) The production of C_5Cl_6 from polychloropentanes and chlorine cannot be regarded in technological investigations as a single process, as the constituent reactions are very different in the thermodynamic respect.

2) Of the five reactions in the process, four are irreversible and may be carried out at any positive temperature, while the last reaction is a reversible process over a wide range of temperatures.

3) The determining step of the multistage process is the final reaction, dechlorination of cyclo-C_5Cl_8.

By-products are formed from molecules with open carbon chains. Since this process is intensified with increase of temperature, a practical consequence of the thermodynamic analysis is the possibility of carrying out Reactions (a), (b), (c), and (d) in one zone, and of lowering the temperature of this zone as much as possible. The decrease of the reaction rates can be compensated by the use of catalysts. On the other hand, for Reaction (e) the temperature must be raised, and adequately complete dechlorination cannot be combined successfully with the first four reactions. Reaction (e) must be completed in another zone. In view of the favorable influence of HCl, as a diluent, on Reaction (e), it is convenient to direct the reaction products from Zone I into Zone II, so that the whole process can be effected in the same reactor.

We calculated the equilibrium yields for Reaction (e) in the 25-1100° temperature range. The results are plotted in Fig. 2. The assumptions made in the calculation should be taken into account in the use of these data. It follows from the thermodynamic analysis that Reaction (e) can be effected most completely if the temperature in Zone II is raised, the process is carried out in a stream of inert gas, and cyclo-C_5Cl_8 is introduced into the system. Experiments to test these directions for investigation of the formation of C_5Cl_6 from polychloropentanes and chlorine were carried out in a flow unit, in a quartz tube 20 mm in diameter. The starting materials were hexachloropentanes, and chlorine from a cylinder. Details of the starting materials, apparatus, experimental procedure, and analytical methods are given in an earlier paper [7]. The reaction between polychloropentanes and chlorine was effected over a catalyst — infusorial earth — at 350°. The results of these experiments are presented in Table 1 and Figs. 3-6. The following notation is used: α is the degree of total conversion of polychloropentanes (determined from the amount of HCl formed); α_u is the degree of useful conversion of polychloropentanes (aggregate yield of C_5Cl_6 and intermediates); γ is the degree of cyclization of C_5Cl_8, equal to (C_5Cl_6 + cyclo-C_5Cl_8: α_u); β is the degree of dechlorination of cyclo-C_5Cl_8, equal to C_5Cl_6 (C_5Cl_6 + cyclo-C_5Cl_8); C_5Cl_6: α_u is the degree of completion of the process; α_u: α is the selectivity.

The following conclusions may be drawn from these results: C_5Cl_6 can be successfully prepared if the reaction temperature is lowered to 350° and a catalyst is used; the selectivity of the process is high, 80-95%

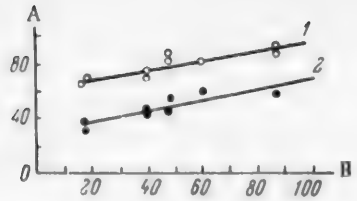

Fig. 3. Effect of the length of the contact zone on the total degree of conversion of polychloropentanes (α) and on the yield of hexachlorocyclopentadiene.
A) Degree of conversion α (1), and yield of hexachlorocyclopentadiene (2) (in %), B) length of the contact zone (cm).

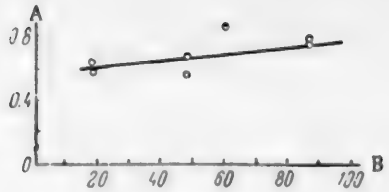

Fig. 4. Effect of the length of the contact zone on the degree of completion of polychloropentane conversion (temperature 350°).
A) Extent of conversion, C_5Cl_6: α_u, B) length of the contact zone (cm).

TABLE 1

Results of Experiments on the Production of Hexachlorocyclopentadiene from Polychloropentanes and Chlorine at 350° in Presence of Infusorial Earth Polychloropentane feed rate 1.00-1.14 g/minute, chlorine in 35.50% excess. Catalyst – infusorial earth (sample No.1)

Expt. No.	Length of contact zone (mm)	α	Yield %				γ	β	$\frac{C_5Cl_6}{\alpha_u}$	$\frac{\alpha_u}{\alpha}$
			C_5Cl_6	C_5Cl_8	cyclo-C_5Cl_8	α_u				
61	180	68	32	15	8	55	73	80	58	81
62	180	68	38	14	12	64	78	76	59	94
64	480	87	45	17	17	79	70	73	58	90
65	480	83	54	12	13	79	85	81	69	95
50	870	87	56	5	11	72	93	83	78	83
72	870	93	59	2	10	71	97	85	83	77

rather than 50% as is reported in the literature [4]; increase of the contact time favors the course of all the irreversible reactions and has no effect on Reaction (e). The yield in this last reaction corresponds to the calculated equilibrium value.

The results of experiments on the effect of temperature in Zone II on the interaction of polychloropentanes with chlorine are presented in Table 2 and Fig. 7.

It follows from these results that Reaction (e) is more complete with increase of the temperature of Zone II. Appreciable amounts of cyclo-C_5Cl_6 begin to be formed at 450°.

For confirmation of the favorable effect of an inert gas, experiments were carried out on dechlorination of cyclo-C_5Cl_8 and on the interaction of polychloropentanes with chlorine in presence and in absence of nitrogen.

The results of these experiments are presented in Table 3 and Fig. 8.

The following conclusions may be drawn from these data: 1) introduction of an inert gas into the system results in a sharp shift of equilibrium in Reaction (e); 2) the effect produced by a given amount of nitrogen is greater with polychloropentanes than with cyclo-C_5Cl_8. For an equal dechlorination effect, more nitrogen must be used in the second case than in the first. This is due to the liberation of HCl if polychloropentanes are used; this has the same significance as nitrogen in Reaction (e).

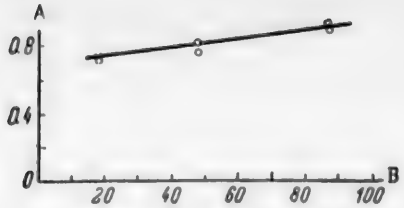

Fig. 5. Effect of the length of the contact zone on the degree of cyclization of octachloropentadiene in the conversion of polychloropentanes (temperature 350°).
A) Degree of cyclization γ, B) length of contact zone (cm).

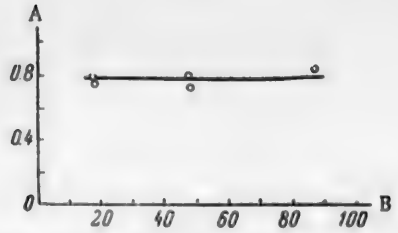

Fig. 6. Effect of the length of the contact zone on the degree of dechlorination of octachlorocyclopentene in the conversion of polychloropentanes (temperature 350°).
A) Degree of dechlorination β, B) length of contact zone (cm).

TABLE 2

Effect of the Temperature in Reaction Zone II on the Interaction of Polychloropentanes with Chlorine in Presence of Infusorial Earth. Polychloropentane feed rate 1.05-1.11 g/minute, chlorine in 17-29% excess. Zone I: t = 350°, l_1 = 620 mm. Zone II: l_2 = 250 mm. Catalyst — infusorial earth (sample No. 2)

Expt. No.	Temperature of Zone II (°C)	α	Yield (%)				β	γ
			C_5Cl_8	C_5Cl_6	cyclo-C_5Cl_8	α_u		
93	350	84	42	12	26	80	62	85
109	350	82	42	8	23	72	65	77
111	400	89	55	8	17	80	77	90
112	400	87	50	12	19	81	73	85
115	450	92	58	4	6	68	91	94
116	450	89	57	7	11	74	84	92

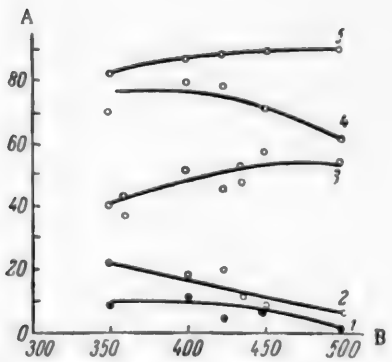

Fig. 7. Effect of the temperature in reaction-zone II on the catalytic conversion of polychloropentanes.
A) Yield (%), B) temperature (°C). Curves: 1) C_5Cl_8, 2) cyclo-C_5Cl_8, 3) C_5Cl_6, 4) α_u, 5) α.

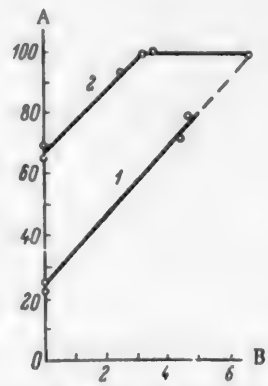

Fig. 8. Effect of nitrogen on the degree of dechlorination (β) of octachlorocyclopentadiene, taken separately and in the course of its formation from polychloropentanes.
A) Degree of dechlorination β (%), B) amount of nitrogen (in moles/mole C_5), Curves: 1) cyclo-C_5Cl_8, 2) polychloropentanes.

TABLE 3

Effect of Nitrogen on Chlorination of Octachlorocyclopentene and on the Reaction of Polychloropentanes (PCP) with Chlorine

Experiment No.	Nitrogen feed rate (moles/ mole C_5)	α*	Yield (%)			
			C_5Cl_6	C_5Cl_8	cyclo-C_5Cl_8	α_u**
Dechlorination of octachlorocyclopentene						
t= 400°, l = 870 mm; feed rate of cyclo-C_5Cl_8 1.29 - 1.38 g/ minute						
99	0	–	22	–	66	88
129	0	–	20	–	70	90
96	4.5	–	56	–	22	78
97	4.7	–	63	–	17	80
Interaction of polychloropentanes with chlorine						
t_1 = 350°, l_1 = 620 mm; t_2 = 425°, l_2 = 250 mm; PCP feed rate 1.06-1.18 g/ minute; chlorine in 8-20% excess						
114	0	91	39	3	21	63
113	0	89	45	3	20	68
121	2.5	86	52	6	3	61
120	3.6	80	58	8	0	66
119	6.7	72	54	4	0	58

* The decrease of α with increase of the amount of nitrogen is due to decrease of the contact time.

** The decrease of α_u is due to less efficient condensation of the reaction products.

TABLE 4

Effect of Octachlorocyclopentene on the Interaction of Polychloropentanes and Polychlorocyclopentanes with Chlorine in Presence of Infusorial Earth. Reduced feed rate of C_5 = 0.8-1.1 g/ minute, chlorine in 20-40% excess. Zone I: t = 350°, l = 620 mm. Zone II: t= 425°, l = 250mm. Catalyst – infusorial earth (sample No.2)

Experiment No.	Content of cyclo-C_5Cl_8 in mixture (%)	α	Yield (%)				β	β_1
			C_5Cl_6	C_5Cl_8	cyclo-C_5Cl_8	α_u		
Polychloropentanes								
113	0	89	45	3	20	68	70	–
114	0	91	39	3	21	63	65	–
124	20	90	71	10	2	83	75	–9
125	20	88	71	12	0	83	78	+9
Polychlorocyclopentanes								
231*	0	88	44	0	43	84	50	–
232*	0	86	44	0	40	84	53	–
311	25	90	89	0	0	89	80	+3
312	25	87	89	0	0	89	77	–10

* t_2 = 380°.

Since the process of C_5Cl_6 production is determined by Reaction (e), the origin of the cyclo-C_5Cl_8 is immaterial. Therefore in experiments on the influence of cyclo-C_5Cl_8 on the yield of C_5Cl_6 the action of chlorine on open-chain and cyclic polychloropentanes was studied. The polychlorocyclopentanes were made by liquid-phase chlorination of cyclopentadiene. The mixture of polychlorocyclopentanes had the following constants: $n_D^{20} = 1.5630$, $d_4^{20} = 1.5904$. The results of the experiments are presented in Table 4. Here β_1 represents the degree of dechlorination of the cyclo-C_5Cl_8 introduced into the process.

These results show that: 1) the total degree of dechlorination of cyclo-C_5Cl_8 (made from polychloropentanes or polychlorocyclopentanes and introduced from outside) under isothermal conditions is independent of the amount of cyclo-C_5Cl_8 introduced, and is at the level of 70-80%; 2) by introduction of cyclo-C_5Cl_8 into the process the yield of C_5Cl_6 from polychloropentanes can be increased from 45 to 70%, and it is possible to select conditions in which the added cyclo-C_5H_8 is not dechlorinated and can be recycled; 3) introduction of cyclo-C_5Cl_8 also has a favorable effect on the conversion of polychlorocyclopentanes. The yield of C_5Cl_6 then reaches 90%.

SUMMARY

1. Thermodynamic calculations relating to the reactions which take place when polychloropentanes interact with chlorine have shown that Reactions (a), (b), (c), and (d) are irreversible and can be carried out at any positive temperature, while Reaction (e), dechlorination of octachlorocyclopentene, is reversible and is determining for the process as a whole.

2. The reaction space should be divided into two zones. The irreversible reactions should take place in Zone I, at the lowest possible temperature which is determined by the catalyst choosen, and partial dechlorination of octachlorocyclopentene should also take place in that zone. The dechlorination of octachlorocyclopentene should be completed in Zone II.

3. The conclusions drawn from thermodynamic calculations concerning the direction of investigations designed to obtain the maximum yield of hexachlorocyclopentadiene were confirmed experimentally. These directions are: decrease of the temperature in Zone I and increase of the temperature in Zone II, introduction of an inert gas, and recirculation of octachlorocyclopentene. The yield of hexachlorocyclopentadiene was then 70%. These means are applicable to the successful production of hexachlorocyclopentadiene from polychlorocyclopentanes. A yield of 90% was obtained in this instance.

The authors express their deep gratitude to R. M. Flid for aid in the calculations.

LITERATURE CITED

[1] R. Riemschneider, Chem. et Ind. 64, 695 (1950); British Patent 614,931; C. A. 43, 4693 (1949); H. Bluestone, R. E. Lidov, I. H. Knaus, and P. W. A. Hoverston, U. S. Patent 2,576,666 (1951); C. A. 46, 6316 (1952).

[2] P. Robitshek and C. T. Bean, Ind. Eng. Ch. 46, 1628 (1954).

[3] W. A. Reeves and J. D. Guthrie, Ind. Eng. Ch. 48, 64 (1956).

[4] E. T. McBee and C. F. Baranauckas, Ind. Eng. Ch. 41, 806 (1949).

[5] E. T. McBee and C. F. Baranauckas, U. S. Patent 2,509,160 (1950); C. A. 44, 7871 (1950).

[6] A. H. Maude and D. S. Rosenberg, U. S. Patent 2,650,942 (1953); C. A. 48, 10066 (1954); British Patent 735,025 (1955); C. A., 49, 14027 (1955).

[7] L. M. Kogan, N. M. Burmakin and N. V. Cherniak, J. Gen. Chem. 28, 27 (1958).*

[8] O. Hougen and K. Watson, Chemical Process Principles, I-II (1948).

[9] M. Kh. Karapet'iants, Chemical Thermodynamics [In Russian] (Moscow, Goskhimizdat, (1953)).

[10] A. A. Vvedenskii, Thermodynamic Calculations in Processes of the Fuel Industry [In Russian] (Leningrad, State Fuel Tech. Press, (1949)).

*Original Russian pagination. See C. B. Translation.

[11] V. V. Korobov and A. V. Frost, Free Energies of Organic Compounds [In Russian] (Moscow Section of the Mendeleev All-Union Chem. Soc., (1950)).

Received March 12, 1957

LARGE UNIT FOR HYDROGEN FLUORIDE POLYMERIZATION OF TERPENES FROM OLEORESIN AND STUMP TURPENTINES, "BENZENE HEAD" CYCLOPENTADIENE, AND UNSATURATED COMPOUNDS FROM CRUDE BENZENE

V. G. Pliusnin, E. P. Babin, and S. I. Chertkova

Ural Branch, Academy of Sciences USSR

Investigations of the polymerization of turpentine terpenes [1, 2] and of cyclopentadiene from the "benzene head" and obtained by purification of crude benzene [3] have shown that the same technological scheme can be used for all these processes.

For determination of the technological data needed for the design of an industrial unit, and for the preparation of sufficient amounts of polyterpene, polycyclopentadiene, and cyclopentadiene–indene–coumarone-styrene resins for industrial trials, a large unit with an output of 20 liters per hour was constructed; this is shown schematically in the diagram.

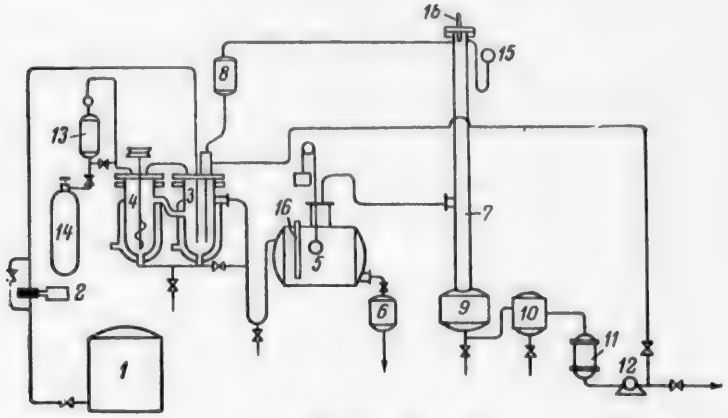

Flow sheet of large unit.

Description of the unit. The raw material is fed into the bottom part of the settler-reactor 3 from the tank 1 by means of the pump 2. Owing to the suction exerted by the screw stirrer in reactor 4, the raw material together with the settled catalyst passes along the lower pipe from the settler–reactor 3 into the reactor 4, where it is vigorously stirred, and is then returned along the upper pipe into the middle part of the settler–reactor 3.

The hydrogen fluoride carried over with the polymer is separated from the latter in the settler–reactor 3. The polymer overflows through the upper outlet and a bend into the still 5. As the catalyzate enters the still 5, the fluorides are continuously decomposed, and hydrogen fluoride and unpolymerized hydrocarbons are distilled off.

The polymer level and temperature in the still can be varied at will, so that conditions may be selected for complete separation of hydrogen fluoride and unpolymerized hydrocarbons.

The finished polymer is withdrawn from the system into a receiver from the still 5 through the condenser 6. Hydrogen fluoride and unpolymerized hydrocarbon vapor pass through the head of the still 5 into the middle portion of the rectification column 7. The unpolymerized hydrocarbon vapor is separated from hydrogen fluoride in the column 7. The hydrogen fluoride is withdrawn from the top of the column and enters the condenser 8, from which it flows by gravity into the middle portion of the settler–reactor 3. The unpolymerizaed hydrocarbons and aqueous hydrogen fluoride are collected in the heated evaporator 9, maintained at a constant level and temperature ensuring boiling of the liquid in the evaporator. From the evaporator 9 the unpolymerized hydrocarbons and aqueous hydrogen fluoride pass into the settler 10. Aqueous hydrogen fluoride is removed through a valve from the lower part of the settler 10, and unpolymerized hydrocarbons are removed at the top, through the condenser 11. A part of the unpolymerized hydrocarbons can be pumped back by means of the pump 12 into the settler–reactor to dilute the catalyzate.

The design of the unit provides for continuous recovery of the catalyst. However, it is possible to recover the catalyst completely in the system, as part of it leaves the system in the form of aqueous hydrogen fluoride. The amount of aqueous hydrogen fluoride depends on the moisture content of the raw material. To make up the loss of hydrogen chloride, a measuring vessel 13 is provided for fresh catalyst, which is supplied from a cylinder 14 containing hydrogen fluoride.

Description of the individual components. The reactors are water-jacketed vessels of equal capacity (19 liters each). The reactor bodies are made from ordinary gas cylinders of internal diameter 205 mm and total height 600 mm. The overflow pipes are at a height of 450 mm. Thus, the working volume of each reactor is 12 liters, and the cooling surface is 0.283 m^2. One of the reactors is provided with a screw stirrer of 2.5 turns. This type of stirrer ensures not only stirring, but also circulation of the liquid in the two communicating reactors. The stirrer rotates at 350 revolutions per minute.

The still for decomposition of fluorides, and distillation of hydrogen fluoride and unpolymerized hydrocarbons is made from 6 mm iron. The diameter of the still is 500 mm, the length is 600 mm, and the capacity is 600 liters. The still is situated in the casing of a sectional electric heater. The sections are placed under the cylindrical portion of the still. The maximum heating area of the still is 0.4 m^2, or about one half of the cylindrical portion.

The column is an ordinary iron tube 75 mm in internal diameter and 2 meters high, packed with rings made from iron wire 2.5 mm in diameter, the external ring diameter being 20 mm. The column, fitted at the top with a manometer 15 and thermometer 16, is placed on an evaporator 20 liters in capacity. The evaporator is enclosed in the casing of an electric heater.

None of the other components of the unit is of any special significance, and a description is not necessary.

Principal operating characteristics of the large unit. In the experiments on polymerization of turpentine terpenes and "benzene head" cyclopentadiene, the purpose was to determine the principal operational characteristics of the equipment for the given process. The parts of the equipment significant in this respect are the reactors and the still for decomposition of organic fluorine compounds. The following are the main operational characteristics of these components: 1) productivity per unit cooling area of the reactors, in terms of unsaturated compounds; 2) the residence time of the raw material in the reactors, or, in other words, the time of contact between the raw material and the catalyst; 3) the time during which the polymers remain in the still for decomposition of the organic fluorine compounds at different temperatures.

The principal operating characteristics of the equipment in one of the experiments are given below. In this experiment 5 kg of hydrogen fluoride was introduced into the reactor per 245 kg of raw material. The hydrogen fluoride balance was not calculated in this experiment, but it should be noted that at the end of the experiment the polymerization of unsaturated hydrocarbons was complete, the same as at the start of the experiment. The productivity of the unit was constant at 19.5 kg of turpentine or "benzene head" per hour. The characteristics of the raw materials are given below.

Characteristics of the raw materials

Raw material	d_4^{20}	n_D^{20}	Iodine number
Stump turpentine	0.8754	1.4765	269
"Benzene head" from Gubakha works	0.8925	1.4822	162

In the polymerization of turpentine, about 14 kg of unpolymerized hydrocarbons (gasoline) was introduced into the reactors to serve as polymer solvent and was circulated in the system. The pressure in the system was 2-2.5 atmos, the reactor temperature was 35-40°, and the temperature in the still was maintained at about 220-230°.

Under these conditions very viscous polymers were obtained, the yields being ~90% from turpentine, and ~48% from "benzene head." The characteristics of "benzene head" polymers and unpolymerized hydrocarbons are given below.

Polymer characteristics

Polymer	Yield (% on raw material)	d_4^{20}	n_D^{20}	Iodine number	Fluorine content (%)
Polymer from terpenes	90.6	0.9464	1.5330	117.8	–
Polymer from cyclopentadiene	47.5	0.9883	1.5385	102.0	0.027
Unpolymerized "benzene head" polymers	50.0	0.8965	1.4975	2.4	–

Vacuum distillation under a residual pressure of 8 mm Hg yielded 37.8% (by weight on the raw material) of a solid polyterpene of melting point 71°, and 43.5% of solid polycyclopentadiene of melting point 68°; these did not differ in any respect from the polymers prepared earlier [1, 2]. Hydrogen fluoride was not liberated under vacuum. Thus, almost completely defluorinated terpene and cyclopentadiene polymers, and "benzene head" free from unsaturated hydrocarbons were obtained.

The principal characteristics of the main components of the unit are as follows.

Productivity per 1 m^2 of reactor cooling surface:

$$\frac{19.5}{0.283 \cdot 2} = 34.5 \text{ kg/hour} \cdot m^2 \text{ on the raw material,}$$

$$\frac{19.5 \cdot 0.475}{0.284 \cdot 2} = 16.3 \text{ kg/hour} \cdot m^2 \text{ on unsaturated compounds.}$$

The pressure in the system, during the steady process, was at a level of 2-2.5 atmos, and the reactor temperature was 35-40°. It was found that the pressure in the system depends entirely in the temperature in the reactors. Therefore the polymerization may be carried out at lower pressures if the productivity is lowered or if the cooling surface of the reactors is increased. In fact, when the productivity was lowered from 19.5 kg/hour to 13.5 kg/hour (on the raw material), the pressure in the system fell to 1.2-1.5 atmos, and the temperature fell to 28-33°.

Up to 100°, the polymerization temperature has no significant effect on polymer quality. However, since the pressure in the system increases with increasing temperature in the reactors, in order to raise the productivity per unit volume of reactor it is expedient to increase the cooling area. For calculations of the cooling area of the reactor, for a reactor temperature of 35-40°, the above-mentioned value of 16.3 kg of unsaturated hydrocarbons per hour per 1 m^2 cooling area may be used, or the calculations may be based on the heat of polymerization, which is approximately 170 kcal per 1 kg of cyclopentadiene*.

* Determined from the heats of combustion of cyclopentadiene and the solid polymer.

The residence time of the raw material in the reactor, or, which is the same thing, the contact time, is a quantity necessary for calculation of the reactor volume. In the present instance, with the raw-feed pump and circulation pump operating at 19.5 kg/hour and 14 kg/hour respectively, the contact time was

$$\frac{12.2 \cdot 0.89}{19.5 + 14} = 0.64 \text{ hour}$$

It was noted earlier that polymerization of unsaturated hydrocarbons was complete in this instance. Therefore a contact time of 0.64 hour is quite sufficient for completion of the polymerization reaction. It must be pointed out that it was not determined whether a contact time of 0.64 hour is the minimum time required to ensure complete polymerization of the unsaturated hydrocarbons.

The residence time of the polymer in the still at a given temperature determines the extent of fluoride decomposition on the one hand, and the extent of removal of unpolymerized hydrocarbons and other organic compounds present in turpentine and "benzene head" on the other. In the experiment under consideration, the temperature in the still was kept constant at about 220°. 33.5 kg of liquid per hour entered the still, including 10.5 kg of polymers per hour. The volume of liquid in the still was on the average 65% of the still capacity, i.e.

$$102 \cdot 0.65 = 65 \text{ liters}$$

Therefore the residence time of the polymer in the still was

$$\frac{65 \cdot 0.9883}{10.5} = 6.2 \text{ hours}$$

In a test of the extent of fluoride decomposition it was found that at 220° the liberation of hydrogen fluoride ceases after about 3 hours of heating. Therefore total decomposition of fluorides can be effected in a still of about half the capacity.

It has been shown [2] that the fluoride-decomposition time depends on the temperature. The fluoride-decomposition time can be decreased still further at higher temperatures, but the temperature in the still should not be kept higher than 220°, because of the risk of overheating at the walls.

These calculations were made for "benzene head." Analogous calculations for turpentines give similar results. The polymers obtained in this experiment are not solids but highly viscous sirupy liquids.

In vacuum distillation of the polymers made in the unit, the yield of liquid polymers was only 8% in the case of "benzene head," 48.0% for oleoresin turpentine, and 52.0% for stump turpentine. The residual solid polymers melted at 68-70°. However, if the terpene and cyclopentadiene polymers are to be used in the rubber industry, the production of solid polymers is not necessary.

The polymers made in the unit are not inferior in quality to solid polymers, and for use at ordinary temperatures viscous polymers are more convenient than solid polymers.

Purification of crude benzene from the Gubakha works in the large unit under the same conditions (pressure and reactor temperature), but with modifications of the operating regime of the still and column and with removal of aromatic hydrocarbons from the system, made it possible to obtain cyclopentadiene–coumarone–styrene resins, and benzene, toluene, and xylene all free from unsaturated hydrocarbons. The yields were: resins 12%, benzene 44.5%, toluene 17.0%, and xylene 8.0%.

Experience with the large unit showed that its design may form the basis of the design of an industrial unit for the production of terpene, cyclopentadiene, and cyclopentadiene–indene–coumarone–styrene resins.

SUMMARY

1. A large unit has been designed for the hydrogen-fluoride polymerization of turpentine terpenes, and unsaturated hydrocarbons from "benzene head" and crude benzene; the principal characteristics of the main sections, necessary for design calculations relating to a large unit, have been determined.

2. The large unit, with an output of 19 liters/hour, can be successfully used for hydrogen-fluoride polymerization of turpentine terpenes and of unsaturated "benzene head" hydrocarbons, and for purification of crude benzene.

LITERATURE CITED

[1] V. G. Pliusnin, S. I. Chertkova and E. P. Babin, J. Appl. Chem. 29, 1265 (1956). *

[2] S. I. Chertkova, V. G. Pliusnin and E. P. Babin, J. Appl. Chem. 29, 7, 1865 (1956). *

[3] V. G. Pliusnin, E. P. Babin and S. I. Chertkova, J. Appl. Chem. 29, 1070 (1956). *

Received December 20, 1956

* Original Russian pagination. See C. B. Translation.

BRIEF COMMUNICATIONS

PREPARATION OF MAGNESIUM PEROXIDE

I. I. Vol'nov and E. I. Latysheva

Products known as "heavy," "semiheavy" and "light" magnesium peroxide are made in a number of countries; their main uses are in medicine for disinfection of the gastrointestinal tract, in hyperacidity, metabolic disturbances, diabetes, ketonuria, gas poisoning, and also in the production of antiseptic ointments, tooth pastes, and dusting powders [13].

It has been reported [4-6] that magnesia products based in MgO_2 can be used with success for disinfection of water under field conditions, for cotton bleaching, and in the rubber industry as vulcanization activators for synthetic rubber. All these products are mixtures of MgO_2, MgO, and $Mg(OH)_2$ with an admixture of $MgCO_3$, in which the MgO_2 content does not exceed 50 wt. %. For example, the products marketed in England [7] contain 25 wt. % MgO_2, and in the U. S. A., 15-50 wt. % MgO_2 [8]. Specifications for commercial magnesium peroxide of Russian manufacture are given in the literature [9].

The question of the existence of individual magnesium peroxides was studied by the present authors under the guidance of Prof. S. Z. Makarov [10]. Solubility studies for the system $Mg(OH_2) - H_2O_2 - H_2O$ at 0 and 20° showed that three compounds, of the composition MgO_2, $MgO_2 \cdot 0.5H_2O$ and $MgO_2 \cdot H_2O$, can exist in equilibrium with H_2O_2 solutions. However, no one has as yet prepared ~ 100% MgO_2. Under laboratory conditions, treatment of $Mg(OH)_2$ with a large excess of 80% H_2O_2 solution, with subsequent drying of the precipitate over P_2O_5 and KOH at room temperature, yields preparations containing ~ 80% MgO_2 by weight, i. e., approaching the composition $MgO_2 \cdot 0.5H_2O$.

The industrial process for production of MgO_2, based on the reaction of magnesium oxide with perhydrol, yields products containing not more than 25% MgO_2 by weight. The electrolytic process proposed by Hinz [11] is not used, while the method based on the interaction of magnesium salts with NH_4OH and H_2O_2 solutions yields very unstable precipitates of poor filterability, with low MgO_2 contents.

In contrast to the above-mentioned processes, the authors of this paper have developed, and tested under plant conditions, a method for the production of a magnesium peroxide preparation containing up to 65 wt. % MgO_2; the method is based on the interaction of magnesium hydroxide suspensions ("milk of magnesia") with H_2O_2 solutions.

EXPERIMENTAL

Our choice of the synthesis conditions for MgO_2 was based on data [12] according to which MgO catalyzes the decomposition of H_2O_2 solutions, and on the solubility isotherm at 20° for the system $Mg(OH)_2 - H_2O_2 - H_2O$ [10]. Preliminary experiments, in which dry MgO or badly slaked magnesia slurry was mixed with perhydrol at room temperature, showed that the reaction between these substances is accompanied by heat evolution and a temperature rise to 80°, and that the H_2O_2 is decomposed completely even when taken in 3-fold excess. No active oxygen is found in the paste. In the interaction of well-slaked MgO (80% moisture content) with perhydrol (in 3-fold excess), the temperature did not rise above 40°, and the paste contained approximately 7% of active oxygen by weight. If a suspension containing 2% $Mg(OH)_2$ by weight was used, the temperature did not rise appreciably above room temperature and H_2O_2 did not decompose even with a 36-fold excess of H_2O_2. The magnesia suspension was prepared by the slaking of previously sifted MgO, in the ratio $MgO : H_2O = 1 : 100$. To accelerate the slaking and the growth of $Mg(OH)_2$ particles, the suspension was heated to the boiling point at intervals. Analysis showed that under these conditions the MgO was completely slaked after 40 hours.

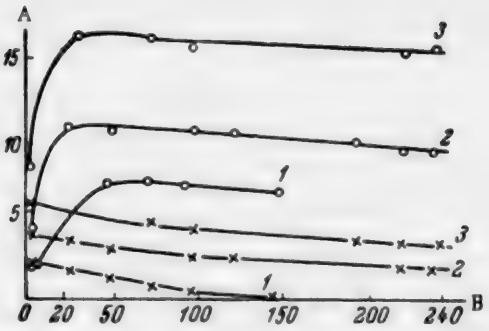

Fig. 1. Variations of the active-oxygen content of the liquid phase and the "residue" in the interaction of magnesium hydroxide suspension with perhydrol.
A) Active-oxygen content (wt. %), B) time (hours). Explanation in text.

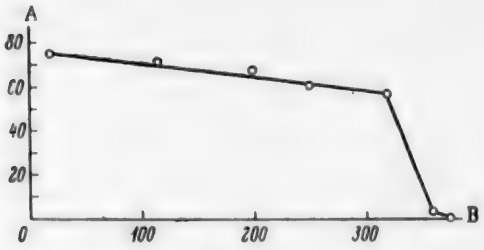

Fig. 2. Thermal decomposition of MgO_2.
A) MgO_2 content (%), B) temperature (°C).

In solubility studies of the system $Mg(OH)_2$–H_2O_2–H_2O in the region of the phase $MgO_2 \cdot 0.5\ H_2O$ the excess of H_2O_2 was roughly 150-fold over the calculated amount [10]. It was necessary to determine the most advantageous and lowest $Mg(OH)_2 : H_2O_2$ ratios for the production of a preparation containing over 25 wt. % of MgO_2 under conditions similar to those in the plant. These ratios were determined by means of numerous experiments in which definite and increasing amounts of perhydrol were added to a definite volume (1 liter) of a suspension containing 2 wt. % $Mg(OH)_2$; the variations of the contents of active oxygen in the liquid phase and "residue" were also studied. The most typical results are plotted in Fig. 1, where the crosses represent the active-oxygen content of the liquid phase (in wt. %), and the circles represent the active-oxygen content of the "residue" (in wt. %). In Fig. 1, Curves 1, 2, and 3 refer respectively to 3.6-fold, 14.4-fold, and 28.8-fold excess of H_2O_2. Consideration of this graph shows that the formation of a product containing over 25 wt. % of MgO_2 can be expected with certainty only if a 20 to 30-fold excess of H_2O_2 is used, as only then does the MgO_2 content of the "residue" exceed 40 wt. %. The graph also shows that equilibrium is reached after about 2 days. The active-oxygen content (H_2O_2 concentration) of the liquid phases, and the active-oxygen content of the "residues" remains almost constant for about 10 days; this shows that the product is stable. The precipitates prepared by this method, in contrast to precipitates formed by the reaction of MgO with perhydrol, or from magnesium salts and NH_4OH and H_2O_2 solutions, can be filtered off easily on cotton cloth. The filtrate contains a considerable amount of H_2O_2, and it can therefore be used in the production of successive batches of MgO_2. In the production of a preparation of a high MgO_2 content, a very important step is the drying of the "residues" made by the above method. According to our results, the drying should be performed at 60-70° under a residual pressure of 10 mm Hg, with a well-developed surface and with a layer height of 10 mm. Results obtained in the vacuum drying of a "residue" containing about 43 wt. % MgO_2, made by the action of a suspension containing 2 wt. % $Mg(OH)_2$ (1 liter) on perhydrol (800 ml), i.e., at the ratio of $Mg(OH)_2 : H_2O_2 = 1 : 28$, are given below:

Drying time (hours)	MgO_2 content (wt. %)	Weight loss (wt. %)
0	42.8	0
1	72.4	44.6
2	73.0	49.5
3	70.9	51.7
4	66.8	53.4
5	66.5	53.4

It is seen that the product reaches constant composition after 4 hours of drying, and contains over 60% MgO_2 by weight. It is stable for 2 years if kept in air-tight packages. When it is heated, as Fig. 2 shows, it loses active oxygen smoothly up to 320°. In the 320-360° range, according to heating-curve data [13], the loss of active oxygen increases abruptly.

SUMMARY

In contrast to methods for the production of MgO_2, based on the reaction of MgO with perhydrol, a method has been developed based on the interaction of magnesium hydroxide suspensions with perhydrol, which yields stable products containing 60-70% MgO_2 by weight.

LITERATURE CITED

[1] K. Sagtetter, Ch. Ztg., 58, 939 (1934).

[2] H. Dienst, Arch. Verdaunungs, 38, 325 (1926); Zbl., II, 102 (1927).

[3] S. Kottek, Munch. Med. Wach., 68, 1396 (1921).

[4] R. von Forreger, J. Chem. Soc. Ind., 25, 298 (1906).

[5] M. Prudhomme, C. r., 112, 1374 (1891).

[6] C. Sturgis, Ind. Eng. Ch., 39, 64 (1947).

[7] V. W. Slater, Chem. and Ind., 5, 45 (1945).

[8] Encyclopedia of Chemical Technology, 10, 38 (1953).

[9] Iu. V. Kariakin and I. I. Angelov, Pure Chemical Reagents [In Russian] (Moscow, State Chem. Press, (1955)).

[10] S. Z. Makarov and I. I. Vol'nov, Bull. Acad. Sci. USSR, Div. Chem. Sci. 5, 765 (1954). •

[11] F. Hinz, U. S. Patent 2,091,129 (1935).

[12] E. A. Fomina, Author's Summary of Candidate's Dissertation, Inst. Phys. Chem. Acad. Sci. USSR (Moscow, (1953)). [In Russian]

[13] I. I. Vol'nov, Proc. Acad. Sci. USSR 94, 477 (1954).

Received February 2, 1957

• Original Russian pagination. See C. B. Translation.

THE USE OF DOLOMITE AS AN OPACIFIER

I. Azimov and A. I. Avgustinik

It is reported in the literature [1-4] that calcium oxide and magnesium oxide may, under certain conditions, favor the crystallization of glass and glaze at 950-1050°. We made use of this fact in the production of a pure white and very cheap enamel glaze for loess—loam ceramics. The method used for preparation of the specimens was described in another paper [5].

The frit was made at 1400°; the temperature during glost firing was raised at the rate of 300° per hour, and held at 1000° for 1 hour. The density of the slip was such as to give a glaze layer 0.4-0.5 mm thick after firing. To aid suspension of the glaze, 2% of bentonite (on the dry weight of the frit) was added with the water. The raw materials consisted of Samarkand feldspar, Maisk coarse sand, and Begabad dolomite, the chemical compositions of which are given in Table 1.

After extensive investigations, the basic composition chosen was enamel No 1, as shown in Table 2.

The frit for this enamel had the following composition (in parts by weight): quartz sand 44, feldspar 31, borax (crystalline) 17, dolomite 17.

This composition yielded a fairly viscous melt at 1400°, and after glost firing the specimens were milk-white without surface defects.

The effects of the following factors were studied: dolomite content, oxide contents, the influence of certain additives, such as fluorine, phosphorus pentoxide, and the oxides of barium, zinc, and lithium.

The methods described earlier [5] were used for determinations of fusibility, contact angle, luster, yellowness, reflection spectra, thermal stability, and the qualitative phase composition of the opacifier. In addition, the whiteness was determined quantitatively by means of a photoelectric whiteness-meter [6], and microhardness by means of the PMT-3 instrument [7]. The absolute value of the whiteness was calculated from the average value for five specimens (each specimen being tested 3-5 times in the apparatus).

The microhardness was also the average for five specimens, the value for each being found from 5-10 determinations.

TABLE 1

Raw material	Chemical composition (wt. %)							
	SiO_2	Al_2O_3	Fe_2O_3	CaO	MgO	K_2O	Na_2O	calcination loss
Samarkand feldspar	68.14	18.02	0.16	0.85	0.07	9.93	2.25	0.58
Maisk quartz sand	96.76	2.11	0.11	0.71	—	—	—	0.31
Begabad dolomite	3.52	Traces	1.11	30.62	19.87	—	—	44.87

TABLE 2

Enamel No.	Chemical composition (wt. %)							
	SiO_2	B_2O_3	Al_2O_3	Fe_2O_3	Na_2O	K_2O	CaO	MgO
1	69.24	6.621	7.113	0.309	3.671	3.276	6.152	3.618
2	72.235	7.021	7.35	0.225	3.893	3.473	3.758	2.042
3	71.03	6.892	7.216	0.257	3.822	3.41	4.708	2.666
4	69.86	6.77	7.087	0.29	3.754	3.349	5.623	3.267
5	68.018	6.571	6.88	0.339	3.644	3.251	7.08	4.22
6	66.96	6.457	6.761	0.367	3.582	3.195	7.909	4.767
7	66.274	6.385	6.684	0.387	3.542	3.159	8.447	5.121
8	65.333	6.284	6.579	0.324	3.486	3.109	9.242	5.642
9	64.309	6.175	6.466	0.44	3.425	3.055	9.993	6.136
10	63.070	6.043	6.327	0.472	3.352	2.99	10.969	6.776
11	61.592	5.886	6.161	0.513	3.264	2.912	12.131	7.54

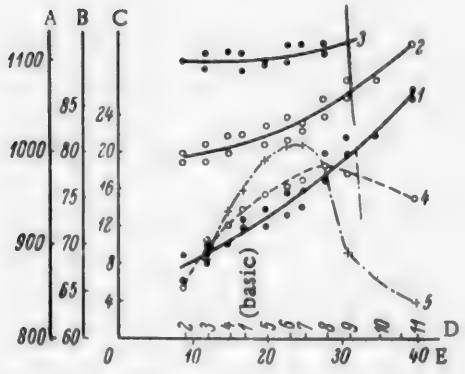

Effect of dolomite content on the properties of the enamel.
A) Temperature (°C), B) reflectance (%), C) luster (in luster numbers), D) dolomite content (wt. parts), E) number of enamel. Curves: 1) temperature of the start of melting of the enamel, 2) temperature of the end of melting, 3) temperature of the start of spreading, 4) reflectance (whiteness), 5) luster.

Effect of variations of the dolomite content. Eleven enamel compositions were studied (Table 2, and figure); the dolomite content was varied in steps of 2-4 weight parts in such a way that the contents of the other components in the batch remained constant.

In enamels Nos 2-4 the frit melt does not flow at 1400°, but it becomes increasingly fluid with increase of the dolomite content. The microhardness of the specimens is in the range of 520-572 kg/ mm^2.

All the specimens have high heat resistance and withstand more than 8 temperature changes from 100 to 20°, by immersion in water. The reflection spectra of all the specimens in the 750-400 mμ region form lines almost parallel to the abscissa axis. The spectrum indicates absence of yellowness. This made it possible to use an instrument with selenium photocells for whiteness determinations.

Thus, increase of the dolomite content lowers the viscosity of the frit melt, raises the fusibility of the enamels, and, up to certain limits, increases the whiteness (up to 28 wt. parts of dolomite) and the luster (up to 23 wt. parts of dolomite), while further increases have an adverse effect on these properties. The other properties of the enamel are not influenced significantly by variations of the dolomite content.

The diagram shows that enamels Nos 5-8 are not inferior to a zircon enamel.

Phase composition of the enamel opacifier. For determination of the phase composition of the enamel opacifier, the basic composition (No 1) was used in the preparation of two new compositions; in one, all the CaO was replaced by MgO (Enamel No 12), while in the other all the MgO was replaced by CaO (Enamel No 13) (after glost firing, these enamels were also white; the whiteness of Enamel No 12 was 77.7%, and of No 13, 65.6%, and No 12 was much more fusible than No 13).

All the specimens used for phase analysis (Enamels Nos 7, 11-13) were heated for a long time (20-60 hours) in a furnace at 1000°. However, the crystals formed in the enamels were so small (about 1μ) that they could not be studied optically, and the x-ray method [5] was used. The x-ray photographs were taken by means of RPK and VRS cameras, and also a flat x-ray camera with a copper anticathode, at 30 kv, 18 ma, and exposures of 6-20 hours.

The x-ray results show that in absence of CaO, in Enamel No 12, the opacifying phase is enstatite ($MgO \cdot SiO_2$), and in absence of MgO (No 13) it is wollastonite ($CaO \cdot SiO_2$). If CaO and MgO, introduced as dolomite, are present together in the enamel, a crystalline phase consisting of diopside ($CaO \cdot MgO \cdot 2SiO_2$) appears.

SUMMARY

1. The crystallizing power of calcium and magnesium oxides, which under certain conditions favor the development of finely-divided crystalline phases, can be used for effective opacification of fusible enamels on ceramics. Dolomite is recommended as a cheap raw material for this purpose.

2. When dolomite is used as opacifier, the crystalline phase is diopside.

3. A formulation is given for a cheap white enamel (Nos 5-8), with a flow temperature of 1000°, for loess ceramics. The molecular composition is:

$$\left.\begin{array}{l} K_2O - 0.106\text{—}0.084 \\ Na_2O - 0.181\text{—}0.143 \\ CaO - 0.39\ \text{—}0.418 \\ MgO - 0.323\text{—}0.355 \end{array}\right\} \quad \begin{array}{l} Al_2O_3 - 0.208\text{—}0.164 \\ Fe_2O_3 - 0.0065 \end{array} \quad \left\{\begin{array}{l} SiO_2 - 3.477\text{—}2.751 \\ B_2O_3 - 0.29\ \text{—}0.229 \end{array}\right.$$

These enamels are composed as follows (in wt. parts): quartz sand 44, feldspar 31, borax (crystalline) 17, and dolomite 20-28.

LITERATURE CITED

[1] I. I. Kitaigorodskii, Plekhanov Inst., Laboratory of Silicate Technology, MARKhOZ [In Russian] (Moscow, (1928)).

[2] V. V. Vargin, K. S. Evstrop'ev, K. A. Krakau, I. M. Prok, and A. I. Stozharov, Physiocochemical Properties of Glass and their Dependence on Composition [In Russian] (State Light Ind. Press, 1937).

[3] A. P. Zak and S. I. Iofe, Trans. State Sci. Res. Inst. Glass (State Light Ind. Press, 1937).

[4] V. P. Barzakovskii and S. K. Dubrovo, Physiocochemical Properties of Glazes for High-Voltage Porcelain [In Russian] (Izd. AN SSSR, 1953).

[5] I. Azimov and A. I. Avgustinik, Chem. and Chem. Technol. 4 (1958).

[6] V. Ia. Lokshin, Technology of Metal Enameling [In Russian] (1955), p. 142.

[7] M. M. Krushchev and E. S. Berkovich, The PMT-2 and PMT-3 Instruments for Microhardness Testing [In Russian] (Izd. AN SSSR, 1950).

Received April 1, 1958

PHOSPHATE ENAMELS

K. P. Azarov and E. M. Chistova

Enamels Laboratory, Novocherkassk Polytechnic Institute

In silicate-free phosphate glasses [1-7] there are two and a half oxygen ions per ion of the p^{5+} glass former; this indicates the presence of "single-bonded" oxygen. The network in such a glass is less strong and more mobile than in a silicate glass, where two oxygen ions are present for each ion of the glass former.

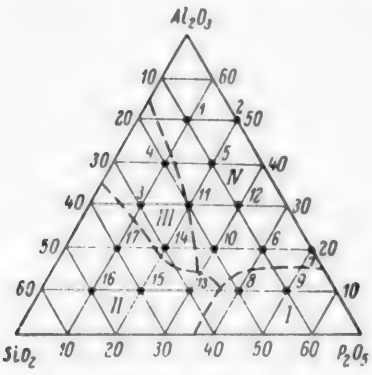

Fig. 1. Glasses of Series I. The numbers of the points correspond to the numbers of the different glasses. Region I) fusible glasses, II) viscous glasses, III) sintered glassy mass, IV) glasses not formed.

Since phosphate glasses are more fusible than silicate glasses, it is of interest to study these glasses in relation to their use as opaque fusible enamels for metals. In view of the great differences between the properties of phosphate and silicate glasses, the effects of different oxides on the properties of phosphate glasses of various types were studied.

The first series of experiments was carried out on the system $Na_2O-SiO_2-P_2O_5-Al_2O_3-B_2O_3$, in order to select compositions which form glasses at a melting temperature of 1200° in 1 hour. The contents of Al_2O_3, P_2O_5, and SiO_2 were varied, with constant contents of Na_2O (20 molar %) and B_2O_3 (10 molar %). The original glass No 19 of Series II is characterized by a high content of SiO_2 and a low content of B_2O_3. Series III (original glass No 64) is characterized by high SiO_2 and B_2O_3 contents. Glasses of Series IV (original glass, No 84) have a low SiO_2 content and a ratio of $P_2O_5 : Al_2O_3 > 1$. Glasses of Series V (original glass, No 105) contain a little SiO_2, and correspond to the ratio $P_2O_5 : Al_2O_3 < 1$. Series VI (original glasses Nos 143 and 171) are alumin phosphate silicate-free glasses (Table 1).

TABLE 1

Compositions of the Original Glasses

Series	Glass No.	Composition of original glass (wt. %)								
		SiO_2	Al_2O_3	P_2O_5	Na_2O	B_2O_3	TiO_2	K_2O	Na_3AlF_6	ZnO
I	8	12.2	10.4	57.7	12.6	7.1	—	—	—	—
	9	5.63	9.57	66.6	11.65	6.55	—	—	—	—
	17	30.8	26.1	18.2	16.0	8.9	—	—	—	—
II	19	30.8	26.1	18.2	16.0	8.9	10.0	—	—	—
III	64	22.4	19.2	13.5	11.6	16.6	7.3	3.6	5.8	—
IV	84	7.4	19.2	28.5	11.6	16.6	7.3	3.6	5.8	—
V	105	8.0	20.5	23.5	12.4	17.8	7.8	3.8	6.2	—
VI	143	—	23.0	40.6	16.5	4.9	—	11.0	—	4.0
	171	—	23.5	32.7	17.4	11.2	6.5	3.5	5.2	—

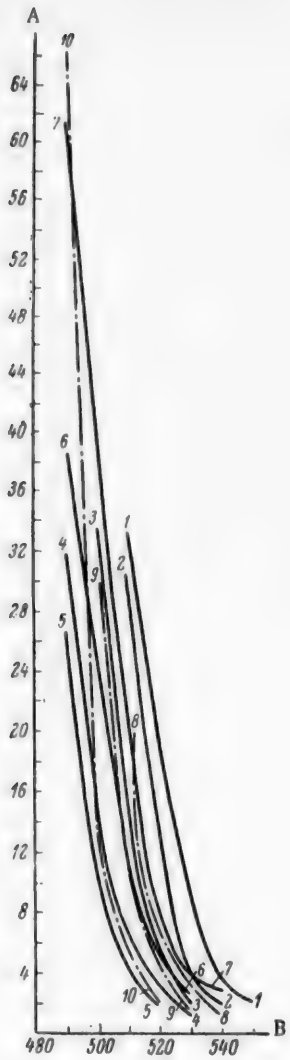

Fig. 2. Viscosities of glasses of Series III, IV, and V in the softening range.
A) Viscosity $\eta / 10^{-8}$ (poises), B) temperature (°C). Replacement of SiO_2 by P_2O_5 1) original glass No 64 (Series III), 2) 5% SiO_2, 3) 10% SiO_2, 4) 15% SiO_2 (glass No 84), 5) 20% SiO_2. Effect of additions of B_2O_3: 4) original glass No 84 (Series IV), 6) 3% B_2O_3, 7) 8% B_2O_3, 8) original glass No 105 (Series V), 9) 3% B_2O_3, 10) 8% B_2O_3.

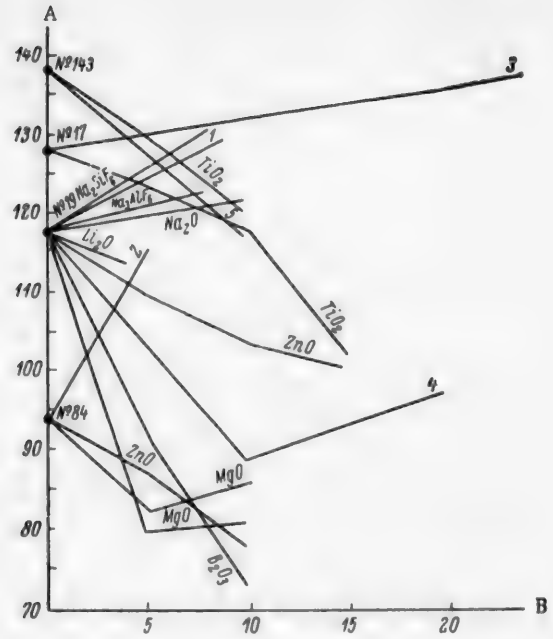

Fig. 3. Linear coefficients of thermal expansion. Nos 17, 19, 84 and 143, original glasses of Series I, II, IV, and VI.
A) Coefficient of thermal expansion $\alpha \cdot 10^{-7}$, B) amount of oxide (wt. %). 1) Replacement of B_2O_3 by Na_2O, 2) B_2O_3 by Na_2O, 3) SiO_2 by P_2O_5, 4) SiO_2 by P_2O_5, 5) P_2O_5 by SiO_2.

Fig. 1 shows that fusible glasses are formed with compositions (molar %) of Al_2O_3 10—20, SiO_2 10—20 and P_2O_5 40—50 (Region I). More viscous glasses were formed on increase of the SiO_2 content (Region II). To glasses Nos 8, 9, and 17 of Series I there was also added 5, 10, and 15 wt. % of TiO_2 respectively as opacifier. The best results with regard to whiteness, absence of a color tinge, and luster were obtained for glass No 17, and, with 10% TiO_2 by weight, for glass No 19, which was the original glass for Series II.

In Series II, III, IV, V, and VI the effects of replacement of some oxides by others, and of addition of the oxides Li_2O, Na_2O, K_2O, MgO, CaO, BaO, ZnO, B_2O_3, TiO_2, and of fluorides to the main composition, on the glass properties were studied.

Fig. 3 shows that the silicate-free glass No 143 has the highest linear coefficient of thermal expansion (20-400°).

Replacement of B_2O_3 by Na_2O in glass No 19 of Series II (Curve 1) and No 84 of Series IV (Curve 2) increases the coefficient of expansion, the increase being greater in Series IV than II*. Replacement of SiO_2 by P_2O_5 in glass No 17 of Series I (Curve 3) results in a moderate increase of the coef-

* Enamel coatings on steel had a network of cracks.

TABLE 2

Enamel Compositions (wt. %)

Enamel No.	SiO_2	Al_2O_3	P_2O_5	Na_2O	B_2O_3	TiO_2	K_2O	Na_3AlF_6	ZnO
119	8.0	20.5	23.5	16.2	17.8	7.8	—	6.2	—
120	8.4	21.6	24.7	17.0	13.5	8.2	—	6.6	—
121	8.9	22.8	26.1	18.0	8.70	8.70	—	6.8	—
132	7.6	19.5	22.4	11.8	16.9	7.5	3.6	5.9	4.70
137	8.0	20.5	23.5	12.4	12.8	7.8	3.8	6.2	5.0
138	8.0	20.5	23.5	12.4	7.8	7.8	3.8	6.2	10.0

ficient of expansion, while in glass No 19 of Series II the coefficient of expansion decreases at first, on replacement of 10% SiO_2 by P_2O_5, and then increases (Curve 4). Replacement of P_2O_5 by SIO_2 in glass No 143 of Series VI (Curve 5) decreases the coefficient of expansion. Additions of Na_2SiF_6, Na_3AlF_6 and Na_2O increase the coefficient of expansion of glass No 19 (Series II); the greatest increase is produced by additions of fluorides. Additions of Li_2O, ZnO, B_2O_3 and MgO to the same glass decrease the coefficient of expansion, the greatest decreases being produced by MgO and B_2O_3. The oxides MgO and ZnO also lower the coefficient of expansion of glass No 84 of Series IV. Titanium dioxide decreases the coefficient of thermal expansion of glasses of Series I (No 17) and VI (No 143).

Viscosity studies in the softening region were carried out with glasses of Series III, IV, and V. It was found (Fig. 2) that the viscosity decreases considerably on replacement of 5, 10, 15 and 20 wt. % of SiO_2 by P_2O_5 in glass No 64. Additions of 3 and 8 wt. % of B_2O_3 increase the viscosity of glass No 84 of Series IV, but decrease the viscosity of glass No 105 of Series V.

Fusibility determinations by the method described previously [8] showed that addition of B_2O_3 makes glass No 84 of series IV less fusible, and glass No 105 of series V more fusible. Additions of cryolite have a favorable effect on the fusibility in Series II and III. Lithium oxide improves fusibility, but confers a yellowish tinge. The oxides K_2O, MgO, CaO make the enamel less fusible. The oxides Na_2O and ZnO slightly improve fusibility.

The following oxides have a favorable effect on opacity in all the series: Al_2O_3, ZnO, B_2O_3, K_2O (in decreasing order). Additions of MgO and CaO have little effect on whiteness, color tinge, or luster.

Experiments showed that the addition of 10-12 molar of TiO_2 in Series II, III, and V, and 16-19 molar % of TiO_2 in Series IV and VI, is sufficient for good opacification. It was noticed that in glasses containing 10 molar % of TiO_2 the opacity is worse and a yellow tinge appears when the molar content of P_2O_5 exceeds that of Al_2O_3. The TiO_2 content of these glasses must be increased in order to improve the opacity and whiteness of these glasses.

Petrographic investigations* showed that replacement of SiO_2 by P_2O_5 results in an increase of crystal size (probably rutile).

In trials of these glasses, enamels were obtained at firing temperatures of 675-775°, with diffuse reflection coefficients in the 75-83% range for coatings 0.2 mm thick. The compositions of these enamels (Table 2) correspond to 10 molar % SiO_2, 15-19 % P_2O_5, 17-19 molar % Al_2O_3, 10 molar % TiO_2, and 10-19 molar % B_2O_3.

Tests for acid resistance with the aid of 4% acetic acid ("spotting test") showed no dulling of the surface after 1 hour.

LITERATURE CITED

[1] W. A. Weyl and N. J. Kreidl, J. Am. Cer. Soc. 24, 11, 372 (1941).

[2] W. A. Weyl, Chem. Eng. News 27, 15, 1048 (1949).

*Performed by A V. Rodionova.

[3] L. R. Blair, and M. D. Beals, J. Am. Cer. Soc. 34, 110 (1951).

[4] B. K. Niklewski and R. H. Ashby, Sheet Met. Ind. 29, 1037 (1952).

[5] W. T. Baldwin, J. Am. Cer. Soc. 31, 5, 115 (1948).

[6] J. E. Stanworth and W. E. S. Turner, J. Soc. Glass Techn. 21, 87, 368 (1937).

[7] W. Heimsoeth and F. B. Meyer, J. Am. Cer. Soc. 34, 12, 366 (1951).

[8] K. P. Azarov, Factory Labs. 6, 748 (1950).

Received December 27, 1957

COMPARISON OF DIFFERENT METHODS FOR THE THERMAL DECOMPOSITION OF HYDROLYTIC LIGNIN*

V. G. Panasiuk

The Dnepropetrovsk Agricultural Institute

The previous communications described the results of experiments on the thermal processing of hydrolytic lignin from cotton hulls and wood. The thermal methods tested included: dry distillation of lignin [1], vacuum-thermal decomposition in the liquid phase [2], and thermal liquefaction [3].

The optimum experimental conditions were the following: dry distillation – time 8 hours, final temperature 500°, atmospheric pressure; vacuum-thermal decomposition (VTD) – time 1.5 hours, final temperature 460°, pressure 40 mm Hg, anthracene oil medium; thermal liquefaction (TL) – time 1 hour, final temperature 380°, pressure 65-80 atmos, solar oil as solvent.

The results of the most typical experiments with cotton-hull lignin are given in Table 1.

It follows from the data in Table 1 that dry distillation gave a low yield of tar with high yields of water and gas. A considerably higher yield of tar was obtained by thermal liquefaction, and the highest yield was in the vacuum process.

It is known that the most valuable of the products formed in the pyrolysis of lignin is tar, which yields phenols and a ligroine fraction, and also carbon suitable for activation.

Table 2 shows what substances, and in what yields, can be obtained from different tars made from cotton-hull lignin.

TABLE 1

Yields in Different Methods of Thermal Decomposition of Cotton-Hull Lignin

Method	Yield (% on lignin)			
	carbon	tar	pyrolysis water	gas and losses
Dry distillation	51.2	8.3	21.4	19.1
Vacuum-thermal decomposition	49.2	38.0	4.4	8.4
Thermal liquefaction	49.1	23.9	7.9	19.1

TABLE 2

Group Composition of Tar Fractions up to 230°, Obtained by Different Methods of Decomposition of Cotton-Hull Lignin

Composition	Yield (% of tar fraction) by method of		
	dry distillation	VTD	TL
Acids	2.1	2.8	2.0
Phenols	46.0	43.3	11.9
Bases	2.0	2.5	2.3
Neutral substances	48.6	51.0	76.8

* Communication VI in the series on thermal processing of hydrolytic lignin.

TABLE 3

Yields in Different Methods of Thermal Decomposition of Lignin from Wood

Method	Yield (% on lignin)			
	carbon	tar	pyrolysis water	gas and losses
Dry distillation	53.5	8.5	29.2	8.8
Vacuum-thermal decomposition	54.2	30.0	8.7	7.1
Thermal liquefaction	54.3	18.4	10.8	16.5

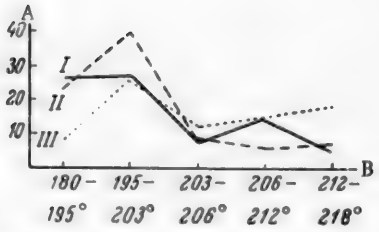

Fig. 1. Yields of phenol fractions from cotton-hull lignin in different thermal processes.
A) Yield (%), B) phenol fractions (°C). Process: I) Dry distillation, II) VTD, III) TL.

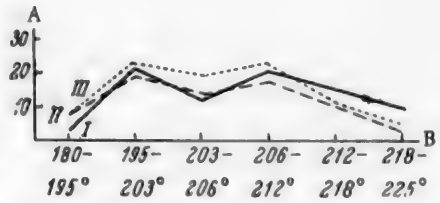

Fig. 2. Yields of phenol fractions from wood lignin in different thermal processes.
A) Yield (%), B) phenol fractions (°C). Process: I) Dry distillation, II) VTD, III) TL.

Since the required product in the VTD and TL processes is a tar fraction boiling up to 230°, the same fraction from dry-distillation tar was investigated for comparison.

The tar fractions up to 230° from the dry-distillation process and vacuum-thermal decomposition are almost identical in group composition, consisting predominantly of phenols and neutral substances. The composition of the tar fraction made by thermal liquefaction is quite different. Neutral substances predominate in this fraction, while the phenol content is about $^1/_4$ of that obtained by the other processes. Calculation of the phenol yields as percentages of the original lignin gives the following results: by dry distillation, 1.75%; by VTD, 12.05%; and by TL, 3.88%.

Curves representing the distillation of phenols into narrow fractions are given in Fig. 1.

It is seen that, irrespectively of the process used for the thermal decomposition, cresol fractions (sum of the 1st and 2nd fractions) predominate; thus, the cresol fractions comprise over 63% in dry distillation, over 65% in VTD, and about 40% in TL.

Chromatographic analysis showed that all the cresol fractions contained o-, m-, and p-cresols; the m-isomer was present in the greatest quantity, and the p-isomer in the least.

Approximately the same yields of decomposition products were obtained in the thermal decomposition of hydrolytic lignin from wood. The results are given in Table 3.

As in the case of cotton-hull lignin, vacuum-thermal decomposition gives the highest tar yields.

Group analysis of the tar fractions up to 230° shows that phenols predominate in the fractions obtained by dry distillation and by VTD. Thus, dry distillation yielded 44.5% of phenols, or 1.51% on the weight of lignin, and VTD yielded 39.5%, or 10.47% on the weight of lignin.

The tar fraction up to 230° obtained by thermal liquefaction is obtained in a very considerable yield, but it contains only 8.5% phenols, or 3.8% on the lignin. Thus, the tars obtained from different lignins but by the same thermal processes are identical in group composition.

The phenols isolated from the tar fractions were distilled. The distillation curves are presented in Fig. 2.

With regard to the amount of each narrow phenol fraction, the situation is quite identical — most of the phenols are distilled off in the 195-212° range. Comparison of the phenols obtained from wood and from cotton hull by the same processes shows that the maximum amount of phenols from hull lignin is distilled off in the 180-203° range.

Paper chromatography revealed the presence of the same phenols as were found in tars obtained from cotton-hull lignin, the only differences being in their quantitative proportions. The phenols from wood lignin contained creosol which was not isolated from hull lignin.

The phenols obtained from cotton-hull lignin contained about 30% m-cresol, about 25% other cresols, about 6% phenol, and about 3% guaiacol. The phenols obtained from wood lignin contained over 35% guaiacol and about 30% cresols.

In summarizing the results obtained for phenols obtained from different hydrolytic lignins by different processes of thermal decomposition, we may note that the nature of the phenols obtained evidently depends only on the raw material used, irrespectively of the thermal processes if the latter are carried out over the same temperature range (up to 500°).

The amounts of light-boiling phenols differ for different thermal processes, but the nature and qualitative proportions of the phenols remains almost constant.

In a discussion of the chemical composition of wood tars, Sumarokov [4] points out that the conditions of thermal decomposition, such as the heating time, temperature, use of vacuum or pressure, and the medium, greatly influence the composition of wood tar, but the available data relate mainly to tar yields.

We carried out thermal decomposition of two different kinds of lignin under the most diverse conditions, namely: ordinary dry distillation under atmospheric pressure, decomposition under vacuum in anthracene oil, and thermal liquefaction under pressure in solar oil. Very different tar yields were obtained. However, the same results were obtained in each case for the qualitative composition of the phenols present in these tars; the composition depends only on the kind of lignin, and not on the thermal process used.

LITERATURE CITED

[1] V. G. Panasiuk et al., Hydrolysis Industry USSR 2 (1953); V. G. Panasiuk, J. Appl. Chem. 26, 7, 763 (1953).*

[2] V. G. Panasiuk, J. Appl. Chem. 30, Nos 4, 5, 6 (1957).*

[3] V. G. Panasiuk, J. Appl. Chem. 31, No 9, 1409 (1958).*

[4] V. P. Sumarokov, Chemistry and Technology of Wood-Tar Processing [In Russian] (1953).

Received March 18, 1957

*Original Russian pagination. See C. B. Translation.

THE DISSOLUTION OF IRON FROM TIN PLATE IN VARIOUS FLUXES

A. I. Vitkin

Apart from its useful functions in hot tinning of iron, a flux consisting of a boiling solution of zinc chloride is the main source of contamination of the tin bath by iron [1]. The mechanism whereby iron passes from the sheet into the tin of the plating bath consists of the dissolution of the iron in the flux, in the form of ferrous chloride, and formation of the compound $FeSn_2$ according to the equation

$$FeCl_2 + 3Sn \rightarrow SnCl_2 + FeSn_2.$$

The $FeSn_2$ crystals formed pass into the liquid tin in the bath.

In order to lower the solubility of iron in fluxes, we investigated various fluxes, consisting mainly of compositions melting below the temperature of liquid tin. The following systems were tested: 70% $ZnCl_2$ + 30% KCl of m.p. ~ 207°, 70% $SnCl_2$ + 30% KCl of m.p. ~ 200°, 65.5% $ZnCl_2$ + 35.5 $SnCl_2$ of m.p. ~ 180°, 40% $ZnCl_2$ + 60% ($SnCl_2 \cdot KCl$) of m.p. ~ 210°, 100% $ZnCl_2$ of m.p. up to 300°, and 100% $SnCl_2$ of m.p. ~ 247°.

The solubility of iron in these flux melts was determined by the following method: 100 g of the flux was melted in a crucible at 340 deg; a specimen of low-carbon steel sheet (08-KP) 30 cm^2 in total area was immersed in the melt for a definite time. The specimens were cut from the same coil of one roll of steel sheet made by the "Zaporozhstal" works. Before immersion, each specimen was degreased, washed, pickled, and again washed thoroughly in cold and hot water before immersion. Only one specimen was immersed in each melt; each experiment was performed in triplicate for each immersion time. The solubility of iron in the flux, calculated per unit specimen area, was found from the difference between the iron contents of the flux before and after immersion. The average of three results for each immersion time was taken.

The results are presented in the form of curves (isotherms) in Fig. 1. It follows from Fig. 1 that the solubility of iron is highest in melts of pure $SnCl_2$. The solubility in melts of pure $ZnCl_2$ is considerably lower. Addition of KCl to $ZnCl_2$ or $SnCl_2$ lowers the solubility of iron considerably; the solubility curve for the $ZnCl_2$-KCl melt lies below the solubility curve for the $SnCl_2$-KCl melt. The isotherm corresponding to the flux $ZnCl_2$ + $SnCl_2 \cdot KCl$ (not shown in the figure) lies between these two bottom curves.

The upper curve, based on Chufarov's data for the dissolution of iron in a boiling flux solution of optimum water content (up to 10%), is of interest. The solubility of iron in such fluxes (similar to those used in hot tinning) is more than 100 times its solubility in a $ZnCl_2$ melt.

However, as is clear from the isotherms (for 340°) in Fig. 2, the solubility of iron can be lowered still further by addition of KCl to the melt. Another effective means was dehydration of the flux ($ZnCl_2$ by calcination of the melt to constant weight; the calcination temperature chosen was above 400°, when water of crystallization is removed. As the bottom curve in Fig. 2 shows, the dissolution of iron almost ceased in the dehydrated flux; dissolution of iron could be prevented completely by the use of the melt under vacuum, with the tin fed in the dry state in a protective atmosphere.

Whereas in the case of zinc chloride fluxes the solubility of iron could be lowered by dehydration of the melt, this could not be achieved with stannous chloride fluxes, owing to the displacement reaction with deposition of tin on the sheet and dissolution of iron in the melt.

$$Fe + SnCl_2 \rightarrow FeCl_2 + Sn$$

DISCUSSION OF RESULTS

It follows from the work of Kochergin and others [2, 4] that the dissolution of iron in fused chlorides is an electrochemical process ($Fe + 2H^+ \rightarrow Fe^{2+} + H_2$), which is a consequence of salt hydrolysis, the degree of which depends on the stability of the complex ions formed in the melts. The stability of complex ions depends on the complex-forming capacity of their central elements and on the polarizing action of the external cations, which increases in the series $K^+ - Na^+ - Ba^{2+} - Ca^{2+}$. These views are fully confirmed by our investigations on the solubility of iron in melts of zinc

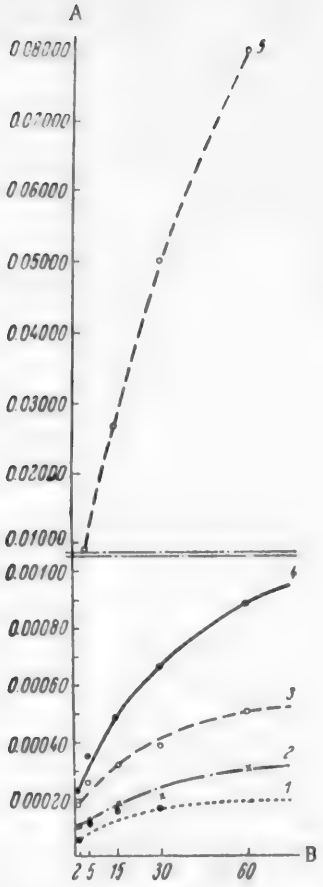

Fig. 1. Course of dissolution of iron in various fluxes at 340°.
A) Solubility of iron (g/ cm^2), B) time (seconds). System and melting point respectively (°C): 1) 70% $ZnCl_2$ +30% KCl, 207; 2) 70% $SnCl_2$ + 30% KCl, 200; 3) $ZnCl_2$ 291; 4) $SnCl_2$, 247; 5) 91% $ZnCl_2$ + 9% H_2O (Chufarov's system), b.p. 200°.

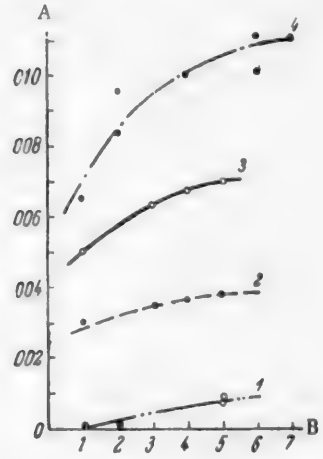

Fig. 2. Course of dissolution of iron in fluxes with different KCl contents at 340°.
A) Solubility of iron (g/ cm^2), B) time (hours). System: 1) $ZnCl_2$ without water of crystallization 2) 70% $ZnCl_2$ + 30% KCl, 3) 90% $ZnCl_2$ + 10% KCl, 4) $ZnCl_2 \cdot (1\text{-}4)\ H_2O$.

tin, and potassium chlorides. In the light of these views, the most suitable additive for flux melts is potassium chloride.

It must be pointed out that in all the earlier investigations the experiments were performed with melts in which displacement reactions did not occur. The absence of a reaction between iron and zinc chloride in one of these investigations [4] is explained by the fact that iron is below zinc in Delimarskii's [5] electrochemical series. However, despite the fact that tin is above iron in these same series, there was a new factor in our experiments — the displacement of tin from its chloride by iron from the sheet. Incidentally, tin is displaced from $SnCl_2$ even by such a noble metal as copper. Evidently the course of the displacement of one metal from its salts by another metal does not always correspond to the positions of these metals in the potential series or to the values of their electrode potentials. The course of displacement (or exchange) reactions may be determined by the thermodynamic method used by Elagina and Palkin, which is based on the principle that these reactions proceed in the direction of formation of products in which the total energy of the crystal lattice

is greater [6]. The energy of salt crystal lattice may be estimated by means of Kapustinskii's formula [7] for the lattice energy of ionic crystals, while the energy of the metal crystal lattice may be estimated from the heat of evaporation of the metal [8]. The whole series of the displacement reactions may then be represented as follows:

$$\underset{665.7}{ZnCl_2 + Fe} \leftarrow \underset{616.88}{FeCl_2 + Zn} \quad (+48.82 \text{ kcal/g-atom} \tag{1}$$

$$\underset{651.1}{ZnCl_2 + Sn} \leftarrow \underset{570.8}{SnCl_2 + Zn} \quad (+80.3 \text{ kcal/g-atom} \tag{2}$$

$$\underset{627.5}{SnCl_2 + Fe} \rightarrow \underset{659.0}{FeCl_2 + Sn} \quad (+31.5 \text{ kcal/g-atom} \tag{3}$$

$$\underset{615.7}{SnCl_2 + Cu} \rightarrow \underset{654.0}{CuCl_2 + Sn} \quad (+38.3 \text{ kcal/g-atom} \tag{4}$$

In fact, zinc is not deposited on sheet iron when it is immersed in a $ZnCl_2$ melt; similarly, Reaction (2) does not proceed to any extent from left to right, and therefore zinc chloride is used as a flux in tinning when contamination of the tin bath by zinc is excluded. However, if a steel or copper plate is immersed in a melt of $SnCl_2$, tin is deposited on the surface. This largely accounts for the higher rate of dissolution of iron in fluxes containing tin, as compared with fluxes containing zinc.

SUMMARY

1. The solubility of iron is much lower in fused fluxes than in flux solutions. The solubility is lowered still further by addition of KCl to the melts, and by dehydration of the melts.

2. The presence of stannous chloride in fused fluxes decreases the solubility of iron somewhat because of the displacement Reaction (3).

3. The direction of the displacement of one metal from its salts by another metal does not always correspond to the positions of the metals in the potential series. These reactions proceed in the direction of formation of products of greater total lattice energy.

LITERATURE CITED

[1] G. I. Chufarov et al., J. Appl. Chem. 26, No 6 (1953). *

[2] V. P. Kochergin et al., J. Appl. Chem. 27, No 9 (1954).*

[3] V. P. Kochergin et al., J. Appl. Chem. 29, No 4, 566 (1956). *

[4] V. P. Kochergin et al., J. Inorg. Chem. 1, 11 (1956).

[5] Iu. K. Delimarskii, J. Phys. Chem. 29 (1955).

[6] E. I. Elagina and A. P. Palkin, J. Inorg, Chem. 1, 11 (1956).

[7] G. B. Bokii, Introduction to Crystal Chemistry [In Russian] (Izd. MGU, (1954)).

[8] S. Dushman, Scientific Foundations of Vacuum Technique (IL, (1950)) [Russian translation].

Received May 24, 1957

* Original Russian pagination. See C. B. Translation.

LIQUID–VAPOR EQUILIBRIUM IN THE SYSTEM ACETALDEHYDE–METHYL ALCOHOL AT ATMOSPHERIC PRESSURE

R. P. Kirsanova and S. Sh. Byk

It is known that oxidation of mixtures of C_3-C_4 hydrocarbons yields a complex mixture of organic compounds containing oxygen, including acetaldehyde and methyl alcohol. Liquid–vapor equilibrium data are necessary for separation of this mixture by distillation. To the best of our knowledge no such data are available for the system acetaldehyde–methanol in the literature.

The purpose of the present investigation was to fill this gap to some extent.

EXPERIMENTAL

Characteristics of the starting materials. Methyl alcohol, of "chemically pure" grade, was carefully dehydrated by means of magnesium methylate, and then distilled. After distillation, it had the following constants: $n_D^{20} = 1.3290$, $d^{20} = 0.7911$. The water content, determined by means of the Fischer reagent, was less than 0.01% by weight. The acetaldehyde was of the "chemically pure" grade, b.p. 20.2° at 760 mm.

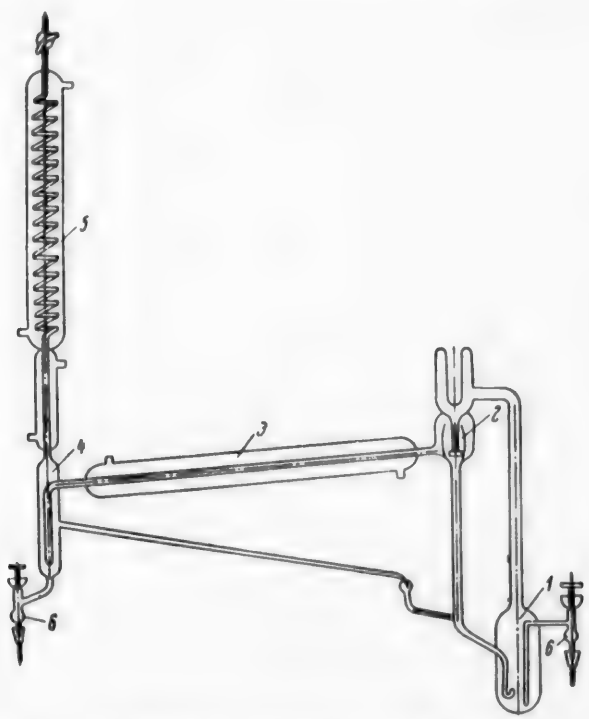

Fig. 1. Apparatus for investigation of liquid–vapor equilibrium. Explanation in text.

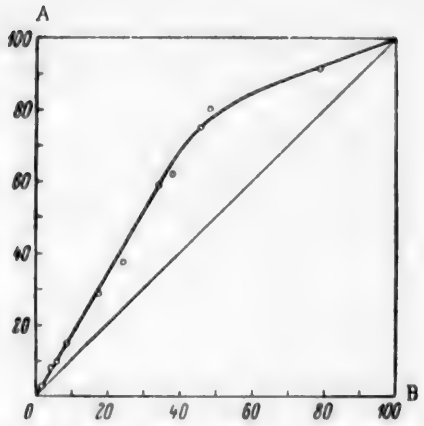

Fig. 2. Boiling point–composition diagram for the system acetaldehyde–methyl alcohol under atmospheric pressure.
A) CH_3CHO in vapor (wt. %), B) CH_3CHO in liquid (wt. %).

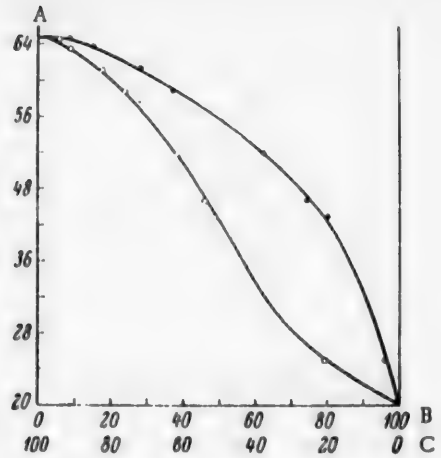

Fig. 3. Distribution of acetaldehyde between the equilibrium phases in the binary system acetaldehyde–methyl alcohol under atmospheric pressure.
A) Temperature (°C), B) CH_3CHO content (wt. %), C) CH_3OH content (wt. %).

Liquid–Vapor Equilibrium in the System Acetaldehyde–Methanol at P = 760 mm Hg

Composition of vapor phase (wt. %)		Composition of liquid phase (wt. %)		Composition of vapor phase (wt. %)		Composition of liquid phase (wt. %)	
acetaldehyde	methanol	acetaldehyde	methanol	acetaldehyde	methanol	acetaldehyde	methanol
3.0	97.0	2.0	98.0	8.0	92.0	4.0	96.0
4.2	95.8	2.4	97.6	9.0	91.0	5.8	94.2
5.0	95.0	2.8	97.2	15.0	85.0	8.8	91.2
6.0	94.0	3.6	96.4	28.8	71.2	17.4	82.6
6.4	93.6	4.2	95.8	37.2	62.8	23.6	76.4
7.6	92.4	4.2	95.8	58.6	41.4	34.6	65.4
11.0	89.0	6.6	93.4	63.0	38.0	38.0	62.0
9.8	90.2	5.0	95.0	80.0	20.0	48.2	51.8
12.0	88.0	7.8	92.2	74.2	25.8	45.4	54.6
12.8	87.2	8.4	91.6	90.6	9.4	79.0	21.0

Method of investigation. Liquid–vapor equilibrium was studied by the dynamic method in an apparatus operating on the principle of thermal-siphon circulation of the vapor–liquid mixture. This type of apparatus has been described in the literature [1, 2], and was used successfully earlier in our studies of other systems [3-5].

The apparatus (Fig. 1) consists of an electrically heated still 1; the vapor–liquid mixture passes from it into the separator 2; the liquid flows back from the separator into the still, while the vapor passes to the condenser 3 and receiver 4.

When the circulation temperature of the vapor–liquid mixture, measured by means of a standard thermometer, became constant, it was considered that equilibrium had been reached. Preliminary experiments showed that equilibrium is established 1-1.5 hours after the start of normal circulation in the apparatus.

The temperature fluctuations of the mixtures studied at equilibrium did not exceed ± 0.2°. It should be noted that the specific properties of the system (the high vapor pressure of acetaldehyde, 760 mm Hg at 20.2°)

led us to introduce certain modifications in the design of the apparatus in order to prevent losses of acetaldehyde, both during circulation of the vapor–liquid mixture, and during the taking of equilibrium samples from the still and receiver. For this reason a vertical coil condenser 5 with a large cooling surface was connected above the condensate receiver which was open to the air, and the sampling stopcocks 6 were provided with ground-glass surfaces so that the samples could be taken without vapor leakage. In addition, the cooling system was modified. Isopropyl alcohol cooled by solid carbon dioxide was used in the condenser instead of water. The temperature of the alcohol at the condenser entry was −50°, and −30° at the exit. Determinations of the material balance showed that under these conditions the losses of acetaldehyde in the system were negligible.

Method of analysis. The acetaldehyde contents of the equilibrium phases were determined by means of hydroxylamine hydrochloride, with an error of ± 0.1 wt. %.

RESULTS

Liquid–vapor equilibrium in the system acetaldehyde–methanol was studied at P = 760 mm Hg over the whole range of acetaldehyde concentrations.

The results are presented in the table and in Figs. 2 and 3.

It follows from the results that the maximum enrichment of the equilibrium vapor phase with acetaldehyde occurs in the region of medium concentrations (~ 50 wt. %) of acetaldehyde in the liquid.

The authors are grateful to K. A. Gol'bert for discussion of the results.

LITERATURE CITED

[1] D. F. Gillespie, Ind. Eng. Ch. 18, 575 (1946).

[2] V. A. Kireev, Iu. N. Sheinker, and E. M. Peresleni, J. Phys. Chem. 26, 352 (1952).

[3] L. I. Shcherbak and S. Sh. Byk, J. Phys. Chem. 30, 1, 56 (1956).

[4] S. Sh. Byk, L. I. Shcherbak, and R. G. Stroiteleva, J. Phys. Chem. 30, 2, 305 (1956).

[5] L. I. Shcherbak, S. Sh. Byk, and M. E. Aerov, J. Appl. Chem. 28, 1120 (1955).•

[6] J. Mithel and D. M. Smith, Ann. Chem. 22, 746 (1950).

Received February 1, 1957

• Original Russian pagination. See C. B. Translation.

CONFERENCE ON MODERN INVESTIGATION METHODS IN THE FIELD OF SILICATES AND CONSTRUCTION MATERIALS

A conference on modern investigation methods in the field of silicates and constructional meterials, organized by the Scientific Engineering and Technical Society, was held from October 14 to 18 in the October Hall of the House of the Soviets in Moscow. The conference was attended by more than 500 delegates representing the scientific community of the capital, and of Leningrad, Kiev, Khar'kov, Tbilisi, Minsk, Alma-Ata, and other towns.

About 70 papers on different subjects related to silicate research were presented at the conference.

The conference was opened by P. P. Budnikov, who, in a short introductory address, outlined the significance of the conference for further development of research methods. This was followed by the following papers at the plenary session: by V. V. Tarasov, on the application of the quantum theory of heat capacities to glass and silicate research; by E. A. Porai-Koshits, on the use of the low-angle method for the x-ray investigation of the structure of materials; by L. S. Palatnik and A. I. Landau, on new methods for the construction of equilibrium diagrams for multicompoent system; by V. V. Lapin, on petrographic research methods; by E. K. Keler, on the method of multiple thermal analysis in silicate research; and by O. P. Mchedlov-Petrosian and V. I. Babushkin on thermodynamic methods for investigation of solid-phase reactions in silicate systems.

V. V. Tarasov showed that his quantum theory of heat capacity of chain and layer structures can be used to reveal the presence of chain, band, and layer formations in silicates, borates, phosphates, and other materials, regardless of their crystalline or glassy state. Studies of heat capacity at low temperatures (20-300° K) can lead to reliable data on forces within and between the chains and layers, and make it possible to determine the force constants. The heterodynamic equilibrium between the chain and layer structures which follows from these considerations reflects the already known fact that the covalent forces within the frameworks (chains or layers) are greater than the ionic forces of interaction between the frameworks (chains or layers) and modifier cations, for which the force constants are lower. The dynamic behavior of structures in Na_2SiO_3, $MgSiO_3$, As_2O_3, Sb_2O_3, Bi_2O_3, Nb_2O_5, $Na_2B_4O_7$ etc., was considered in the light of this theory. It was shown that the mechanical and thermal properties of frameworks and other structures are determined by the values of the force constants of the most elastic bonds of the structure, i.e., the bonds within the framework itself. In the case of chain and layer structures, a consequence of their heterodynamic character is that the weakest bonds play the determining role.

E. A. Porai-Koshits reported on the principles involved in the development of the method of low-angle x-ray scattering, which can be used for determinations of slight changes in the dimensions, shapes, and distribution of submicroscopic heterogeneity regions in solid structures. His theoretical and experimental modifications of the method made it possible to establish the existence of submicroscopic heterogeneity regions in sodium borosilicate glasses which had not been subjected to any chemical action; this is an important contribution to the theory of the glassy state.

L. S. Palatnik reported on his topoanalytical theory of multicomponent heterogeneous systems, which leads to a new method for construction of phase diagrams and determination of the chemical composition of phases in such systems without the use of physical or physicochemical methods of analysis. The method is based on the use of a generalized "center of gravity" rule in conjunction with other thermodynamic principles.

V. V. Lapin presented the principles of petrographic investigations of articles made from synthetic stone, and drew attention to the importance of a multiple approach, which involves the use of x-ray and electron

microscope methods, etc., in conjunction with chemical methods. Attention was drawn to difficulties in the production of certain materials, and to shortages of qualified workers.

E. K. Keler described the method of multiple thermal analysis and its uses in studies of mineral reactions at high temperatures. He described improvements in the technique of multiple thermal analysis, originally described by him in 1939-1940 and, independently, by G. N. Voronkov.

O. P. Mchedlov-Petrosian and V. I. Babushkin described the use of thermodynamics in studies of solid-phase reactions, with the systems $Al_2O_3-SiO_2$, $CaO-SiO_2$, $CaO-Al_2O_3$ and the decomposition of dolomite being used as examples. It was shown that the modification of clays, the burning of cement, etc., can be explained by the use of these methods. The paper was followed by critical comments by Ia. S. Olishanskii, and by statements by A. V. Ralko and L. S. Palatnik in support of the views advanced by the speakers.

At the plenary session on October 18, B. V. Deriagin presented a paper on methods for particle-size determination; he showed that air-permeability methods, based on the Poiseuille regime of air flow, give theoretically larger errors with increase of the dispersity than do methods based on molecular flow of highly rarefied air.

The paper by G. S. Gzimek (Poland) dealt with the influence of the raw materials and other factors on the shape of alite grains.

R. R. Barta and N. I. Gregor (Czechoslovakia) and G. G. Frank (Democratic German Republic) reported on the nature and subject matter of the scientific research work carried out by Czechoslavak and German silicate chemists.

Between the plenary sessions, on October 15, 16, and 17, the sections on cements and cement products, ceramics and refractories, and physiocochemical methods for investigation of silicates and glass, held their meetings.

The largest number of papers was presented in the section on cements. These papers can be classified in the following groups.

1) Use of radioactive isotopes in cement research (papers by B. V. Volkonskii and L. G. Sudakov, P. F. Konovalov and E. I. Morozov, M. G. Tolochkova, and F. G. Banit).

2) Phase analysis of hydrothermal-hardening products (papers by Iu. M. Butt, A. A. Maier and L. N. Rashkovich, T. M. Berkovich, D. M. Kheiker, O. I. Gracheva and N. I. Kupreeva, O. M. Astreeva, and L. Ia. Lopatnikova and V. I. Mikhailova).

3) Methods for studying processes in the hydration of cements (papers by B. V. Ratinov, T. I. Rozenberg and I. A. Smirnova, O. M. Astreeva, L. Ia. Lopatnikova and V. I. Mikhailova, I. V. Kravchenko, S. D. Okorokov, and S. L. Golynko-Vol'fson).

4) Methods of chemical spectroscopy (papers by S. M. Roiak and Z. A. Kel'tseva, E. I. Nagerova, and I. V. Bogdanov).

5) Investigations of the specific surface of cements (papers by D. S. Sominskii and R. L. Koloshin, D. S. Sominskii and G. S. Khodakov, A. S. Panin, and N. N. Tsiurup).

6) Investigations of the properties of concretes (papers by V. I. Soroker and I. S. Vainshtok, V. V. Strel'nikov, K. E. Gorianov and A. V. Mikhailov, S. K. Noskov, E. E. Kalmykova, and others).

The papers aroused great interest in the audience, and in some cases, especially in discussions of methods for determinations of specific surface, there were vigorous exchanges of opinion.

In the section on ceramics and refractories many papers dealt with the use of sonic methods for determination of the elasticity modulus (papers by E. I. Kozlovskaia, Z. I. Veselova, G. N. Voronkov, M. P. Volarovich, and A. S. Gurvich). The papers by G. V. Kukolev, L. A. Shchukareva and N. V. Pitak, and I. F. Ponomarev dealt with the water retention and plasticity of clays. Among other subjects discussed at this section was the determination of properties of materials at high temperatures (papers by F. Ia. Galakhov, V. I. Averianova, N. V. Solomin, A. I. Avgustinik and L. V. Kozlovskii, L. I. Kariakin, and P. D. Piatikop). The paper by D. N. Poluboiarinov and G. N. Volosevich was concerned with methods for regulation of the crystallization and properties of single-oxide ceramics; Iu. Ia. Zaiduk and Iu. G. Shteinberg discussed studies of the

properties of glazes and underglaze layers. The paper by A. E. Fradkin on methods for determination of residual stresses in porcelain aroused special interest.

The section on physicochemical methods for investigation of silicates and glass also included papers on the use of radioactive tracers (papers by V. A. Dubrovskii and T. S. Dubrovskaia, and K. M. Bespalov). A number of papers in this and in other sections touched on questions of calorimetry (papers by E. F. Stroganov, G. M. Matveev and Kh. B. Kokonov, N. N. Sinel'nikov, K. G. Krasil'nikov, and V. F. Kiselev). As in the cement section, some of the papers dealt with spectroscopy (papers Kh. I. Zil'bershtein, O. N. Nikitina, and N. N. Semenova), x-ray methods of investigation (V. N. Rozhanskii and L. A. Feigin), the use of luminescent tracers for studies of the flow of glass (V. V. Polliak), etc.

The summarizing resolutions carried by the sections note the great interest of the conference delegates in the questions discussed.

I. I. Ginzburg presented a special communication, at the request of the All-Union Committee on Clays, at the ceramics section. At his invitation, those interested in studied of clay raw materials attended a special meeting at which they received instruction from a mineralogy specialist on sampling techniques and selection of characteristic and informative tests.

After the resolution at the plenary session of October 18 had been read and adopted, P. P. Budnikov in his concluding address referred to the fruitful work of the conference, which was evidence of the achievements of Soviet science in this field.

The representative of the People's Republic of Poland, G. S. Gzimek, then proposed the creation of an international organization for silicate science and industry in the countries of the Peoples' Democracies. This proposal, intended to create closer contacts between scientists working in this field, and to facilitate the exchange of advanced experience in silicate industry and science, was enthusiastically supported by the delegates.

P. P. Budnikov and O. P. Mchedlov-Petrosian.

EDITORIAL NOTE

The question of gas–liquid interaction regimes in various types of equipment has been discussed in this Journal. Different views on this question have been put forward in the following papers published so far: "Hydrodynamic conditions in the ascent of a gas through a liquid layer" by R. A. Melikian (J. Appl. Chem. 30, No 1, 38, 1957); "The hydraulic conditions which arise in sieve and bubble-cap equipment" by the same author (J. Appl. Chem. 31, No 4, 550, (1958), and "The nature of the gas–liquid disperse system" by M. E. Pozin, I. P. Mukhlenov, and E. Ia. Tarat (J. Appl. Chem. 30, No 1, 45, 1957). It is clear from the material already published, and received by the Editorial Office since, that in the majority of cases the questions are only formally controversial, owing to lack of precise definition. In reality, both sides hold similar views in a number of respects. Therefore, despite the fact that the editorial files contain more papers on this subject by the same authors, it has been decided to terminate this discussion.

BOOK REVIEW

Handling and Uses of the alkali metals. Advances in Chemistry Series, No 19. Washington, American Chemical Society, 1957, 177 p.

There are hardly any books or monographs on the alkali metals, either in Russian or in foreign languages. The book by M. Sittig, recently published in the U.S.A. (M. Sittig. Sodium, its Manufacture, Properties and Uses. New York. 1956) has to some extent filled the gap in the literature on sodium, which occupies a leading position among the alkali metals. However, their technological importance continues to increase. In addition to sodium, which has extensive industrial uses, lithium is now becoming increasingly important in the metallurgy of titanium and zirconium. Therefore a new book on the alkali metals — a rare event in the world of books — is naturally of interest to workers in the fields of chemistry and technology of these metals.

The book "Handling and Uses of the Alkali Metals" is a collection of articles published in the Advances in Chemistry Series. They comprise the papers presented at a symposium on the alkali metals, organized by the American Chemical Society in April 1956.

The 19 chapters of the book can be classified into three unequal groups: 5 articles deal with lithium, 12 with sodium and its derivatives, and 2 with potassium. There is a bibliography at the end of each chapter. The text is profusely illustrated by diagrams, flow sheets, and photographs.

In our opinion, two of the chapters in lithium are of special interest: "Some practical aspects of handling lithium metal," by H. C. Meyer, and "Uses of lithium metal," by W. M. Fenton, D. L. Esmay, R. L. Larsen, and H. H. Schroeder. The authors discuss the uses of lithium in organic synthesis, in metallurgy, as a reducing agent in certain organic reactions, and the uses of lithium and organolithium compounds as polymerization catalysts. It is also noted that metallic lithium may be used as a heat-transfer medium. Useful information is also given in the other chapters on lithium: "Lithium and other alkali metal polymerization catalysts," by F. C. Foster and J. L. Binder, "The binary system sodium—lithium," by W. H. Howland and L. F. Epstein. The results of research work are presented in these last two articles.

The data on sodium and some of its compounds are presented more extensively.

The chapters "Sodium handling at Argonne National Laboratory," by F. A. Smith, and "Sodium handling equipment," by J. F. Cage, contain brief descriptions of sodium handling equipment — an electromagnetic pump, a magnetic flow meter, and certain instruments.

The chapter "Corrosion resistance of metals and alloys to sodium and lithium," by E. E. Hoffman and W. D. Manly, contains very condensed information on factors which influence corrosion of materials in liquid metals. The corrosion resistances of certain metals and alloys used in work with liquid sodium and lithium are compared.

The chapter "Manufacture, handling, and uses of sodium hydride," by M. D. Banus and A. A. Hinckley, deals with handling techniques and uses of sodium hydride (preparation of other metal hydrides, preparation of sodium alcoholates, reduction of metal salts, condensation reactions).

The short chapter "Sodium peroxide production story," by H. R. Tennant and R. B. Schow, contains an interesting section on the continuous production of sodium peroxide in the U.S.A. (Ashtabula, Ohio).

The chapter "Preparation of sodium superoxide," by W. H. Schechter and R. H. Shakely, describes research work on the production of sodium superoxide by the treatment of sodium peroxide with oxygen at high temperatures and pressures.

The chapter "Preparation of metal powders by sodium reduction," by T. P. Whaley, deals with conditions for the formation of powders of nickel, iron, manganese, cobalt, cadmium, and certain other metals by reactions of dispersed metallic sodium with chlorides of these metals.

A chapter of undoubted interest to Soviet readers deals with a very topical subject: "Present and potential uses of sodium in metallurgy." The author is the eminent American technologist W. J. Kroll, known for his method for the production of titanium by the reduction of $TiCl_4$ with magnesium. The uses of metallic sodium as reducing agent for the production of pure metals and alloys are considered in this chapter. The production of titanium by reduction of titanium tetrachloride by sodium is discussed.

This brief account of the chapters on sodium may be completed by a mention of two other chapters. One is by K. L. Lindsay, entitled "Reactions of sodium with organic compounds." The other is in the field of the analytical chemistry of sodium; it is entitled "Determination of sodium monoxide in sodium." The authors are V. L. Hansley and R. A. Kolbeson.

The last two chapters of the book are on the subject of potassium and its derivatives, and are both written by the same authors, C. B. Jackson and R. C. Werner.

The chapter "Manufacture of potassium and sodium–potassium alloys" contains an excessively brief description of the thermal process for the production of potassium and its sodium alloys. A flow diagram of the continuous production of metallic potassium is given.

The chapter "Manufacture and use of potassium superoxide" gives a very concise account of a unit for the production of potassium superoxide (KO_2), with an output of 3 tons per day, and of the uses of this chemical for respiratory purposes.

With regard to the book as a whole it must be stated that most of the articles are rather short and give only general outlines of the subjects discussed. The information in some of the chapters is not particularly new (for example, the articles by Smith and Cage on sodium handling).

The book was written by 33 authors. It gives the impression that the editors did not always succeed in obtaining consistent presentation.

Despite these defects, the book constitutes a definite contribution to the literature on alkali metals. It will be of use to chemists, technologists, and planners concerned with the technology and uses of the alkali metals and their derivatives. The book is also of some interest to metallurgists in the new titanium industry.

"Handling and Uses of the Alakali Metals" should be translated into Russian. This would form a valuable addition to the Russian Translation of Sittig's book on sodium, which is being published by the Foreign Literature Press.

I. Ia. Volkind

SIGNIFICANCE OF ABBREVIATIONS MOST FREQUENTLY ENCOUNTERED IN SOVIET PERIODICALS

FIAN	Phys. Inst. Acad. Sci. USSR.
GDI	Water Power Inst.
GITI	State Sci.-Tech. Press
GITTL	State Tech. and Theor. Lit. Press
GONTI	State United Sci.-Tech. Press
Gosenergoizdat	State Power Press
Goskhimizdat	State Chem. Press
GOST	All-Union State Standard
GTTI	State Tech. and Theor. Lit. Press
IL	Foreign Lit. Press
ISN (Izd. Sov. Nauk)	Soviet Science Press
Izd. AN SSSR	Acad. Sci. USSR Press
Izd. MGU	Moscow State Univ. Press
LEIIZhT	Leningrad Power Inst. of Railroad Engineering
LET	Leningrad Elec. Engr. School
LETI	Leningrad Electrotechnical Inst.
LETIIZhT	Leningrad Electrical Engineering Research Inst. of Railroad Engr.
Mashgiz	State Sci.-Tech. Press for Machine Construction Lit.
MEP	Ministry of Electrical Industry
MES	Ministry of Electrical Power Plants
MESEP	Ministry of Electrical Power Plants and the Electrical Industry
MGU	Moscow State Univ.
MKhTI	Moscow Inst. Chem. Tech.
MOPI	Moscow Regional Pedagogical Inst.
MSP	Ministry of Industrial Construction
NII ZVUKSZAPIOI	Scientific Research Inst. of Sound Recording
NIKFI	Sci. Inst. of Modern Motion Picture Photography
ONTI	United Sci.-Tech. Press
OTI	Division of Technical Information
OTN	Div. Tech. Sci.
Stroiizdat	Construction Press
TOE	Association of Power Engineers
TsKTI	Central Research Inst. for Boilers and Turbines
TsNIEL	Central Scientific Research Elec. Engr. Lab.
TsNIEL-MES	Central Scientific Research Elec. Engr. Lab.—Ministry of Electric Power Plants
TsVTI	Central Office of Economic Information
UF	Ural Branch
VIESKh	All-Union Inst. of Rural Elec. Power Stations
VNIIM	All-Union Scientific Research Inst. of Meteorology
VNIIZhDT	All-Union Scientific Research Inst. of Railroad Engineering
VTI	All-Union Thermotech. Inst.
VZEI	All-Union Power Correspondence Inst.

Note: Abbreviations not on this list and not explained in the translation have been transliterated, no further information about their significance being available to us. — Publisher.

SCIENTIST - TRANSLATORS WANTED

For over a decade, Consultants Bureau, Inc. has provided Western scientists with high quality cover-to-cover translations of Soviet scientific journals. Our unique contracts with the Soviet government are constantly revised to include more extensive coverage of technical activity in the USSR. In order to produce these journals at the high standards set down by both the Soviet and American governments, it is of prime importance to maintain a large staff of scientist-translators who can translate with precision in their specific scientific field. It is our strict policy to assign a translator only that material which is within his scope.

As part of our current and future* expansion programs, we have openings for a limited number of scientist-translators who can translate in the fields covered by the following journals:

Journal of General Chemistry

Antibiotics
Biochemistry
Bulletin of Experimental Biology and Medicine
Entomological Review
Microbiology
Pharmacology and Toxicology
Plant Physiology

Automation and Remote Control
Industrial Laboratory
Instruments and Experimental Techniques
Measurement Techniques

Czechoslovak Journal of Physics
Soviet Journal of Atomic Energy
Soviet Physics - Acoustics
Soviet Physics - Crystallography
Soviet Physics - Technical Physics

Our basic requirements are that the scientist-translator have a native command of English, a minimum degree of B.S. in his specific field, and a thorough knowledge of the contemporary technical terminology of his scientific discipline.

Translation may be done at home on a full or part-time basis.

For further information, please contact:

Translation Editor
CONSULTANTS BUREAU, INC.
227 West 17th Street
New York 11, New York

*We expect, in the near future, to initiate a program of translation from the growing amount of important Chinese scientific literature available. In preparation, we are accepting applications from Chinese to English translators.